Establishment of High Cell Density Fed-Batch Microbial Cultures at the Microwell Scale

An EngD Thesis submitted to

University College London

By

Mary Alice Gallaway Lunson

Declaration

'I, Mary Lunson confirm that the work presented in this thesis is my own. Where information has been derived from other sources, I confirm that this has been indicated in the thesis.'

Acknowledgements

Firstly, I would like to thank my supervisor from UCL Gary Lye for his continued support and guidance throughout this project. I would also like to thank my secondary supervisor from UCL Darren Nesbeth. I would like to thank my industrial supervisors Gary Finka, Steve Warr and Andy Kaja in Biopharm Process Research at GSK for giving me the opportunity to gain experience in the biopharmaceutical industry and access to resources such as 3D-printing facilities. In addition, I would like to thank GSK and the EPSRC for funding this project.

I would like to thank everyone in the Biopharm Process Research group at GSK, Stevenage for making my time in the group so enjoyable. In particular, I would like to thank Jed Smith for providing me with the microbioreactor k_La characterisation data that he generated prior to me starting the project, and Julian Chesshyre and Ioannis Voulgaris for their invaluable expertise in microbial fermentation and their support throughout the project. I would like to thank Alex Linvingstone for his assistance with the pilot scale fermentation and Katy Newell for her support with small scale purification. I would also like to thank Pat Marder for all her support with media and bioreactor preparation.

I would like to thank Michael Gray from 3D-printing Platform, Technology and Science, Research & Development at GSK, and the UCL Design and Fabrication Facility, in particular Simon Dawes, for their assistance with design and development of the microbioreactor feeding system. I also like would like to thank the EPSRC Engineering Instrument Pool (no longer in existence) for the loan of the high speed camera.

Finally, I would like to thank my family, particularly my parents, for their continued support throughout my studies.

Abstract

The rate limiting steps of biopharmaceutical process development are clone evaluation and process optimisation. To improve the efficiency of this step, miniature bioreactors are increasingly being used as a tool for high throughput experimentation. At industrial scale, microbial cultivations are usually performed in fed-batch mode to allow for high cell density cost-effective processes; however, many commercially available miniature bioreactors do not have an inbuilt feeding capacity. There are several challenges that need to be addressed to establish high cell density fed-batch cultivation at microscale: attaining high oxygen mass transfer rates, achieving good mixing for the duration of the culture and implementation of an industrially relevant feeding strategy requiring low volume additions.

The overall aim of this project was to develop a scale-down fermentation platform suitable for the study and optimisation of high cell density cultures. The first objective of this work was to evaluate options for fed-batch cultures in a commercially available 24-well shaken microbioreactor. To achieve this, two feeding strategies were evaluated using an *E. coli* strain expressing a domain antibody: *in situ* feeding by the enzymatic release of glucose from polymeric starch, and direct feeding using a bespoke feed delivery system. *In situ* feeding was investigated as it is a simple option that does not require a physical method of feed delivery; cellular productivity was enhanced in comparison to batch cultures, however the glucose release was insufficient to sustain high cell density cultures representative of laboratory and pilot scale processes. To enable direct and continuous feed delivery to the microbioreactor a bespoke 3D-printed feeding system was developed that can operate at flow rates of 20μL h^{-1} and above, and enables up to twelve fed-batch cultures to be run in parallel. *E. coli* fermentations were performed on complex medium containing glycerol with direct feeding of a 23% w/v glycerol solution initiated at around 18 hours.

The second objective of this project was to establish an industrially relevant feeding strategy in the microbioreactor, comparable to a laboratory scale fed-batch process. To this end, the direct feeding strategy was refined in terms of cell growth and product expression; the feed rate and concentration were modified, the DO set point was increased, and a pre-feeding hold period was implemented to allow for consumption of the inhibitory by-products generated in the batch phase. It was found that direct feeding enhanced biomass production by ~70% and product expression by ~2.4 fold in comparison to non-fed cultures.

The third objective of this work was to demonstrate the applicability of the new feeding system as a tool for process optimisation experiments. The effect of IPTG concentration and post-

induction temperature on product expression was performed using the both the microbioreactor feeding system and the 1L laboratory scale process. The data trends were consistent between scales; product expression was enhanced at a higher post-induction temperature, and IPTG concentration did not affect product expression over the concentration range tested. This demonstrates that the microbioreactor, is predicative of the 1L laboratory scale process terms of sensitivity to change in process conditions

The fourth objective of this work was to characterise the microbioreactor in terms of oxygen transfer capability and fluid mixing. To achieve this aim, the volumetric oxygen mass transfer coefficient (k_La) and liquid phase mixing time (t_m) of the microbioreactor were determined. The impact of shaking frequency, total gas flow rate and fill volume on oxygen transfer and fluid mixing were investigated and the optimum operating conditions were determined. Within the operating ranges of the miniature bioreactor system, it was found that oxygen transfer was dependant on both shaking frequency and gas flow rate, but was independent of fill volume. The oxygen mass transfer coefficient, k_La increased with both increasing shaking frequency (500-800rpm) and gas flow rate (0.1-20 mL min^{-1}) over the range 3-101h^{-1}; this is at the lower end of the range for conventional stirred tank reactors. It was demonstrated that the miniature bioreactor system is well mixed under the range of operating conditions evaluated. The liquid phase mixing time, t_m under non-aerated conditions increased with shaking frequency and decreased with fill volume over the range 0.5-15s.

The final objective this project was to demonstrate suitability of the microbioreactor as a scale-down model of an industrial fermentation process. 50L pilot scale, 1L laboratory scale, and 4mL microbioreactor fed-batch fermentations were performed under optimum conditions. The 4mL microbioreactor fed-batch process was shown to better predict the 50L pilot-scale process than the 1L laboratory-scale process based on cell growth, product expression and product quality. This could be explained by mixing and oxygen mass transfer phenomena. At 1L scale, oxygen mass transfer and fluid mixing are most efficient, meaning cell growth and productivity were the highest of the three processes. It appears that the limitations in oxygen mass transfer in the microbioreactor and fluid mixing in the 50L scale vessel, results in a comparable cellular environment, and therefore cell growth, productivity and product quality.

In summary, this work has demonstrated the ability to conduct high cell density, fed-batch microbial cultures in parallel, using a shaken miniature bioreactor system. A bespoke, 3D-printed feed delivery system was developed allowing for twelve industrially-relevant microbial fed-batch cultures to be run in parallel. The microbioreactor fed-batch cultures were shown to be predictive of, a 50L pilot scale process in terms of cell growth, productivity and product quality.

EngD Impact Statement

The use of parallel miniature bioreactors in early stage biopharmaceutical process development can reduce development time and cost, due to increased throughput of strain screening and process optimisation experiments. Improving the efficiency of biopharmaceutical process development allows for a greater number of medicines to reach patients sooner. In this work a bespoke feeding system was developed for a commercial 24-well microbioreactor system. It was shown that this has the potential to enable strain screening and process optimisation experiments to be performed under industrially relevant fed-batch conditions, reducing the frequency of scale-up failures and therefore development time and cost. Other potential applications of this feeding system in the biopharmaceutical industry are high throughput media evaluation, and small scale protein production for characterisation studies.

In addition to the biopharmaceutical industry, the feeding system developed in this work could also be a useful tool for research activities in other industries such as the renewable energy and food industries, for example for the development of biorefinery processes. The feeding system would also be suitable for use in academia; the system is 3D-printed and therefore fabrication is inexpensive. It could therefore be useful for academic research that requires the scale-up or scale-down of fed-batch processes, and could also be used for small scale protein production for characterisation or activity studies. The system would be an asset to establishments that are already using microwell bioreactors in batch mode, and are would like the flexibility to run fed-batch cultures to enhance their research programme, to generate results more representative of industrial fermentation process conditions.

Contents

List of Tables

List of Figures

Nomenclature

Abbreviation	Description
4-AAP	4-Aminoantipyrine
ADH	Alcohol dehydrogenase
ADP	Adenosine diphosphate
AGU	Amyloglucosidase units
AK	Acetate kinase
ATP	Adenosine triphosphate
CS	Citrate synthase
BFL	Micro-24 cassette with direct sparging and a single baffle
BLI	Bio-Layer Interferometry
BPR	Biopharmaceutical Process Research
CA	Cellulose acetate
CAD	Computer assisted design
CER	Carbon dioxide evolution rate ($kg\ m^3\ h^{-1}$ or $mmol\ L^{-1}\ h^{-1}$)
CFD	Computational fluid dynamics
CFU	Colony forming units
CHO	Chinese hamster ovary
CPP	Critical process parameter
CQA	Critical quality attribute
CV	Coefficient of variance
dAb	Domain antibody
DCW	Dry cell weight ($g\ L^{-1}$)
DNA	Deoxyribonucleic acid
DO	Dissolved oxygen
DoE	Design of experiment
E. coli	*Escherichia coli*
EGFR	Epidermal growth factor receptor
EOB	End of batch
ETFE	Ethylene tetrafluoroethylene
Fab	Fragment antigen binding domain
Fc	Fragment crystalline domain
Fv	Variable domain
FcCCD	Face-centred central composite design
GFP	Green fluorescent protein

GK	Glycerol kinase
G6P-DH	Glucose 6-phosphate dehydrogenase
GPO	Glycerol 6-phosphate oxidase
HCDC	High cell density culture
HCP	Host cell proteins
HK	Hexokinase
HOS	High order structure
HPLC	High performance liquid chromatography
Ig	Immunoglobulin
IgG	Y-Immunoglobulin
IPTG	Isopropyl β-D-1-thiogalactopyranoside
ISFET	Ion sensitive field effect transistor
mAb	Monoclonal antibody
MBR	Micro or miniature bioreactor
MDH	L-malate dehydrogenase
Micro-24	Miniature 24-well shaken bioreactor
MSBR	Miniature stirred bioreactor
MTP	Microtitre plate
NAD^+	Nicotinamide adenine dinucleotide
$NADP^+$	Nicotinamide adenine dinucleotide phosphate
OTR	Oxygen transfer rate (mmol L^{-1} h^{-1} or kg m^{-3} h^{-1})
OUR	Oxygen uptake rate (mmol L^{-1} h^{-1} or kg m^{-3} h^{-1})
OUR_{max}	Maximum oxygen uptake rate (mmol L^{-1} h^{-1} or kg m^{-3} h^{-1})
PBS	Phosphate buffered saline
PEI	Polyethylenimine
PES	Polyethersulfone
POD	Peroxidase
PRC	Micro-24 cassette with headspace sparging
PTA	Phosphotransacetylase
PTFE	Polytetrafluoroethylene
PTS	Platform Technology and Science
QbD	Quality by design
REG	Micro-24 cassette with direct sparging
RPM	Revolutions per minute (min^{-1})
SDS-PAGE	Sodium dodecyl sulphate–polyacrylamide gel electrophoresis
SEC	Size exclusion chromatography

SPR	Specific productivity (mg g^{-1} L^{-1})
SRW	Standard round well (microtitre plate)
STR	Stirred tank reactor
TCA	Tricarboxylic acid
VBNC	Viable but not culturable
VVM	Gas volume flow per liquid volume unit per minute
WCW	Wet cell weight (g L^{-1})

Symbol	Description
a	Gas-liquid interfacial area per unit volume of fluid (m^2 m^{-3})
C_a	Glucose per unit volume of matrix in Equation 1.14 (mg mm^{-3})
C_s	Glucose solubility per unit volume of matrix in Equation 1.14 (mg mm^{-3})
C_L	Liquid phase oxygen concentration (mmoL L^{-1})
C^*_L	Liquid phase oxygen concentration in equilibrium with the gas phase (mmoL L^{-1})
D	Diffusion coefficient in Equation 1.14 (mm^2 s^{-1})
D_f or d_f	Maximum flask diameter (m)
D_i or d_i	Impeller diameter (m)
D_T	Tank diameter (m)
g	Gravitational acceleration (m s^{-2})
H_T	Tank height (m)
k_L	Liquid phase mass transfer coefficient (m s^{-1})
$k_L a$	Volumetric oxygen mass transfer coefficient (s^{-1} or h^{-1})
m	Microbial maintenance requirement of oxygen (mmol O$_2$ g^{-1} h^{-1})
M_s	Carbon source mass flow rate (g h^{-1})
M_{glc}	Mass of glucose released in Equations 1.14 and 1.15 (mg)
N	Stir speed (rpm)
N_{cd}	The rotational speed at which the complete dispersion of the gas phase occurs
OD$_{600}$	Optical density at 600nm
q_{O2} or Q_{o2}	Specific oxygen consumption rate (h^{-1})
Q	Volumetric flow rate (m^3 s^{-1})
Q_{air}	Volumetric air flow rate (m^3 s^{-1})
P_o ($P/\rho N^3 di^5$)	Ungassed impeller power number (dimensionless)
P_{og} ($P_g/\rho N^3 di^5$)	Gassed impeller power number (dimensionless)

Ph	Phase number as described in Equation 1.9 (dimensionless)
P_g	Gassed power (W or KW)
P_{ug}	Ungassed power (W or KW)
$Re_f\,(\rho N d_f^2/\mu)$	Flask Reynolds number
$R_{ei}\,(\rho N di^2/\mu)$	Impeller Reynolds number (dimensionless)
s	Sample Standard deviation
S_F	Substrate concentration (g L^{-1})
t_{90}	Mixing time for 90% homogeneity (s)
t	Time (s)
t_o	Feed start time (h)
t_{90}	Mixing time at 90% homogeneity
t_m	Mixing time (s)
U	Amyloglucosidase units
$U_{tip}\,(\pi ND_i)$	Impeller tip speed (m s^{-1})
v	Volume (m^3)
V_H	IgG heavy chain
V_L	IgG light chain
v_s	Superficial gas velocity (m s^{-1})
w	Weight (kg)
X	Biomass concentration (g L^{-1})
$\bar{x}$	Sample mean
X_{final}	Final biomass concentration (g L^{-1})
$Y_{x/o2}$	Yield of biomass on oxygen
$Y_{x/s}$	Yield of biomass on substrate
z	Number of discs in Equation 1.15
Z	Term in Equation 5.1

Greek symbol	**Description**
ε_T	Local energy dissipation rate (W Kg^{-1})
$\bar{\varepsilon}_T$	Average energy dissipation rate (W kg^{-1})
$(\varepsilon_T)_T$	Energy dissipation rate close to the tank wall (W kg^{-1})
μ	Viscosity (N s m^{-2})
μ	Specific growth rate (h^{-1})
μ_{max}	Maximum specific growth rate (h^{-1})
ρ	Density (Kg m^{-3})
σ	Liquid surface tension (N m^{-1})

τ_p Probe response time (s)

Chapter 1. Introduction

1.1. Biopharmaceutical industry overview

Biopharmaceutical market sales were estimated to be $281 billion per year in 2016 (Moorkens *et al.*, 2017). Monoclonal antibodies are the largest class of these 'biologic' medicines and account for 66% of annual sales (Figure 1.1). Sales of monoclonal antibodies reached approximately $106.9 billion in 2016; a 205% increase from 2008, when sales were $35 billion (Kesik-Brodacka, 2018). By 2017 more than 58 antibodies had been approved (Chung, 2017). The total cost to develop a biopharmaceutical product is estimated to exceed $1.2 billion and the average development time from discovery through to registration is 12 years. The high development cost is largely due to the majority of molecules in development failing to make in through to registration (Steinmeyer and McCormick, 2008).
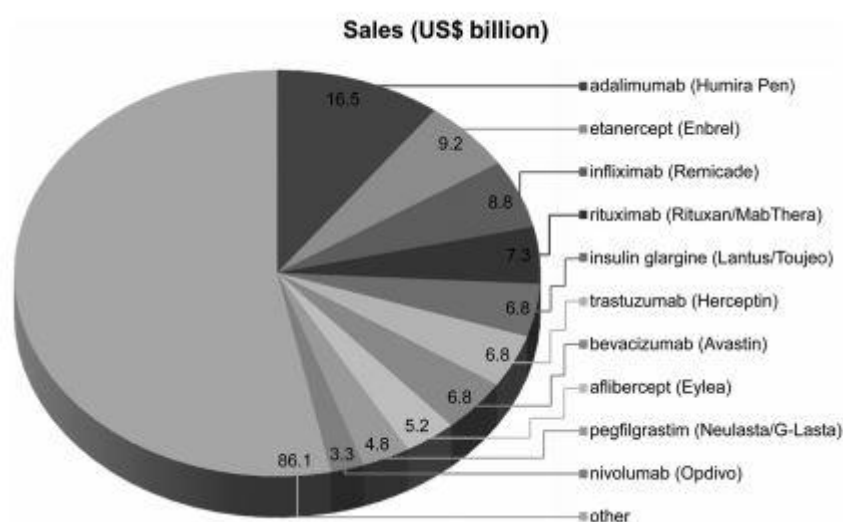
Figure 1.1. Top selling biopharmaceuticals in 2016 (figure reproduced from Kesik-Brodacka, 2018)

1.2. Expression systems used for production of biopharmaceuticals

The majority of approved biopharmaceuticals are produced in one of three host systems: *Escherichia coli*, yeasts and mammalian cells, primarily Chinese hamster ovary (CHO) cells. The expression system used for protein production is dependent on the properties of the protein of interest including the molecular weight and any required post-translational modifications (PTMs); PTMs are changes in the primary structure of a protein such as glycosylation, deamidation and oxidation, that can modify the high-order structure (HOS) and therefore biological function (Orphanou and Gervais, 2018). The metabolic machinery required for PTMs is only present in eukaryotic cells (Butler, 2005; Zhu, 2012). In 2011, of the 211 approved biopharmaceuticals 31% were produced in *E. coli*, 15% in yeast and 43% in mammalian cells (Berlec and Strukelj, 2013). Table 1.1 summarises advantages and limitations of the various expression systems.

1.2.1. The *E coli* expression system

E. coli is the preferred expression system for non-glycosylated proteins due to its well characterised genetics, rapid growth and high yield production (Huang, Lin and Yang, 2012). *E. coli* recombinant protein expression is either cytoplasmic, periplasmic, or in a few cases secreted into the growth medium (Berlec and Strukelj, 2013). Cytoplasmic protein expression is the simplest and most commonly used expression strategy, however downstream processing is more challenging. The main disadvantages of cytoplasmic expression are the high level of host cell proteins (HCPs) released during primary recovery, the inability to form correct disulphide bonds, the presence of intracellular proteases and inclusion body formation (Berlec and Strukelj, 2013). In some cases, inclusion body formation is considered to be an advantage, as they contain few contaminating proteins and have a high density (1.3 mg mL^{-1}), allowing for separation from other cellular components by centrifugation; high yields can be achieved and downstream processing is considered efficient (Berlec and Strukelj, 2013). Another advantage to inclusion body formation is the versatility to express a range of proteins (Huang, Lin and Yang, 2012). The limitation of inclusion body formation is that a refolding step is required; refolding steps can be slow and are not always effective and result in dilution of the product stream (Berlec and Strukelj, 2013).

Periplasmic expression is a favourable option since the *E. coli* periplasm contains only 4% of the total host cell proteins; this means that fewer processing steps are required further downstream. The main limitation of expression in the periplasm is that the recombinant protein

requires an appropriate leader peptide which then has to be removed during downstream processing (Berlec and Strukelj, 2013). Generally, *E. coli* is unable to secrete proteins (Nandakumar, Cheung and Marten, 2006), however four mechanisms to induce the secretion of proteins have been reported. The first method is the use of engineered strains with secretion mechanisms from pathogenic Gram-negative bacterial strains. The second strategy involves carrier proteins that are secreted by an unknown mechanism. The third involves the use of mutants with defects in the outer membrane, although this may influence cell growth, and the fourth strategy is the co-expression of lysis promoting proteins (Ni and Chen, 2009; Berlec and Strukelj, 2013). Literature suggests that in the case of functional antibody fragments, expression in the periplasmic space, where conditions are suitable for correct disulphide bond formation, is currently the most commonly used method in industry (Bothmann and Pluckthun, 2000; Sonoda *et al.*, 2011; Wang *et al.*, 2013; Lee and Jeong, 2015)

1.3. Domain antibodies (dAbs)

Antibodies are glycoproteins secreted by B cells in response to a foreign organism or antigen, that bind to the foreign target triggering an immune response Antibodies belong to the immunoglobulin (Ig) superfamily (Buss *et al.*, 2012). Figure 1.2 shows the structure of a γ-immunoglobulin (IgG); most therapeutic monoclonal antibodies (mAbs) are of this isotype. The fragment antigen binding domain (Fab) is formed by the combination of the hypervariable regions of the heavy and light chains. The fragment crystallisable domain (Fc) is composed of two constant domains of the heavy chain and is responsible for effector function (Buss *et al.*, 2012).

Whole monoclonal antibodies are mainly produced in CHO cells which allow for human-like N-glycosylation. Mammalian cells, however, have limitations relating to bioprocessing and scale-up (Table 1.1); this results in high production costs and comparatively low productivity (Spadiut *et al.*, 2014). However, antibody fragments can be effectively produced in microbial strains (Holt *et al.*, 2003). The absence of glycosylation on the Fv and Fab regions means that engineering and cultivation of microbial host organisms is possible (Spadiut *et al.*, 2014). Domain antibodies (dAbs) are either composed of a mouse or human single, unpaired V_H or V_L domain, or the unpaired variable domain (V_{HH}) from antibodies naturally expressed in shark and camelid species (Boder and Jiang, 2011). dAbs have many advantages over mAbs including small size, stability, solubility, tumour uptake and blood clearance (Zarschler *et al.*, 2013). The biophysical properties of dAbs mean they are promising in cancer and other therapeutic areas;

dAbs are able to refold after thermal denaturation and reacquire antigen-binding activity (Boder and Jiang, 2011)

The three main microbial expression systems for antibody domain production are *S. cerevisiae*, *P. pastoris* and *E. coli* (Spadiut *et al*., 2014). Zarschler *et al* (2013) demonstrated the production of up to 200 mg L^{-1} of functional soluble epidermal growth factor receptor (EGFR)-specific dAbs using a genetically engineered *E. coli* strain and high cell density cultivation media (Zarschler *et al.*, 2013).
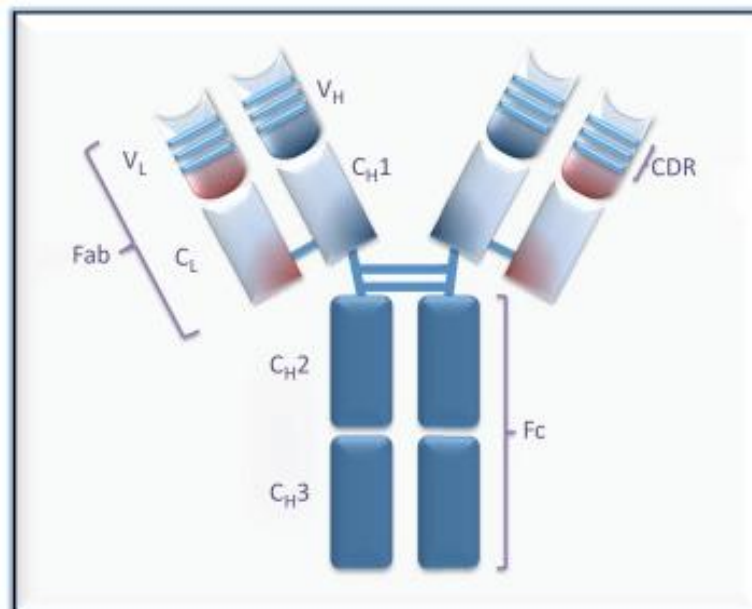
Figure 1.2. Structure of a Y-immunoglobulin, IgG (figure reproduced from Buss et al., 2012). V_H is the heavy chain variable domain, C_H1, C_H2 and C_H3 are the three constant domains of the heavy chain. V_L is the light chain variable domain and C_L1 is the light chain constant domain. The Fab domain is the fragment antigen binding domain and Fc is the crystallisable domain. The CDRs are complementarity-determining regions, which bind to the antigen directly.

Table 1.1. Advantages and disadvantages of bacterial, yeast and mammalian expression systems (information from Rai and Padh, (2001); Berlec and Strukelj, (2013); Fischer, Handrick and Otte, (2015), unless otherwise indicated)

Expression system	Advantages	Limitations
Bacterial	- High growth rates resulting in high volumetric productivity - High cell densities can be achieved - Simple and inexpensive media - Well characterised genetics	- No post-translational modifications or glycosylation in either N- or O-linked conformation - Inclusion body formation - Incorrect folding of proteins - Release of endotoxins and HCPs during recovery of cytoplasmic proteins *E coli* has toxic cell wall pyrogens
Yeast	- Relatively high growth rate - Simple, inexpensive media - High cell densities can be achieved - Advanced genetics so can readily be manipulated - Complete genome sequence available - High copy plasmids - Able to secrete proteins - Able to glycosylate target proteins	- Hypermannosylation hindering proper folding - Inappropriate non-human glycosylation of human glycoproteins (Frenzel, Hust and Schirrmann, 2013)
Mammalian (CHO cells)	- Mammalian post-translational modifications possible - Robust growth in serum-free and chemically defined media - Relatively good safety profile in terms on human pathogenic virus replication. - Stable expression of the gene of interest (GOI) with the desired productivity and product quality. CHO genome available (Xu *et al.*, 2011)	- Differences in glycosylation between rodent and human cell lines and human tissues - Time consuming due to the slow growth rates - Limited scalability compared to *E. coli* - Complex and expensive nutrient media required - Low product concentration

1.4. Engineering characterisation of bioreactors for microbial cultivation

1.4.1. Oxygen demand in microbial systems

Oxygen is used by aerobic microorganisms for growth (Garcia-Ochoa and Gomez, 2009). In many microbial processes, oxygen transfer is the rate-determining step as oxygen is only sparingly soluble in water (Zhong, 2010). The concentration of oxygen in the fermentation broth depends on the oxygen transfer rate (OTR) of oxygen from gas bubbles to the liquid phase and the rate that oxygen is consumed by the microorganism in the culture broth, the oxygen uptake rate (OUR). The OUR is calculated using Equation 1.1 and has units of mmol O_2 L^{-1} h^{-1}, where, q_{O2} is the oxygen consumption rate (h^{-1}), μ is the specific growth rate (s^{-1}), $Y_{X/O2}$ is the yield of biomass on oxygen, X is the biomass concentration (g L^{-1}) and m is the maintenance requirement of oxygen (mmol O_2 g^{-1} h^{-1}).

Each microorganism has a different specific q_{o2}. Çalik, Yilgör and Demir, (2006) reported a q_{O2} of an *E. coli* K12 strain to be 0.031-0.641 kg(O_2) kg^{-1}(biomass) h^{-1} during an 11-hour batch fermentation, using defined media containing glucose in the pH range 5.0-7.8. The q_{o2} is assumed to be constant during all phases of microbial growth although there is experimental data that contradicts this assumption (Çalik, Yilgör and Demir, (2006); Garcia-Ochoa and Gomez, 2000). The maximum oxygen uptake rate (OUR_{max}) occurs at the end of the exponential phase when the most cells are growing at the highest rate.

$$OUR = q_{O_2}X + mX = \frac{\mu}{Y_{X/O_2}} + mX \tag{1.1}$$

1.4.2. Oxygen mass transfer and fluid mixing requirements for microbial cultivation

A cylindrical stirred tank reactor (STR) is the most common reactor configuration used in bioprocessing. The main challenge in reactor design for aerobic microbial applications is to achieve adequate mixing and aeration to provide sufficient oxygen for cell growth (Doran, 2013). The rate of oxygen transfer per unit volume of fluid (OTR) is proportional to the concentration gradient; the proportionality constant is the volumetric oxygen mass transfer coefficient, k_La (Equation 1.2) (Garcia-Ochoa and Gomez, 2009). k_L (m s^{-1}) is the liquid phase mass transfer coefficient and a is the gas-liquid interfacial area per unit volume of fluid (m^2 m^{-3}). C_L is the oxygen concentration (mmol L^{-1}) in the broth and C^*_L is the oxygen concentration in the broth at equilibrium with the gas phase (mmol L^{-1}). The difference between C^*_L and C_L represents the concentration difference driving force for mass transfer. The maximum mass transfer rate can therefore be approximated by $k_La.C^*_L$ (Garcia-Ochoa and Gomez, 2009).

There are many empirical correlations to determine $k_L a$ (Table 5.7), and methods for theoretical predictions of $k_L a$, such as computational fluid dynamics (CFD) have also been developed (Kelly, 2008; Sharma, Malhotra and Rathore, 2011). The OTR is affected by physical properties of the culture broth, operating conditions, bioreactor geometry and the presence of biomass. The OTR can be enhanced though increasing stirrer speed, total gas flow rate or oxygen concentration in the gas phase (Garcia-Ochoa and Gomez, 2009)

$$OTR = k_L a(C^*_L - C_L)$$
(1.2)

Efficient mixing of the culture broth is required to maintain a homogeneous environment for cell culture. Mixing promotes an optimal environment by blending soluble media components, dispersing gasses in the form of small bubbles, maintaining solid particles in suspension, promoting heat transfer, and where necessary dispersing immiscible liquids throughout the whole volume of liquid. Vessel geometry, liquid height and the presence of baffles and sparger design all influence mixing in STRs (Doran, 2013).

The power input into a bioreactor is the energy required to move the fluid by either mechanical or pneumatic agitation. Efficient mixing with minimum energy requirements is an important consideration in reducing operating costs (Bates, Fondy and Corpstein, 1963). The power required to mix non-aerated fluids depends on the vessel and impeller geometries, and the physical properties of the fermentation broth (Bates, Fondy and Corpstein, 1963; Doran, 2013). The relationship between these variables can be quantified using dimensionless analysis. The most important dimensionless group for mixing characterisation is the Reynolds Number. The impeller Reynolds number (Re_i) for a stirred tank reactor is shown in Equation 1.3 where ρ is the liquid density, N is the impeller rotational speed, D_i is the impeller diameter and μ is the liquid viscosity. The Re_i represents the ratio of the inertial forces acting on the liquid to the intrinsic viscous forces of the liquid (Doran, 2013).

The ungassed power (P_{ug}) required to achieve fluid mixing is described by the Power number (P_o) (Equation 1.4). In the turbulent regime ($Re_i > 10^4$), P_o is independent of power number and in the laminar regime ($Re_i < 10$). P_o is directly proportional to the fluid viscosity (Doran, 2013). The presence of a dispersed gas phase reduces the density of the fluid and causes gas-filled cavities to form behind the impeller blades. This reduces impeller resistance to rotation causing a significant drop in the power requirement. In the case of a six-flat-blade disc turbine (Rushton turbine), most commonly used for microbial fermentations due to the effective gas distribution,

the gassed power requirement is typically 30-40% of the ungassed power requirement (Oosterhuis and Kossen, 1981; Doran, 2013).

$$Re_i = \frac{\rho N d_i^2}{\mu} \qquad \qquad (1.3)$$

$$Po = \frac{P_{ug}}{\rho N^3 d_i^5} \qquad \qquad (1.4)$$

The liquid phase mixing time, t_m, is the time taken to achieve a specific degree of homogeneity, typically 95%. The mixing time is measured by monitoring the concentration of an inert tracer at one or multiple points in the vessel (van't Riet and van der Lans, 2011). Nienow (1997) proposed a mixing time correlation for vessels with an aspect ratio (H_T:D_T) and equipped with a single impeller (Equation 1.5), where $\bar{\varepsilon}_T$ is the mean energy dissipation rate (Equation 1.6). This correlation assumes that the D_i/D_t and $(\varepsilon_T)_T/\bar{\varepsilon}_T$, where $(\varepsilon_T)_T$ is the local energy dissipation rate (ε_T) closest to the wall at its lowest value, are the same for all impeller geometries. Equation 1.5 shows that mixing time can be reduced by increasing both D_i:D_t and $\bar{\varepsilon}_T$ (Nienow, 1998). Cooke (1993) described a correlation for '90% mixing time' (t_{90}), for 20-60 litre STRs with H_T:D_T of 1-3 equipped with three Rushton Turbines (Equation 1.7) (Cooke, 1993).

Gogate, Beenackers and Pandit, (2000) reported mixing times for an STR with multiple impeller geometries at agitation speeds up to 1200 rpm of less than 40s and less than 10s for a single Rushton turbine. Saito *et al.*, (1992) reported mixing times in a similar range of 5-20s for 6-blade Scaba Radial Flow Gas-Dispersing Turbine (SRGT) and Rushton turbine impellers at agitation speeds of 100 to 450 rpm and gas flow rates of 0.5-1 VVM. The energy dissipation rate is reduced at larger scales; at 1000m^3 scale mixing times are in the order of 100s seconds due to the lower $\bar{\varepsilon}_T$, which is significantly higher than the time for oxygen mass transfer of approximately 10s. To reduce the mixing time to the order of 10s from 100s a 1000-fold increase in the power input is required (Equation 1.5) (van't Riet and van der Lans, 2011)

$$t_m = 5.9 T^{\frac{2}{3}} (\bar{\varepsilon}_T)^{-\frac{1}{3}} \left(\frac{D_i}{D_t}\right)^{-\frac{1}{3}} \qquad \qquad (1.5)$$

$$\bar{\varepsilon}_T = \frac{P}{\rho V} \qquad \qquad (1.6)$$

$$t_{90} = 3.3Pog^{-\frac{1}{3}}N^{-1}\left(\frac{H_L}{D_i}\right)^{2.43}$$

<div align="right">(1.7)</div>

1.5. Microbial cultivation at microscale

The introduction of microbioreactors (MBRs) has enabled the development of scale down models of industrially relevant upstream processes. At microscale high throughput bioprocess screening and optimisation studies are performed at the microlitre or millilitre scales; volumes as low as 20μL have been employed for fermentation process development activities (Micheletti and Lye, 2006). Upstream process development is traditionally carried out at laboratory scales with typically 6-8 reactors with a volume of 1-30L being used per project. The use of MBRs allows for 24-48 reactors to be operated by a single researcher at any one time, thus reducing labour costs (Bareither and Pollard, 2011). Operating at the microscale has many other advantages such as reduced space requirements, reduced sterilisation and cleaning requirements, reduced set-up and shut-down times and the capability for automation (Schapper *et al.*, 2009; Bareither and Pollard, 2011). The high-throughput experimentation possible with MBRs enables the implementation of quality by design (QbD) approaches (Bareither and Pollard, 2011). A QbD approach involves designing quality into a product by the establishment of design space. A design space is defined by key and critical process parameters (KPPS and CPPs) and their acceptable ranges, indentified by process optimisation experiments (Rathore and Winkle, 2009). To indentify the parameters that have an impact on one or more critical quality attributes (CQAs), and the interactions between these parameters, a design of experiment (DoE) approach is commonly used (Islam *et al.*, 2007; Rathore and Winkle, 2009). MBRs have a range of applications including medium selection, strain optimisation by metabolic engineering or directed evolution, and bioprocessing of natural products as well as for process development (Betts and Baganz, 2006).

The main limitations of MBRs compared to laboratory or pilot scale reactors are the lack of instrumentation for process monitoring and control available, the reduced capacity for off-line sampling. This means at present generally there is a trade-off between data quality and quantity and experimental throughput (Betts and Baganz, 2006) (Figure 1.3.). Table 1.2 summarises the literature on the technical and performance specification for a range of miniature bioreactor systems currently available. Table 1.3 summarises the final cell densities (X_{final}) and maximum specific growth rate (μ_{max}) reported in the literature for microbial cultivations using microtitre plates or miniature STRs.
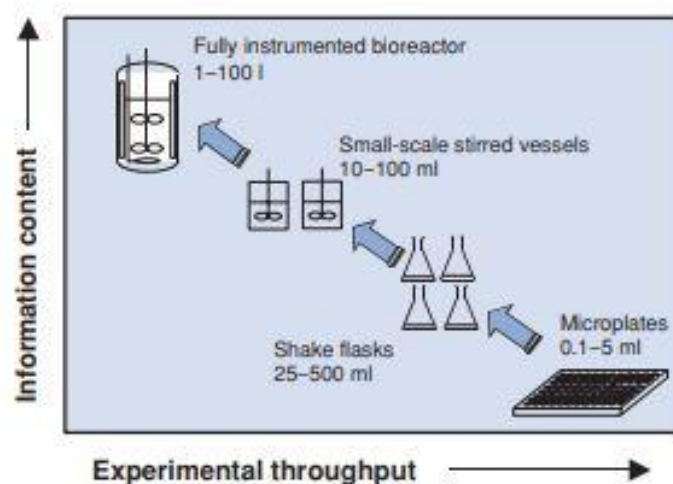
Figure 1.3. The trade-off between the volume of process information and experimental throughput with scale. Figure reproduced from Doig *et al*. (2006) .

1.5.1. Shaken miniature bioreactor systems

There are two main types of shaken miniature bioreactor systems: shake flasks and microtitre plates (MTPs). Shake flasks have a working volume range 10-500mL and varieties of different forms are available. Shake flasks are either made of glass or plastic and can be baffled or unbaffled. Shaking can be orbital or linear and culture temperature is maintained using a temperature-controlled cabinet. Factors that affect cultivation and the cell density achieved are fill volume, vessel size and geometry, the presence of baffles and their geometry, agitation speed and plug type used to seal the vessel (Betts and Baganz, 2006). The advantages of shake flasks are that they are inexpensive and easy to operate, however the lack of on-line monitoring of parameters such as pH and dissolved oxygen (DO) is a limitation. Instrumented shake flasks are now available and are designed to monitor and possibly control fermentation parameters online (Betts and Baganz, 2006).

Shake flasks rely on surface aeration and k_La values are in the range 150 h^{-1} to 277 h^{-1} , which are sufficient to support microbial growth, have been reported (Kato and Tanaka, 1998; Wittmann *et al.*, 2003). The presence of baffles can enhance the k_La, but at higher shaking speeds splashing can occur blocking the gas-permeable plug (Betts and Baganz, 2006).

Microtitre plates (MTPs) are available in a range of formats from 6-1,536 wells; 24, 48 and 96 are most commonly used for bioprocessing applications. The vessel geometry can either be square-shaped or cylindrical: square geometries can provide a high OTR however turbulence can cause splashing of cultures, whereas cylindrical geometries prevent splashing as well as

maintaining an adequate OTR. Online monitoring is achieved through non-invasive fluorescent technologies for monitoring DO and pH. This often lowers the cost of MTPs and micro-bioreactors as it allows for use of sensors as disposables and therefore the sensors do not contribute to the cost of the device itself (Chen *et al.*, 2009).

Mixing in MTPs is achieved via orbital shaking, and cultures are aerated by surface aeration, sparging or electrochemical gas production (Table 1.2.). A modified flask Reynolds number (Re_f) was defined by Büchs *et al.* (2000) (Equation 1.8), where d_f is the maximum inside flask diameter. Buchs *et al.* 2001 described a phenomenon unique to fluid flow in shaken bioreactors, and identified two flow regimes: 'in-phase' and 'out-of-phase'. The' in-phase' flow regime occurs when the majority of the liquid circulates around the vessel wall in synchronisation with the motion of the shaking platform. Fluid flow is 'out-of-phase' when only a small fraction of liquid moves along the vessel wall and the majority of the liquid remaining stationary on the base of the flask reducing mixing efficiency. A dimensionless number, the phase number (Ph) describes this phenomenon (Equation 1.9). The phase number can be calculated from Equation 1.9 where d_o is the shaker diameter, d_f is the inner diameter of the shaken vessel, V is the liquid volume and N is the shaking frequency. According to Buchs *et al* (2001) for operating conditions where $Ph<1.26$ fluid flow will be 'in-phase' and for $Ph<1.26$ fluid flow will be 'out-of phase.

There are several challenges of working in microtitre format: minimising evaporation rate while maintaining aeration and gaseous exchange rates, achieving parallel process control at small scale, and the implementation of feed strategies for fed-batch control.

$$Re_f = \frac{\rho N d_f}{\mu} \tag{1.8}$$

$$Ph = \frac{d_o}{d_f} \left\{ 1 + 3\log_{10}\left[\frac{\rho(2\pi N d_f{}^2)}{4\mu}\right]\left(1 - \sqrt{1 - \frac{4}{\pi}\left(\frac{V^{1/3}}{d_f}\right)^2}\right)^2 \right\} \tag{1.9}$$

1.5.2 Miniature stirred bioreactors

Miniature stirred bioreactors (MSBRs) are modelled on conventional lab-scale STRs. The working volume of a MSBR is typically between MTPs and shake flasks ranging from 8-250ml (Table 1.2.). MSBRs usually have one to three impellers; the use of turbine impellers, dual paddle impellers and a novel one-sided paddle have all been reported (Table 1.2.) (Puskeiler *et al.*, 2005; Betts, Doig and Baganz, 2006; Hortsch, Stratmann and Weuster-Botz, 2010). Agitation can also be achieved using a magnetic stirrer bar or gas-inducing impeller (Puskeiler, Kaufmann and Weuster-Botz, 2005; Klein, Schneider and Heinzle, 2013) MSBRs can achieve relatively high $k_L a$ values which are comparable to laboratory scale bioreactors; a $k_L a$ of $1600h^{-1}$ was reported by Puskeiler *et al*. (2005), however this was for a novel MSBR with a gas-inducing impeller. Aeration is achieved by direct sparging or surface aeration (Table1.2). The high oxygen transfer capabilities of MSBRs mean that the growth of organisms with high growth rate such as *E. coli* can be supported. Mixing times are relatively short in comparison to conventional STRs due to the high power input per unit volume (P_g/V). MSBRs have the potential for multiplexing of up to 48 MSBRs, and are compatible with automation platforms (Puskeiler and Weuster-Botz, 2005; Betts and Baganz, 2006; Bournazou *et al.*, 2017). Fed-batch operation and online-monitoring are also possible with MSBRs (Tables 1.2. and 1.3.).

Table 1.2. Summary of MBRs reported in the literature and their the technical and performance specification (table modified from Betts and Baganz (2006))

Device	Format	Volume (ml)	Agitation	Aeration	pH, DO and OD instrumentation	k_La (hr^{-1})	k_La measurement method	Multiplexing	Manufactured by / Reference
Fedbatch-Pro	Based upon shake flask	50-500	Orbital shaker	Surface	pH (sterilisable probe)	NR	N/A	16	Dasgip www.eppendorf.com
Micro-24	MTP	4-6	Orbital shaker	Gas sparging	pH and DO (optical probes)	32-57 (non-sparged)	Dynamic gassing out	24	Micro-24 MicroReactor (www.pall.com) (Isett *et al.*, 2007; Chen *et al.*, 2009)
SimCell	Microfluidic chip	0.3-0.7	Rotation of MBR chips	Surface via membrane	pH, DO and OD (at-line via cell-reading station)	Up to 500	CFD estimation	1500	Seahorse Bioprocessors (www.seahorsebio.com)
MBR array with parametric control	MTP	0.25	Orbital shaker	Electrochemical O$_2$ generation	pH (ISFET);OD (optically)	NR	N/A	8	(Maharbiz *et al.*, 2004)
SensorDish® reader	MTP	1	Orbital shaker	Surface	pH and DO (optical probes)	NR	NA	6-24	PreSens (www.presens.de) (Kocincova *et al.*, 2008)
BioLector® Basic	MTP	<1	Orbital shaker	Surface (headspace sparging)	pH, DO and OD (optical probes)	NR	NA	48	m2p Labs (www.m2p-labs.com) (R Huber *et al.*, 2009; Kensy *et al.*, 2009)

Device	Format	Volume (ml)	Agitation	Aeration	pH, DO and OD instrumentation	k_La (hr^{-1})	k_La measurement method	Multiplexing	Manufactured by / Reference
BioLector® Pro	MTP with microfluidic chip	<1	Orbital shaker	Surface (headspace sparging)	pH, DO and OD (optical probes)	NR	NA	32	m2p Labs (www.m2p-labs.com) (Buchenauer *et al.*, 2009; Funke *et al.*, 2010)
Micro-Matrix	MTP	1-5	Orbital shaking	Surface (headspace sparging)	pH and DO (optical probes)	3.2-204.9	Static gassing out	24	Applikon (www.applikon-bio.com) (Applikon, 2020)
Polymer MBR	STR	0.15	Magnetic stirrer bar	Surface via membrane	pH, DO and OD$_{600}$ (optical probes)	20-75	Dynamic gassing out	8	(Szita *et al.*, 2005; Zhang *et al.*, 2006)
Cuvette with magnetic stirrer	STR	2	Magnetic stirrer bar	Sparger	pH, DO and OD$_{600}$ (optical probes)	9.8-44.4	NR	NA	(Kostov *et al.*, 2001)
Stirrer-Pro Flask	STR	200-275	Magnetic stirrer bar	Sparger	pH and DO (sterilisable probe)	NR	NA	8	Dasgip (www.dasgip.com)
Xplorer	STR	Up to 100	Single turbine impeller	Sparger	pH, DO and OD probes	400	Dynamic gassing out	16	BioXplore (www.bioxplore.net) (Gill *et al.*, 2008a, 2008b)
Cellstation	STR	Up to 35	Dual paddle impeller	Sparger	pH, DO and OD$_{600}$ (optical probes)	NR	N/A	12	Fluorometrix (www.fluorometrix.com)

Device	Format	Volume (ml)	Agitation	Aeration	pH, DO and OD instrumentation	k_La (hr^{-1})	k_La measurement method	Multiplexing	Manufactured by / Reference
MSBR	STR	18	Triple Turbine Impeller	Sparger	pH, DO and OD$_{600}$ (optical probes)	Up to 480	Dynamic gassing-out	NR	(Betts and Baganz, 2006; Betts, Doig and Baganz, 2006)
Bioreactor Block	STR	8-12	Gas-inducing single impeller	Gas-inducing single Impeller	DO (optically); pH and OD$_{600}$ (plate reader)	700-1600	Dynamic gassing-out	48	(Puskeiler, Kaufmann and Weuster-Botz, 2005)
MTP with agitator	MTP	1	Single agitator	Sparger	DO, pH and OD$_{600}$ (optically)	2-26	Sulphite oxidation method	24	(Harms *et al.*, 2006)
Single microwell with agitator	STR	1	Single agitator	Sparger	DO, pH and OD$_{600}$ (optically)	68-300	Sulphite oxidation method	24	(Harms *et al.*, 2006)
MSBR	STR	8-12	Single one-sided paddle impeller	Surface aeration	pH and DO (optical probes)	Up to 540	Sulphite oxidation method	48	(Hortsch, Stratmann and Weuster-Botz, 2010)
MiniBio	STR	50-800	Triple turbine or marine impellers	Sparger	pH and DO probes	NR	NA	32	Applikon (www.applikon-bio.com)
ambr250[TM]	STR	100-250	Double Rushton turbine	Sparger	pH and DO probes	10-500	NA	24	TAP Biosystems (www.tapbiosystems.com) (Bareither *et al.*, 2013)

Device	Format	Volume (ml)	Agitation	Aeration	pH, DO and OD instrumentation	k_La (hr^{-1})	k_La measurement method	Multiplexing	Manufactured by / Reference
MSBR	STR	10	Magnetic stirrer bar	Sparger	DO (optically)	26.8-48.5	Determined during yeast cell cultivation	8	(Klein et al., 2013)
ambr® 15 fermentation	STR	10-15 (8-12 with gas bubbles)	Single Rushton-type impeller	Sparger	pH and DO	150-210	NR	48	(Velez-Suberbie *et al.*, 2018)

NA = not applicable, NR = not reported

Table 1.3. Summary of X_{final} and μ_{max} achieved in miniature bioreactors reported in the literature

Device	Format	Working volume (mL)	Strain	Q_{air} (vvm)	Agitation/shaking speed (rpm)	X_{final} (g L^{-1})	μ_{max} (h^{-1})	Reference
MTP with agitator	MTP	1	*E. coli*	NR	NR	NR	NR	(Harms *et al.*, 2006)
BioLector® Basic (www.m2p-labs.com)	MTP	0.8-1.0	*E. coli*	NA (surface aeration)	1400 (orbital shaking)	11-13 (*in situ* feeding)	NR	(R Huber *et al.*, 2009; Kensy *et al.*, 2009; Toeroek *et al.*, 2015)
BioLector® Pro (www.m2p-labs.com)	MTP with microfluidic chip	0.5	*E. coli*	NA (surface aeration)	800 (orbital shaking)	NR	NR	(Buchenauer *et al.*, 2009; Funke *et al.*, 2010)

Device	Format	Working volume (mL)	Strain	Q_{air} (vvm)	Agitation/shaking speed (rpm)	X_{final} (g L^{-1})	μ_{max} (h^{-1})	Reference
MBR array with parametric control	MTP	0.25	*E. coli*	NA (electrochemical oxygen generation up to 10 μmol/h reported)	175 (orbital shaking)	NR, 0.23* (without oxygen input) 0.39* (with oxygen input)	NR	(Maharbiz *et al.*, 2004)
MTP integrated with an automated liquid handling system	MTP	0.96	*E. coli*	NA (surface aeration)	1000	~7	NR	(Tan *et al.*, 2018)
Air-Well mini fermenter	MTP with an air sparging device	1	*E. coli*	200ms pulse width 5s pulse period	NA	~ 3	NR	(Deantonio *et al.*, 2014)
Micro-Matrix	MTP	2	*E. coli*	NR (headspace sparging)	NR	~ 34*.	NR	(Becker *et al.*, 2017)
MicroReactor (Micro-24 prototype)	MTP	6	*S. oneidensis*	NR	500 (orbital shaking)	NR, OD$_{600}$ = 1.31	0.20 (calculated from t$_d$)	(Tang *et al.*, 2006)
Micro-24 (www.Pall.com)	MTP	4-6	*E. coli*	NR	800 (orbital shaking)	~ 6.9*	0.82	(Isett *et al.*, 2007)
			P. pastoris	NR	800 (orbital shaking)	~20	NR	
Cuvette with magnetic stirrer	STR	2	*E. coli*	2	300	~2.7*	NR	(Kostov *et al.*, 2001)

Device	Format	Working volume (mL)	Strain	Q_{air} (vvm)	Agitation/shaking speed (rpm)	X_{final} (g L^{-1})	μ_{max} (h^{-1})	Reference
MSBR	STR	10	*S. tendae*	NA (surface aeration)	1200	~20	~0.20	(Hortsch *et al.*, 2010)
Xplorer BioXplore (**www.bioxplore.net**)	STR	100	*E. coli*	1	1000	3.8±0.05 (8.8 with improved aeration rates and oxygen enrichment)	0.68±0.01	(Gill *et al.*, 2008a)
Xplorer BioXplore (**www.bioxplore.net**)	STR	100	*B.subtilis*	1	1500	9.0±0.05	0.45±0.01	
MSBR	STR	10	*E. coli*	1	3000	3.5-4.0	0.44±0.03	(Betts *et al.*, 2006)
Bioreactor Block	STR	10	*E. coli*	1	2080	7.6 20.5 (fed-batch)	0.52	(Puskeiler *et al.*, 2005)
MSBR	STR	1	*E. coli*	NR	NR	NR	NR	(Harms *et al.*, 2006)
MSBR	STR	10	*S. pombe*	Magnetic stirrer disk	2000	~1.5 (chemostat)	NR	(Klein *et al.*, 2013)
MSBR	STR	58	Bioluminescent *E. coli*	Magnetic stirrer	NR	0.85*(chemostat)	$D = 0.28$	(Gu *et al.*, 1996)

Device	Format	Working volume (mL)	Strain	Q_{air} (vvm)	Agitation/shaking speed (rpm)	X_{final} (g L^{-1})	μ_{max} (h^{-1})	Reference
MSBR	STR	80	*B. anthracis*	1	700	OD$_{600}$ = 2.98 (non-aerated), 4.01 (aerated between 16h and 17h	NR	(Mukhopadhyay *et al.*, 2010)
ambr®15 single-use fermenter	STR	10	*E. coli*	1	710-2585 (DO control cascade)	37.3 ± 2.93	Run 1: 0.25 ± 0.004 h^{-1} Run 2: 0.23 ± 0.004 h^{-1}	(Velez-Suberbie *et al.*, 2018) (www.tapbiosystems.com)

NA = not applicable, NR = not reported, *D* = dilution rate

*Calculated from the OD$_{600}$s reported assuming one OD$_{600}$ unit corresponds to 0.3 g L^{-1} DCW (Soini, Ukkonen and Neubauer, 2008).

1.6. Scale-up of microbial cultures in STRs

The objective of scale-up of a laboratory or microscale fermentation process is to maintain the optimal environmental conditions, such as pH temperature and dissolved oxygen, to minimise the risk of batch failure at pilot or manufacturing scales (Diaz and Acevedo, 1999). 'Rules of thumb' are typically used as the basis for scale translation. Geometric similarity is required for scale-up by 'rules of thumbs'; an acceptable range of equivalency of a D_i:D_T of 0.3-0.45, a H_T:D_T of less of equal to 2, and either two or three impellers was defined, as exact geometric similarity is rarely achieved (Junker, 2004). Matched P_g/V, matched k_La or OTR, matched impeller tip speed U_{tip} (Equation 1.10) and matched Re_i and t_m are all used as bases for scale translation depending on the particular application (Junker, 2004). The situations where each 'rule of thumb' is typically applied and the possible impacts of scale-up are described in Table 1.4.

$$U_{tip} = \pi N D_i \hspace{8cm} \textbf{1.10}$$

Table 1.4. Examples of 'Rules of thumb' scale-up criteria (information from Junker, 2004 and Schmidt, 2005 unless otherwise stated).

Scale up criteria	Application of scale-up criteria	Possible impacts of scale-up using specified criteria
Matched impeller tip speed, U_{tip}	Used when the relationship between shear and morphology for mycelial cultures is not well characterised.	Reduction of Pg/V, which can negatively affect aeration efficiency, however the Pg/V can be improved by multiple impellers
Matched P_g/V	Used for scale-up of fermentation processes that require high energy inputs such as *E. coli* cultures.	t_m and U_{tip} increase, this can result in overestimating the motor size requirements.
Matched *OTR* or k_La	Frequently used for microbial fermentations. The low solubility of oxygen means maintaining oxygen transfer is of high importance. However, the k_La changes during a fermentation process, making it difficult to quantify.	P_g/V changes in proportion to k_La at equal v_s, therefore there can be an effect on t_m and U_{tip} (Najafpour, 2007)
Matched Re_i	Aeration is not included in the R_{ei}, so scale-up based on matched k_La is not successful for many fermentations	Increase in t_m and reduction in turbulence (Smith, Tavlarides and Placek, 1990)
Matched t_m	Used for fed-batch *E.coli* or yeast fermentations, to prevent the formation of nutrient and metabolite concentration gradients	Increase in shear forces (U_{tip}); this effect is greater at higher viscosities.

1.7. Fed-batch *E. coli* cultivation

1.7.1. High cell density *E. coli* cultivation

Cost-effective, high productivity *E. coli* fermentation processes can be achieved by performing high cell density culture (HCDC) processes. HCDC reduces the required culture volume, , reduces waste water and lowers production costs and capital investment (Lee, 1996; Shiloach and Fass, 2005). The absolute upper limit of attainable dry cell weight (DCW) is approximately 200 g L^{-1} for *E. coli* (Salehmin *et al*., 2013), and above a dry cell weight of 220 g L^{-1} culture fluidity is lost (Mori *et al.*, 1979; Lee, 1996). However, the practical upper limit of bioreactor operation is approximately 190 g L^{-1} as above this dry cell weight the cells form a paste; the high viscosity negatively impacts mixing and transport processes such as oxygen transfer, heat transfer and carbon dioxide transfer. Exponential growth becomes difficult to maintain once biomass concentration is above about 50 g L^{-1}, after which biomass concentration increases slowly due to oxygen mass transfer limitations (Salehmin, Annuar and Chisti, 2013).

Acetate is a product of *E. coli* metabolism, when carbon flux is greater than the biosynthetic demands and capacity for energy generation; this is phenomenon is known as overflow metabolism. It is generated when growth rate is above a threshold value and glucose is the carbon source. The threshold growth rate for acetate production in defined media for fed-batch processes is between $0.14h^{-1}$ and $0.17h^{-1}$ (Lee, 1996, Eiteman and Altman, 2006). The main cause of acetate production is saturation of the tricarboxylic acid cycle (TCA) cycle and electron transport chain. An acetate concentration of 0.3 g L^{-1} has been shown to inhibit *E. coli* cell growth, and a concentration of 2 g L^{-1} has been shown to inhibit recombinant protein expression (Meyer, Leist and Fiechter, 1984; Sun *et al.*, 1993). Acetate is produced at a much lower concentration when glycerol is used as the substrate due to the lower rate of transport into the cell, leading to a reduction in flux of carbon through glycolysis (Mccleary and Stock, 1994; Lee, 1996); however this results in a lower maximum specific growth rate (Lee, 1996). The formation of acetate can be reduced by both process and genetic modifications (Eiteman and Altman, 2006). A process can be modified to prevent acetate formation, by forcing cells to grow below the threshold specific growth rate for acetate production; this can be achieved by restricting the supply of glucose in fed-batch or continuous cultivation, or by lowering the culture temperature to 26 to 30^{0}C. The inhibitory effects of acetate can also be reduced by removal of the acetate formed during the fermentation by dialysis. An alternative strategy for reducing acetate production is by metabolic engineering of *E. coli* (Lee, 1996; Eiteman and Altman, 2006).

In fed–batch mode, substrate inhibition and acetate formation is reduced by gradually feeding a growth limiting substrate. There are four main feeding strategies:

- Constant rate feeding where nutrients are fed into the fermenter at a predetermined rate; the specific growth rate (μ) decreases due to the increase in cell culture volume and cell concentration.
- Stepwise feeding where a greater amount of nutrients are supplied at higher cell densities,
- Exponential-feeding where cells are grown at a constant specific growth rates. Exponential feeding is often applied to the pre-induction growth phase.
- Feeding controlled in response to parameters measured online such as pH and DO (Salehmin, Annuar and Chisti, 2013) .

Metabolic changes due to product formation usually decrease the glucose consumption capacity of the cells so the feed rate should be reduced to avoid glucose accumulation (Glazyrina *et al.*, 2010). The specific growth rate is maintained between $0.1h^{-1}$ and $0.3h^{-1}$ to avoid acetate formation. Dry cell weights of 128 g L^{-1} and 148 g L^{-1} have been achieved with glucose and glycerol feeding respectively (Lee, 1996).

The feeding rate during fed batch operations can be calculated using Equation 1.13. M_s is the mass flow rate of carbon source, t is the time, S_F is the substrate concentration in feeding solution, μ is the specific growth rate, $Y_{x/s}$ is the biomass yield on carbon substrate, m is the specific maintenance coefficient (g g(DCW)$^{-1}$ h^{-1}), X is the biomass concentration, V is the culture volume and t_0 is the time feeding was started in hours (Yee and Blanch, 1992; Lee, 1996)

$$M_s(t) = F(t)S_F(t) \qquad \qquad \textbf{1.11}$$

$$= \left(\frac{\mu}{Y_{x/s}} + m\right)X(t)V(t) \qquad \qquad \textbf{1.12}$$

$$= \left(\frac{\mu}{Y_{x/s}} + m\right)X(t_0)V(t_0)exp[\mu(t - t_0)] \qquad \qquad \textbf{1.13}$$

Feedback control schemes have also be developed to control substrate addition. There are two methods of feedback control: pH-stat and DO-stat (Mori *et al.*, 1979; Riesenberg *et al.*, 1991; Liew, Rajendran and Middelberg, 2010; Bang *et al.*, 2018). The pH stat method is more

suitable when semi-defined or complex media are used, as the change in DO is not as large as with minimal or defined media due to the cells utilising complex carbon-nitrogen substrates together with the primary carbohydrate source. The feeding rate can also be controlled based on online carbon evolution rate (CER), which is roughly proportional to the carbohydrate consumption rate (Lee, 1996).

1.7.2. Options for fed-batch operation for small scale bioreactors

The main objective of small scale fed-batch cultures is to achieve cell densities comparable to laboratory or pilot scale STR fed-batch cultures (Panula-Perala *et al.*, 2008). This is a challenge at small scale due to relatively few commercially available devices allowing for fed-batch and pH controlled fermentations, that have multiplexing capabilities and are inexpensive (Jeude *et al.*, 2006). In an attempt to operate in fed-batch mode at a small-scale two main strategies have been employed: (i) *in-situ* feeding via diffusion or enzymatic release and (ii) direct feeding via liquid additions.

1.7.2.1. In-situ fed-batch systems

Jeude *et al.* (2006) described an elastomer polymer disc system containing glucose that is gradually released into the culture. Cultures of *Hansenula polymorpha* expressing green fluorescent protein (GFP) were grown in shake flasks in both batch and fed-batch modes. Glucose release from the discs is proportional to the square root of time until the glucose is almost depleted. Equation 1.14 describes glucose release from the discs where M_{glc} is the mass of released glucose (g), A is the surface area of the disc, D is the diffusion coefficient (mm^2 s^{-1}), C_a is the amount of glucose per unit volume of matrix (mg mm^{-3}), C_s is the solubility of glucose per unit volume of matrix (mg mm^{-3}) and t is the time (s). Equation 1.14 is only valid if the remaining concentration in the polymer is above the solubility of glucose. Assuming all parameters are constant for a disc besides time *(t)* Equation 1.14 can be modified to give Equation 1.15, where z is the number of discs, $\dot{m}_{glc}$ is the mass stream of glucose (mg h$^{-0.5}$), to calculate the mass released from a disc. Velocity increases approximately linearly with disc thickness.

Using this approach, an 85% increase in biomass yield and 23.4 g L^{-1} dry cell weight was achieved, which corresponded to a yield of biomass on glucose comparable to a conventional STR of 0.38-0.47; the GFP yield also increased by a factor of thirty-five in comparison to batch cultures. This improvement in biomass and GFP yield was attributed to the reduction in overflow metabolism (Jeude *et al.*, 2006). A similar approach was used by Sanil *et al.* (2014),

who used magnesium hydroxide-loaded pH managing hydrogels (m-pHmH) for pH control, in combination with a glucose-releasing hydrogel for fed-batch *E. coli* cultures in shake flasks; a 394% increase in volumetric plasmid production was achieved (Sanil, Maralingannavar and Gadgil, 2014).

$$M_{glc} = A \cdot (2 \cdot D \cdot C_s \cdot C_a \cdot t)^{0.5} \qquad \qquad \textbf{1.14}$$

$$M_{glc} = z \cdot \dot{m}_{glc} \cdot t^{0.5} \qquad \qquad \textbf{1.15}$$

`

An alternative strategy described by Panula-Perala *et al.*, (2008) is the enzymatic release of glucose from a starch polymer immobilised in an agar storage gel. This approach is an advancement of the elastomer polymer disc method as it allows for the controlled release of glucose into the medium through enzymatic degradation of starch; the amount of glucoamylase added to the culture determines the glucose release rate (Panula-Perala *et al.*, 2008). High concentrations of starch would decrease oxygen transfer rate due to increased medium viscosity so a two-phase system was used; a gel as the starch reservoir and a liquid cultivation medium. The gel was optimised so that the diffusion of starch into the medium did not limit the enzymatic reaction and the gel could resist mechanical shaking. 10% w/w starch embedded into the gel provided enough glucose for a cell density of 30 g L^{-1} to be achieved in the liquid phase assuming all the starch available is processed and one gram glucose yields approximately 0.5g cell dry weight. Glucoamylase from *Aspergillus niger* (AG 300L) was used for the enzymatic release of glucose from starch. In 96-well plates an 8-to 10-fold increase in product yield was observed in comparison to medium without the starch reservoir due to the higher cell density and higher percentage of soluble protein.

A liquid phase cultivation systems is commercially available as, Enbase® EnPresso® B Growth System (Enpresso, Germany). A second cultivation system, Feed in Time (FIT) (m2p-labs, Germany), was also previously available but has recently been discontinued. Higher cell densities are achieved in gel format compared to liquid phase systems due to the greater substrate supply; however liquid phase systems are more convenient as direct centrifugation and removal of the cell pellet is possible and also they can be used at a larger scale. The EnBase® system has been shown to be compatible with *E coli* cultivation using a rocking-motion type bioreactor, which are not often used for microbial cultivations due to their lower oxygen transfer rate (Glazyrina *et al.*, 2010). Glazyrina *et al.*, (2010) achieved an OD$_{600}$ value of 30 (10 g L^{-1} dry cell weight) using the EnBase® system in a rocking-motion type bioreactor, compared to an

OD_{600} value of 3-4 in conventional batch mode, and an OD_{600} value of 60 (20 g L^{-1} dry cell weight) in fed-batch mode using an exponential glucose feeding regime and oxygen pulsing.

The scalability of the Enbase® technology from microscale to pilot scale was demonstrated by Glazyrina *et al.*, (2012) using an *E. coli* process for the production of recombinant alcohol dehydrogenase (ADH). Cultivations were performed in deep-well plates with a working volume of 3ml and in bioreactors at 2L and 60L scales. Cell growth and protein yield were shown to be comparable at all three scales. Glazyrina *et al.* (2012) also reported that EnBase® can be used as a starter culture for high cell density cultivations; an final OD_{600} value of 120 corresponding to approximately 40g L^{-1} DCW was achieved using EnBase® as an overnight starter culture followed by exponential glucose feeding ($\mu = 0.2h^{-1}$) (Glazyrina *et al.*, 2012).

1.7.2.2. Direct feeding methods

Direct feeding at small scale can be achieved by the manual or automated intermittent addition of substrates. This method of feeding has been demonstrated for mammalian cell culture where intermittent feeding occurs over a longer time period and less frequently in comparison to microbial cultures due to the lower growth rate. Silk *et al.* (2010) first described a method for fed-batch mammalian cell culture in 24 standard round-well (SRW) microtitre plates. CHO cells were fed via manual additions of bolus feed containing glucose and other nutrients and bicarbonate for pH control. Similar cell growth and antibody formation in 24-SRW plates (800μL) and 50mL shake flasks were achieved; the peak viable cell densities of 8 ± 0.5 x 10^6 and 9 ± 1.3 x 10^6 mL^{-1} respectively and the final titres were both approximately 1.5g L^{-1} at both scales (Silk *et al.*, 2010). Accurate liquid handling and contamination from repeated manual additions are challenges with intermittent feed additions without automation (Lye *et al.*, 2003; Silk *et al.*, 2010). The process described by Silk *et al.* (2010) can be used with standard shaking platforms and fully automated on robotic platforms.

Intermittent feeding at the microscale can also be achieved by pulsing feed directly into each well. This feeding strategy has been demonstrated with shake flasks and microbioreactors. Weuster-Botz, Altenbach-Rehm and Arnold, (2001) described a method for parallel feeding in shake flasks with pH control. Feeding was achieved using a syringe pump with a substrate reservoir via a substrate distribution system to individual miniature valves on each shake flask; volumes as small as 20μl could be added at a pump flow rate of 1mL min^{-1}. This system was demonstrated to be accurate with substrates of varying viscosities and was also used for pH control (Weuster-Botz, Altenbach-Rehm and Arnold, 2001). A commercially available microbioreactor system manufactured by Applikon® Biotechnology, the micro-Matrix, allows for intermittent feeding of 50nL or less per pulse using pressurised feed vessels; the feed

delivery to each well is controlled via microvalves (Applikon, 2018) This system is based on a 10ml 24-well square-well microtitre plate with a working volume of 1-7ml. Each well has individual gas supplies into the headspace and independent pH, DO and temperature control.

Most direct feeding strategies at microscale reported in the literature are intermittent or pulsating, however there are a few examples of continuous feeding. van Leeuwen *et al.* (2009) developed a Hagen-Poiseuille micropump that allows for a constant feed rate and is compatible with microtitre plates. The micropump works on the principle that by generating a pressure difference (0-1 bar) over a capillary tube with a defined internal diameter (20μm) and length (10-20cm), the desired flow rate, from zero to a few hundred nL min^{-1}, can be achieved. Manufacturing cost of the pump is low and parallelisation is simple (van Leeuwen et al., 2009). A miniature STR with an inbuilt capacity for pumped feed delivery, the ambr15$^{®}$f manufactured by Sartorius Stedim, has recently entered the market (Sartorius Stedim, no date). Velez-Suberbie *et al.* (2018) achieved an *E. coli* biomass concentation of approximately 37 g L^{-1} using this device, and demonstrated scalability to a 1L-scale laboroatory process using matched P_g/V.

A microfluidic chip was described by Funke *et al.*, (2010) that replaces the base of a conventional 48-well microtitre plate and allows controlled dosage of nanolitre liquid volumes from one well to another. This is the principle behind the commercially available system manufactured by m2p labs, the BioLector$^{®}$ Pro. The microfluidic device contains a micropump that allows for pH control and microscale fed-batch fermentations by a predetermined feeding profile and a controlled rate of highly concentrated feeding solution. Funke *et al.* (2010) demonstrated fed-batch *E. coli* fermentations performed using the microfluidic feeding device for glucose feeding and pH control. The glucose concentration in the media at the start of the fermentations was zero, and a 500 mg L^{-1} glucose feed dosed at a rate of 2μL h^{-1} was added at the start of the cultivation, resulting in a dosage of 500 mg h^{-1}. The authors reported that the pH could be sufficiently controlled to pH 7 ± 0.2 using this device, however biomass concentration was monitored by backscattering and the final off-line OD$_{600}$ measurements were not reported (Funke *et al.*, 2010).

1.8. Critical review of the literature

The current trend in upstream bioprocess development is towards high-throughput small scale experimentation using miniature bioreactors or microtitre plates (Section 1.5 and Tables 1.2 and 1.3). Operating at microscale is economically advantageous as it reduces labour and media costs and increases experimental throughput, which results in lower development costs. There are a number of commercially available devices with working volumes in the range 1-250mL that

allow researchers to perform up to 48 cultivations simultaneously (Table 1.2). However, at the present the majority of these devices cannot achieve the high cell densities comparable to a conventional bioreactor (Section 1.5, Table 1.4). There are two main challenges that need to be addressed to achieve high cell densities at the microscale: meeting oxygen demand and implementation of fed batch feeding strategies at suitable rates for microbial cultivation.

It has been demonstrated that oxygen transfer rates comparable to conventional bioreactors can be achieved at the microscale (Table 1.2). Aeration strategies used at microscale, are surface aeration or gas sparging either directly into the culture media or into the headspace. Agitation is achieved by shaking or stirring via one or multiple impellers. At present most examples of scale-up of microbial cultures from microscale are in batch mode, and there are far fewer examples of fed-batch cultures due to the difficulties with implementing feeding strategies. To date examples of fed-batch feeding strategies at the microscale are mainly *in-situ* strategies where there is no requirement for a physical delivery mechanism. However the disadvantages of *in-situ* feeding are the restricted control of glucose release rates, and the limited scalability. There are also a few examples of direct feeding using at the microscale using strategies such as a manual bolus additions, pulsing feeding using syringe pumps and constant additions using micropumps; however the majority of these haven't shown the delivery at rates likely to be required to match pilot scale fed batch operations.

1.9. Project aim and objectives

Given the need for industrially relevant feeding strategies at microscale to allow for high throughput bioprocess development, the aim of this project is to develop a scale-down fermentation platform suitable for the study and optimisation of high cell density cultures. The specific focus will be on implementing an industrially relevant fed-batch feeding strategy to a commercially available, 24-well, shaken microbioreactor, the Pall Micro-24 MicroReactor system (Pall, Port Washington). Studies will be performed based on the expression of a domain antibody produced in *E. coli*. The objectives of this work are:

1. To evaluate different options for introducing fed-batch operation with the microbioreactor including both *in situ* and direct feeding methods.
2. To establish an industrially relevant feeding strategy in the microbioreactor to enable *E. coli* cultures that are predictive of a laboratory scale fed-batch process in terms of cell growth and product expression.

3. To demonstrate the applicability of the new feeding system as a tool for high throughput fermentation process optimisation experiments.

4. To characterise the microbioreactor in terms of oxygen transfer capability and fluid mixing, to compare to the laboratory and pilot scale bioreactors.

5. To show that the optimised microbioreactor, fed-batch process is comparable to laboratory scale and pilot scale processes in terms of cell growth, product expression, and product quality.

1.10. Project background

This EngD project started in 2013, when the only commercially available microbioreactor systems were the ambr$^{®}$15 cell culture (miniature STR) and the Pall Micro-24 MicroReactor (shaken microtitre plate), neither of which have the capability of direct, continuous feeding. Therefore, the motivation for this project was that lack of options for performing industrially relevant fed-batch cultures at microscale. Since the start of this project there have been significant advancements in microbioreactor technologies, and there are now several devices that have an inbuilt feeding capacity as described in Section 1.7.2.2.

This project was completed in collaboration with GSK. The scope of the project was to develop a scale-down model of the GSK platform microbial fermentation process, for screening and development activities; therefore, evaluation of the microbioreactor as a scale-down model of other fed-batch processes was out of scope. In addition, due to intellectual property reasons, GSK were only able to provide one *E.coli* strain for development and evaluation of the microbioreactor feeding system.

Chapter 2. Materials and Methods

2.1. Glycerol stock preparation

A w3110 *E. coli* strain expressing a dAb was provided by GlaxoSmithKline (GSK) (Stevenage, UK). A master cell bank 20% v/v glycerol stock ($OD_{600} \sim 1$) was used to inoculate a 500mL total volume Ultra Yield^{TM} shake flask (Thomson Instrument Company, California, USA) containing 100mL of GSK in-house cell banking complex media. The media was sterilised by autoclaving at 121°C for 20 minutes. A stock solution of 15 mg mL^{-1} tetracycline in 70% ethanol was added to the flask at a concentration of 15μg mL^{-1}. The flasks were sealed with foam bungs or AirOtop™ Enhanced Seals (Thomson Instrument Company, California, USA). Two cell banks were prepared during the project; cell bank 1 was used for the fermentations described in Chapter 3, and cell bank 2 was used for the fermentations described in Chapters 4 and 5. The inoculation OD_{600} was ~0.05 for cell bank 1 and ~0.0002 for cell bank 2. The cultures were incubated in a Shaker X incubator (Kuhner, Switzerland) at 37^{0}C, 230 rpm for 4 hours (cell bank 1) or 6 hours (cell bank 2) to a final OD_{600} value of 1-2. The cultures were then cooled on ice and 80% w/v glycerol was added to a final concentration of 20% w/v glycerol. 1.1mL of culture was aliquoted into chilled labelled cryogenic sterile vials and stored at -80^{0}C.

2.2. Shake flask seed cultures

2.2.1. Micro-24 and 1L scale processes

100mL of the cell banking media was added to a 500mL Ultra Yield^{TM} shake flask. Tetracycline was added to a final concentration of 15 μg mL^{-1}, and GSK in-house antifoam was added to a final concentration of 500ppm. The flask was inoculated with a glycerol stock vial to an OD_{600} of 0.05. The flasks were sealed with foam bungs or AirOtop™ Enhanced Seals.The cultures were incubated in a Shaker X incubator at 37^{0}C, 230rpm for ~ 3 hours, then at 30^{0}C, 230rpm for ~ 3 hours to a final OD_{600} ~2-3. This method was used for the fermentations in Chapter 3. The shake flask cultures used for the fermentations in Chapters 4 and 5 were prepared as described above, with the exceptions that the Ultra Yield^{TM} Flasks were inoculated to an OD_{600} of 0.02. The shake flask cultures were grown 7-9 hours at 30°C, 120rpm to OD_{600} values of 2-3.

2.2.2. 50L scale process

500mL of the cell banking media was added to a 2.5L Ultra Yield^{TM} shake flask. Tetracycline was added at a concentration of 15µg mL^{-1}, and antifoam to a final concentration of 500ppm. The media was inoculated with a glycerol stock to an OD_{600} of 0.0000001. The flasks were sealed with AirOtop™ Enhanced Seals. The cultures were incubated in a Kuhner Shaker X incubator (Kuhner, Switzerland). The shake flask cultures were gown overnight for ~21.5 hours at 30°C, 100rpm to OD_{600}s of 2-3.

2.3. 1L scale batch and fed-batch fermentations

2.3.1. 1L vessel description

1L batch and fed-batch fermentations were performed using a DASGIP$^{®}$ Parallel Bioreactor System (Eppendorf, Germany). The DASGIP$^{®}$ system had eight 2.1L glass vessels with a 400mL to 1.5L working volume. The internal tank diameter was 0.094m, and the vessel had an aspect ratio h_t/D_t of 3.2. Each vessel was equipped with a direct overhead impeller drive. The impeller shaft was equipped with 3 Ruston turbines with a diameter of 0.046m, resulting in a D_i/D_t ratio of 0.49. The three Rushton turbines were positioned 0.019m, 0.075m and 0.131m from the base of the vessel. Each vessel was fitted with an L-sparger, cooling finger, OxyProbe or OxyProbeII (D = 0.012m) polarographic DO sensor (Broadley James, Bedford), a FermProbe (D = 0.012m) pH electrode (Broadley James, Bedford), condenser, a sampling port with valve, and 3 feed line ports for the acid, base and glycerol feed lines.

2.3.2. 1L scale batch and fed-batch fermentation processes

1L batch and fed-batch fermentations were performed using the DASGIP$^{®}$ system with 4-8 bioreactors run in parallel. Each bioreactor as filled with 1L of proprietary GSK complex media containing 70% w/v glycerol and yeast extract (Becton Dickinson, New Jersey, USA). The media was sterilised by autoclaving at 121°C for 20 minutes. Tetracycline was added at a concentration of 15µg mL^{-1}, and antifoam was added at a concentration of 500ppm. The bioreactors were inoculated with the seed cultures (Section 2.2.1) to an OD_{600} of 0.001 to 0.05. The temperature was controlled to 30^{0}C. The pH was controlled to pH 7.0 with 25% v/v NH_4OH and 35% v/v H3PO4. The DO was controlled to 30% or 40% using a control cascade; the first response was an increase in agitation speed (400-1200rpm), the second response was an increase in total gas flow rate (1-2vvm) and the third response was oxygen enrichment (21%-100%).

The fed-batch cultures were grown in batch mode for ~11-21 hours, depending on the inoculation OD_{600}. Feeding was triggered by a DO spike observed when the initial glycerol had been exhausted; the feeding was programmed to start when the DO had remained at ≥60% for a 5-minute period. The cultures were fed with GSK in-house 70% w/v glycerol feed solution containing yeast extract at 6 mL h^{-1} for ~6 hours until the OD_{600} was 70-90. The cultures were then induced with 0.22μm filter sterilised 100μM Isopropyl β-D-1-thiogalactopyranoside 100mM IPTG and the feed rate was reduced to 3.5 mL h^{-1}. The cells were harvested after a further 40-48 hours. 5-10mL samples were taken during the fermentation; at a minimum, samples were taken pre-induction and every 24-hours post-induction. Samples were taken for OD_{600} measurement, DCW determination, glycerol and acetate concentration analysis, and dAb titre analysis as described in Sections 2.10.1, 2.10.4 and 2.10.7.

The induced batch cultures were inoculated to an OD_{600} 0.05 grown for ~ 5 hours until the OD_{600} was ~ 1. The cultures were then induced with 100μM IPTG and grown for a further 45 hours. 5-10mL samples were taken at a minimum pre-induction (5 hours), and twice daily post-induction. The non-induced batch cultures were inoculated to an OD_{600} of 0.05, and grown for ~21 hours until the OD_{600} was ~60. 5-10mL samples were taken at the end of batch only.

At harvest the cultures were cooled to ≤10^{0}C, whilst maintaining the DO ≥30%. 24 2mL aliquots were taken from each vessel and were centrifuged using an 5415D Centrifuge (Eppendorf, Germany). The supernatant of the 24 Eppendorf tubes was pooled and stored at -20^{0}C for purification by Protein A chromatography for product quality analysis by size exclusion chromatography – high performance liquid chromatography (SEC-HPLC) (Sections 2.10.6)

2.4. Micro-24 System description

The Micro-24 System (Pall, Port Washington) consists of 24 miniature bioreactors in deep well microtitre plate format with a total volume of 10mL and a working volume of 3-7mL. Each well is equipped with a heating element for temperature control, a thermocouple for temperature monitoring and fluorescent sensor spots that allow for optical monitoring of pH and DO. The microtitre plates are made of polycarbonate, irradiated by e-beam and are clamped to a base plate via a vacuum seal; the shaking speed of the base plate can be adjusted between 0 to 800rpm. DO and pH control is achieved via gas injection through a 0.2μm hydrophobic sparge membrane. Typically, for aerobic microbial cultures, oxygen is used for DO control, and either dilute ammonia gas alone or with a carbon dioxide source is used for pH control. There are three cassette designs available: REG, PRC and BFL. For the REG and BFL cassette

designs, gas is injected through a membrane on the base of the well directly into the liquid phase, whereas for the PRC cassette design the gas is injected up a central sparge tube and into the headspace (Figure 2.1). The BFL plate design also has a single baffle. There are three types of well closure: Type A closures that are single use and have a neoprene check valve and sterile membrane barrier; Type D closures that are also single-use but only have a sterile membrane barrier; Type E closures that are autoclavable and have a stainless steel check valve but no sterile membrane. For microbial applications Type D closures are typically used. The Micro-24 system has previously described by a range of authors (Isett *et al.*, 2007; Chen *et al.*, 2009; Betts *et al.*, 2014).
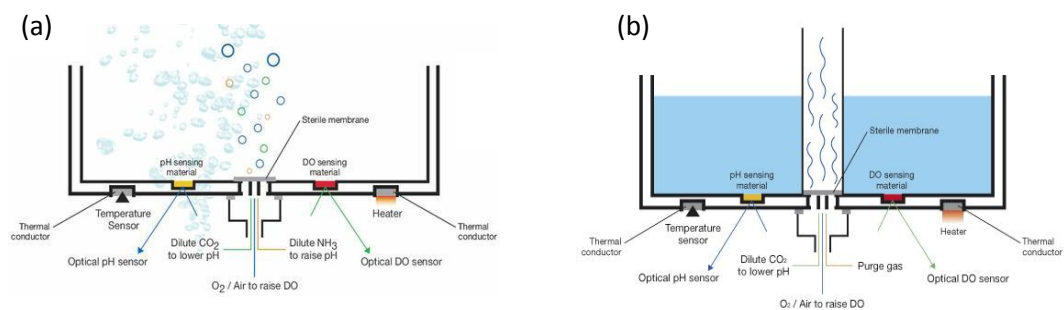
Figure 2.1. Micro-24 cassette configuration. (a) REG cassette and (b) PRC cassette (Figure reproduced from Pall Corporation, (2012))

2.5. Micro-24 fed-batch cultures by *in situ* feeding

The EnPresso® B growth system (Enpresso, Germany) was used for the *in situ* Micro-24 fed-batch cultures. EnPresso® B is designed to increase cell growth and recombinant protein expression in microbial cultures. It utilises the proprietary EnBase® technology for the controlled release of glucose from a polysaccharide substrate.

2.5.1. Glucose release kinetics of the EnPresso® B growth system in shake flasks and the Micro-24

The manufacturers protocol for the EnPresso® B growth system was used for the shake flask incubations. 100ml of sterile water was added to seven 500mL Ultra Yield™ shake flask (Thomson Instrument Company, California). 4 EnPresso® B tablets containing the polysaccharide substrate, organic nitrogen for pH control, minerals, vitamins and trace elements, tetracycline ($15\mu g$ mL^{-1} final concentration) and antifoam (500ppm final concentration) were added to each flask. Glucoamylase was then added to 6 of the flasks to a final concentration of either 1.5, 3 or 6 U h^{-1}. Each glucoamylase concentration was run in

duplicate, and an additional flask was used as a negative control (no glucoamylase addition). The flasks were incubated for 24 hours at 30°C, 250rpm. 1mL samples were taken during the incubation for glucose concentration analysis using a Cedex Bio Analyzer (Section 2.10.7.1). The 24-hour incubation was staggered over two runs. Samples were taken at 2, 4, 6, 8, 10,5, 17.5, 19, 21, and 24 hours. For the Micro-24 incubations, 200ml of sterile water was added to a 500mL Ultra Yield flask. 2 Enpresso® tablets, tetracycline (15μg/mL final concentration) and antifoam (500ppm final concentration) were added to each flask. The flask was then incubated at 37°C, 230rpm until the tablets had completely dissolved. The contents of the flask were then divided into 30mL aliquots. Glucoamylase was then added to each aliquot to a final concentration of either 0, 1.5, 6 or 18 or 30 U h^{-1}. 5mL of each 30mL aliquot was added to 5 wells of a Micro-24 REG plate, except for the 0 U h^{-1} concentration which was added to 4 wells. The plate was incubated at 30°C, 800rpm for 76 hours. Duplicate samples were taken at 3, 17, 25, 41, 44, 48 and 66 hours and analysed on the Cedex Bio Analyzer for glucose concentration (Section 2.10.7.1).

2.5.2. Micro-24 non-induced and induced fed-batch cultures by *in situ* feeding

The protocol enclosed with the EnPresso® B growth system was used for the Micro-24 fed-batch cultures. 100ml of sterile water was added to two 500mL Ultra Yield™ flasks. 4 EnPresso® B tablets, tetracycline and antifoam were added to the flask. The flasks were then incubated at 37°C, 230rpm until the tablets had completely dissolved. 3mL of media from one of the flasks was added to each well of a REG cassette. The second flask was then inoculated with the seed culture (Section 2.2.1.) to an OD_{600} of 0.05. The content of the inoculated flask was divided into 20mL aliquots. Glucoamylase was then added to each aliquot to a final concentration of either 0, 24, 72 or 120 U L^{-1}. 1mL of each aliquot was then added to 5 wells of a Micro-24 REG plate to give final glucoamylase concentrations of 0, 6, 18 and 30 U L^{-1}. 4 wells containing the proprietary GSK complex media containing 70% w/v glycerol were also run as controls. The plate was incubated at 30°C, 800rpm for 39 hours. The DO was controlled to 30% by direct sparging of 100% oxygen, and the pH was controlled to pH 7 by direct sparging with 15% ammonia and 100% carbon dioxide). Samples were taken at 14, 18, 22 and 39 hours.

The same method as described above was used for the induced cultures, with the exception that a glucoamylase concentration of 18 U L^{-1} was used for all 24 wells. The plate was incubated at 30°C, 800rpm for ~14 hours. At 14 hours 400μL of EnPresso® B booster solution containing 0 U L^{-1} 15 U L^{-1}, 60 U L^{-1} or 180 U L^{-1} of glucoamylase (final concentration of 0 U L^{-1} 1.5 U L^{-1}, 6 U L^{-1} or 18 U L^{-1}), and 1mM IPTG (final concentration of 100μM) were added to the cultures. Eight samples were taken at 14 hours (induction), and duplicate samples were taken at 22 hours

and 38 hours (harvest). Samples were taken for OD_{600} measurement, DCW determination, glucose and acetate concentration analysis, and dAb titre analysis (induced cultures) as described in Sections 2.10.1, 2.10.4 and 2.10.7.

2.6. Micro-24 fed-batch cultures by direct feeding

2.6.1. Bespoke Micro-24 feed delivery system development

2.6.1.1. Micro-24 feeding device design and fabrication

During the course of this research a feeding device was developed to enable the direct connection of parallel feed lines to the Micro-24 cassette as described in Chapter 3. The development process involved five iterations of the device (Table 2.1, Figures 3.13 and 3.15). Version 1 or the device was designed and fabricated by the Biopharmaceutical Research (BPR) department, GSK Stevenage, Versions 2-4 by the UCL Design and Fabrication Facility, and Version 5 by 3D Printing, Platform Technology and Science PTS 3D-printing facility, GSK, Stevenage. Table 2.1 describes each version of the device. The final version of the feeding device (Version 5) was designed using SpaceClaim 3D Modelling Software (Anasys, Massachusetts, USA) for the computer assisted design (CAD) drawing and the device was printed out of VeroWhitePlus^{TM} (RGD835) and VeroBlackPlus^{TM} (RGD835) (Stratasys, Minnesota, USA) using a Stratasys Connex 500 3D-Printer (Stratasys, Minnesota, USA).

2.6.1.2. Micro-24 feeding system set up

An AL-1200 12-channel syringe pump (World Precision Instruments, Florida) was used for feed delivery. 12 3mL hypodermic Plastipak™ Luer-Lock syringes (Becton Dickinson, New Jersey, USA) were filled with 3mL of GSK glycerol feed, either 70% or 23% glycerol, containing yeast extract. The syringes were then connected to the feed line tubing via luer-lock connectors. A range of tubing and connectors were tested to during the development of the feeding system (Table 2.2). A hypodermic needle was then attached to the other end of the tubing via luer-lock connectors; 21 gauge 1.5 inch, 18 gauge 1 inch, and 20 gauge 1 inch (Becton Dickinson, New Jersey, USA or Henke-Sass, Wolf, Germany) were tested. 0.5mL of feed was dispensed manually to prime the feed lines up to the needles. The needles were then pushed through the Micro-24 caps and the primed feed lines were then clamped to the Micro-24 cassette using the bespoke feeding device (Section 2.6.1.1). The syringes were then fitted into the syringe pump. The final feeding system comprised of Upchurch Scientific Tefzel$^{®}$ Ethylene tetrafluoroethylene

(ETFE) HPLC tubing (IDEX Corporation, Illinois, USA), Upchurch Scientific luer connectors, and 20G 1 inch needles (Table 2.1).

The Micro-24 lid could not accommodate the feeding device, so an inverted plastic box was used to maintain the environment temperature; this was used for Versions 1-5 of the feeding system. A 3D-printed bespoke lid was subsequently developed (Figures 3.16 c and d) and used with the final version of the feeding system. A stand was also developed to hold the feeding device containing the Micro-24 caps and needles during sampling (Figures 3.16a and b). The stand was composed of two separate 3D-printed pieces attached together with 6 hexagonal nickel-plated brass spacers. The lid and sampling stand were designed and fabricated as described above (Section 2.6.1.1.).

2.6.1.3. Syringe pump validation

A calibration curve of actual flow rate against the flow rate set on the syringe pump was generated for flow rates of 0 -100 μL h^{-1}. At each flow rate twelve syringes were filled with either water, a feed solution containing 70% glycerol (w/v) or a feed solution containing 23% glycerol (w/v). The feed lines were assembled and primed as described in Section 2.6.1.2. Each needle was inserted into the cap of a pre-weighed Eppendorf tube (Eppendorf, Germany). The syringe pump was run for 0.5-2 hours at the required flow rate, and the Eppendorf tube was then re-weighed to determine the volume added. This procedure was repeated three times. This syringe pump was validated using water and the 70% glycerol solution using 18G 1" needles, and with the 23% glycerol feed solution using both 18 gauge 1 inch and 20 gauge 1 inch needles.

2.6.1.4. Feed drop size approximation

The drop size was determined for two needle sizes (18 gauge 1 inch and 20 gauge 1 inch) using both the 70% and 23% glycerol feed solutions. Drop formation at a flow rate of 120 μL h^{-1} was videoed and the volume of the drop was approximated by the time taken for the drop to fall of the end of the needle.

2.6.1.5. Micro-24 feeding system sterility validation

The feeding system was assembled as described in Section (2.6.1.2), using Version 4 of the feeding device (Section 2.6.1.1., Table 2.1). The syringe pump was programmed to deliver 540μL at a flow rate of 20μL/h (total time of 27 hours). The Micro-24 was run at 800rpm with a temperature set point of 37°C, and without DO or pH control. The change in DO over the 27-

hour period was monitored. After 20 hours, the OD_{600} was measured to determine if any cell growth had occurred (Section 2.10.1).

2.6.2. Initial fed-batch cultures

4mL of proprietary GSK complex media containing yeast extract (Becton Dickinson, New Jersey) and glycerol was added to each well of a REG cassette, and tetracycline (15mg L^{-1} final concentration) and antifoam (500ppm final concentration). The media in the plate was inoculated with the seed cultures (Section 2.2.1.) to give a final inoculation OD_{600} of 0.05. The cultures were gown for ~14 hours to an OD_{600} of 40-60. The DO, pH and temperature were controlled to 30%, pH7 and 30^0C respectively as described in Section 2.5.2. At 14 hours, a 70% w/v glycerol feed solution containing yeast extract was added at a flow rate of 24µL h^{-1} to 6-12 wells for 6 hours using the syringe pump, and an additional 6-12 wells were run as non-fed controls. The feeding system was assembled as described in Section 2.6.1.2. At ~21 hours the cultures were induced with 100µM IPTG and the feed rate was reduced to a flow rate of 14µL h^{-1}. The cultures were harvested at 65-69 hours. 0.5 mL L^{-1} of antifoam was added manually at induction and then every 24 hours to prevent excessive foaming. Samples were taken at end-of-batch (EOB) and at harvest for OD_{600} measurement, DCW determination, glycerol and acetate concentration analysis, and dAb titre analysis as described in Sections 2.10.1, 2.10.4 and 2.10.7.

Table 2.1. Overview of the development of the Micro-24 parallel feeding device.

Device version	Description	Material of construction	Fabrication method	Compatible connectors	Sterilisation method
1	Single plate device with two holes per well to accommodate the Micro-24 caps and feed line needles (refer to Chapter 3 Figures 3.13a and b).	Aluminium	Milling	Any luer-lock connectors	Autoclaving or 70/30 Ethanol
2	Three-plate device: Two plates to accommodate the Micro-24 lines and feed line needles and connecters. Top plate to clamp the feed lines to the bottom plates (refer to Chapter 3 Figures 3.13c, d and e).	Aluminium, stainless steel screws	Milling	Male luer lock with lock ring with 1/16" hose barb	Autoclaving or 70/30 Ethanol
3	Two-plate device: Two plates to accommodate the Micro-24 lines and feed line needles and connecters). Two clamps that each clamp 12 feed lines to the plates	Acrylic, stainless steel screws	Milling	Male luer lock with lock ring with 1/16" hose barb	70/30 Ethanol
4	Two-plate system: Two plates to accommodate the Micro-24 lines and feed line needles and connecters. Two clamps; each clamp 12 feed lines to the plates (refer to Chapter 3 Figures 3.13f and g, Appendix B, Figures B.1-B.4.).	Polytetrafluoroethylene (PTFE), stainless steel screws	Milling	Male luer lock with lock ring with 1/16" hose barb P-677 adapter, male Luer to female M6 flat-bottom (Upchurch Scientific). The device could only accommodate 12 feed lines using these connectors.	Autoclaving or 70/ 30 ethanol
5	One-plate device: One double-layered plate to accommodate the Micro-24 lines and feed line needles and connecters. Two clamps; each clamp 12 feed lines to the plate (refer to Chapter 3 Figure 3.15, Appendix B, Figures B.5-B.7)	VeroWhitePlus^{TM} (RGD835), stainless steel screws	3D-printing	P-677 adapter, male Luer to female M6 flat-bottom (Upchurch Scientific)	70/30 Ethanol

Table 2.2. Tubing and connectors used with the different versions of the parallel feeding device.

Tubing type	ID (in)	OD	Wall thickness	Connectors	Versions of feeding system
Platinum-cured silicon (Cole-Parmer)	1/16 (1.6mm)	1.8 (3.2mm)	1/32 (0.8mm)	Luer to barb connectors for 1/16" tubing (Cole-Parmer) secured with cable ties	1,2
C-Flex® tubing	1/16 (1.6mm)	1.8 (3.2mm)	1/32 (0.8mm)	Luer to barb connectors for 1/16" tubing (Cole-Parmer) secured with cable ties	3, 4
Upchurch Scientific, Tefzel® HPLC tubing (ETFE)	0.040" (1.02mm)	1/16 (1.6mm)	0.011" (0.29mm)	P-200Nx, flangeless ferrule, P-207, flangeless nut, standard knurl, M6 flat-bottom port, P-680 adapter, female Luer to female M6 flat-bottom, P-677 adapter, male Luer to female M6 flat-bottom (Upchurch Scientific)	4, 5

2.6.3. Micro-24 feeding strategy optimisation

2.6.3.1. Implementation of a post-induction feed rate equivalent to the 1L scale process (per gram of biomass)

The method described in Section 2.6.2 with modifications to the inoculation technique, the feed concentration, yeast extract supplier, post-induction feed rate and antifoam concentration, was used for these cultures. Prior to inoculation, the seed culture was diluted to an OD_{600} of 0.2 in 500mL of proprietary GSK complex media containing tetracycline (15mg L^{-1} final concentration) and antifoam (500ppm final concentration). A REG cassette was filled with 3mL of GSK complex media containing glycerol and yeast extract (Sigma Aldrich, Missouri, USA), tetracycline (15 µg mL^{-1}) and antifoam (800ppm final concentration). 1mL of the diluted seed culture was then added to the REG cassette to give a final inoculation OD_{600} of 0.05. A 23% w/v glycerol feed solution containing yeast extract (Sigma Aldrich, Missouri) was used instead of the 70% w/v glycerol solution, and 1mL of culture broth was removed prior to feeding. The pre-induction feed rate was 58 µL h^{-1}, and the post-induction feed rate was 26 µL h^{-1}.

2.6.3.2. Micro-24 batch cultures for metabolite analysis

Micro-24 batch cultures were performed as described in Section 2.6.2, with the exception that the cultures were not fed and were harvested at 21-24 hours. 4-8 wells were sacrificed at each time point for OD_{600} measurement, DCW determination, glycerol and acetate concentration analysis as described in Sections 2.10.1 and 2.10.7.

2.6.3.3. Fed-batch cultures with a pre-feeding hold period and higher DO set point

The same method as described in Section 2.6.3.1. was used for these fed-batch cultures, with the exception that the DO set point was increased to 60%, and a pre-feeding hold period of 3 or 5 hours was implemented to allow for acetate consumption.

2.6.3.4. Implementation of a pre-induction feed rates equivalent to the 1L scale process per gram of biomass

The same method as described in Section 2.6.3.3. was used for these fed-batch cultures, with the exception that a pre-induction feed rate 43 µL h^{-1} was implemented.

2.6.3.5. Measurement of Micro-24 evaporation rate

A dye-based method was used to determine the evaporation rate. The change in absorbance of an Erioglaucine disodium salt solution was measured over time. A calibration curve of absorbance at 625nm against concentration was generated for Erioglaucine disodium salt

concentrations in the range of 1μM-8μM as the corresponding A_{625} values for this concentration range were within the linear range of the spectrophotometer. A concentration of 1μM was determined to be a suitable to be used as the start concentration of the experiment (A_{625} = 0.110±0.004). A design of experiment (DoE) approach was used determine the evaporation rate from a REG cassette under microbial operating conditions. Table 2.3 describes the factors and the experimental ranges studied. A 3-factor-2-level, face-centered, central composite design (fcCCD) with six centre points was used for this experiment (Islam *et al.*, 2007). The experiment method as described in Section 2.6.3.1. All experiments were run at 800rpm. The DoE design was run in duplicate. The DoE response models were generated using JMP$^{®}$ 13 software (SAS Institute, North Carolina).

Table 2.3. Evaporation rate experiment factors and ranges

Factor	Low value (-1)	Centre point (0)	High value (+1)
Fill volume (mL)	3	4	5
Temperature (°C)	28	30	32
Total gas flow rate (mL min^{-1})	0	7.5	15

2.7. Micro-24 and 1L scale fed-batch fermentation process optimisation DoE

A 2-factor, 2-level full factorial design was used for the Micro-24 and 1L scale fermentation process optimisation experiments as described in Table 2.4 (Islam *et al.*, 2007). 4-6 replicates of each factor combination were run in the Micro-24; two separated runs were performed, one at a post-induction temperature of 30^{0}C and one at 25^{0}C. At 1L scale each factor combination was run in duplicate. The DoE response models were generated using JMP® 13 software. The Micro-24 and 1L scale processes were performed as described in Sections 2.3. and 2.6.3.4, with the exception that at a post-induction temperature of 25^{0}C the post-induction feed rate was reduced to 22 μL L^{-1} h^{-1} and 2.6 mL h^{-1} respectively.

Table 2.4. Micro-24 and 1L scale process optimisation DoE factors and ranges

Factor	Low value (-1)	High value (+1)
IPTG concentration (μM)	100	250
Post-induction temperature (°C)	25	30

2.8. Micro-24 engineering characterisation

2.8.1. Determination of the oxygen mass transfer coefficient (k_La)

The static gassing-out method as described by Betts *et al*. (2014) was used to determine k_La values with water and GSK complex media containing 70% w/v glycerol. A single well containing the required volume of deionised water or complex media was sparged with nitrogen until the DO reached 0% saturation. The nitrogen was then turned off and the well was sparged with air at the required flow rate and the change in DO concentration with time was monitored. K_La values were determined for REG and PRC and BFL cassette designs. For the REG cassette experiments with complex media antifoam was added to a final concentration of 500ppm. A Design of Experiment (DoE) approach was used to determine how k_La values varied with operating conditions. A 3 factor-2 level face centred central composite design with 6 centre points was used (Islam et al., 2007). The factors studied were agitation speed, air flow rate and fill volume (Table 2.5). The DoE response models were generated using JMP® 13 software. All experiments were performed at 30°C.

Table 2.5. Micro-24 k_La characterisation DoE factors and ranges

Factor	Low value (-1)	Centre point (0)	High value (+1)
Fill volume (mL)	3 (4 for BFL)	5.5 (4.5 for BFL)	7 (5 for BFL)
Agitation speed (rpm)	500	650	800
Total gas flow rate (mL min^{-1})	0.1	10.05	20

2.8.2. Liquid phase mixing time (t_m)

Mixing times (t_m) of the REG and PRC cassettes were measured using the iodine decolourisation method (Carreau, Patterson and Yap, 1976; Takahashi *et al*., 1985; Betts *et al*., 2014). The required volume of 5 mM iodine solution was added to a single well of a PRC or REG cassette. Sodium thiosulphate solution (1.8 M) was then added to the iodine solution; an equivalent ratio of 1.4 was used as described by Carreau et al. (1976). Bespoke cassette mimics were used for these experiments that consisted of a single well with a Perspex® box constructed around it. The Perspex® box was filled with glycerol to prevent image distortion. For all experiments shaking was started before sodium thiosulphate addition Sodium thiosulphate was added at a position of ~1cm above the liquid surface. Fluid flow was visualised using a DVR Fastcam (Photron, California, USA). The camera was set to record at

125 frames per second with a shutter speed of 1/frame rate and with normal gain. A resolution of 640 x 480 pixels was used for all experiments.

A DoE approach was used to determine how mixing time values varied with operating conditions; the DoE design was a 2 factor-2 level face centred central composite design with 6 centre points (Islam et al., 2007). The factors studied were agitation speed and fill volume; the factor ranges were the same as for the k_La characterisation (Table 2.6). All experiments were performed under non-aerated conditions at 30°C. The DoE response models were generated using JMP® 13 software. Additional experiments outside the DoE design were performed at 2mL and 3mL fill volumes for both cassette designs.

Table 2.6. Micro-24 liquid phase mixing time (t_m) determination DoE factors and ranges

Factor	Low value (-1)	Centre point (0)	High value (+1)
Fill volume (mL)	3	5.5	7
Agitation speed (rpm)	500	650	800

2.9. 50L fed-batch fermentations

2.9.1. 50L vessel description

50L batch and fed-batch fermentations were performed using a 75L Chemap fermenter with a 50L working volume (Infolabel AG, Switzerland). The internal tank diameter was 0.316m, and the vessel had an aspect ratio H_t/D_t of 3.2. The vessel was equipped with a bottom-driven impeller drive. The impeller shaft was equipped with 3 equally spaced Ruston turbines with a diameter of 0.110m, resulting in a D_i/D_t ratio of 0.35. The vessel was fitted with an L-sparger, VisiFerm DO (D = 0.012) optical DO sensor (Hamilton, Nevada), an InPro3100i (D = 0.012m) pH electrode (Mettler Toledo, Switzerland), cooling jacket, condenser, a sampling port and 3 feed line ports for the acid, base and glycerol feed lines. The vessel had four 0.025m x 0.770m diametrically opposed baffles.

2.9.2. 50L fed-batch fermentation process

The 75L Chemap system was filled with 50L of complex media containing 70% w/v glycerol and yeast extract (Sigma Aldrich, Missouri, USA). The vessel was inoculated to an OD_{600} of ~0.001. The DO was controlled to 40% using a control cascade; the first response was an increase in agitation speed (350 to 900 rpm), the second response was an increase in total gas

flow rate (0.7-1.2vvm) and the third response was oxygen enrichment (21%-34%). The pH was controlled to pH7 using 35% w/v phosphoric acid and 25% w/v ammonium hydroxide, and the temperature was controlled to 30^0C. The vessel was maintained at a 0.2bar overpressure. The cells were grown in batch mode for ~22 hours. Feeding was triggered when DO spiked to 70%, due to exhaustion of the glycerol, and remained at ≥70% for 5 minutes. The cultures were fed with the proprietary GSK 70% w/v glycerol feed containing yeast extract (Sigma Aldrich, Missouri) at a flow rate of 330 g h^{-1} for ~6 hours. The cultures were then induced with 100μM IPTG and the feed rate was reduced to 192.5 g h^{-1} manually.

Samples were taken pre-induction (28 hours), 42 hours, 49 hours, and at harvest (68 hours). Samples were taken for OD_{600} measurement, DCW determination, glycerol and acetate concentration analysis, and dAb titre analysis as described in Sections 2.10.1, 2.10.4 and 2.10.7. Two 900mL aliquots were harvested. One aliquot was centrifuged with Polyethylenimine (PEI) and the other without PEI; 38mL of 9.5% PEI (pH 7) was added and left at room temperature for 15 minutes. The aliquots were then centrifuged using an Avanti-J26 Centrifuge Harvest with a J 8.1000 Centrifuge rotor (Beckman Coulter, USA) at 7000rpm for 60 minutes. The supernatant was stored at -20^0C for Protein-A chromatography for product quality analysis by SEC-HPLC (Section 2.10.6) and the pellets were discarded.

2.10. Analytical methods

2.10.1. OD_{600} measurement and cell weight determination

Cell dry weights were determined by aliquoting 1ml of culture broth into pre-weighed 2ml microfuge tubes and then centrifuging at 13000rpm for 20 minutes. The supernatant was removed, and the microfuge tubes were centrifuged for a further 5 minutes at 13000rpm. Any remaining supernatant was then removed and the microfuge tubes were re-weighed using a 770 Balance (Kern & Sohn GmbH, Germany), to determine cell wet weight per ml of culture broth. The pellets were then incubated at 105^0C in an OBT4 heating block (Grant Instruments, Royston) for 24-48 hours and reweighed to determine the cell dry weight per mL of culture broth. The optical density was measured at 600nm using a Ultraspec 4330 pro spectrophotometer (Amersham, Buckinghamshire). Samples were diluted with phosphate buffered saline (PBS), pH7.2, as appropriate so the measured OD_{600} was in the linear range of the spectrophotometer.

2.10.2. Cell lysate preparation

1ml of culture broth was centrifuged using a 5415D Centrifuge (Eppendorf, Germany) in a 2mL microfuge tube at 13000rpm for 20 minutes. The supernatant was removed and transferred to

another microfuge tube and stored at -20°C. The pellet was resuspended in 1ml of 10 mM Tris-HCl pH 7.5, and was then subjected to three freeze-thaw cycles; the pellet was frozen at -80°C and then thawed at 40°C in a Sub6 water bath (Grant Instruments, Royston). The resuspended pellets were then sonicated for 30 seconds at 5um amplitude using a Soniprep 150 plus (MSE (UK) Ltd., London, United Kingdom). The sonicated samples were then centrifuged at 13000 rpm for 20 minutes and the supernatant removed and stored at -20°C.

2.10.3. SDS-PAGE analysis

SDS-PAGE was performed on both supernatant and cell lysate samples. 25µL of 4x NuPAGE® sample buffer and 10µL of 10x NuPAGE® reducing agent (Thermo Fisher Scientific, Massachusetts) were added to 65µL of sample and the resulting mixture was then incubated at 90^{0}C for 5 minutes in a MJ Research PTC-200 Thermal Cycler (GMI, Minnesota, USA) or 70^{0}C in an OBT4 heat block Grant Instruments, Royston, United Kingdom). 5-10µl of each sample and reference standard was loaded onto a NuPAGE® Bis-Tris Mini Gel (Thermo Fisher Scientific, Massachusetts) in a Novex Xcell SureLock^{TM} Mini-Cell Electrophoresis System (Thermo Fisher Scientific, Massachusetts), containing 800mL of NuPAGE™ MES SDS Running Buffer (Thermo Fisher Scientific, Massachusetts); 5-10µL of SeeBlue® Plus2 Pre-stained standard (Thermo Fisher Scientific, Massachusetts) was also loaded onto the gel. The gel was run at 200V (100-125 mA) for 35 minutes. On completion of the run the gel was stained with Instant Blue stain (Expedeon, Cambridgeshire) for 2-3 hours on a shaking platform. The gel was photographed using a Molecular Imager® Gel Doc™ EZ Imager with ImageLab3.0 software (Bio-Rad, California).

2.10.4. Octet® RED384 titre analysis

The titre of the dAb was quantified by Protein A binding affinity using an FortéBio Octet® RED38 (Pall Corporation, Port Washington). The Octet® RED384 uses Pall FortéBio's proprietary Bio-Layer Interferometry (BLI) to measure the interaction between the Protein A sensors and the protein of interest (Pall, no date). The Protein A sensors were equilibrated in either complex medium (extracellular samples) or 10mM Tris-HCl, pH 7.5 (intracellular samples) for 10 minutes and then placed into each sample for 120 seconds at 400rpm, 30^{0}C; each sample was run in triplicate. To quantify the dAb present in the samples a standard curve was generated from reference standard material provided by GSK; the material was diluted to 10µg mL^{-1}, 50µg mL^{-1}, 100µg mL^{-1}, 250µg mL^{-1}, 500µg mL^{-1}, 750µg mL^{-1} and 1000µg mL^{-1} in the same matrix as the fermentation samples (complex media or Tris-HCl buffer, pH 7.5). The standards and samples were analysed using the initial slope of the binding curve. A 5-paraemter logistic regression equation was fitted to the standard curve. A new standard curve was generated for each assay (Appendix D. Figure D.1.)

2.10.5. Plasmid stability analysis

100μL of culture sample was diluted in cell banking media by a factor of 10^{-5}-10^{-8}. These were plated out in duplicate onto LB agar plates with and without tetracycline (15 μg mL^{-1}). The plates were grown at 37^0C for 18-48 hours in a Heraeus Kelvitron T Drying Oven (Thermo Fisher Scientific, Massachusetts, USA). The number of colony forming units on each plate (CFUs) were counted. The plasmid stability was calculated using Equation 2.1.

$$Plasmid\ stability\ (\%) = \left(\frac{CFUs\ on\ vLB\ agar+Tet}{CFUs\ on\ vLB\ agar}\right) \times 100 \qquad (2.1)$$

2.10.6. Product quality analysis by HPLC-SEC

2.10.6.1. Purification by Protein A chromatography

Fermentation samples were purified by Protein A chromatography on a Tecan Freedom Evo$^{®}$ system with Infinite$^{®}$ M200 Pro plate reader (Tecan, Switzerland). 10-40mL harvest samples were stored at -80^{0}C at harvest and thawed prior to purification. The samples were centrifuged after thawing using a Sovall Evolution RC Centrifuge (Thermo Fisher Scientific, Massachusetts) with a Sorvall SS-34 Centrifuge rotor (Thermo Fisher Scientific, Massachusetts) at 20,000 rpm for 30 minutes. A protease inhibitor tablet and Benzonase$^{®}$ (Merck, New Jersey) at a concentration of 25U mL^{-1} were added. The samples were incubated at room temperature at 150rpm for ~3 hours until the material could pass through a 500mL polyethersulfone (PES) 0.22μm, 40cm^2 membrane Stericup$^{®}$ Filter Unit (Merck, New Jersey), or a Corning$^{®}$ 500mL, cellulose acetate (CA) 0.22μm, 33.2cm² membrane Vacuum Filter System (Corning, New York).

The samples were then purified on the Tecan system using 200μL MabSelect SuRe$^{®}$ RoboColumns (GE Healthcare, Sweden). The columns were equilibrated with 4 column volumes (CVs) of 55mM Tris base, 45mM acetic acid, pH 7.5 at a flow rate of 4.17μL s^{-1}. The columns were loaded with 5.5-6mL of load sample at a flow rate of 2.83μL s^{-1}, and then washed with 5CVs of 55mM Tris base, 45mM acetic acid, 100mM sodium caprylate, 300mM sodium acetate, pH 7.5, at a flow rate of 4.17μL s^{-1} followed by 4CVs of 55mM Tris base, 45mM acetic acid, pH 7.5 at a flow rate of 4.17μL s^{-1}. The columns were eluted in 10 x 100μL fractions using 1.8mM sodium acetate, 28.2mM acetic acid, pH 3.6 at a flow rate of 2.83μLs^{-1}. After elution, the columns were regenerated using 4CVs of 0.5M sodium hydroxide at a flow rate of

8.33µL s^{-1}, and the columns were stored in 20% ethanol. The fractions were collected in an UV-STAR® Microplate, 96-well plate (Greiner bio-one GmbH, Austria). The fractions were pooled based on the protein concentration determined by the absorbance at 280nm measured using an Infinite® M200 Pro plate reader. The pooled samples were subsequently diluted in PBS, pH7.2 to 1 mg mL^{-1} to load onto the HPLC-SEC system for aggregate analysis (Section 2.10.6.2).

2.10.6.2. HPLC-SEC for aggregate analysis

A standard GSK HPLC-SEC method was used to determine sample aggregate levels. 10µL of sample was injected onto a TSKgel G2000SWXl, 7.8 x 300mm column with a particle size of 5µm, and a pore size of 125Å (Tosoh Biosciences, Japan). A mobile phase of 100mM sodium phosphate (monobasic), 200mM NaCl, pH6.8, 5% n-Propanol was used at a flow rate of 0.5mL min^{-1}. Protein content was detected by UV absorbance at a wavelength of 214nm. Prior to analysis the samples were stored on an autosampler at 5^{0}C ± 3^{0}C.

2.10.7. Metabolite analysis

Metabolite analysis was performed using a Cedex HT Bio Analyzer (Roche Diagnostics, Germany). The principles of the individual assays are described below in accordance with the manufacturer's guidelines.

2.10.7.1. Measurement of glucose concentration

The glucose concentration was quantified based on the reaction scheme shown in Equations 2.2 and 2.3 catalysed by hexokinase (HK) and glucose 6-phosphate dehydrogenase (G6P-DH). The formation of NADPH was measured photometrically by UV-spectroscopy at a wavelength of 340nm. The production of NADH is directly proportional to the glucose concentration as shown in Equations 2.2 and 2.3.

$$\text{Glucose} + \text{ATP} \xrightarrow{\text{HK}} \text{Glucsoe-6-phosphate (G-6-P)} + \text{ADP} \qquad \textbf{(2.2)}$$

$$\text{G-6-P} + \text{NADP}^+ \xrightarrow{\text{G6P-DH}} \text{Gluconate-6-phosphate} + \text{NADPH} + \text{H}^+ \qquad \textbf{(2.3)}$$
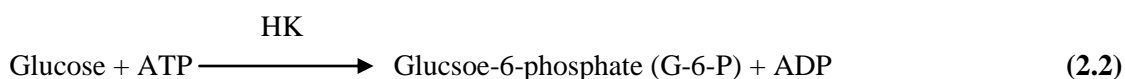
2.10.7.2. Measurement of acetate concentration

The acetate concentration was quantified based on the reaction scheme shown in Equations 2.4-2.7 catalysed by acetate kinase (AK), phosphotransacetylase (PTA), citrate synthase (CS), and L-malate dehydrogenase (MDH). The rate of NADPH was measured photometrically by UV-spectroscopy at a wavelength of 340nm. The oxalacetate produced in Equation 2.7. is used for the reaction catalysed by citrate synthase in Equation 2.6. The production of NADH related to the to the acetate concentration as the presence of acetate will result in the consumption of the oxalacetate produced in Equation 2.4. and a shift in the reaction equilibrium towards NADH production.

$$\text{Aceatate} + \text{ATP} \xrightarrow{\text{AK}} \text{Acetylphosphate} + \text{ADP} \tag{2.4}$$

$$\text{Acetylphosphate} + \text{CoA} \xrightarrow{\text{PTA}} \text{Acetyl-CoA} + \text{Phosphate} \tag{2.5}$$

$$\text{Acetyl-CoA} + \text{Oxalacetate} + H_2O \xrightarrow{\text{CS}} \text{Citrate} + \text{CoA} \tag{2.6}$$

$$\text{L-Malate} + NAD^+ \xrightarrow{\text{MDH}} \text{Oxalacetate} + NADH + H^+ \tag{2.7}$$

2.10.7.3. Measurement of glycerol concentration

The glycerol concentration was quantified based on the reactions shown in Equations 2.8 to 2.10 catalysed by glycerol kinase (GK), glycerol 6-phosphate oxidase (GPO) and peroxidase (POD). The 4-(p-benzoquinone-monoimino)-phenazone formed is a red dye that has an absorbance of 512nm. The increase in absorbance at 512nm, is directly proportional to the glycerol concentration as shown in Equations 2.8 to 2.10.

Glycerol + ATP $\xrightarrow{\text{GK}}$ Glycerol-3-phosphate + ADP **(2.8)**

Glycerol-3-phosphate + O$_2$ $\xrightarrow{\text{GPO}}$ dihydroxyacetone phosphate (DHA) + H$_2$O$_2$ **(2.9)**

H$_2$O$_2$ + 4-aminoantipyrine (4-AAP) + 4-cholophenol (4-CP) $\xrightarrow{\text{POD}}$

4-(p-benzoquinone-monoimino)-phenazone **(2.10)**
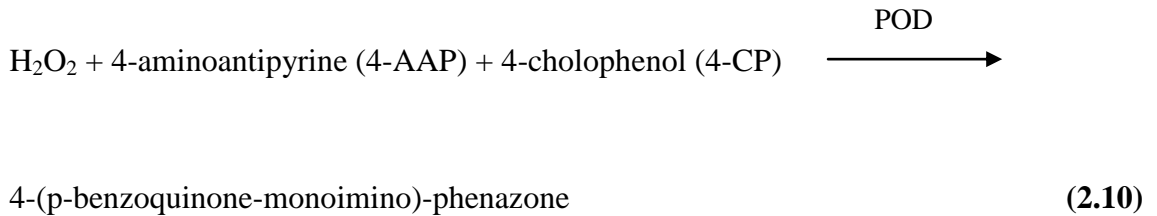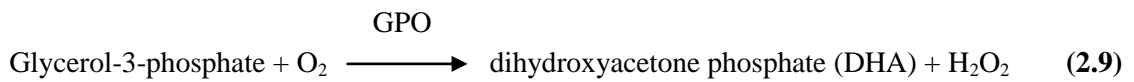
2.11. Statistics

2.11.1. Standard deviation

The standard deviation (*s*) was calculated using Equation 2.11.

$$s = \sqrt{\frac{\Sigma(x-\bar{x})^2}{(n-1)}}$$ **(2.11)**

2.11.2. Coefficient of variance (CV)

The coefficient of variance (CV) was calculated using Equation 2.12.

$$CV = \left(\frac{s}{\bar{x}}\right) \times 100$$ **(2.12)**

Chapter 3: Evaluation of fed-batch options in microwell scale fermentations

3.1. Introduction and aim

Recent trends in upstream bioprocess development are towards high throughput screening using microbioreactors (Section 1.5). These allow for large quantities of process information to be generated earlier in the development process and at a lower cost. Quality by Design (QbD) principles can also be implemented allowing for the translation of more efficient and robust processes to manufacturing scale (Section 1.5.).

When miniature bioreactors were first commercialised in the mid 2000s (Table 1.2.), they were only capable of batch operation despite the fact that most industrial fermentation processes operate in fed-batch mode. More recently (2017), the first miniature bioreactors with a feeding capacity were commercialised. Table 1.3 summarises the miniature bioreactors currently available and the feeding mechanism of each. The microbioreactor system used in this work consists of 24 miniature bioreactors with a working volume of 3-7mL (Pall Corporation, 2012). Each well has independent DO, pH and temperature and agitation is via orbital shaking control (Section 2.4.); however, it does not have a built-in feeding capacity.

The aim of this chapter was to investigate fed-batch options for high cell density *E. coli* cultures at the microwell scale. In this work two feeding strategies were implemented to microwell scale *E. coli* fermentations for domain antibody production. The first method investigated was *in situ* feeding by the enzymatic release of glucose from a polysaccharide polymer as described in Section 1.7.2. This avoids the requirement for a physical feed delivery system. The second method was the development of a bespoke feed delivery system for direct addition of feed solutions into individual microwells (Section 1.7.2.2.). The performance of the two methods was compared to a 1L scale fed-batch fermentation process previously developed for the expression system studied.

3.2. 1L scale batch and fed-batch fermentations of a w3110 *E. coli* strain producing a domain antibody ('platform process')

A dAb production process established at laboratory, pilot and manufacturing scales was used as a benchmark for the implementation of fed-batch feeding strategies at the microwell scale. In the current workflow, screening of *E. coli* strains is performed at microscale in batch mode.

The best clones identified by these screening experiments are then run at 1L scale in fed-batch mode to establish the optimum fermentation conditions to be transferred to pilot and manufacturing scales. Implementation of feeding at microscale would enable generation of large amounts of process optimisation data under industrially relevant conditions, reducing the number of laboratory scale experiments required. To fully understand the dAb production process to be scaled-down to Micro-24 scale, batch and fed-batch fermentations were performed at 1L scale under platform process conditions. The strain used for all fermentations in this thesis was a w3110 *E. coli* strain producing a dAb protein provided by Biopharm Process Research, GSK, Stevenage.

3.2.1. 1L batch fermentations

Three 1L batch fermentations were run in parallel under platform conditions as described in Section 2.3. The cultures were induced in the early exponential phase at an OD_{600} value of 1.2-1.4. Figure 3.1(a) shows that upon induction with IPTG, cell growth was severely retarded until approximately 20 hours post-induction. Also, SDS-PAGE analysis showed that both intracellular and extracellular dAb expression was minimal throughout the cultures (Figure 3.2). After around 25 hours the cells began to grow rapidly; this is most likely due to degradation of the tetracycline antibiotic initially added to the medium resulting in plasmid loss from the cells. As shown in Figure 3.2 the dAb was not produced during this second growth phase. Figure 3.1(b) shows the corresponding on-line process data. A rapid decrease in the DO was seen in the first 5 hours and at around 20 hours corresponding to the two separate stages seen in the growth curves. In each case the bioreactor control software responds with changes in agitation speed and/or gas flow rate to maintain the DO at the set point of 30%.

Factors such as the cell bank, IPTG batch and IPTG concentration were investigated as potential causes of the retardation of cell growth and minimal product expression post-induction; however none of these modifications improved cell growth or dAb expression (data not shown). It was hypothesised that the retardation of cell growth was due to product toxicity or a metabolic shift towards product expression over cell growth. As the cultures were induced in the early exponential phase, with either scenario there was insufficient biomass for detectable dAb expression. The inhibition of cell growth upon induction due to the metabolic burden of recombinant protein production has been well documented (Dong, Nilsson and Kurland, 1995; Heyland, Blank and Schmid, 2011; Lecina *et al.*, 2013). Toxicity effects of recombinant proteins leading to inhibition of cell growth have also been widely reported (Doherty, Connolly and Worrall, 1993; Dong, Nilsson and Kurland, 1995; Miroux and Walker, 1996; Dumon-Seignovert, Cariot and Vuillard, 2004; Rosano and Ceccarelli, 2014).
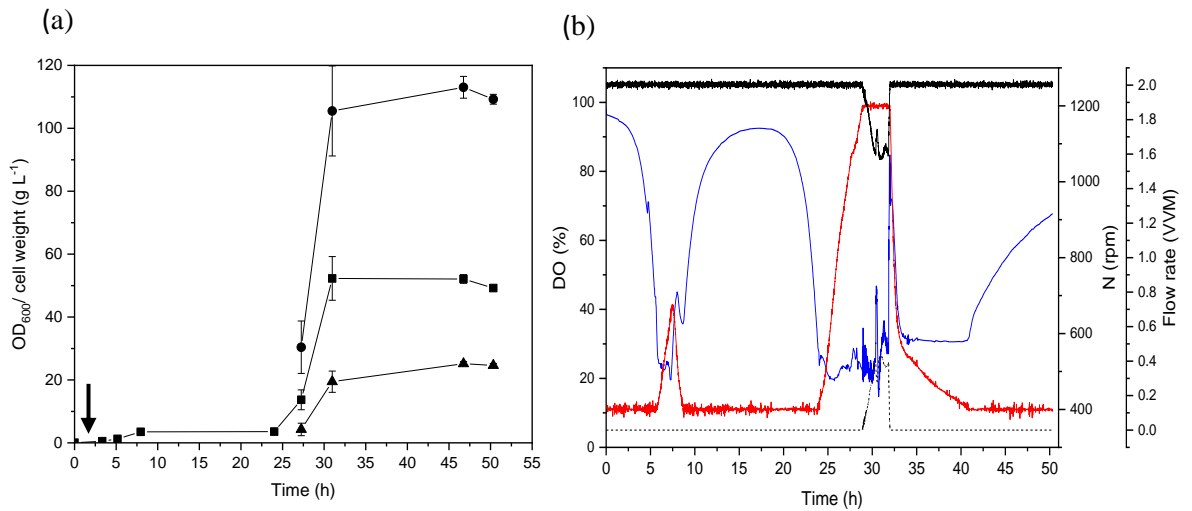
Figure 3.1. 1L batch culture kinetics of w3110 *E. coli* producing a dAb protein. (a) Cell growth profiles: OD_{600} (■), WCW (●) and DCW (▲), induction with IPTG (black arrow). (b) DO control: DO is indicated by the blue line, stirrer speed (N) is indicated by the red line, air flow rate is indicated by the solid black line, and oxygen flow rate is indicated by the dashed black line. The fermentations were performed as described in Section 2.3.2. The cultures were induced at 5.2 hours at OD_{600} values of 1.2-1.4. The DO, pH and temperature set points were 30%, pH7 and 30°C respectively. The error bars represent one standard deviation from the mean (n=3).
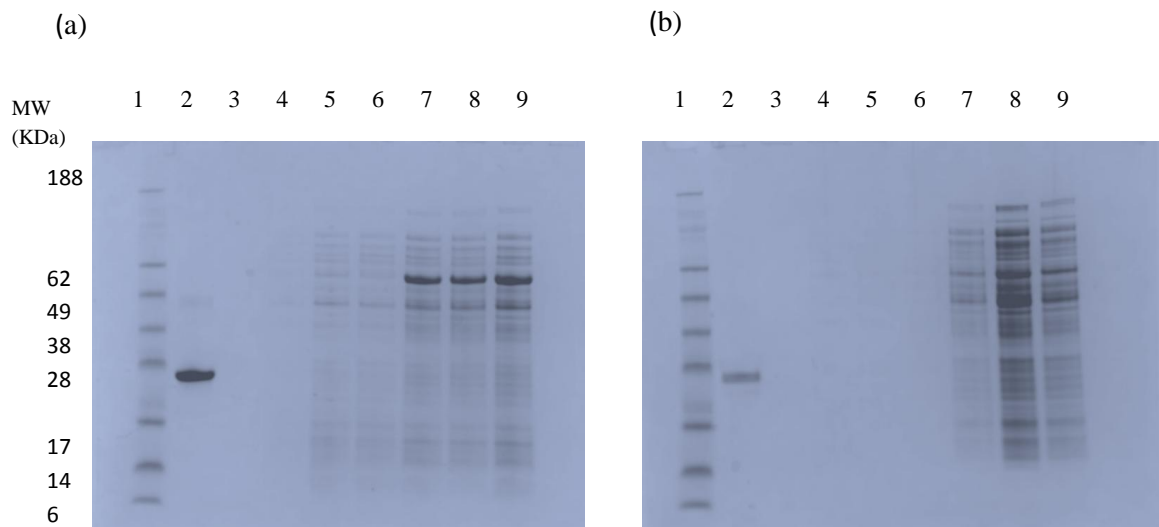
Figure 3.2. SDS-PAGE analysis of 1L batch cultures of w3110 *E. coli* producing a dAb protein. (a) extracellular dAb, and (b) intracellular dAb. The fermentations were performed as described in Figure 3.1 and SDS-PAGE was run as described in Section 2.10.3. Lane order: Lane1- SeeBlue® Plus2 Pre-stained molecular weight ladder, Lane 2-dAb reference standard (1 g L^{-1}), Lane 3-blank, Lanes 4,5,6 -24 hour samples, and Lanes 7,8,9-50-hour samples. The loading volume was 10μL.

3.2.2. 1L Fed-batch fermentations

Three 1L fed-batch fermentations were run in parallel. The batch phase of the cultures was performed as described in Section 3.2.1., with the exception that the cultures were not induced in the early exponential phase. At the end of the batch phase, feeding at a flow rate of 6 mL h^{-1} was triggered by a spike in the DO (60%) at 12-13 hours, corresponding to the exhaustion of the glycerol present in the medium (Figure 3.3(a) and (c)). The cultures were induced after six hours of feeding at a DCW of 34-36 g L^{-1}; at induction the feed rate was reduced to 3.5 mL h^{-1} and the fermentations were continued for a further 46 hours (Figure 3.3).

The cells grew rapidly in the initial batch phase; this corresponds to the consumption of the start concentration of glycerol in the media (Figures 3.3(a)). There was an increase in the oxygen flow rate at the end of the batch phase corresponding to the high oxygen uptake rate (Figure 3.3(c)). After feeding was triggered by the DO spike, the growth rate dropped as a result of the controlled glycerol addition (Figure 3.3(a)). The oxygen flow rate dropped post-induction as a result of the lower metabolic activity during product formation (Figure 3.3(c)). In terms of dAb titre, Figure 3.3(b) shows that dAb production occurred from approximately 3 hours post-induction, and dAb movement into the culture media was observed from around 10 hours post-induction. At harvest the total titre was 1.7 g L^{-1} and 68% of the dAb produced was extracellular.

In comparison to the batch fermentations (Section 3.2.1.) the maximum biomass concentration increased by approximately 75% (Table 1). The total dAb titres achieved were 1.3-2 g L^{-1}, significantly higher than the batch cultures where product expression was minimal (Table 3.1); this supports the hypothesis that the low induction biomass concentration was the reason for the lack of product expression. Also, no further cell growth was observed post-induction in the fed-batch cultures (Figure 3.3(a)), which is consistent with the low cell growth in the batch cultures post-induction (Figure 3.31(a)). The glycerol concentration was minimal during feeding, indicating that cell growth and product expression were carbon-limited, minimising the generation of inhibitory by-products such as acetate (Figure 3.3(a)).

Overall, these 1L batch and fed-batch fermentation data indicate that: (a) achieving a sufficient pre-induction biomass concentration, and (b) having a feeding strategy that allows for continuous controlled feeding are key factors in achieving high dAb titres. These will need to be accurately mimicked in the scale-down microwell fermentation processes.
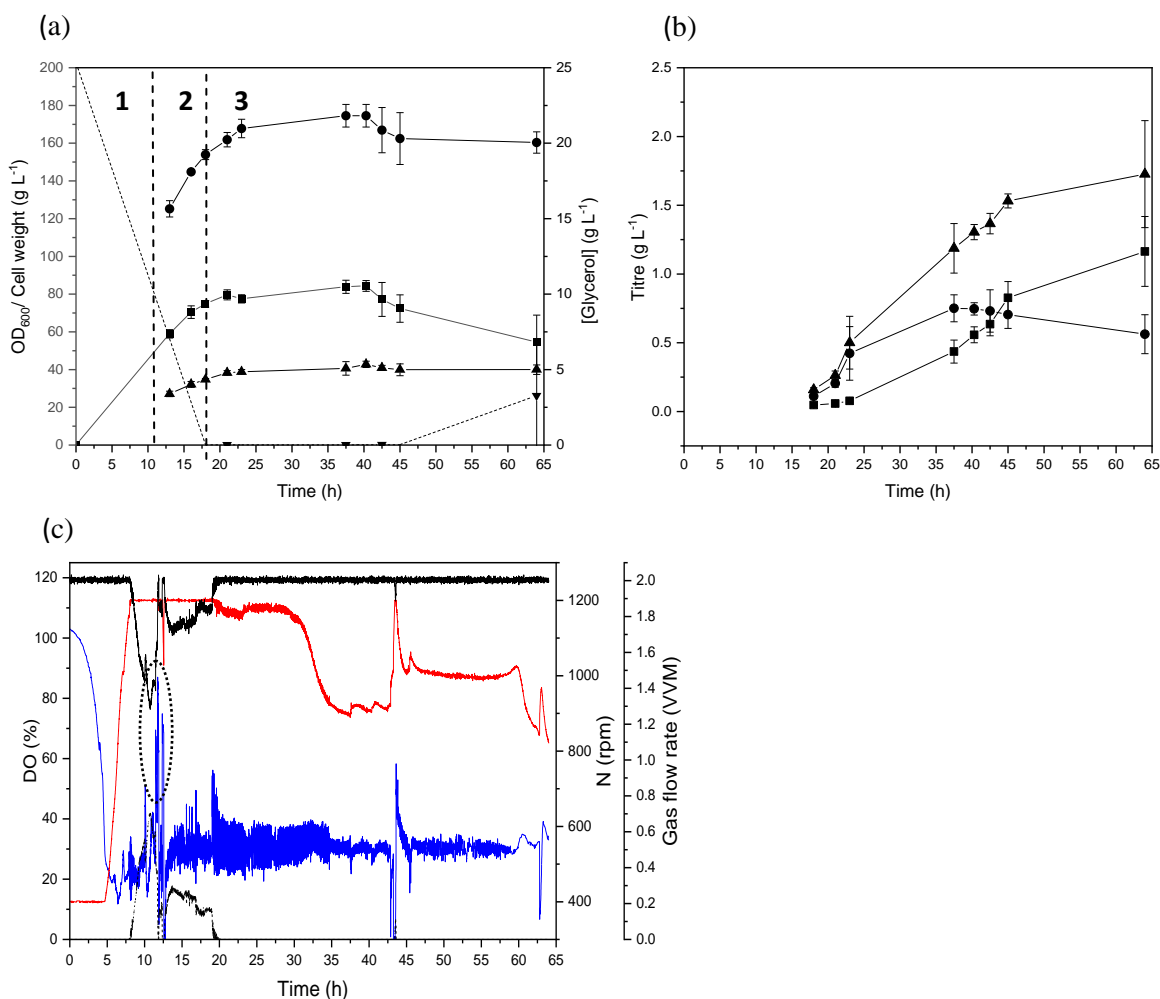
Figure 3.3. 1L fed-batch cultures of w3110 *E. coli* producing a dAb protein. (a) Cell growth and glycerol profiles: OD_{600} (■ with solid line), WCW (● with solid line), DCW (▲ with solid line), glycerol (▼ with dashed line). Phase 1 is the batch phase, phase 2 is the pre-induction fed-batch phase, and phase 3 is the post-induction fed-batch phase. (b) dAb titres by Octet® RED384: Extracellular (■ with solid line), intracellular (● with solid line) and total (▲ with solid line). (c) Online profiles: DO is indicated by the blue line, stirrer speed (N) is indicated by the red line, air flow rate is indicated by the solid black line, and oxygen flow rate is indicated by the dashed black line. The DO spike that triggered the feeding is indicated by the black dotted ring. The fermentations were performed as described in Section 2.3.2, and the analytical assays were carried out as described in Section 2.10. Feeding was triggered by a spike in the DO at 12-13 hours. The cultures were induced at 18 hours at OD_{600} values of 73-77. The DO, pH and temperature set points were 30%, pH7 and 30°C respectively. The error bars represent one standard deviation from the mean (n=3).

3.3. Implementation of microwell fed-batch fermentations

3.3.1. Microwell fed-batch cultures with *in situ* feeding using the EnPresso® B growth system

3.3.1.1. Glucose release kinetics from the EnPresso® B growth system

The first feeding strategy investigated was *in situ* feeding by the enzymatic release of glucose from a polysaccharide polymer (Section 1.7.2.1) using the EnPresso® B growth system. This growth system consists of media containing a polysaccharide polymer, and a glycoamylase enzyme that breaks down the polysaccharide polymer to glucose. The glucose release rate can be controlled by the glucoamylase concentration added to the culture. *In situ* feeding is an attractive option for feeding at microscale as it does not require a physical method of feed delivery, however is does require a change in media composition compared to the existing platform process. Furthermore, the scalability of *in situ* feeding is questionable due to the cost and availability of the reagents at large scale and the limited process control compared to direct feeding.

To determine the maximum glucose concentration attainable within a reasonable timeframe, and the minimum glucoamylase concentration required to achieve this, shake flask and microbioreactor incubations were performed in the absence of cells. Initial investigations were performed in shake flasks so there was a sufficient volume of media for multiple samples to be taken for glucose concentration analysis (Section 2.10.7.1). Figure 3.4(a) shows the glucose release rate in shake flasks over a 24-hour period, using glucoamylase concentrations of 0, 1.5, 3 and 6 U L^{-1}. The glucoamylsae concentrations investigated were selected based on the manufacturer's recommendation of 1.5 U L^{-1}.

Glucose release was linear for the duration of the 24-hour incubation period with all the glucoamylase concentrations investigated (Figure 3.4(a)); this suggests that the maximum glucose release was not achieved. Figure 3.4(b) shows that the glucose release rate increased linearly with glucoamylase concentration, indicating that at all enzyme concentrations tested the polysaccharide polymer was in excess. The equation of the line fitted to the data in Figure 3.4(b) was used to estimate the required glucoamylase concentration to achieve a glucose release matching the pre-induction glycerol consumption at 1L scale. The average pre-induction glycerol consumption rate at 1L scale was estimated to be 2.84 g L^{-1} h^{-1} based on the total amount of glycerol consumed at induction (Figure 3.3(a)); therefore the required glucoamylase concentration was approximated to be 53.4 U L^{-1}. Extrapolation of Figure 3.4(b) assumes that the glucoamylase concentration remains the rate limiting factor and that the polysaccharide polymer is always in excess. However, it is likely the graph will plateau as the concentration of the polysaccharide polymer becomes rate-limiting. Consequently, 30 U L^{-1} was selected as the maximum glucoamylase concentration tested in the microbioreactor.

The glucoamylase concentrations tested in the microbioreactor were 6, 18, 30 U L^{-1}, and a 0 U L^{-1} control. Five wells at each glucoamylase concentration and 4 control wells were run in parallel, and two wells were sampled at each time point. At glucoamylase concentrations of 18 U L^{-1} and 30 U L^{-1} a maximum glucose concentration of 18-20 g L^{-1} was achieved in the 66-hour incubation period (Figure 3.4(c)); this indicates that the maximum amount of glucose that can be released from the polysaccharide polymer is around 20 g L^{-1}. At glucoamylase concentrations of 0 U L^{-1} and 6 U L^{-1} the initial glucose release rates were comparable in shake flasks and the microbioreactor as indicated by the solid lines in Figure 3.4(c). These initial experiments suggested that 18 U L^{-1} is likely to be the optimum pre-induction glucoamylase concentration; therefore the microbioreactor cultures were performed at 6, 18 and 30 U L^{-1}.

Figure 3.4(d) shows the glucose release rate with a glucoamylase concentration of 18 U L^{-1} and the glycerol consumption rate in the 1L scale fed-batch process. This indicates that the maximum glucose release rate is likely to be insufficient to maintain the high cell densities required for high volumetric productivity.
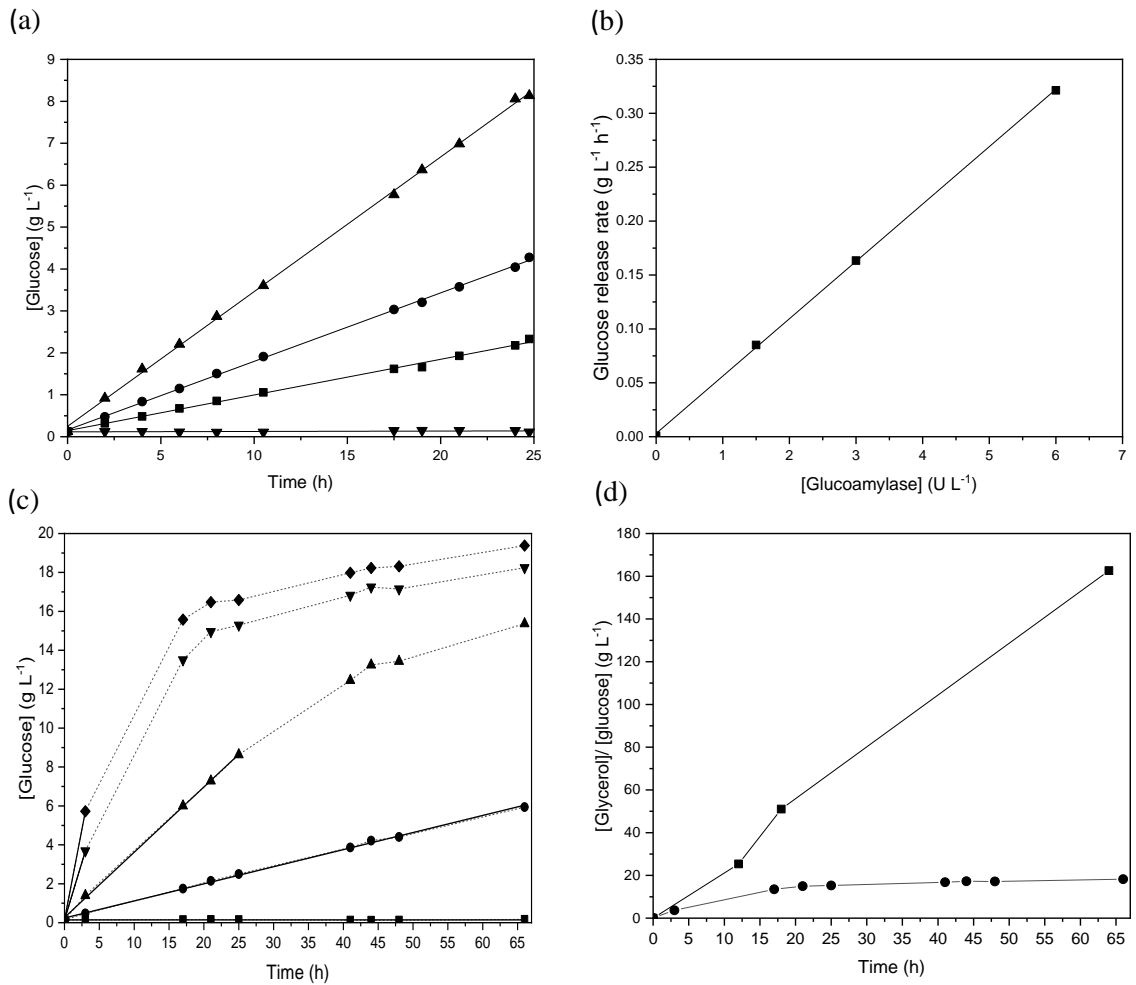
Figure 3.4. Glucose release from the EnPresso® B growth system in shake flasks and the Micro-24. (a) Glucose release in shake flasks using glucoamylase concentrations of 0 U L^{-1} (▼)1.5 U L^{-1} (■), 3 U L^{-1} (●) and 6 U L^{-1} (▲). Each glucoamylase concentration was run in duplicate, and two runs were performed to generate glucose release profiles over a 24-hour period. (b) Glucose release rate in shake flasks with increasing glucoamylase concentration. (c) Glucose release in the Micro-24 using glucoamylase concentrations of 0 U L^{-1} (■), 1.5 U L^{-1} (●), and 6 U L^{-1} (▲), 18 U L-1 (▼) and 30 U L^{-1} (♦). (d) Glucose release in the Micro-24 using a glucoamylase concentration of 18 U L-1 (●), and glycerol consumption in a typical 1L scale process (■). The solid black lines indicate the initial glucose release rate. Five wells of each glucoamylase concentration were run in parallel (four at 0 U L^{-1}), and two wells were sampled at each time point. The shake flask and Micro-24 incubations were carried out as described in Section 2.5.1. Solid lines in (a), (b) and (c) were fitted by linear regression.

3.3.1.2. Micro-24 fed-batch cultures using the EnPresso® B growth system

Initial fed-batch cultures were performed without induction to determine the maximum biomass concentration attainable using the EnPresso® B growth system, and the minimum glucoamylase concentration required to achieve this during an overnight culture (14-24 hours). The acetate concentration was also monitored as it has been widely reported that a high acetate concentration can be detrimental to cell growth and product expression (Xu, Jahic and Enfors, 1999; Enjalbert *et al.*, 2015; Anane *et al.*, 2017).

Figure 3.5(a) shows that at both 18 U L^{-1} and 30 U L^{-1} of glucoamylase, a maximum OD$_{600}$ value of 17-20 was achieved within 24 hours, whereas at 6 U L^{-1} a maximum OD$_{600}$ value of 9-11 was achieved. The final biomass concentrations at 18 U L^{-1} and 30 U L^{-1} were also comparable at approximately 6 g L^{-1} (Figure 3.5c). This suggests that at glucoamylase concentrations above 18 U L^{-1} the glucose release rate stops being growth rate limiting. A low glucose release rate, and therefore cell growth rate, was observed in the absence of glucoamylase (Figure 3.5); a final biomass concentration of 4.8 g L^{-1} was achieved (Figure 3.5b). In the absence of cells, glucose release was shown to be minimal over a 66-hour period (Figure 3.4c), suggesting that the observed glucose release can be attributed to the presence of cells, possibly due to a native glucoamylase enzyme secreted by the cells or released by cell lysis.

The glucose concentration profiles (Figure 3.5(c)) show that with a higher glucoamylase concentration there was a greater accumulation of glucose in the media in the early stages of the cultures. The rate of the subsequent glucose consumption was also greater; a higher maximum growth rate (μ_{max}) is possible with a higher glucose concentration, until the glucose concentration reaches inhibitory levels. An accumulation of acetate was seen at all three glucoamylase concentrations (Figure 3.5(d)). The maximum acetate concentration appears to be similar for 18 U L^{-1} and 30 U L^{-1} at approximately 1.6 g L^{-1} at 10 hours. At 14-hours the acetate concentration was higher at 30 U L^{-1} at 1.10 g L^{-1}, compared to 0.4 g L^{-1} at 18 U L^{-1}. This suggests that between 10 and 14 hours the acetate production rate is greater at 30 U L^{-1}, which is consistent with the greater glucose consumption rate at 30 U L^{-1} (Figure 3.5(c)); the comparable cell growth to of cultures at 18 U L^{-1} and 30 U L^{-1} also indicates a greater amount of overflow metabolism at 30 U L^{-1} (Figure 3.5(a) and (b)).

There was good consistency between the six replicates taken at 23 hours and 39 hours in terms of cell growth, with CVs of 1-11% for the OD$_{600}$ values, at all glucoamylase concentrations. The controlled growth rate enabled maintenance of the DO and pH at set point for most of the culture duration without the need for activation of the microbioreactor and DO control loops (Figure 3.5(e)). The microbioreactor DO control was operational from approximately 9-11 hours at 6 U L^{-1}, and from approximately 9-14 hours at 18 U L^{-1} and 30 U L^{-1} (Figure 3.5(e)).

The effect of using double concentrated media on cell growth was also investigated (Figure 3.6). There was an improvement in the final biomass concentration using the double concentrated media, with a maximum biomass concentration of 11 g L^{-1} at both 18 U L^{-1} and 30 U L^{-1} glucoamylase addition, compared to 6 g L^{-1} with single concentrated media (Figure 3.6(a)). However, there was no significant improvement in the initial growth rate; at 14 hours, the OD$_{600}$ values were 15-18 for both media concentrations at glucoamylase concentrations of 18 U L^{-1} and 30 U L^{-1} (Figure 3.6(b)). The lack of improvement in the initial growth rate with a higher starting concentration of the polysaccharide polymer could be attributed to the increase in the media viscosity. An increase in viscosity would have a detrimental effect on mixing and oxygen transfer (Sections 1.4 and 5.2). There was also a greater accumulation of glucose and acetate during the early stages of the culture at all glucoamylase concentrations using the double concentrated media, which is consistent with greater overflow metabolism (Figure 3.6(c) and (d)).

A pre-induction glucoamylase concentration of 18 U L^{-1} was used for all subsequent induced cultures as the maximum biomass was achieved at 14-18 hours (Figure 3.5a); this allowed for the pre-induction phase to be run overnight. Also, the acetate concentration of approximately 0.4 g L^{-1} at 14-18 hours was comparable to the pre-induction acetate concentration at 1L scale of 0.2 g L^{-1} (Section 4.7, Figure 4.6(b)). Single concentrated media was used as there was no improvement in the initial growth rate using double concentrated media, and there was an increase in acetate accumulation.

The cultures were induced using IPTG at 14 hours as described in Section 2.5.2. A bolus of glucoamylase at either 0, 1.5, 6 or 18 U L^{-1} and a 'booster solution' containing additional polysaccharide substrate and nutrients was also added to each well. The cultures were then grown for a further 24 hours. Eight wells were harvested at 14-hours and the remaining sixteen were induced. Figures 3.7(a) and (b) show that cell growth was comparable at all post-induction glucoamylase concentrations, which suggests the glucoamylase was in excess and the amount of polysaccharide polymer was growth rate limiting. Also, the glucose and acetate concentration profiles post-induction were consistent for all post-induction glucoamylase concentrations, and the cultures without any further glucoamylase additions (Figure 3.7(c) and (d)). This further indicates that the glucoamylase was in excess, and therefore subsequent glucoamylase additions did not influence cell growth or product expression. There was approximately a 50% increase in biomass concentration between 14 and 24 hours, and after 24 hours the biomass concentration gradually declined (Figures 3.7(a) and 3.7(b)). Cell growth post-induction was not observed at 1L scale. This indicates that the low rate of product formation in a consistent manner using *in situ* feeding allows for dAb expression and cell growth to occur simultaneously, due to either a reduction in the metabolic burden of protein expression, or reduced product toxicity effects.

Figure 3.8 shows dAb production using the EnPresso$^{®}$ B growth system. The maximum total titre at 39 hours was approximately 0.25 g L^{-1} at all post-induction glucoamylase concentrations, and without any further glucoamylase addition at induction. Figure 3.9 shows an SDS-PAGE gel of duplicate samples from cultures at each glucoamylase concentration. It is apparent that there was variation in dAb expression between duplicate wells; therefore the variation in dAb production in Figure 3.8 is likely to be due to well-to-well variation rather than an effect of the post-induction glucoamylase concentration. Specific productivities (SPRs) at harvest were comparable to the 1L scale fed-batch process (Table 3.1). However, due to the limited glucose release rate the maximum biomass concentration was insufficient to achieve the high cell density cultures required for comparable volumetric productivities.
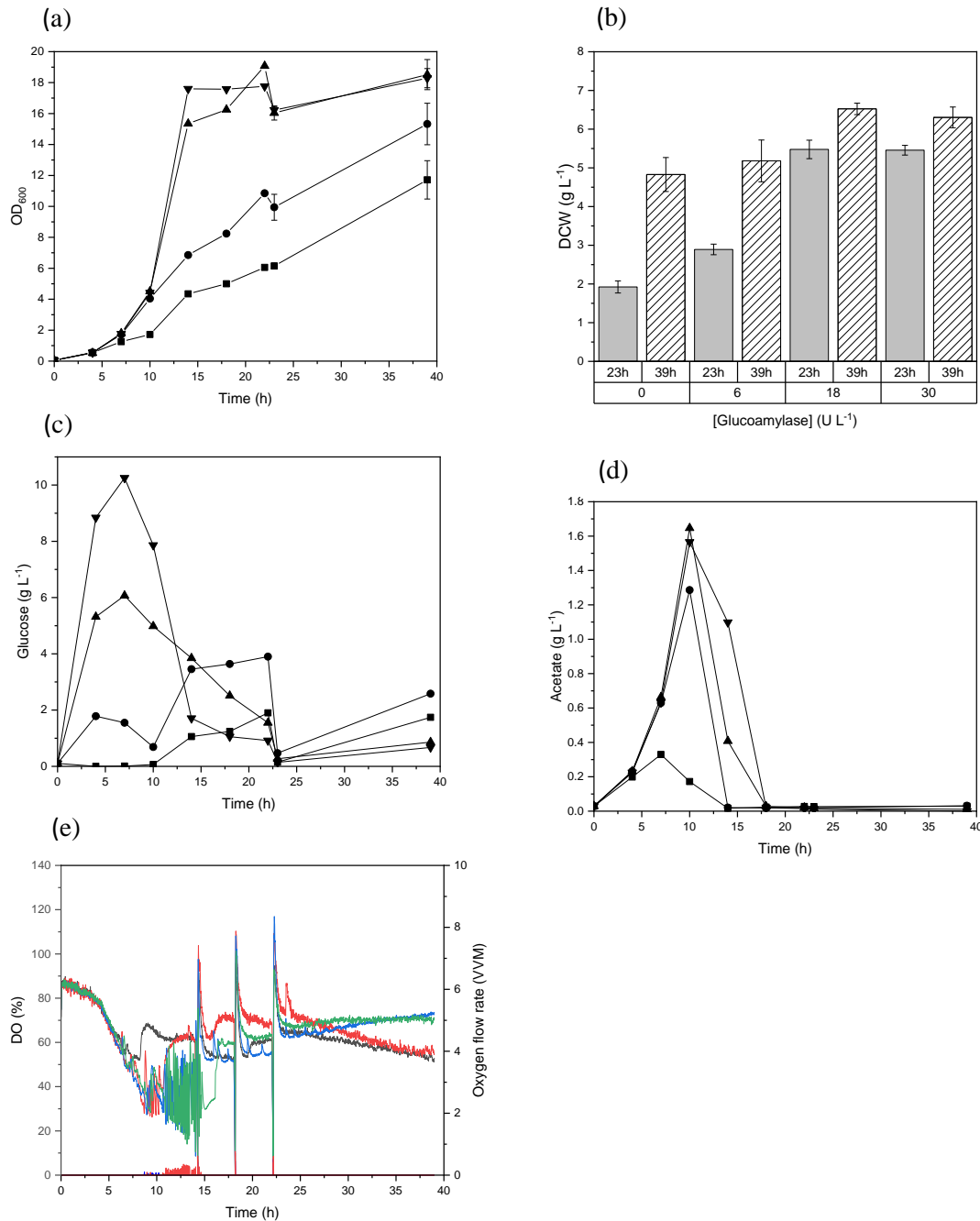
Figure 3.5. Micro-24 fed-batch, non-induced cultures of the w3110 *E. coli* producing a dAb protein using the EnPresso® B growth system. (a) OD_{600} values of cultures with a glucoamylase concentration of 0 U L^{-1} (■), 6 U L^{-1} (●), 18 U L^{-1} (▲) and 30 U L^{-1} (▼). (b) DCW values at 23 hours and 39 hours for each glucoamylase concentration tested. (c) Soluble glucose concentrations for glucoamylase concentrations of 0 U L^{-1} (■), 6 U L^{-1} (●), 18 U L^{-1} (▲) and 30 U L^{-1} (▼). (d) Acetate concentration for glucoamylase concentrations of 0 U L^{-1} (■), 6 U L^{-1} (●), 18 U L^{-1} (▲) and 30 U L^{-1} (▼). (e) DO cultures with glucoamylase concentrations of 0 U L^{-1} (grey line), 6 U L^{-1} (red line), 18 U L^{-1} (blue line) and 30 U L^{-1} (green line). The DO, pH and temperature set points were 30%, pH7 and 30°C respectively. Five wells of each glucoamylase concentration were run in parallel (four at 0 U L^{-1}), and two wells were sampled at each time point. The Micro-24 cultures were carried out as described in Section 2.5.2, and the analytical assays were carried out as described in Section 2.10. Error bars represent one standard deviation from the mean (n = 6).

(a)

(b)

(c)

(d)
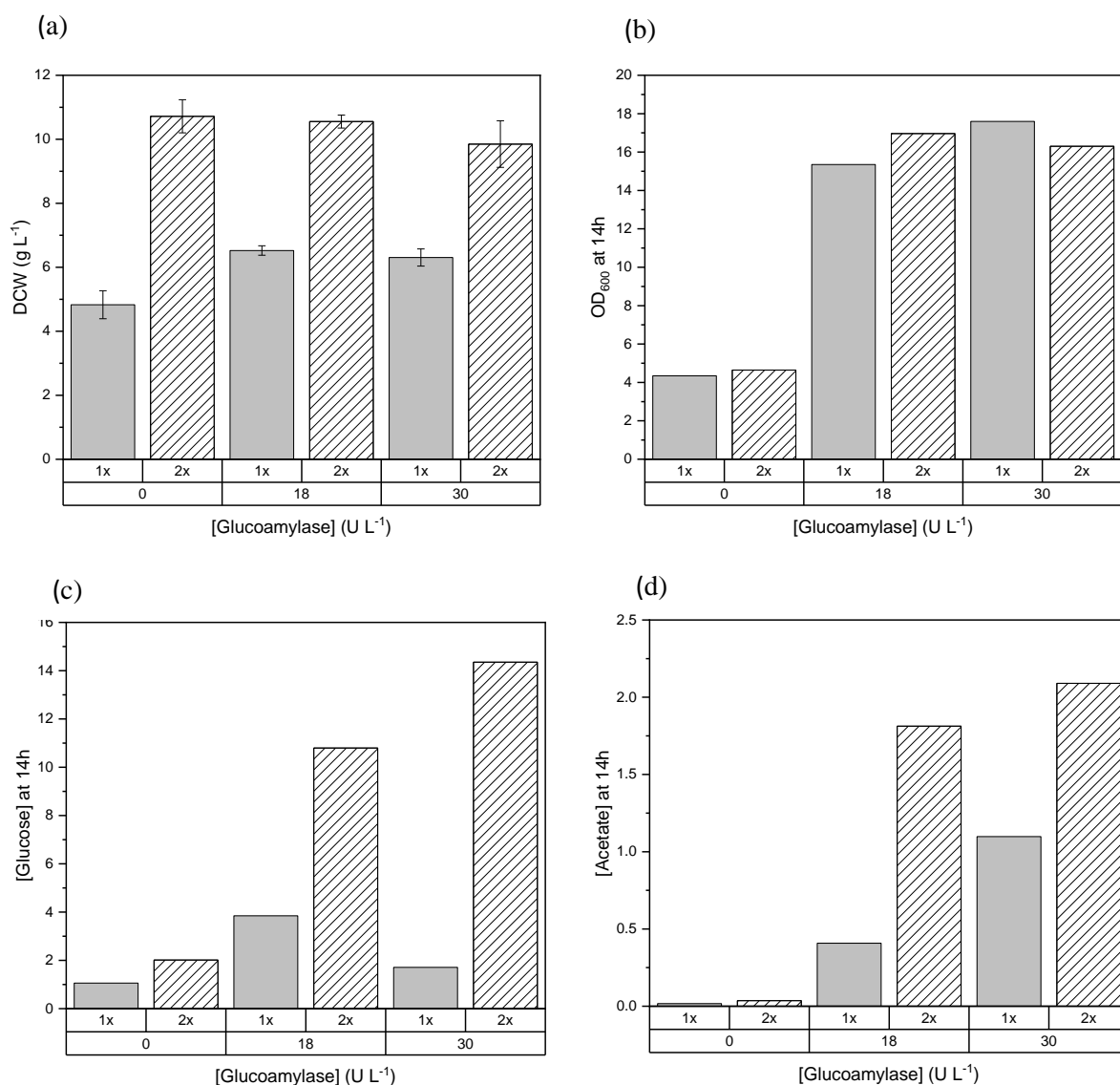
Figure 3.6. Micro-24 fed-batch, non-induced cultures of w3110 *E. coli* producing a dAb protein using the EnPresso® B growth system (2 x concentrated). (a) DCW at harvest, (b) OD_{600} values at 14 hours, (c) glucose concentration at 14 hours, and (d) acetate concentration at 14 hours. Five wells of glucoamylase concentrations of 0 U L^{-1}, 18 U L^{-1} and 30 U L^{-1}, were run in parallel (four at 0 U L^{-1}), and two wells were sampled at each time point. The Micro-24 cultures were carried out as described in Section 2.5.2, and the analytical assays were carried out as described in Section 2.10. Error bars in (a) represent one standard deviation from the mean (n = 5).

(a)

(b)

(c)
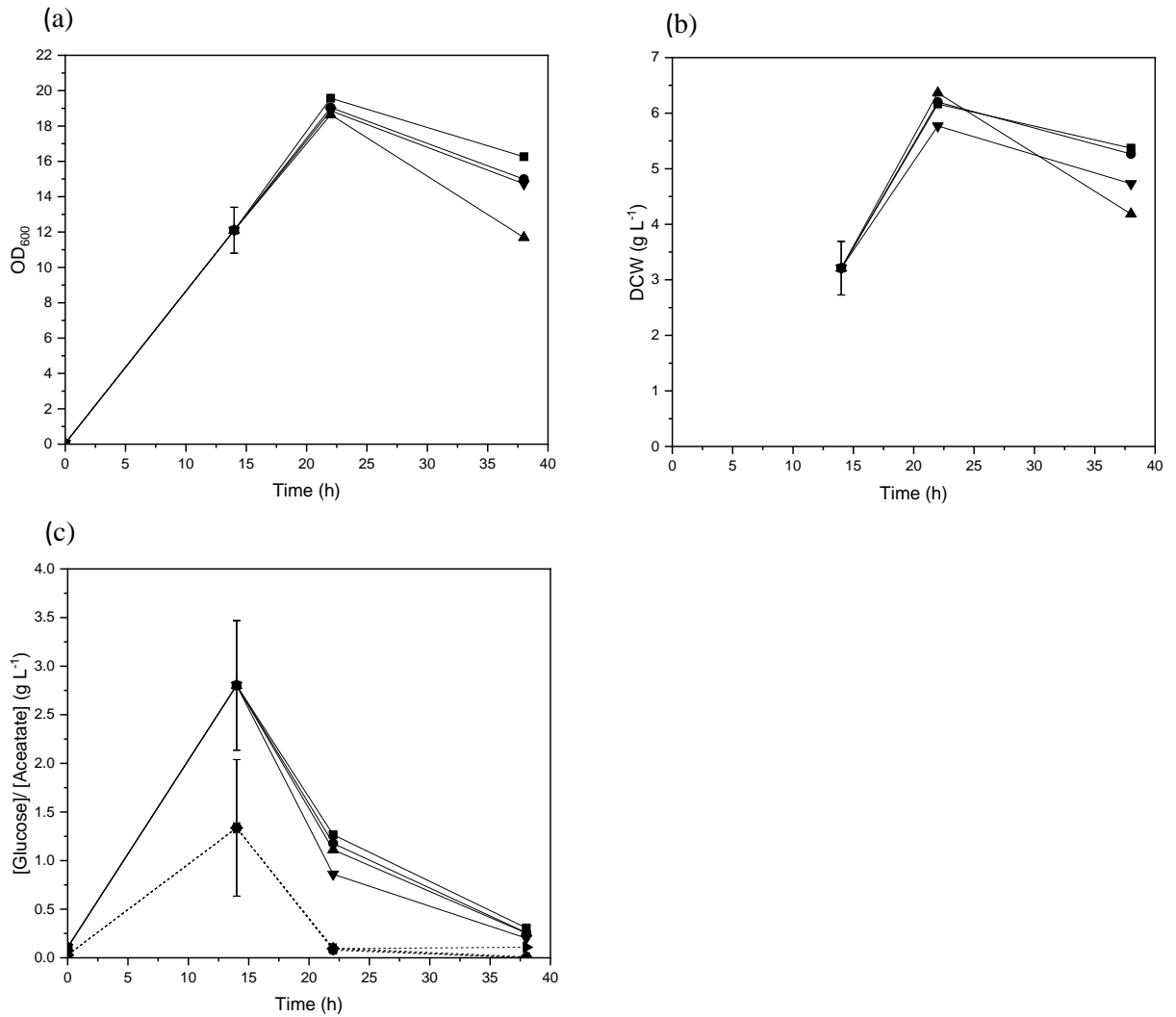
Figure 3.7. Micro-24 induced fed-batch cultures of w3110 *E. coli* producing a dAb protein using the EnPresso® B growth system. (a) OD_{600} values of cultures with post-induction glucoamylase concentrations of 0 U L^{-1} (■), 1.5 U L^{-1} (●), 6 U L^{-1} (▲) and 18 U L^{-1} (▼). (b) DCW values of cultures with a post-induction glucoamylase concentration 0 U L^{-1}(■), 1.5 U L^{-1} (●), 6 U L^{-1} (▲) and 18 U L^{-1} (▼). (c) Glucose and acetate concentration of cultures with post-induction glucoamylase concentrations of 0 U L^{-1}(■), 1.5 U L^{-1} (●), 6 U L^{-1} (▲) and 18 U L^{-1} (▼). The glucose concentration is indicated by the solid lines and the acetate concentration is indicated by the dashed lines. Six wells of each post-induction glucoamylase concentration were run in parallel. Eight wells were sampled at 14.3 hours, and two wells of each glucoamylase concentration were sampled at 22 and 39 hours. The Micro-24 cultures were carried out as described in Section 2.5.2, and the analytical assays were carried out as described in Section 2.10. The error bars at 14.3 hours represent one standard deviation from

- 85 -
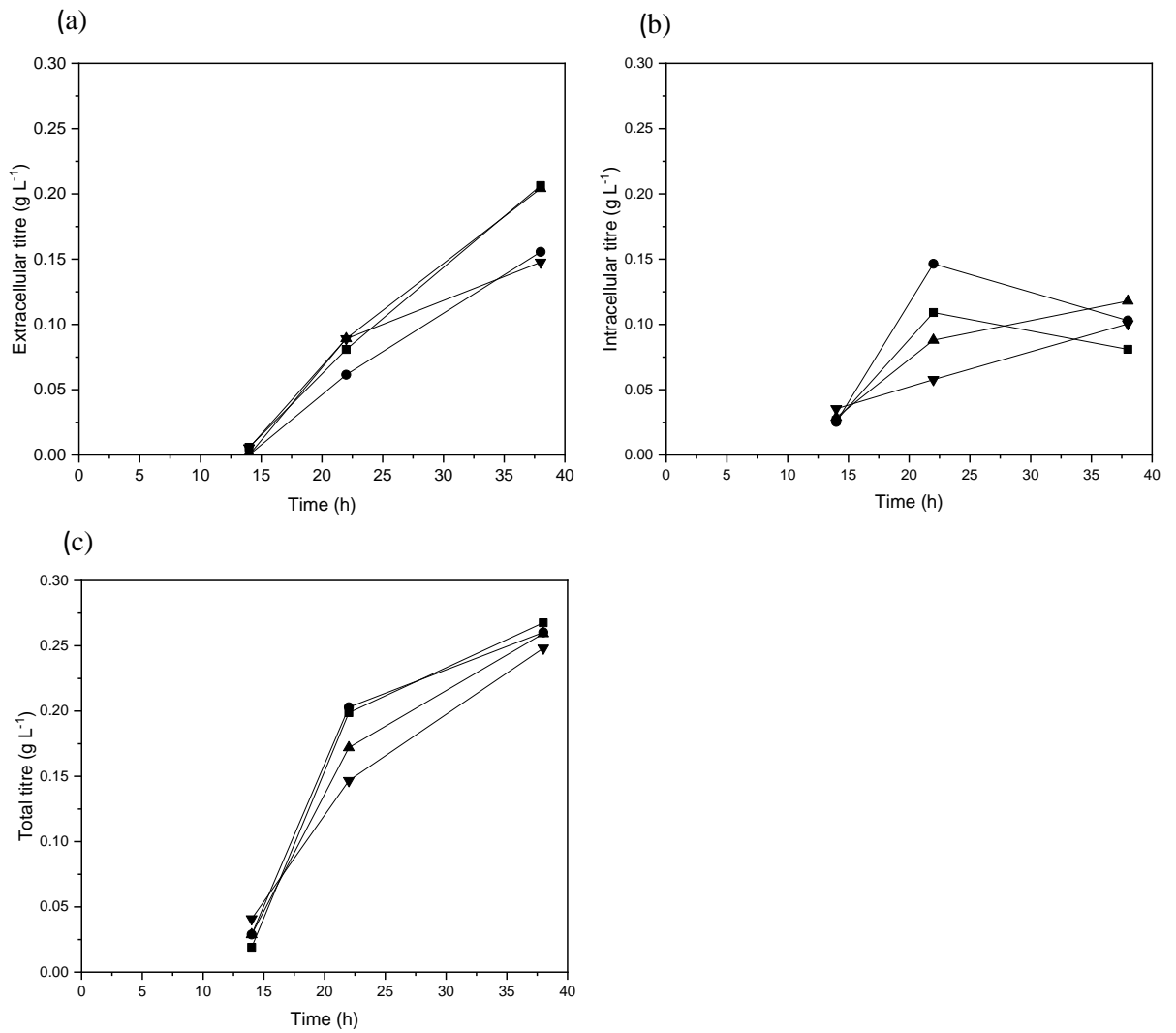
Figure 3.8. dAb titres of Micro-24 induced fed-batch cultures of w3110 *E. coli* using the EnPresso® B growth system, with post-induction glucoamylase concentrations of 0 U L^{-1} (■), 1.5 U L^{-1} (●), 6 U L^{-1} (▲) and 18 U L^{-1} (▼). (a) Extracellular titre, (b) intracellular titre, (c) total titre. Six wells of each post-induction glucoamylase concentration were run in parallel, and two wells were sampled at each time point. The Micro-24 cultures were carried out as described in Section 2.5.2, and the Octet® RED384 titre assays were carried out as described in Section 2.10.4.
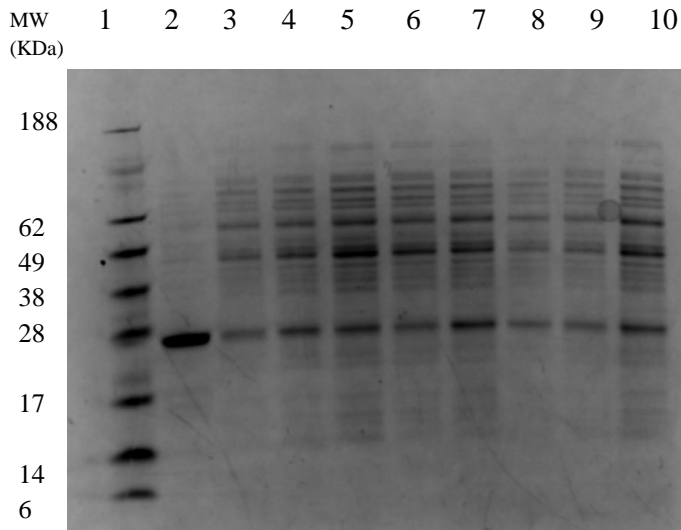
Figure 3.9. SDS-PAGE gels of extracellular samples from Micro-24 fed-batch cultures of w3110 *E. coli* producing a dAb protein using the EnPresso® B growth system. The fermentations were performed as described in Section 2.3 and SDS-PAGE gel was run as described in Section 2.10.3. Lane order: Lane1- SeeBlue® Plus2 Pre-stained standard, Lane 2- dAb reference standard (1 g L^{-1}), Lanes 3 and 7- 0 U L^{-1} samples, Lanes 4 and 8- 1.5 U L^{-1} samples, Lanes 5 and 9- 6 U L^{-1} samples, and Lanes 6 and 10- 18 U L^{-1} samples. The loading volume was 8uL.

3.3.2. Micro-24 fed-batch cultures by direct feeding

To achieve the high cell densities that were not feasible by *in situ* feeding, direct feeding was implemented to the microbioreactor using a 12-channel syringe pump. Initially six fed cultures were set up as described in Section 2.6.1.2. Six 3mL syringes were filled with glycerol feed and 1/16 inch internal diameter platinum cured silicon tubing was attached to each syringe using luer connectors. A 21G 1.5 inch hypodermic needle was attached to the opposite end of the tubing. Each needle was pushed through a well cap into an individual well. These initial experiments revealed that due to the high shaking speeds of the microbioreactor, the needles and caps were not secure in the cassette. Also, reinserting the needles in the same position after sampling was difficult, and could have compromised sterility. To address these issues, a bespoke device was developed to secure the needles and caps to the cassette.

3.3.2.1. Devolvement of a bespoke feeding device

Figures 3.12(a) and (b). Show the first version of the feeding device. The device comprised of an aluminium plate with one hole for the Micro-24 cap filter and a second smaller hole to house the feed line needle. This device secured the caps to the cassette due to the weight of the plate; however there was still some movement of the needles in the caps. The first version of the

feeding device was used to perform initial fed-batch cultures (Figures 3.10 and 3.11). Initially six wells were run in parallel. The 1L scale platform fed-batch process was replicated; the same temperature, pH and DO set points and volumetric feed rates were used as described in Section 2.3.2. However, the feeding was started manually at 15 hours, when an apparent spike in the DO was observed along with a drop in the oxygen flow, as a DO triggered feed start is not possible in microbioreactor control software. Six non-fed cultures were also run as a control. These cultures were induced at the same time as the fed cultures i.e. at the end of the batch phase. There was a loss of pH control in one of the six wells at approximately 13 hours prior to feeding, so cell growth and dAb titre data was generated for five fed cultures. The biomass concentration (DCW) attained in the fed cultures was 68% higher than the non-fed cultures (Figures 3.10a and b), and 5-fold higher than the fed-batch cultures using *in situ* feeding. This confirms that the low biomass concentrations achieved using the EnPresso[®] B growth system was due to the limited glucose release rate and not the oxygen transfer and mixing capabilities of the Micro-24.

In comparison to the 1L scale process, the initial growth rate in the batch phase was lower in the microbioreactor; the DO spike occurred approximately 3 hours later in the microbioreactor at 15 hours (Figure 3.11(b)). This is likely to be due to the enhanced k_La of the 1L vessels compared to the microbioreactor (Section 5.2). In both cases the maximum biomass concentration was achieved at induction after 6 hours of feeding; induction of the 1L scale and microbioreactor processes was at 18 hours and 21 hours respectively. The final DCW of the microscale fed-batch cultures was around 90% of the 1L scale process (Table 3.1), demonstrating the potential for high cell density cultures using the microbioreactor by direct feeding.

Figure 3.10(c) shows the harvest dAb titre and harvest volume of each well. There was significant variation in the titres, with the total titres ranging from 0.04 to 0.71 g L^{-1}. This suggests that there may have been variation in the feed additions between wells. The culture volumes at harvest were also inconsistent; the wells with lower product expression also had a lower volume at harvest confirming an issue with feed delivery. Another factor that may have contributed to the variation in the harvest volumes and titres is differences in evaporation rates between wells. Evaporation is unlikely to be significant in batch cultures; however it is an important consideration in fed-batch cultures at microscale due to the extended culture times and high surface area-to-volume ratio (Silk *et al.*, 2010; Wiegmann, Martinez and Baganz, 2018).

Figure 3.11 shows example online profiles of the non-fed (a) and fed (b) cultures. There was a period of oxygen limitation at the end of the batch phase (12-15 hours) when the oxygen demand was greatest. There were also significant oscillations in the DO profile during feeding, which are likely to be due to dropwise feed addition (Figure 3.12(b)). The low feed rates

required using the microbioreactor meant that a feed droplet formed at the end of the needle and eventually fell into the culture broth due to gravity; this occurred at 1 drop every 3-8 minutes (Section 4.5). Therefore, the oxygen demand of the cells would have oscillated during the cultures.

Overall these initial fed-batch cultures demonstrated that biomass concentration and productivity can be enhanced by implementation of feeding to the microbioreactor. However, it also showed that there were significant challenges that needed to be addressed. The key challenges identified were the improvement of well-to-well reproducibility, improvement of the DO control, and maintenance of sterility. Factors that were identified as possible causes of the well-to-well variation were leakage at the connectors, the accuracy of the syringe pump at the low flow rates required, and variation inherent to the microbioreactor, such as gassing and evaporation rate across the cassette.

To secure the needles to the microbioreactor cassette, a new feeding device that clamped the feed lines to the Micro-24 cassette was developed (Figure 3.12). The first iteration of the new feeding device design (Version 2) is shown in Figures 3.12(c), (d) and (e). The device was designed to accommodate twenty-four feed lines, to secure the needles and caps to the device, and to be autoclavable. The device was fabricated out of aluminium to facilitate autoclaving. The needles were secured in to the device by a top plate that was screwed on top of the connectors after the needles had been inserted (Figure 3.12(c) and (d)). Although this addressed the issue of securing the feed line to the cassette, the complexity of the device meant that sampling was impractical; the time to disassemble the device, perform the required manipulations i.e. sampling and liquid additions, and then reassemble to plate was typically 45-60 minutes. During this time the cells were without DO, pH or temperature control, which appeared to negatively impacted cell growth, as only using the bottom plate of the device to simplify the assembly process improved cell growth (Figure 3.13(a)). Removing the top two plates significantly reduced sampling times; however the feed lines were not completely secure in the device. Also, the device was relatively heavy at 429 grams and there was concern this may cause damage to the microbioreactor shaker motor.

Version 3 of the feeding device was similar to Version 2. The top plate was replaced with adjustable clamps so it was simpler to take feed lines in and out the device. Also, the diameter of the holes to accommodate the microbioreactor cap filters were reduced slightly so that the caps would be lifted out the microbioreactor cassette along with the feeding device, eliminating the need for the device to be disassembled and reassembled during sampling. Version 3 of the device was fabricated from acrylic to reduce the weight, however the acrylic became deformed in the autoclave so was not used for any fermentations.

Version 4 of the feeding device was identical to Version 3 with the exception that it was fabricated from Polytetrafluoroethylene (PTFE), with stainless steel spacers so that it was autoclavable (Figure 3.12(f)and (g)). Also, since PTFE is relatively soft, an additional four spacers were required to support the top of the device (Figure 3.13(f) and (g) and Appendix B Figures B.1-B.4). The sampling time was significantly reduced from 45-60 minutes to 10-20 minutes using Version 4 of the feeding device. Simplification of the sampling procedure also meant that it was straightforward to run twelve cultures simultaneously. To further reduce the sampling time the syringe pump and feeding device were transported together to the laminar flow hood, as opposed to removing the syringes from the syringe pump and then replacing them after sampling. Furthermore, the feeding system was assembled at the start of run prior to inoculation, rather than at the end of the batch phase prior to feeding. This reduced sampling time to 5-15 minutes depending on the number of samples to be taken and liquid additions required. However, Version 4 was still quite heavy at 374 grams as PTFE has a high density at 2.2 g m^{-3} (Wypych, 2016), and after repeated runs this started to cause problems with the microbioreactor shaker motor. Also, because PTFE is relatively soft the orbital shaking caused the screws holding the plates and spacers together to come loose.

Figure 3.13 shows cell growth kinetics using Version 1, Version 2, the bottom plate of Version 2, and Version 4 of the feeding device. The harvest DCWs varied considerably between the different versions of the feeding device (Figure 3.13(b)), however there was also variation in the OD$_{600}$ values pre-feeding (Figure 3.13(a)), indicating that at least some of the variation was unrelated to feed delivery. This could be due to the inherent variability of the microbioreactor, or related to the process such as the media composition or seed culture conditions. Wells were excluded if there was a loss in DO or pH control, if there was excessive foaming, or leakage at the connectors. Figure 3.13 shows that there was not a significant improvement in the reproducibility between versions of the feeding device. Therefore, other factors such as the type of tubing, type of connectors and the feed rate/concentration were investigated (Chapter 4).

To reduce the mass of plate and eliminate the need for the use of metal spacers and screws a 3D-printed version of the plate was designed and fabricated (Version 5, Figures 3.14). The device was designed using SpaceClaim 3D Modelling software and was printed out of VeroWhitePlus^{TM} (plate) and VeroBlackPlus^{TM} (clamps) using a Stratasys Connex 500 3D-printer. The 3D-printied device weighed 45% less than Version 4 with a mass of 205 grams, and there were no issues with the microbioreactor shaker motor using this device. Autoclavable resin was not available at the time of printing so this device was sterilised by spraying with 70/30 v/v denatured ethanol.

3.3.2.2. Ancillary 3D-printed components

A stand to hold the feeding device during sampling was designed and 3D-printed to ensure the needles remained sterile during sampling, to reduce the chances of cross contamination between wells, and for the safety of the operator (Figures 3.15(a) and (b) and Appendix B, Figures B.11-B.13)). The standard lid to maintain the microbioreactor environment temperature did not fit over the feeding device and feed lines, so a new lid was designed and 3D-printed (Figures 3.15(c) and (c) and Appendix B, Figure 10). Prior to the completion of the 3D-printed lid an upturned plastic storage box was used to maintain the environment temperature. This was sufficient to maintain the environment temperature at 26°C, and the well temperature at 30°C; however it was unable to maintain the environment below ambient temperature, and it caused some wear to the feed lines. The 3D-printed lid was not completed until towards the end of the project, so with the exception of the microbioreactor data shown in Figure 5.9, all other microbioreactor fermentations were performed using the storage box as a temporary lid.
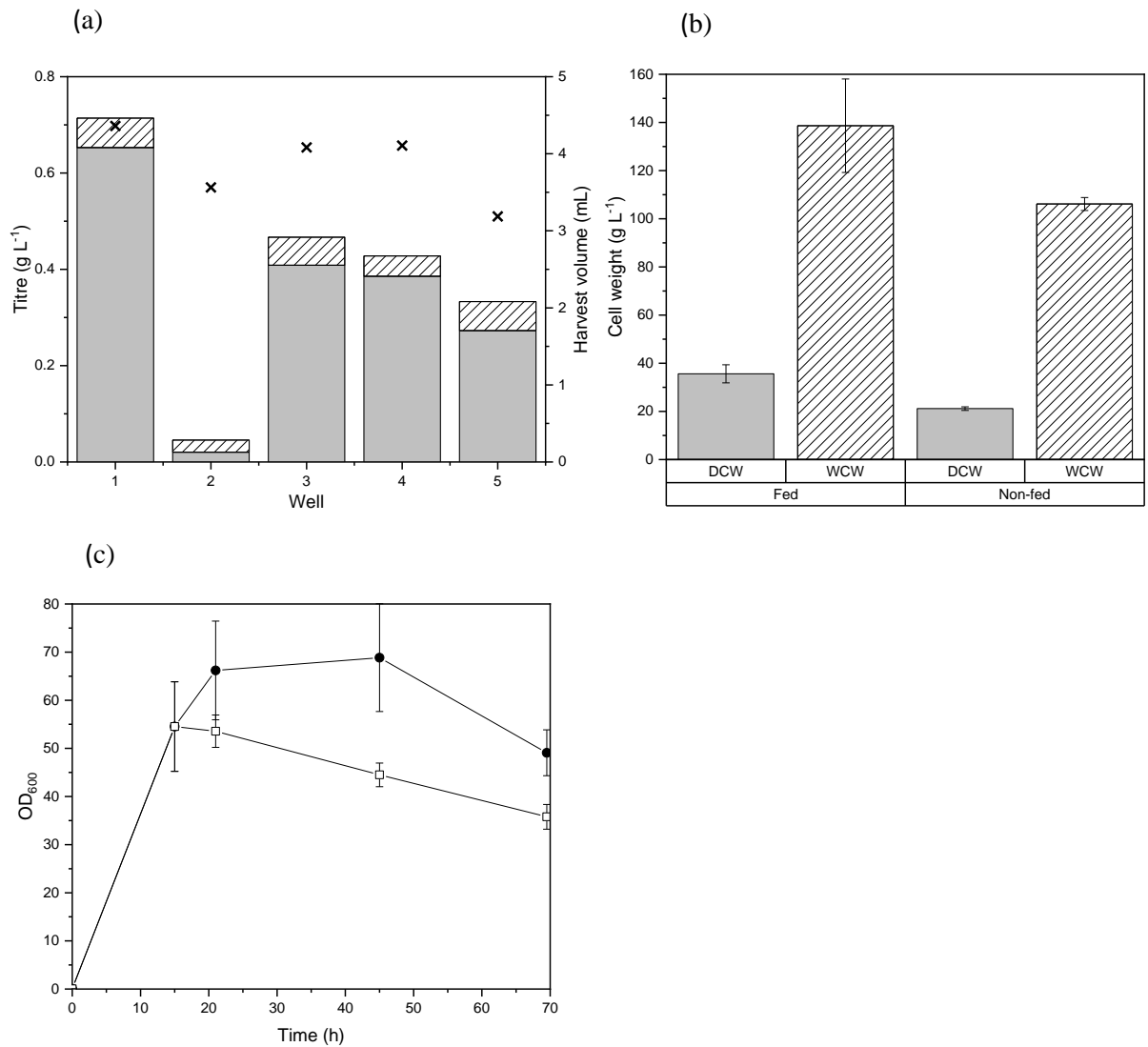
Figure 3.10. Offline data of Micro-24 non-fed batch and fed-batch cultures of w3110 *E. coli* producing a dAb protein, using feeding device Version 1. (a) dAb titres by Octet® RED384 and the well volumes at harvest (x). The grey bars represent the extracellular titres and the dashed bars represent the intracellular titres. (b) WCWs and DCWs. (c) OD_{600} profiles: Fed (● with solid line) and non-fed (□ with solid line). The fermentations were performed as described in Section 2.6.2., and the analytical assays were carried out as described in Section 2.10. Feeding was started manually at 15 hours. The cultures were induced at 21 hours at OD_{600}s of 49-73. The DO, pH and temperature set points were 30%, pH7 and 30°C respectively. The error bars represent one standard deviation from the mean (n=4).
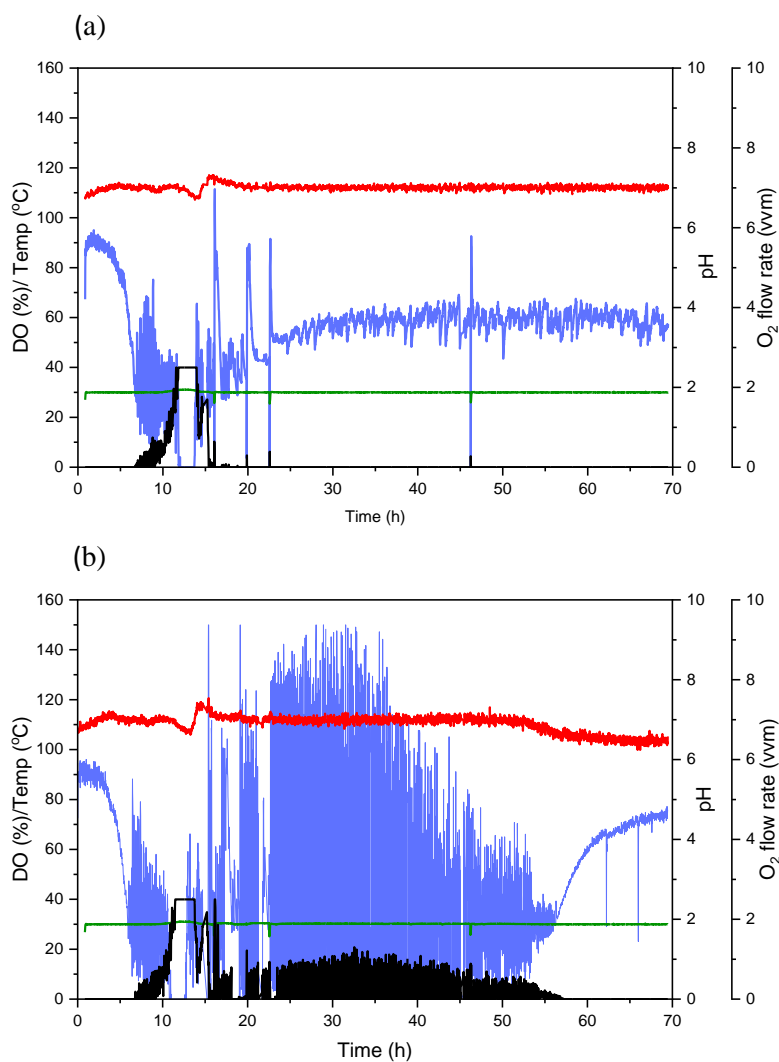
Figure 3.11. Online profiles of Micro-24 non-fed batch and fed-batch cultures of w3110 *E. coli* producing a dAb protein, using feeding device Version 1. (a) Non-fed, batch online profiles and (b) fed online profiles for a single well. The DO is indicated by the blue line, oxygen flow rate indicated by the black line, pH is indicated by the red line, and temperature is indicated by the green line. The fermentations were performed as described in Section 2.3. Feeding was started manually at 15 hours. The cultures were induced at 21 hours. The DO, pH and temperature set points were 30%, pH 7 and 30°C respectively.
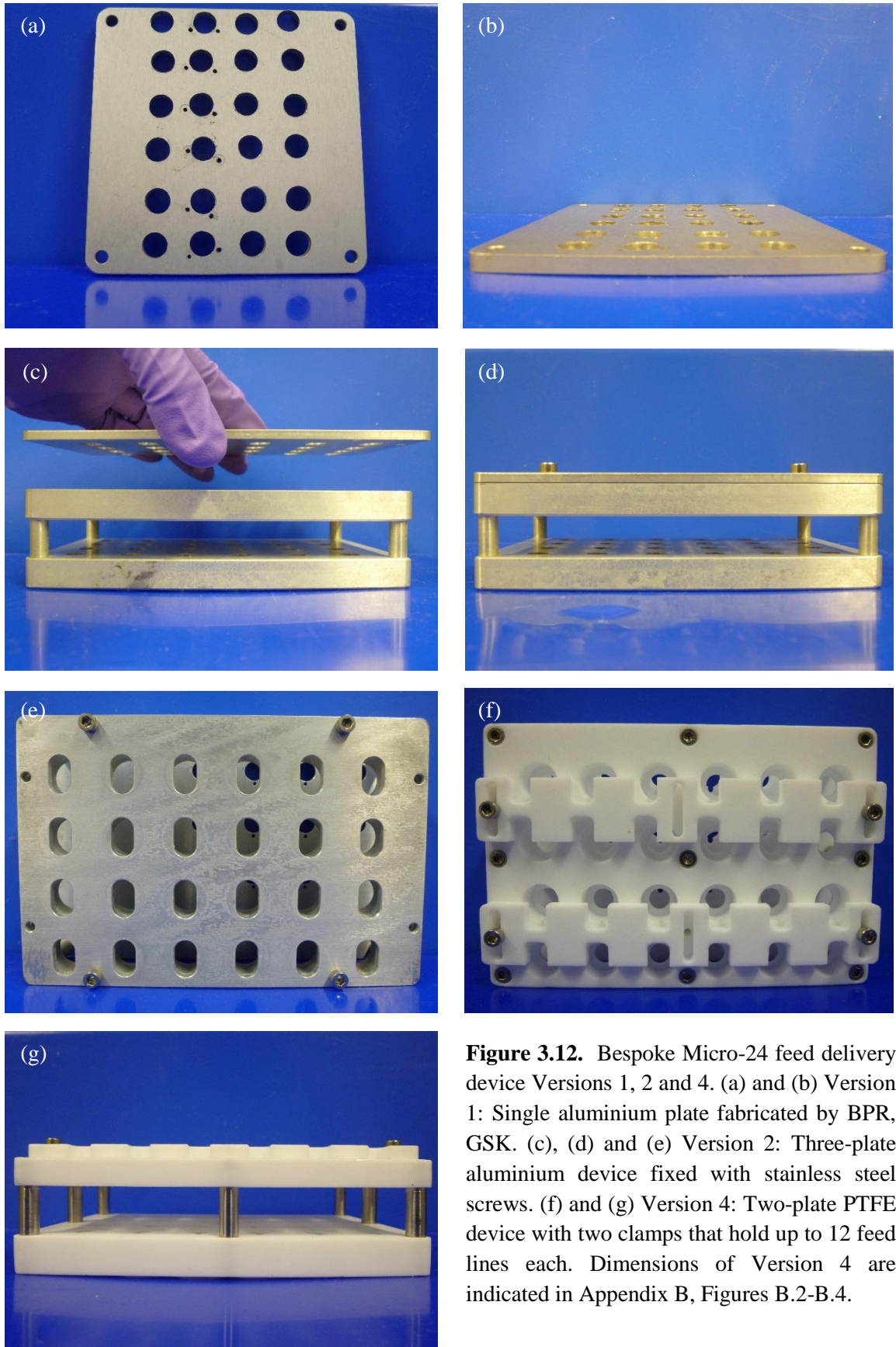
Figure 3.12. Bespoke Micro-24 feed delivery device Versions 1, 2 and 4. (a) and (b) Version 1: Single aluminium plate fabricated by BPR, GSK. (c), (d) and (e) Version 2: Three-plate aluminium device fixed with stainless steel screws. (f) and (g) Version 4: Two-plate PTFE device with two clamps that hold up to 12 feed lines each. Dimensions of Version 4 are indicated in Appendix B, Figures B.2-B.4.
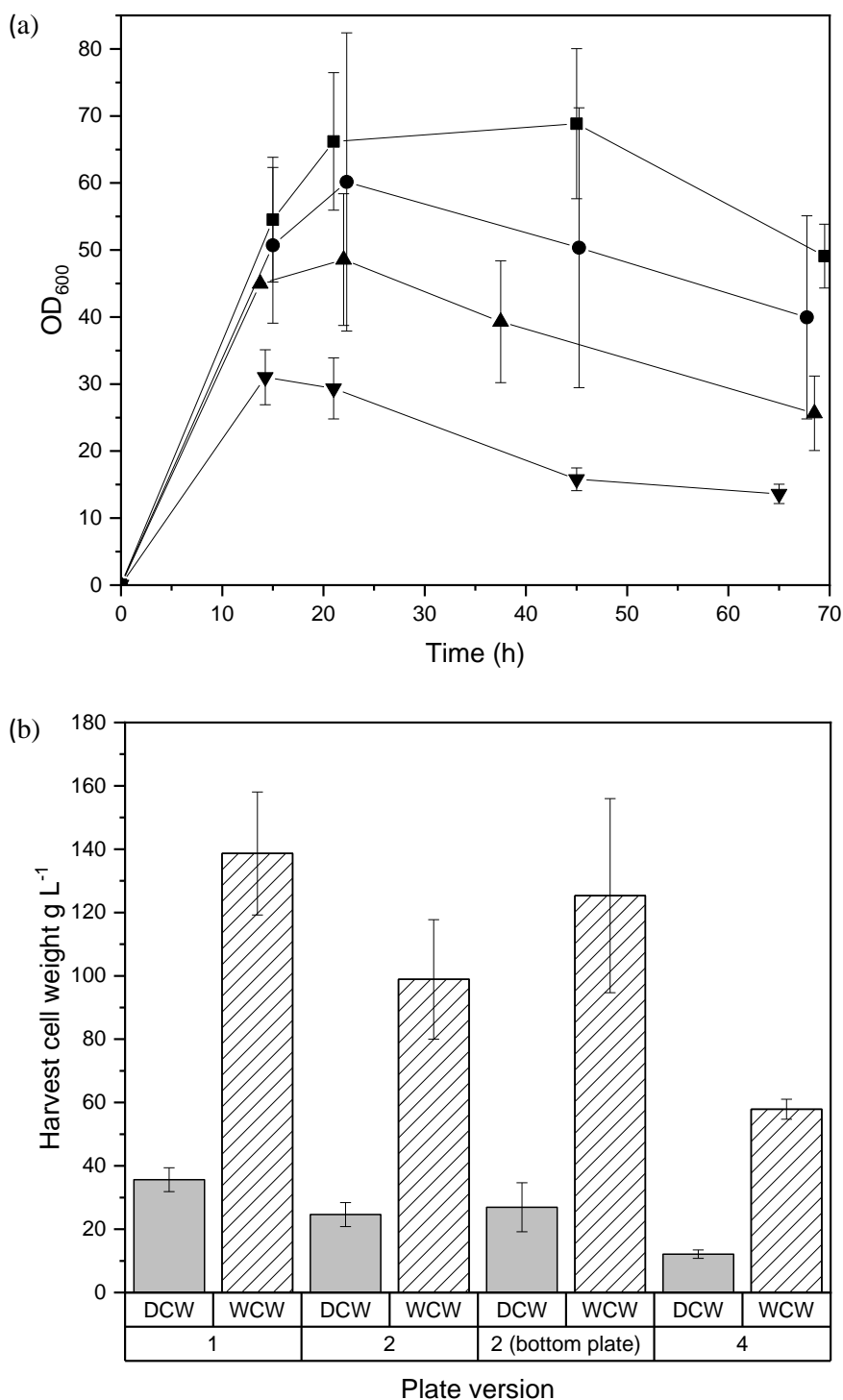
Figure 3.13. Micro-24 fed-batch cultures of w3110 *E. coli* producing a dAb protein, using feeding device Versions 1, 2, the bottom plate of 2, and 4. (a) OD_{600} profiles of feeding device Version 1(■), Version 2 (▲), the bottom plate of Version 2 (●), and Version 4 (▼). (b) WCWs and DCWs. The fermentations were performed as described in Section 2.6.2. Feeding was started manually at 13.7-15 hours. The cultures were induced at 21-22.3 hours. The DO, pH and temperature set points were 30%, pH 7 and 30°C respectively. The error bars represent one standard deviation from the mean (Version 1 n = 4, Version 2, n = 8, bottom plate of Version 2 n = 8, and Version 4 n= 6). OD_{600} and cell weight measurements were performed as described in Section 2.10.1.
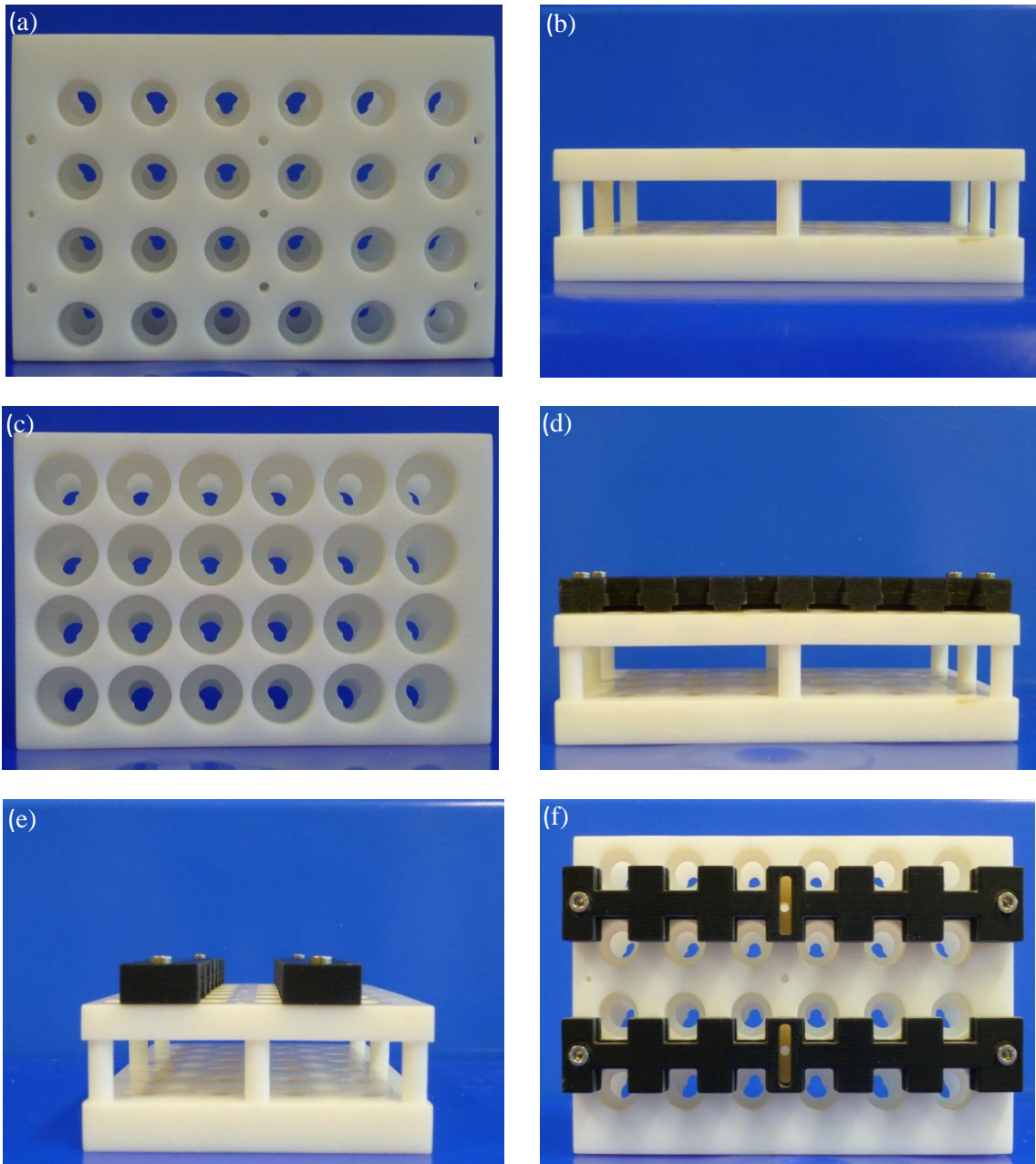
Figure 3.14. Final 3D-printed bespoke Micro-24 feed delivery device (Version 5). The device was designed using SpaceClaim 3D Modelling software and was printed out of VeroWhitePlus™ (plate) and VeroBlackPlus™ (clamps). (a) top (b) side (without clamps). (c) bottom, (d) side (with clamps) (e) front (with clamps), (f) top (with clamps). Dimensions of Version 5 are indicated in Appendix B, Figures B.5-B.9
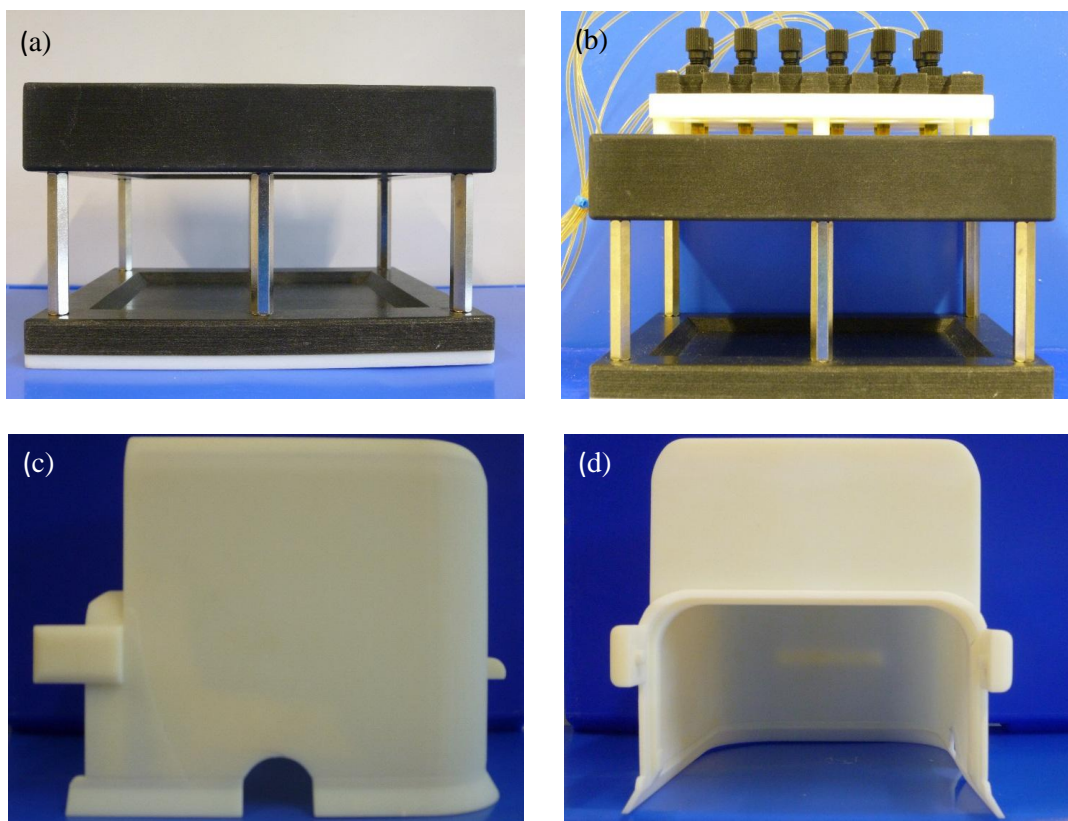
Figure 3.15. 3D-printed Micro-24 lid and sampling stand. The lid and stand were designed using SpaceClaim 3D Modelling software and were printed out of VeroWhitePlus^{TM} (stand and lid) and VeroBlackPlus^{TM} (stand) as described in Section 2.6.1.2. (a) sampling stand without the feeding device and (b) sampling stand with feeding device Version 4 containing 12 feed lines. (c) miniature bioreactor lid (side with cut out for the feed lines), (d) miniature bioreactor lid (back). Dimensions of the lid and sampling stand are indicated in Appendix B, Figures B.10 and B.11-B.13 respectively.

Table 3.1. Summary of the 1L scale and microbioreactor batch and fed-batch processes

System	Initial volume (mL)	Mode of operation	Feeding strategy	$[X]_{final}$ (g L^{-1})	$Y_{x/s}$ (OD g^{-1}) (pre-induction)	Harvest total titre (g L^{-1})	Harvest total SPR (mg g^{-1} L^{-1})	% Extracellular dAb
DASGIP® Parallel Bioreactor System	1000	Batch	N/A	24.1	ND	None	NA	NA
	1000	Fed-batch	Direct	40.0	1.47	1.73	43.3	68
Micro-24 MicroReactor System	4	Fed-batch	*In situ*	5.4	ND	0.27	42.1	77.4
	4	Fed-batch	Direct (Ver. 1)	35.6	**1.31	0.49	13.7	87.8
	4	Fed-batch	Direct (Ver. 2)	23.4	**0.99	ND	ND	ND
	4	Fed-batch	Direct (Ver. 2 bottom plate)	31.4	**1.32	ND	ND	ND
	4	Fed-batch	Direct (Ver. 4)	12.1	**0.58	ND	ND	ND

*Calculated based on the assumption that the starting glycerol concentration was 25 g L^{-1}. ND: not determined.

3.4. Summary

The aim of this chapter was to investigate fed-batch options for high cell density *E. coli* cultures at microwell scale. To this end two feeding methods were investigated: *in situ* feeding by the enzymatic release of glucose, and direct feeding using a bespoke feed delivery system. The cell growth and volumetric productivity achieved using these two feeding strategies were compared to an established 1L scale fed-batch dAb production process.

Table 3.1 summarises the harvest biomass concentration, total dAb titre and specific productivity (SPR). The data clearly show that implementation of direct feeding to the microbioreactor enhances cell growth compared to *in situ* feeding; the harvest DCW was up to 5-fold higher with direct feeding compared to *in situ* feeding (Table 3.1). Initial productivity data using Version 1 of the feed delivery device indicates that the improvement in biomass concentration results in an improvement in volumetric productivity.

The SPR achieved with *in situ* feeding of 42.1 mg g^{-1}, is comparable to the SPR achieved at 1L scale of 43.3 mg g^{-1}, and is approximately 3-fold higher than the SPR attained with direct feeding of 13.7 g L^{-1}. This suggests that SPR is improved when product expression occurs in a highly-controlled manner i.e. with direct feeding using a peristaltic pump at 1L scale, or *in situ* feeding at microscale. In contrast, with direct feeding using the bespoke microbioreactor feed delivery system, feed additions occur in a dropwise manner causing fluctuations in the rate of product formation and therefore the DO; this appears to negatively affect the cellular productivity. The negative impact of fluctuating DO control on cellular productivity in *Yarrowia lipolytica* was demonstrated by Kar *et al*., 2010, who used an automatic valve to close the air flow line on a 20L agitated vessel intermittently, to mimic DO concentration gradients in large scale vessels. A reduction in mRNA expression was observed in the periods where the air line valve was closed (Kar *et al*., 2010).

This initial fed-batch data indicates enhancement of biomass concentration and volumetric productivity can be achieved by direct feeding. To improve productivity, the oscillations in metabolic activity should be reduced by modification of the feed rates/concentrations and tuning of the DO control parameters. Optimisation of the feeding strategy using the 3D-prinited feeding device is described in Chapter 4.

Chapter 4: Establishment of reproducible direct feeding in the microbioreactor

4.1. Introduction and aim

In the previous chapter, two fed-batch feeding strategies were investigated as options for the implementation of fed-batch cultures to a microwell-based, bioreactor system; *in situ* feeding by the enzymatic release of glucose from a polysaccharide polymer (Section 3.3.1), and direct feeding using a bespoke feed delivery system (Section 3.3.2). It was found that *in situ* feeding enhanced cellular dAb expression, however the maximum biomass concentration was insufficient to achieve volumetric productivities comparable to an established 1L-scale fed-batch process (Table 3.1). Higher cell densities, and therefore volumetric productivities were attainable with direct feeding, but there was significant well-to-well variation in cell growth and product expression (Figures 3.10 and 3.13, and Table 3.1). The aim of this chapter is to refine the direct feeding strategy to enable the implementation of industrially relevant fed-batch *E. coli* cultures in the microbioreactor, that are comparable to the laboratory scale fed-batch process in terms of cell growth, product expression and DO control. To improve the reproducibility and refine the microbioreactor feeding strategy several possible causes of variation were considered: the batch complex media composition, the feed line assembly, the seed culture conditions, the accuracy of the syringe pump, the needle type used, and the production of inhibitory by-products.

4.2. Amendments to the batch complex media (yeast extract source and antifoam concentration)

It had been observed that a precipitate formed in the batch complex media after autoclaving. From previous experience at GSK, it was found that the company the yeast extract was purchased from affected whether a precipitate formed or not during the autoclaving process; a precipitate formed with Becton Dickinson yeast extract but not with Sigma Aldrich yeast extract. To eliminate the possibility that that precipitate was blocking the microbioreactor sparger membranes compromising pH and DO control, the yeast extract supplier for both the microbioreactor and 1L scale fermentations was changed from Becton Dickinson to Sigma Aldrich. The antifoam concentration added to the microbioreactor at the start of the fermentation was also increased from 500ppm to 800ppm, as in previous fermentation data was lost due to excessive foaming.

4.3. Improvement of the feed line assembly

Leakage at the feed line connectors was identified as another possible cause of variation in feed delivery, and also a possible source of contamination. Inspection of the feed lines revealed that the flexible C-Flex® tubing was becoming damaged under the cable ties, causing the liquid medium to leak at the connectors. The connectors also became deformed in the autoclave causing the feed lines to become obstructed and leakage to occur. The tubing and connectors were changed to Upchurch Scientific ethylene tetrafluoroethylene (ETFE) connectors and ETFE Tefzel® HPLC tubing (IDEX Corporation, Illinois, USA). This eliminated the need for cable ties and therefore tubing remained intact and the leakage stopped. Also, the feed lines could be autoclaved multiple times without compromising their integrity, which made the assembly process less laborious. The needle type used was also changed from 1.5 inch needles 1 inch needles as there was evidence that the needles were becoming blocked with culture broth and/or feed over extended culture periods; the 1 inch needles sat sufficiently high enough above the liquid surface that the needles did not contact the liquid even when the cassette was shaken at 800rpm.

4.4. Influence of seed conditions on the growth rate in the microbioreactor

There was significant variation in the lag phase, and therefore the end-of-batch time, between microbioreactor fermentation experiments (Figure 4.1(a)); it was hypothesised that this was due to variation in the inoculum. To investigate whether the temperature step-down from $37^{\mathbf{o}}$C to $30^{\mathbf{o}}$C during the seed cultures was causing variation in the state of the cells used to inoculate the microbioreactor, the inoculum development process was changed to a fixed incubation temperature of $30^{\mathbf{o}}$C and a longer incubation time (Section 2.2.1).

Figure 4.1(b) shows the DO profiles for the microbioreactor cultures using the modified seed conditions, for cultures with a DO set point of either 30% or 60%. The lag phase and early exponential growth phase were consistent suggesting that the temperature step-down used previously for seed culture preparation was causing variation in the inoculum, and therefore cell growth in the microbioreactor. For both DO set points the controller kicked-in after around 6 hours and it was possible to maintain the DO of the cultures at around 60% and 30% respectively. The large spikes seen in the DO profiles between 12-16 hours are due to the cassette being removed for sampling.

The importance of inoculum age on *E. coli* cell growth has been reported in the literature. The affinity for glucose of *E. coli* differs depending on the growth phase due to differences in the expression of proteins involved in glucose uptake, MgL and LamB. This means that variation

in the age of the inoculum, will result in differences in cell glucose affinity and therefore cell growth (Death and Ferenci, 1994; Ferenci, 1999). At high incubation temperatures, cell growth is enhanced and therefore less controlled; this means it is more difficult to achieve equivalent end points of multiple seed cultures at high incubation temperatures. Methods that have been employed to improve the reproducibility of the seed cultures are temperature reduction to 20-25°C, or utilisation or a slow release glucose system for *in situ* feeding (Robert Huber *et al.*, 2009; Rosano and Ceccarelli, 2014). The modified seed conditions, a fixed incubation temperature of 30°C and a longer incubation time, were used for all subsequent fermentations.
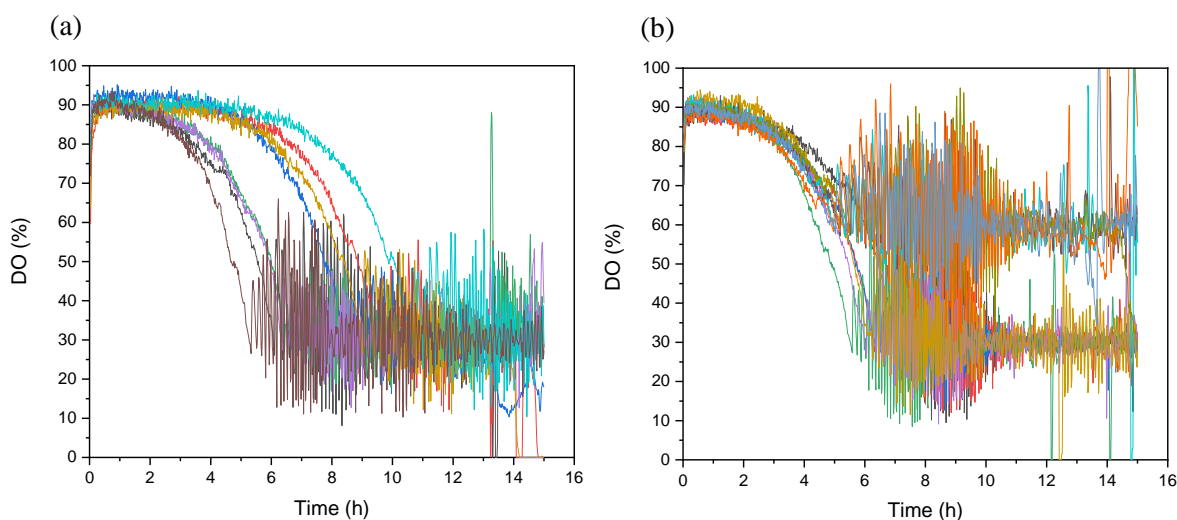
Figure 4.1. DO profiles of the batch phase of fed-batch microbioreactor fermentations inoculated with seed cultures with and without a temperature step-down. (a) DO profiles for eight Micro-24 batch fermentations inoculated with seed cultures grown at 37°C for 3 hours and then 30°C for 3 hours. (b) DO profiles for eight Micro-24 batch fermentations inoculated with seed cultures grown for 7-9 hours at 30°C. The seed cultures and Micro-24 cultures were performed as described in Sections 2.2.1, and 2.6.2 and 2.6.3 respectively.

4.5. Validation of the microbioreactor feeding system

The accuracy of the syringe pump was identified as another possible cause of the well-to-well variation observed (Figure 3.11). The offset of the syringe pump was determined by measuring the volume dispensed from each of the twelve feed lines in a set time period at a range of flow rates; the flow rates tested were 10-100μL h^{-1} as the target feed flow in the microbioreactor fermentations were within this range. A calibration curve of the experimentally determined flow rate against the theoretical flow rate set on the syringe pump were generated for two glycerol feed concentrations and two needle sizes. Figure 4.2(a) shows the calibration curves generated using a 70% w/v glycerol feed with both 18 gauge needles and 20 gauge needles, and

23% glycerol feed with 20 gauge needles. Neither the amount of glycerol in the feed, and hence the viscosity, or the needle size affected the accuracy of feed delivery (Figure 4.2(a)). The calculated offset of the syringe pump, i.e. the difference between the set-point and measured values, was 3-5μL, meaning the accuracy of feed delivery improved with increasing flow rate.

It was also observed that the reproducibility across the twelve channels deteriorated at flow rates below 20μL h^{-1} (data not shown). The post-induction flow rate used for all microbioreactor fermentations prior to these validation experiments was only 14μL h^{-1}, which may have caused variation in feed delivery and therefore dAb expression. A diluted feed at higher flow rates was therefore used for all subsequent fermentations; a 33% feed (23% w/v glycerol) was selected based on the accuracy of the syringe pump, a working volume of 3-5mL, and the maximum syringe volume of 3mL. The feed rates were also corrected to account for the offset of the syringe pump. To accommodate the increased volume of feed added to each well using the 23% w/v feed compared to the 70% w/v feed, 1mL of culture broth was removed prior to feeding.

The influence of needle size on drop formation was investigated to establish if narrower bore needles would reduce the drop size creating a more continuous feed delivery. It was hypothesised that this would reduce the fluctuations in oxygen demand of the cells and therefore improve the DO control. Figure 4.2(b) shows that the drops formed using the 20 gauge needles were 8-10μL in volume, and approximately half the size of the drops formed using the 18 gauge needles (~20μL). Figure 4.3 shows a DO profile and corresponding oxygen flow profile of a one hour period post-induction of three microbioreactor fed wells, at a DO set point of 30% using 20 gauge needles. The variation in the DO was between 10-80%, and the variation in the oxygen flow rate was between 0-3 mL min^{-1}. Assuming each trough of the DO profile (or peak of the oxygen flow profile) corresponds to a feed drop addition, then the drop size would be 1.5-3μL; it is likely the reduction in surface tension caused by the orbital shaking results in a decrease in drop size compared to drop formation under static conditions (Tolman, 1949; Navascues, 1979). This suggests that the needle bore size is unlikely to make a significant difference to the DO control as frequency of feed drop addition is primarily determined by the shaking frequency.

The sterility of the feeding system was validated by performing an incubation in the absence of cells. Six wells filled with complex media were fed with 70% w/v glycerol feed at 37°C for 27 hours. To establish the source of any contamination, media control and feed control wells were also run; the feed control wells had the equivalent total volume of feed added by the syringe pump added manually at the start of the run, and the media control wells contained complex media only. This meant that the source of any contamination cold be traced back to the media, the feed, or the bespoke feeding system. Figure 4.4(a) shows that the biomass concentration remained minimal under all conditions with OD$_{600}$ values of <0.1 in all cases. Variation in the

OD$_{600}$ values could be due to the evaporation during the incubation, resulting in the media becoming more concentrated than the media used to zero the spectrophotometer. The DO also remained constant confirming that the feeding system remained sterile (Figure 4.4(b)).

(a)

(b)
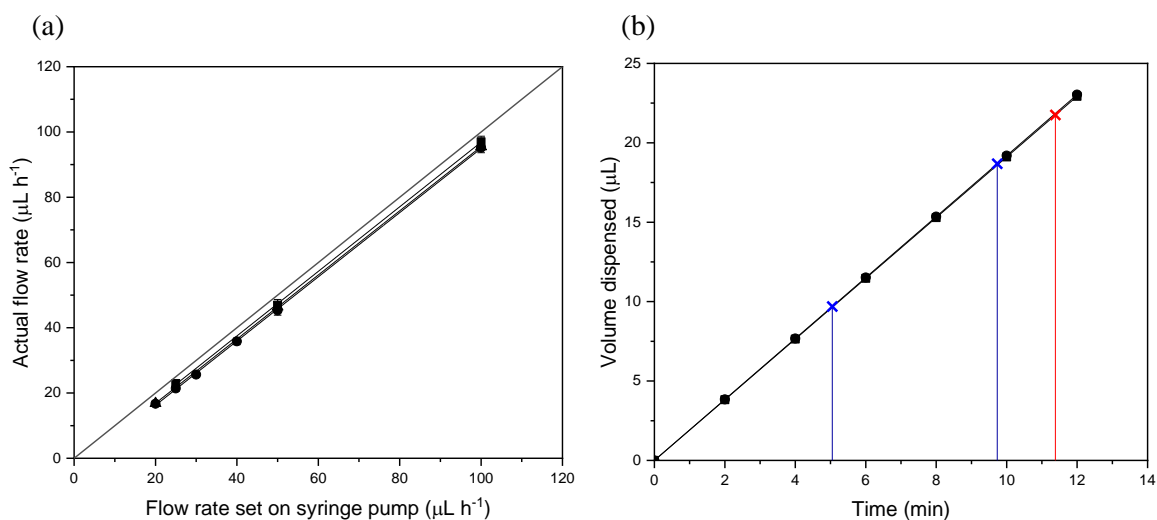
Figure 4.2. Validation of the Micro-24 feeding system syringe pump. (a) Calibration curve of the actual flow rate against the theoretical flow rate with: 70% w/v glycerol, 18 gauge needles (■), 23% w/v glycerol, 18 gauge needles (●) and 23% glycerol, 18 gauge needles (▲). The calibration curve was generated as described in Section 2.6.1.3. The error bars represent one standard deviation about the mean (n = 11-12). (b) Drop size approximation with 18 gauge needles and 20 gauge needles. Volume dispensed using the 18 gauge needles (■), and the volume dispensed using the 20G needles (●) over a 12 minute period at a flow rate of 120μL h^{-1}. The red cross with vertical line indicates the drop formed using the 18 gauge needles, and the blue crosses with vertical lines represent the drops formed using the 20G needles. The drop size was approximated by recording the drop formation on the needle to determine the time taken for a drop to form at 120μL h^{-1}. The drop formation experiments were performed as described in Section 2.6.1.4
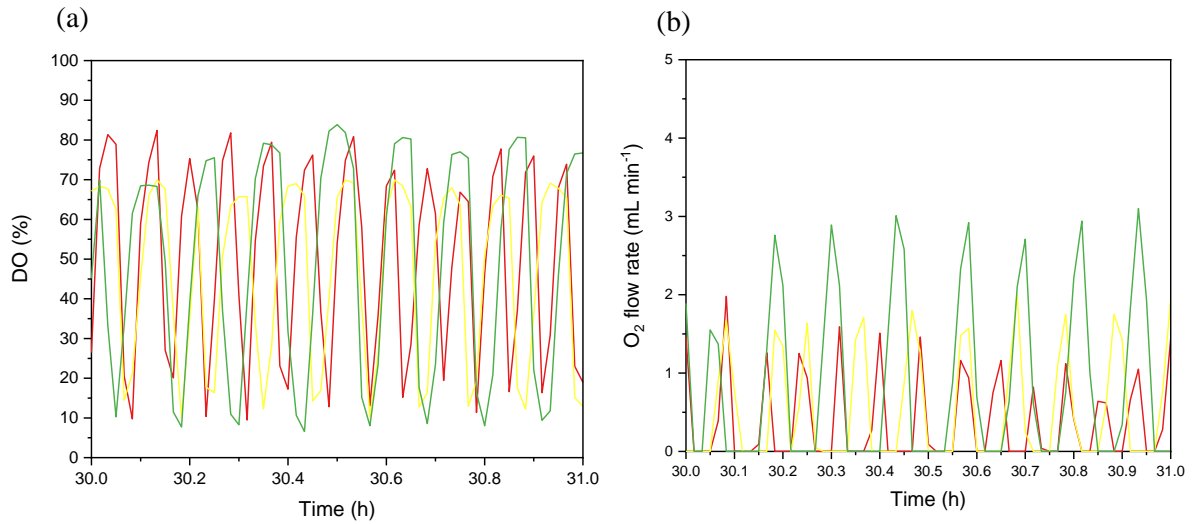
Figure 4.3. DO and oxygen flow rate profiles of a one hour period post-induction of three wells from a standard Micro-24 fed-batch fermentation. (a) DO profiles and (b) oxygen flow rate profiles. The fermentations were carried out as described in Section 2.6.3.3.
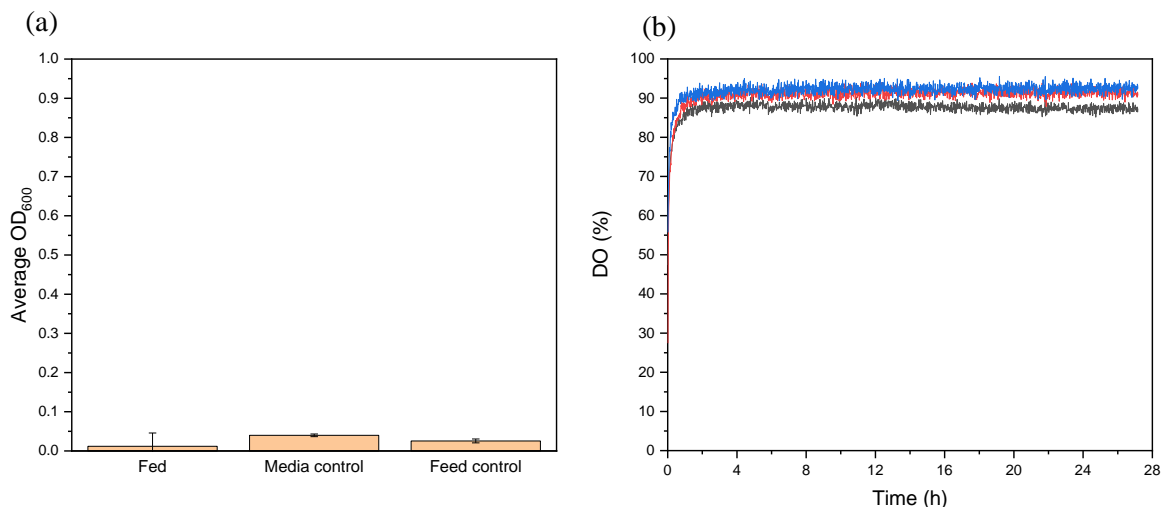
Figure 4.4. Sterility validation of the Micro-24 direct feeding system. (a) OD_{600} values of the fed wells and media and feed controls after the 27-hour incubation at 37°C. The error bars represent one standard deviation from the mean (n = 6). (b) Example DO profiles of the fed wells and media and feed controls for the 27-hour incubation at 37°C. The incubations were performed as described in Section 2.6.1.5, and the OD_{600} values were measured as described in Section 2.10.1.

4.6.   Microbioreactor evaporation rate

Evaporation during fermentation is proportionally greater at microscale compared to laboratory or pilot scale, due to the higher surface-area-to-volume ratio. Evaporation is not normally an issue in batch cultures, however it can have a significant impact in fed-batch cultures due to the extended culture times, if volume loss is not compensated for with feed addition (Silk *et al.*, 2010). The REG cassette evaporation rate was investigated using a 3-factor-2-level, face-centered, central composite experimental design (fcCCD) with six centre points as described in Section 2.6.3.5 The factors investigated were operating temperature (28-32°C), total gas flow rate (0-15mL min^{-1}), and fill volume (3-5mL). The factor ranges were sected based on the operating conditions used for a standard microbioreactor fed-batch fermentation.

The operating temperature and the total gas flow rate both had a significant effect on evaporation rate, with p-values of 0.0004 and <0.0001 respectively (Figure 4.5 and Table A.1 Appendix A). The fill volume did not have a significant effect on evaporation rate over the volume range tested (3-5mL); however the percentage volume loss will increase at lower fill volume, and therefore the concentration factor will be greater.   There was an interaction between total gas flow rate and temperature (p = 0.0002); the total gas flow rate had a greater effect on the evaporation rate at higher operating temperatures (Figure 4.5.). At high gas flow rates, less convection will occur in the headspace and therefore there will be less re-condensation, and the overall evaporation rate will be higher (Shepherd, Hadlock and Brewer, 1938; El-Dessouky *et al.*, 2002). This effect will be enhanced at higher temperatures where evaporation from the liquid into the headspace is greater (Figure 4.5 and Table A.1 Appendix A).

The total gas flow rate during a standard fed-batch fermentation was determined to be 1-9mL min^{-1} from total gas volume data for ten wells. At a fill volume of 4mL and operating temperature of 30°C, the model predicts an evaporation rate of 363-561µL day^{-1} for the highest total gas flow rate of 9mL min^{-1}. In a standard fed-batch fermentation using the 33% diluted feed an average of ~505µL of feed is added per day; therefore, the feed additions should compensate for any evaporation during the microbioreactor fermentations.
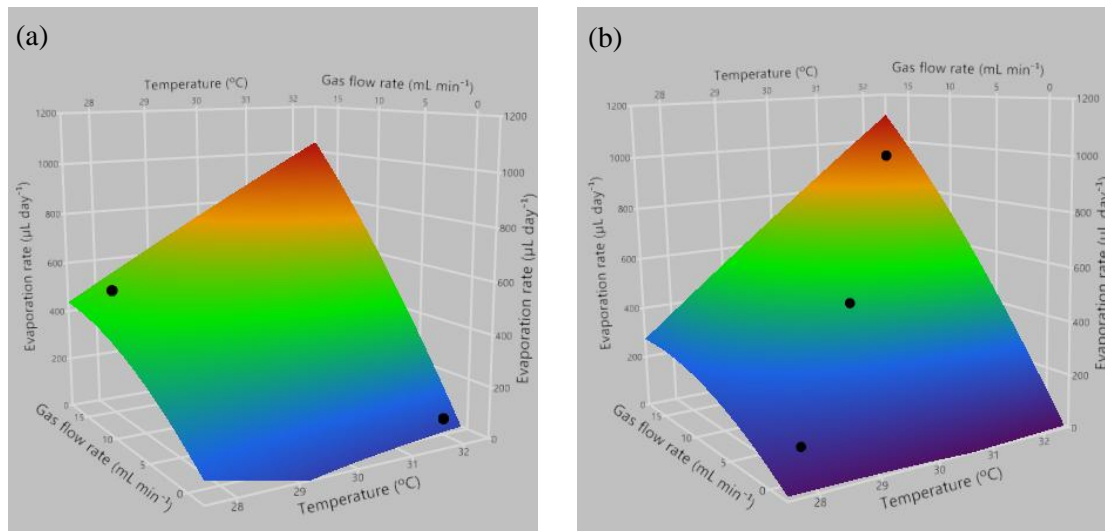
Figure 4.5. Micro-24 evaporation rate data using a REG cassette. (a) Response surface for temperature and total gas flow rate at a 3mL fill volume; (b) response surface for temperature and total gas flow rate at a 5mL fill volume. All experiments were run at 800rpm. A 3-factor-2-level, face-centered, central composite design (fcCCD) with six centre points was used, and the DoE design was run in duplicate. The DoE response models were generated using JMP® 13 software (SAS Institute, North Carolina, USA). These experiments were performed as described in Section 2.6.3.5 The black dots represent the experimental data points.

4.7. Feeding strategy optimisation

Acetate inhibits cell growth and recombinant protein expression by saturation of the TCA cycle, the electron transport chain or a combination of both (Contiero *et al.*, 2000). Various strategies have been employed to overcome acetate inhibition (Section 1.7.1):

- Maintaining the growth rate below the minimum rate for acetate production, the critical growth rate (μ_{crit}), via feed rate in the case of fed-bath cultures or dilution rate for chemostat cultures (Jensen and Carlsen, 1990).
- Utilisation of other carbon sources such as glycerol.
- The use of genetically engineered strains lacking enzymes involved in acetate production such as phosphotransacetylase (PTA) (Contiero *et al.*, 2000) .

To investigate whether acetate accumulation was affecting the reproducibility of the microbioreactor, the acetate concentration during a batch fermentation was measured (Section 2.10.7.2). Figure 4.6(a) shows that the end-of-batch (EOB), pre-feeding, acetate concentration at 14 hours was 9-14 g L^{-1}. Table 2.1 summarises the inhibitory concentrations of acetate reported in the literature and the effects on cell growth and/or product expression. Acetate concentrations of 0.3 g L^{-1} have been shown to inhibit cell growth, and concentrations of 2 g L^{-}

[1]or above have been shown to inhibit product expression (Table 4.1); therefore, the acetate accumulation in the microbioreactor is likely to be inhibitory to both cell growth and product expression. The EOB acetate concentration at 1L scale was ~0.2 g L^{-1} (Figure 4.6(b)), and the maximum acetate concentration was 2 g L^{-1}. This is consistent with the higher end-of -batch biomass concentration at 1L scale of ~27 g L^{-1}, compared to 14-17 g L^{-1} in the microbioreactor (Figure 4.6). This corresponds to a yield of biomass on glycerol of 0.99 g g^{-1} for the 1L-scale process and 0.63 g g^{-1} for the microbioreactor process.

It was hypothesised that the higher EOB acetate concentration in the microbioreactor compared to the 1L scale process could be due to DO in the microbioreactor oscillating below the 30% set point (Figures 4.3). To investigate if this, microbioreactor fermentations were performed at a DO set point of 60%, to ensure the DO remained above 30% for the duration of the fermentation. Wells where the pH and/or control failed at any point during the fermentation were excluded. The EOB acetate concentration was generally higher at DO set point of 30% compared to a DO set point of 60% , however in both cases, there was significant well-to-well variation, with CVs of 20% (n = 3) and 47% (n = 6) for the cultures at a DO set points of 30% and 60% respectively. After a further 6 hours, the acetate concentration dropped in both cases as previously observed (Figures 4.6(a) and 4.7); at a DO set point of 60% the acetate had been almost completely consumed (0.2-1.2 g L^{-1}), whereas at 30% there was still 1-9 g L^{-1} in the culture broth (Figure 4.7).

To reduce the acetate concentration during the pre-induction fed-batch phase, the DO set point was increased to 60%, and a hold period was implemented to allow the acetate that accumulated in the batch phase to be consumed by the cells before feeding commenced. To determine the minimum hold period duration required so that the pre-feeding acetate concentration was not inhibitory to cell growth or dAb expression, 3 and 5-hour hold periods were investigated (Figure 4.8). Figure 4.8(a) shows that the implementation of a 3- or 5-hour hold did not affect cell growth with pre-induction OD_{600} values of 50-70 in both cases. Figure 4.8(b) shows that dAb expression was inhibited with increasing acetate concentration. A similar relationship is apparent between the pre-feeding acetate concentration and pre-induction OD_{600} values, indicating that the primary reason for variation in dAb expression is due to the variation in the pre-induction biomass concentration (Figure 4.8(c)), caused by the inconsistencies in the pre-feeding acetate concentration. Figures 4.8(b) and (c) indicate that the pre-feeding acetate becomes inhibitory at concentrations of 0.5 to 1 g L^{-1}. The acetate concentration was consistently below 1 g L^{-1} with a 5-hour hold time, however was much more variable with a 3-hour hold time at 1 to 6 g L^{-1} (Figures 4.8b and c). A 5-hour pre-feeding hold time was used for all subsequent microbioreactor fed-batch fermentations.

A reduced pre-induction feed rate equivalent to the 1L scale process per gram of DCW was also tested, to determine if overfeeding may be causing variation in the pre-induction biomass concentration (Figure 4.8). Figure 4.8 shows that the reduced feed rate did not affect the pre-induction biomass concentration or dAb expession; however the yield of biomass on glycerol ($Y_{x/s}$) was enhanced, as a comparable biomass concentration was achieved with approximately a 27% reduction in the glycerol added (Figure 4.8(a)). A pre-induction feed-rate equivalent to the 1L-scale process per gram of biomass was used for all subsequent microbioreactor fed-batch cultures.
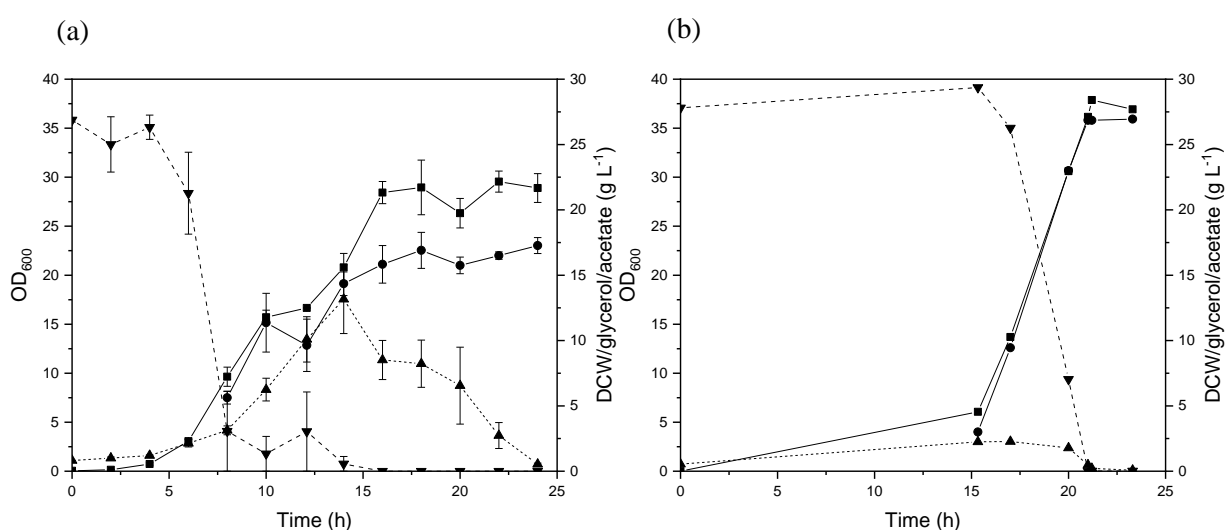
Figure 4.6. Cell growth and metabolite profiles for Micro-24 and 1L batch fermentations. (a) Micro-24 OD_{600} (■ with solid line), DCW (● with solid line), glycerol concentration (▼ with dashed line), and acetate concentration (▲ with dashed line). Two fermentations were combined to generate the 24-hour profiles. Four wells were sacrificed at each time point. The error bars represent one standard deviation from the mean (n = 2-4). (b) 1L scale OD_{600} (■ with solid line), DCW (● with solid line), glycerol concentration (▼ with dashed line), and acetate concentration (▲ with dashed line) (n = 1). The fermentations were performed as described in Sections 2.6.3.2, and the analytical assays were carried out as described in Section 2.10., with the exception that OD_{600} samples were diluted in complex media instead of PBS.
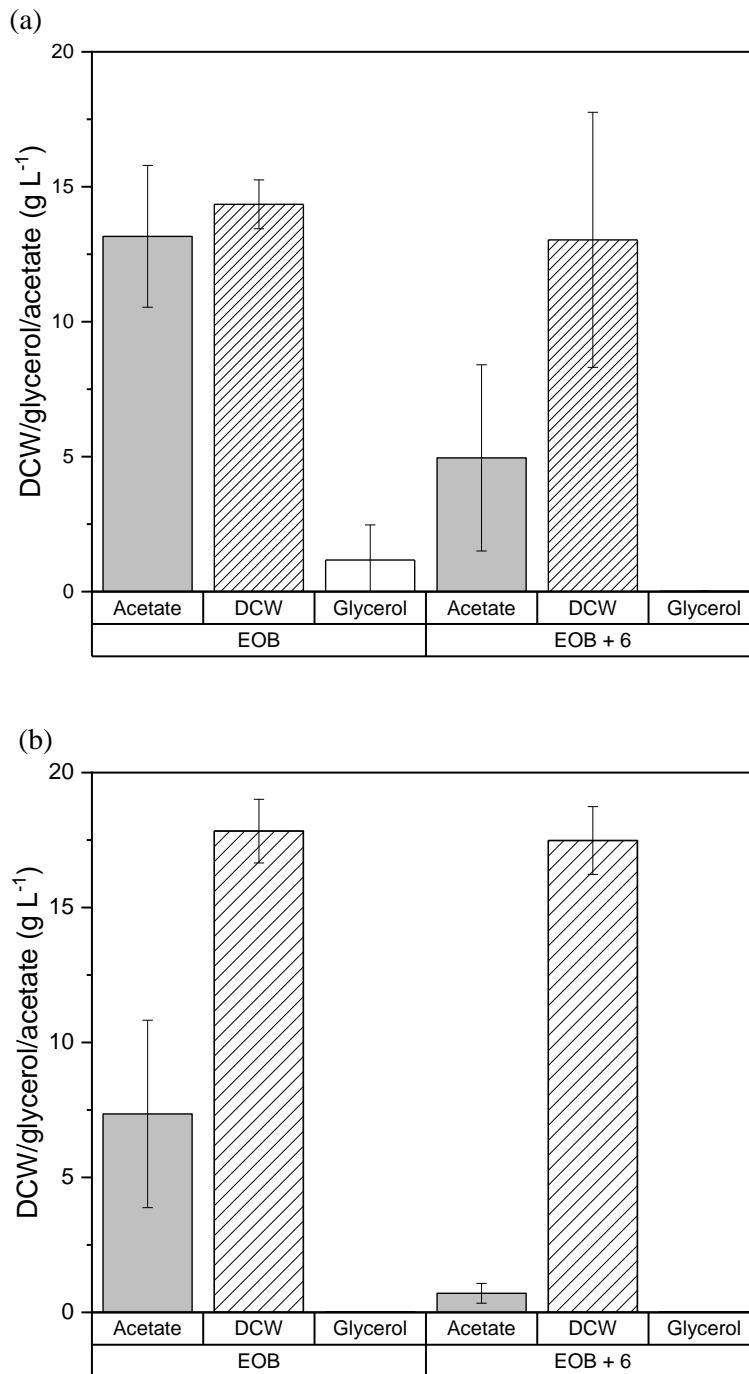
Figure 4.7. Micro-24 batch fermentations with DO set points of 30% and 60%. (a) EOB and EOB + 6 hours DCW, glycerol and acetate concentrations for the set point of 30%. (b) EOB and EOB + 6 hours DCW, glycerol and acetate concentrations for the set point of 60%. The error bars represent one standard deviation from the mean (n = 4-6). The fermentations were performed as described in Section 2.6.3.2 and the analytical assays were performed in Section 2.10.

Table 4.1. Summary of acetate inhibition of cell growth and product expression reported in the literature.

Author	Expression system	Vessel type	Mode of operation	Batch media	Feed	Critical growth rate (μ_{crit}) (h^{-1})	Inhibitory effect of acetate on cell growth	Inhibitory effect of acetate on product expression
Jensen & Carlsen (1990)	*E. coli* MclO61 strain producing X-hGH	1.3L STR	Chemostat	Complex (glucose) (sodium acetate added)	NA	0.4	72% reduction at >6g L^{-1} acetate	86% reduction at >6g L^{-1} acetate 33% reduction >2.4g L^{-1} acetate
Pan *et al.* (1987)	*E. coli* B 54125	Shake flask	Batch	Minimal (glucose) and complex (glucose)	NA	NR	Reduction <2 g L^{-1} acetate (more pronounced with complex media)	NA
Mayer *et al.* (2014)	*E. coli* strain producing interferon	STR	Chemostat	Minimal (glucose) and complex (glucose)	NA	0.4 (minimal media) 0.2 (complex media)	25% reduction at 0.3 g L^{-1} acetate (minimal media) NR for complex media	NR
Luli & Strohl (1990)	Various *E. Coli strains* producing a delta endotoxin	10L STR	Batch	Complex (glucose)	Glucose	NR	Reduction at > 5 g l^{-1} acetate (based on acetate inhibition model derived from experimental data.	NR

Author	Expression system	Vessel type	Mode of operation	Batch media	Feed	Critical growth rate (μ_{crit}) (h^{-1})	Inhibitory effect of acetate on cell growth	Inhibitory effect of acetate on product expression
Landwall & Holme (1977)	*E. coli* B	2.5L and 1L STRs	Fed-batch (with and without dialysis)	Defined (glucose)	Glucose	NR	350% increase in biomass concentration with dialysis with a 1:11 volume ratio (acetate concentrations of 10 g L^{-1} and 0.2 g L^{-1} for cultures without and with dialysis)	NA
Macdonald & Neway (1990)	*E. coli* MM-294-1 producing interleukin-2	14L STR (3 Ruston turbines)	Fed-batch (glucose maintained to 8 ±1 g L^{-1}) and chemostat	Defined (glucose)	Glucose	NR	NR	Reduction in IL-2 expression (% of total protein) at 50mM-100mM (3-6 g L^{-1}) acetate
Lasko *et al.* (2000)	Various wild type *E. coli* strains	250mL STR	Batch	Complex (glucose/glycerol)	N/A	NR	Growth rate decreases linearly from ~0.8 to ~0.4 at acetate concentrations of 0-12 g L^{-1} in the presence of glycerol. Growth rate decreases exponentially from ~0.7 to ~0.02 at acetate concentrations of 0-9 g L^{-1} in the presence of glucose.	NA

Author	Expression system	Vessel type	Mode of operation	Batch media	Feed	Critical growth rate (μ_{crit}) (h^{-1})	Inhibitory effect of acetate on cell growth	Inhibitory effect of acetate on product expression
Nakano *et al.* (1997)	*E. coli* K12	Shake flask and 1L STR	Batch	Defined (glucose/glycerol 40% w/v)	NA	NR	Shake flask: Inhibition of cell growth > 1 g L^{-1} acetate (glycerol), and >0.5 g L^{-1} acetate (glucose) STR: 20% reduction at ~5 g L^{-1} acetate (glucose)	NA
Sun *et al.* (1993)	*E. coli* JM109 and RR1 producing TGFα-PE40	Shake flask 23L STR	Batch	Complex medium (glucose)	NA	NR	Reduction in cell growth of JM109 in shake flasks and STR at 2 g L^{-1} (acetate)	38.0% reduction TGFα-PE40 in JM109 in shake flasks and 38.6% reduction in the STR at 2 g L^{-1} acetate 21.2% Reduction in TGFα-PE40 expression in RR1 in shake flasks at 5 g L^{-1} acetate
Turner *et al.* (1994)	*E. coli* JM107 producing α-amylase	14L STR	chemostat (sodium acetate added)	Defined (galactose)	NA	NR	11.6% reduction in growth rate at 5 g L^{-1} acetate and 50% decrease at 8 g L^{-1} acetate	α-amylase expression was almost completely inhibited at 7.4 g L^{-1} acetate and started again at acetate concentration < 1 g L^{-1}.

Author	Expression system	Vessel type	Mode of operation	Batch media	Feed	Critical growth rate (μ_{crit}) (h^{-1})	Inhibitory effect of acetate on cell growth	Inhibitory effect of acetate on product expression
Yang (1992)	*E. coli* XL1-Blue producing β-galactosidase	Shake flask, 2.5L STR	Complex (glucose)	Batch (shake flask), fed-batch (STR)	Glucose	0.1	~50% reduction in biomass with 20mM (1.18 g L^{-1}) acetate addition in shake flasks	~50% reduction in β-galactosidase at μ > 0.1 h^{-1}
Shimizu *et al.* (1988)	*E. coli* HB101 producing β-galactosidase	2L STR	Complex (glucose)	Fed-batch	Glucose	NR	Cell growth stopped at 0.23M (~13.6 g L^{-1}) acetate in fed-batch cultures using the STR	β-galactosidase production decreased with 0.17M (~10 g L^{-1}) acetate

(a)

(b)

(c)
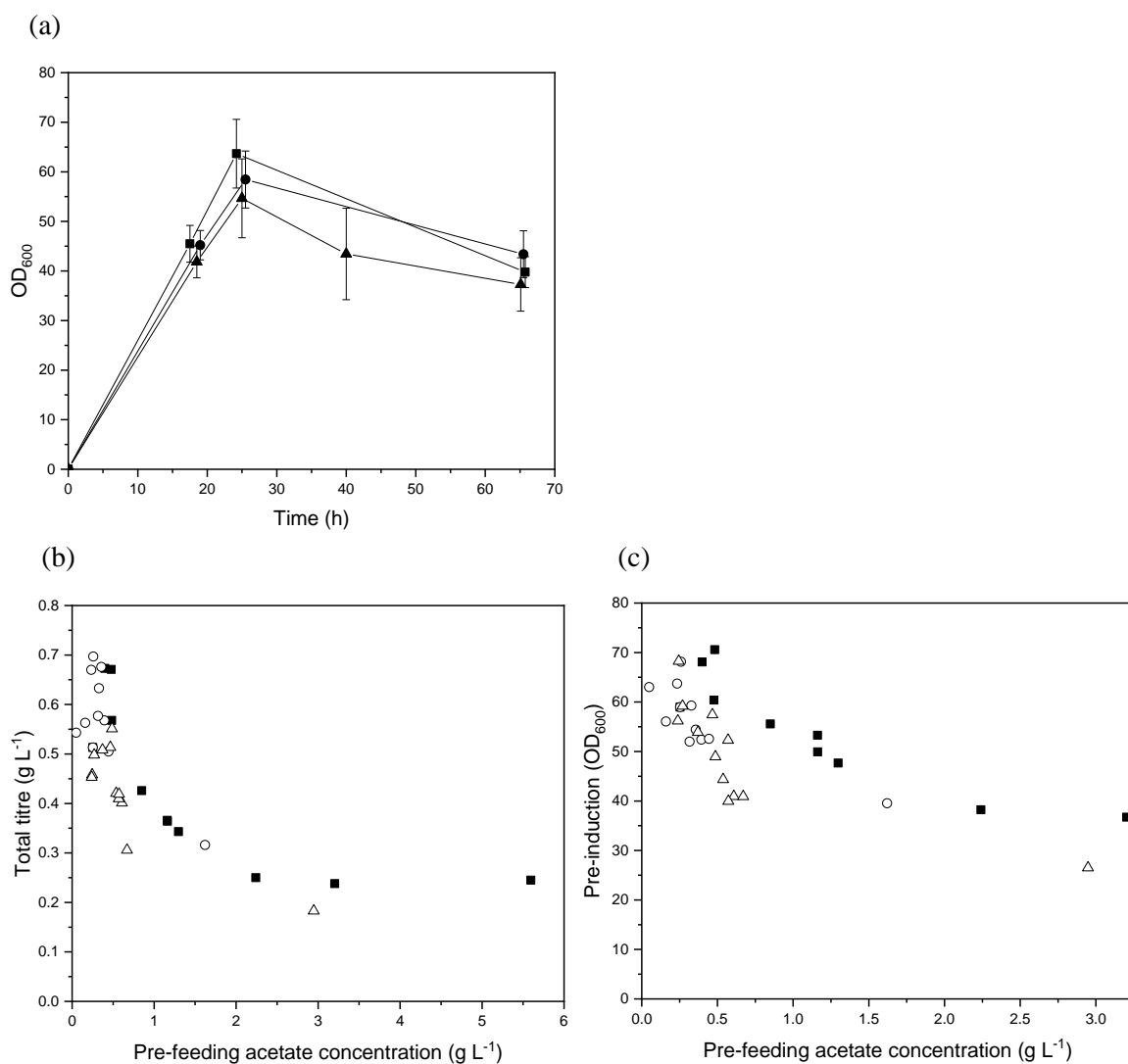
Figure 4.8. Micro-24 fed-batch fermentations with a 3-hour hold time, 5-hour hold time, and 5-hour hold time with a reduced pre-induction feed rate. (a) Micro-24 OD_{600} values for fermentations with a 3-hour hold time (■), 5-hour hold time (●), and 5-hour hold time with a reduced pre-induction feed rate (▲). The error bars represent one standard deviation from the mean (n = 5-10). (b) Total dAb titre against pre-feeding acetate concentration for fermentations with a 3-hour hold time (■), 5-hour hold time (○), and 5-hour hold time with a reduced pre-induction feed rate (Δ). (c) Pre-induction OD_{600} against pre-feeding acetate concentration for fermentations with a 3-hour hold time (■), 5-hour hold time (○), and 5-hour hold time with a reduced pre-induction feed rate (Δ). The data for all fed wells is included in (b) and (c). The fermentations were performed as described in Sections 2.6.3.3 and 2.6.3.4., and the analytical assays were performed in Section 2.10.

4.8. Microbioreactor reproducibility and data exclusion criteria

Due to the well-to-well variation observed in the microbioreactor, a set of well exclusion criteria were defined. This enabled a rational and consistent approach to data exclusion from anomalous wells. Wells where there was a loss of pH control at any point during the fermentation were excluded as previously described (Section 4.7). Based on the acetate inhibition data described in Section 4.7, wells with a pre-feeding acetate concentration of >1g L^{-1} were also excluded. Figure 4.9(a) shows the cell growth profiles for four wells from two identical experiments; wells 1 and 3 are from one experiment and Wells 2 and 4 are from a repeat run. Wells 1 and 3 both had a pre-feeding acetate concentration of 0.66 g L^{-1}, and wells 2 and 4 had a pre-feeding acetate concentration of 0.95 g L^{-1} and 1.19 g L^{-1} respectively. Figure 4.9(a) shows that the biomass concentration did not increase in the pre-induction fed-batch phase in wells 2 and 4 which had a pre-feeding acetate concentration of ~1 g L^{-1}; however there was a significant increase in biomass towards the end of the culture. The SPRs of the cultures with a high harvest biomass concentration due to growth late in the fermentation were significantly lower than the cultures where no late cell growth was observed (Figure 4.9(c)). This suggests either plasmid loss, or a mixture of culturable and viable but not culturable (VBNC) cells were present.

Plasmid stability analysis was performed to determine if the cell growth towards the end of the culture was due to plasmid loss. Figure 4.9(b) shows that the number of colony forming units (CFUs) was similar with and without tetracycline for all wells, indicating that the plasmid had not been lost. The number of CFUs was significantly less for the wells with a higher pre-feeding acetate concentration (wells 2 and 4). This suggests that the cell population was a mixture of culturable cells and cells in a VBNC state. There are two main theories of the VBNC state of *E. coli* cells; the first is that it is a life cycle process whereby the cells can revert back to a culturable state, the second is that it is an end of life process (McDougald *et al.*, 1998). Studies have indicated that resuscitation of cells in a VBNC state is due to the presence of the few remaining culturable cells, which stimulate the dormant cells by secretion of signal molecules via an unknown molecular mechanism (Kaprelyants, Mukamolova and Kell, 1994; McDougald *et al.*, 1998; Weichart and Kell, 2001; Pinto, Santos and Chambel, 2015). It has also been reported that amino acids can stimulate resuscitation (Pinto *et al.*, 2011; Pinto, Santos and Chambel, 2015). To ensure that the cultures used for process optimisation experiments were comparable, wells that did not show an increase in biomass pre-induction and then grew rapidly towards the end of the culture, were excluded from data analysis.

Figure 4.10 shows parity plots to comparing the ranking of twelve fed wells, from four different fermentations in terms of the pre-induction OD_{600} values; a ranking of 1 corresponds to the lowest OD_{600} value and a ranking of 12 corresponds to the highest OD_{600} value. The microbioreactor unit and the wells used were identical for all experiments. The wells used for

the 3-hour hold time experiments were identical and the wells used for the 5-hour hold time were also identical; however, the 3-hour and 5-hour experiments had one well different to each other. Figure 4.10 shows that there was good consistency between experiments in terms of cell growth, and generally the same wells performed well in all experiments. Thus, the same microbioreactor unit was used for all subsequent experiments so it could accurately be predicted which wells should be fed to generate the most reproducible data.
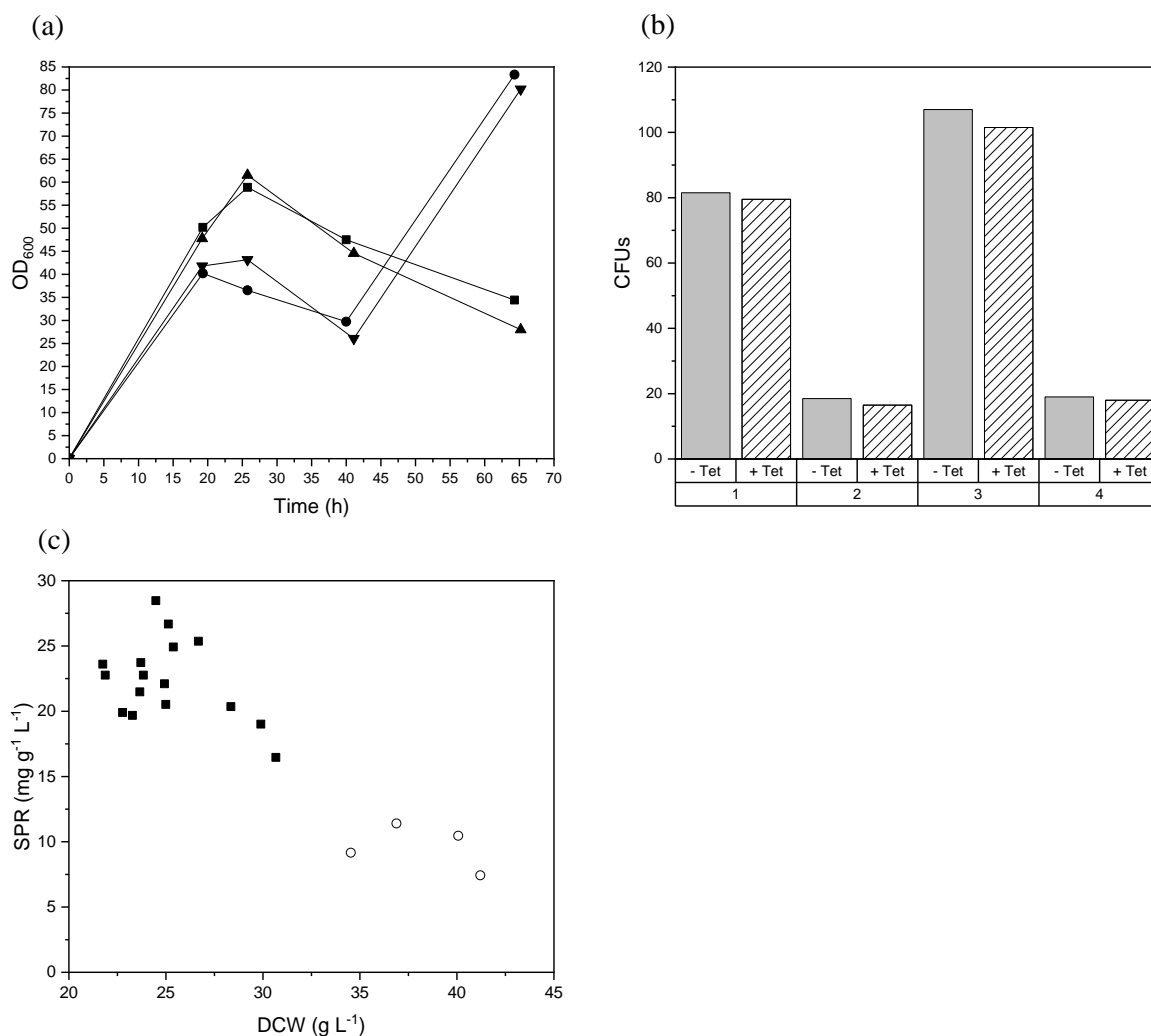
Figure 4.9. Comparison of Micro-24 cell growth, plasmid stability and product expression. (a) OD_{600} profiles of four wells from two identical experiments. Experiment 1: Well 1 (■) and Well 2 (●). Experiment 2: Well 3 (▲) and Well 4 (▼). (b) Number of CFUs grown on agar plates from harvest samples of Wells 1, 2, 3 and 4, with and without tetracycline. (c) SPR against DCW for 20 wells from two fermentations. The fermentation conditions were identical with the exception of the pre-induction feed rate (Experiment 1: 54μL h^{-1}, Experiment 2: 43μL h^{-1}). Wells without growth at the end of the fermentation (■) and wells with growth at the end of the fermentation (○). The fermentations were carried out as described in Section 2.6.3.3. and 2.6.3.4., and the analytical assays were carried out as described in Section 2.10.
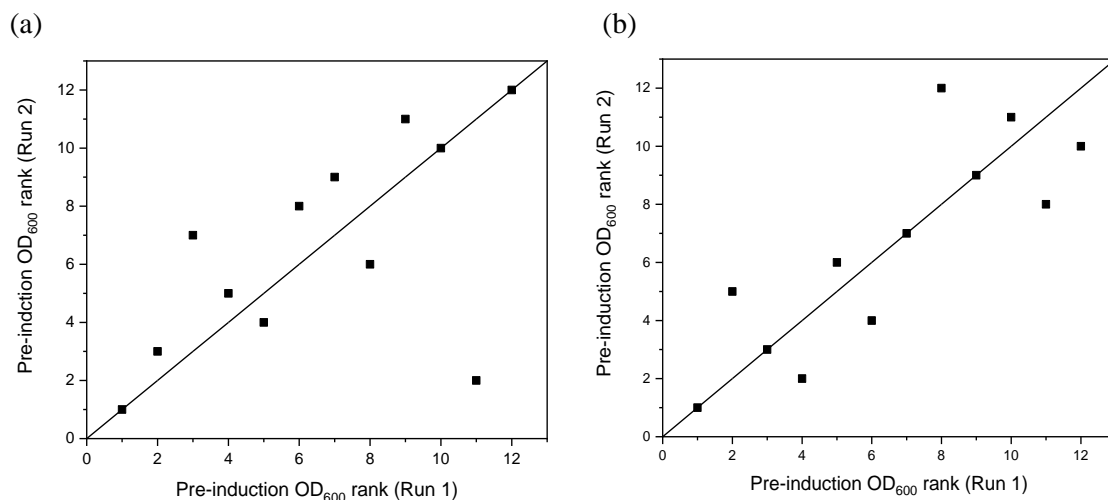
Figure 4.10. Parity plots of well rankings based on pre-induction OD_{600} values for two Micro-24 fed-batch fermentations with a 3-hour pre-feeding hold time (a), and a 5-hour pre-feeding hold time (b). 1 corresponds to the lowest pre-induction OD_{600} value and 12 corresponds to the highest pre-induction OD_{600} value. The fermentation conditions were identical for all experiments with the exception of the pre-feeding hold time, and the pre-induction feed rate of the second 5-hour hold time experiment was reduced to $43\mu L$ h^{-1} from $54\mu L$ h^{-1}. The fermentations were carried out as described as in Section 2.6.3.3. and 2.6.3.4., and the OD_{600} values were measured as described in Section 2.10.1.

4.9.   Optimised microbioreactor feeding strategy

Figures 4.11 and 4.12 show the final microbioreactor feeding strategy and bespoke feed delivery system as described in Sections 4.2-4.7, which were used for all subsequent microbioreactor fermentations. Data from certain wells were excluded based on the exclusion criteria described in Section 4.8. The maximum number of wells that can be fed in parallel is twelve, due to the practicality of sampling and the requirement of a second syringe pump with more than twelve fed wells.
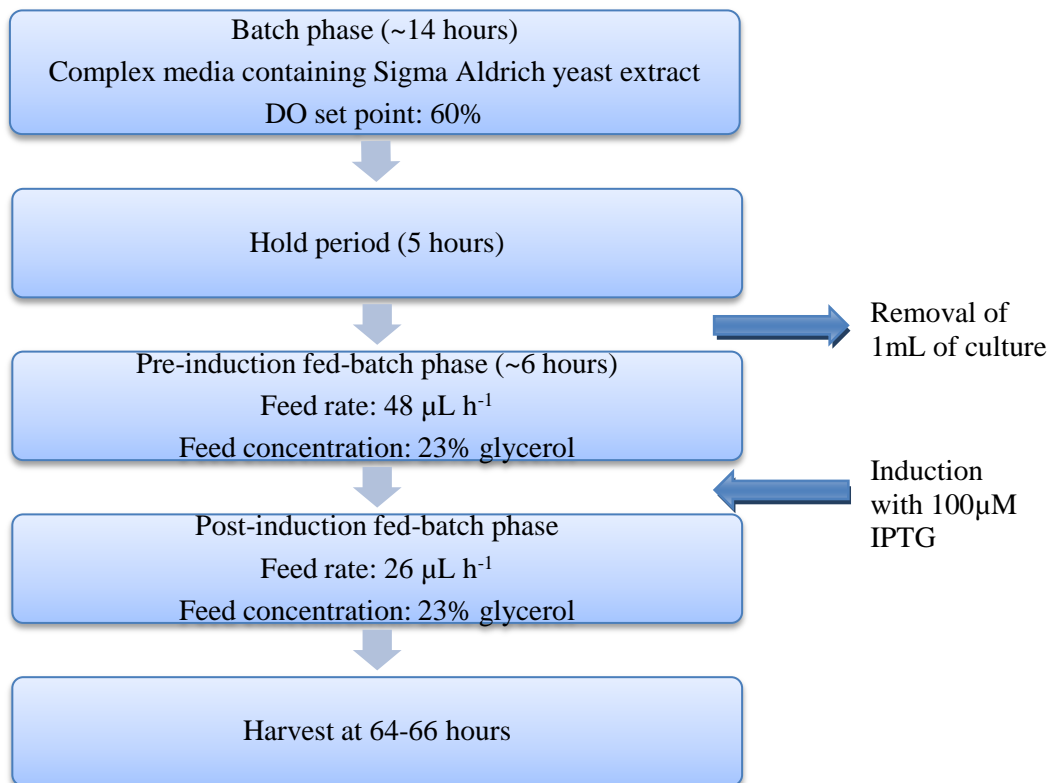
Figure 4.11. Final Micro-24 fed-batch feeding strategy. The fermentation conditions were performed as described as in Section 2.6.3.4
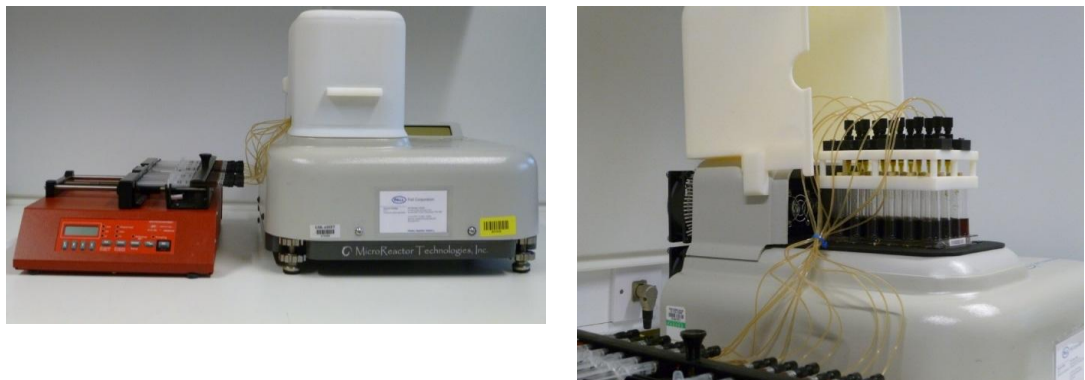
Figure 4.12. Final Micro-24 bespoke feed delivery system with twelve feed lines. The feeding device and temperature control lid and stand were designed using SpaceClaim 3D Modelling software and were printed out of VeroWhitePlus[TM] (stand and lid) and VeroBlackPlus[TM]. The connectors are ethylene ETFE Upchurch Scientific connectors and the tubing was ETFE Tefzel® HPLC tubing.

4.10.   Application of the microbioreactor feeding system for process optimisation

Having optimised the microbioreactor feeding system, its application for fed-batch fermentation process optimisation was examined. Two factors were investigated: post-induction temperature and IPTG concentration, based on previous knowledge of the dAb expression system. Due to the variability of the microbioreactor described in Sections 4.7. and 4.8. it was decided that only two factors would be investigated and six replicates of each condition would be performed. Post-induction temperature was selected as previous experience at 1L scale showed that post-induction temperature has a significant effect on dAb expression. IPTG concentration was selected as it is independent of the microbioreactor control loops and is known to have an impact on dAb expression levels. A 2-factor-2-level, full facetorial design was used, and the DoE design was run in duplicate as described in Section 2.7. An indentical DoE was performed at 1L scale as a comparison. In order keep the cultures under growth rate limiting conditions at both post-induction temperatures, at 25°C the feed rate was reduced by 25% based on the assumption of a temperatue coefficient (Q10) of two i.e. the rate of biochemical processes will double with a 10°C temperature increase (Hegarty, 1973; Herendeen, Vanbogelen and Neidhardt, 1979; Farewell and Neidhardt, 1998).

Figures 4.13(a) and (b) and 4.14(a) show that at both 1L scale and microbioreactor scale the post-induction conditions did not affect the post-induction biomass concentration. This is consitent with previous observations that cell growth ceases upon induction (Sections 3.2.1. and 3.2.2.). Figures 4.13(a) and (b) show that at 1L scale the total titre was 90-150% higher at a post-induction temperature of 30°C than 25°C. In addition, and a greater amount of product was extracellular at 30°C; at 30°C ~50% was extracellular, whereas only ~30% was extracellular at 25°C (Figures 4.13(c) and (d)). This is likely to due to increased leakage at 30°C caused by high periplasmic protein concentrations (Takagi *et al.*, 1988; Donovan, Robinson and Glick, 1996; Schofield *et al.*, 2016). In the microbioreactor, at both 30°C and 25°C the percentage extracellular titre was 55-70% (Figure 4.14b). This indicates that either there was increased cell lysis, or membrane permeability due to exposure to incorrectly folded protein (Skerra and Pluckthun, 1991; Donovan, Robinson and Glick, 1996). The rise in the DO observed towards the end of the microbioreactor cultures suggests cell lysis (data not shown). The microbioreactor data showed a similar trend to the 1L scale data (Figure 4.14(b)); the total titres were significantly higher at 30°C than 25°C. Data from eight out of twenty-four microbioreactor wells were excluded as described in Section 4.8. The well-to-well variation was greater at 30°C than at 25°C; at a 250μM IPTG concentration and a 30°C post-induction temperature, only one well passed the exclusion criteria.

Figure 4.15 shows the surface response plots for total titre, extracellular titre and total SPR for both the 1L scale and microbioreactor processes; the overall response surface behaviour is

comparable at both scales, (Figures 4.15(a)-(f)), however the total titres were approximately three-fold higher at 1L scale, primarily due to the lower biomass concentration attainable in the microbioreactor (Section 4.6 and Table 4.2.). The SPRs at microbioreactor scale were approximately 60% of the SPRs at 1L scale (Figures 4.15(e) and (f), and Table 4.2). This could possibly be due to cell lysis occurring earlier in the microbioreactor and to a greater degree than in the 1L scale process. It could also possibly be attributed to inclusion body formation, as inclusion bodies would have been lost in the centrifugation step after sonication of the resusupended pellets (Sharma, 1986; Weir and Sparks, 1987; Esfandiar *et al.*, 2010; Bao *et al.*, 2016; Maggi and Scotti, 2017).

At both 1L and microbioreactor scale the post-induction temperature had a significant effect on the dAb expression, however IPTG concentration did not influence dAb expression (Figure 4.15 and Tables A.2 to A.7 in Appendix A). Experiments at higher post-induction temperatures would be required to determine if 30°C is the optimum post-induction temperature, or if a higher temperature could improve productivity without causing inclusion body formation, incorrectly folded proteins or increased product degradation due to proteolytic cleavage (Cabilly, 1989; Chalmers *et al.*, 1990; Kosinski, Rinas and Bailey, 1992; Donovan, Robinson and Glick, 1996). The IPTG concentration did not have a significant effect on dAb expression, suggesting that at concentration of 100μM the IPTG was in excess, and therefore an increase in IPTG concentration did not affect dAb expression. This is consistent with model predictions by Laffend and Shuler (1994), that full induction can be achieved at IPTG concentrations of 1mM-100mM depending on the plasmid copy number. If any future experiments were to be performed, the DoE should be modified to include IPTG concentrations below 100μM, to determine if comparable or improved productivity can be achieved at a lower IPTG concentration, as this would reduce manufacturing costs.
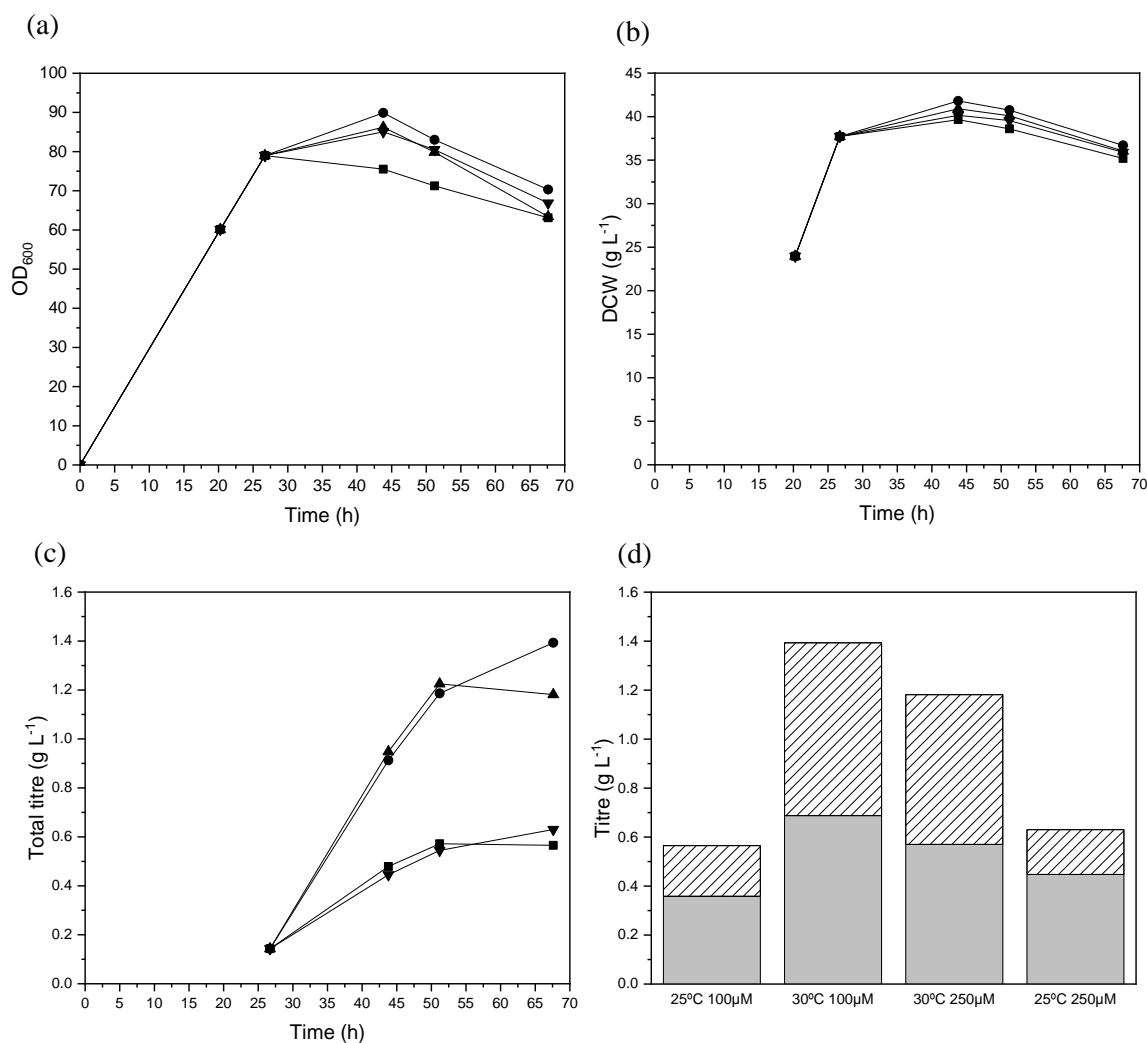
Figure 4.13. 1L-scale fed-batch fermentations at a post-induction temperature of 25°C and 30°C, and an IPTG concentration of 100μM and 250μM. (a) OD_{600} profiles for 25°C, 100μM IPTG (■), 30°C, 100μM IPTG (●), 30°C, 250μM IPTG (▲) and 25°C, 100μM IPTG (▼) . (b) DCW profiles for 25°C, 100μM IPTG (■), 30°C, 100μM IPTG (●), 30°C, 250μM IPTG (▲) and 25°C, 250μM IPTG (▼). (c) Total titre profiles for 25°C, 100μM IPTG (■), 30°C, 100μM IPTG (●), 30°C, 250μM IPTG (▲) and 25°C, 250μM IPTG (▼). (d) Breakdown of harvest intracellular and extracellular titre for 25°C, 100μM IPTG, 30°C, 100μM IPTG, 25°C, 250μM IPTG and 30°C, 250μM IPTG. The grey bars represent the intracellular titre and the dashed bars represent the extracellular titre. Each condition was run in duplicate. The fermentations were carried out as described as in Section 2.7., and the analytical assays were carried out as described in Section 2.10.
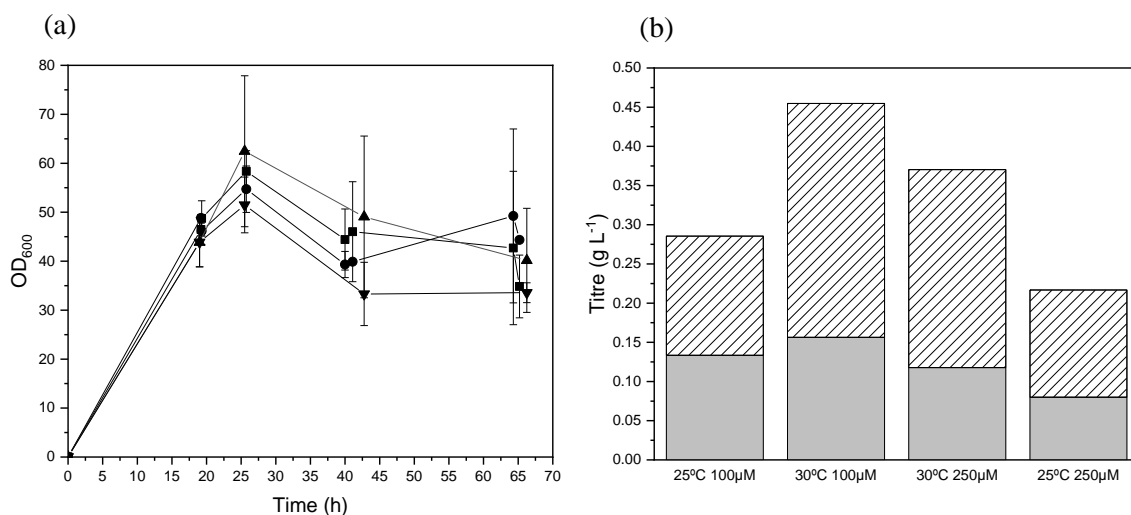
Figure 4.14. Micro-24 fed-batch fermentations at a post-induction temperature of 25°C and 30°C, and an IPTG concentration of 100μM and 250μM. (a) OD_{600} profiles for 25°C, 100μM IPTG (▲), 30°C, 100μM IPTG (■), 30°C, 250μM IPTG (●) and 25°C, 250μM IPTG (▼). (b) Breakdown of harvest intracellular and extracellular titre for 25°C, 100μM IPTG, 30°C, 100μM IPTG, 25°C, 250mM IPTG, and 30°C, 250μM IPTG. The grey bars represent the intracellular titre and the dashed bars represent the extracellular titre. The error bars represent one standard deviation from the mean (n = 1-6). The fermentations were carried out as described as in Section 2.7, and the analytical assays were carried out as described in Section 2.10.

Table 4.2. Comparison of the final biomass concentrations, titres and SPRs ac achieved using the 1L bioreactor and microbioreactor, under the conditions evaluated in the DoE (Section 4.10)

Post-induction temperature (°C)	IPTG concentration (μM)	X_{final} (g L^{-1})		Total titre (g L^{-1})		Extracellular titre (g L^{-1})		Total SPR (mg g^{-1} L^{-1})	
		1L scale	Microbioreactor (4mL)	1L scale	Microbioreactor (4mL)	1L scale	Microbioreactor (4mL)	1L scale	Microbioreactor (4mL)
30	100	36.70	24.23	1.393	0.455	0.705	0.298	37.93	21.83
30	250	40.90	25.71	1.181	0.370	0.611	0.253	32.77	16.30
25	100	36.05	24.00	0.565	0.285	0.207	0.152	16.19	11.64
25	250	35.90	23.08	0.630	0.217	0.183	0.137	17.54	9.67
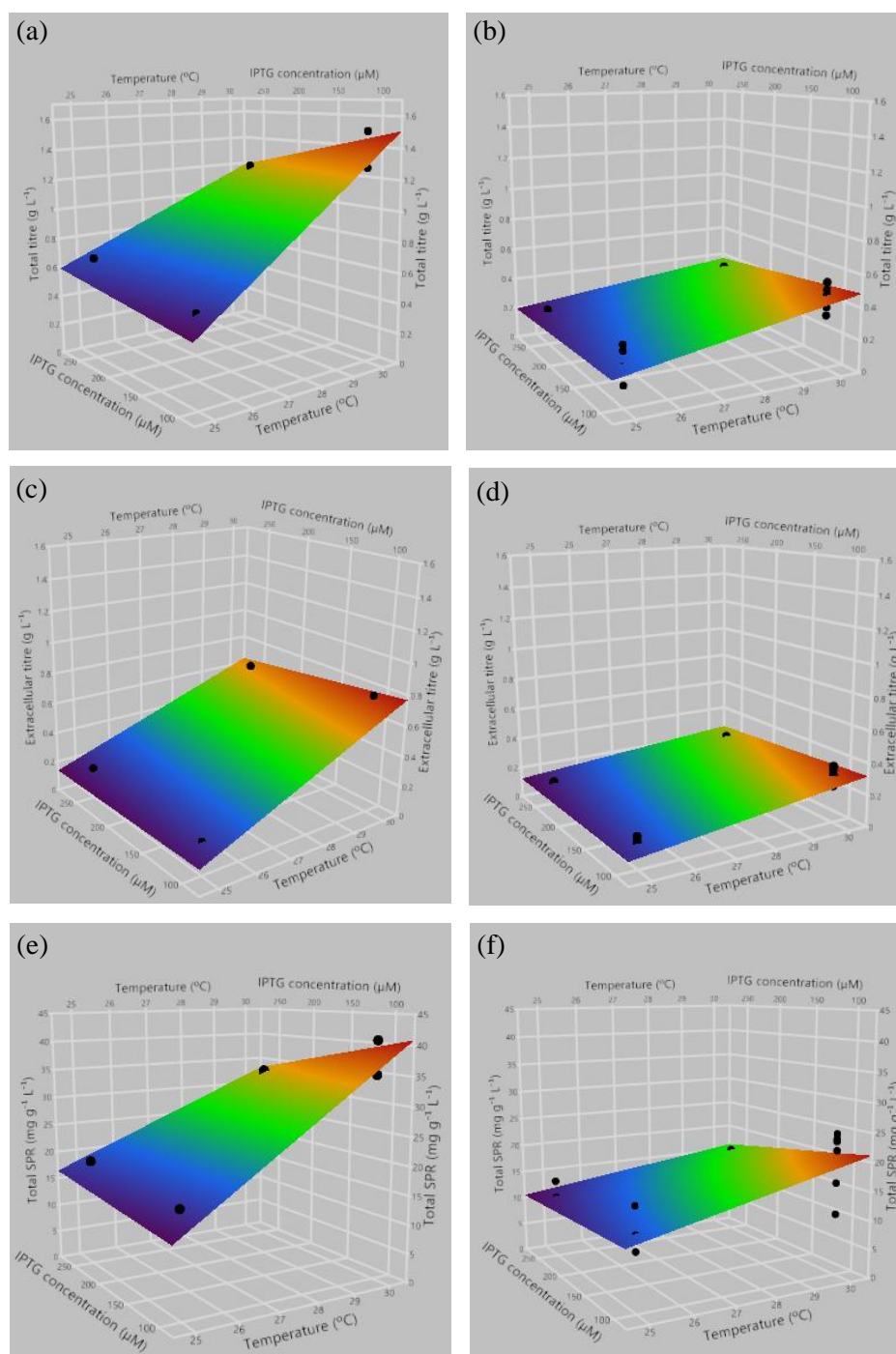
Figure 4.15. 1L scale and Micro-24 process optimisation DoE surface response plots for total titre, extracellular titre and total SPR. (a) 1L scale total titre surface response plot showing the effect of post-induction temperature and IPTG; (b) equivalent Micro-24 total titre surface response plot; (c) 1L scale extracellular titre surface response plot showing the effect of post-induction temperature and IPTG; (d) equivalent Micro-24 extracellular titre surface response plot; (e) 1L scale total SPR surface response plot showing the effect of post-induction temperature and IPTG; (f) equivalent Micro-24 total SPR surface response plot. A 2-factor-2-level, full facetorial design was used, and the DoE design was performed in duplicate. The DoE response models were generated using JMP® 13 software (SAS Institute, North Carolina, USA). These experiments were performed as described in Section 2.7, and the analytical assays were carried out as described in Section 2.10.

4.11. Summary

The aim of this chapter was to refine the direct feeding strategy to establish industrially relevant *E. coli* cultures in the microbioreactor, that were comparable to a laboratory scale fed-batch process in terms of cell growth, product expression and DO control. A feeding strategy was established for the microbioreactor by developing a bespoke feed delivery system, and refining the feeding strategy in terms of feed rate and concentration, concentration of inhibitory by-products, and dissolved oxygen control. The observed well-to-well variation in cell growth and product expression was shown to be caused by high acetate levels pre-feeding. The reproducibility was improved by increasing the DO set point to 60%, and the implementation of a 5-hour hold period for acetate consumption.

The source of the variation in the pre-feeding acetate concentration appears to the inherent to the microbioreactor, as wells performed consistently between experiments. An exclusion criteria was defined based on the pH and DO control, pre-feeding acetate concentration and the pre-induction biomass concentration, to ensure only meaningful data was included in experimental analysis.

Finally, to exemplify the use of the microbioreactor in a DoE-driven, fed-batch fermentation optimisation procedure, experiments investigating the effect of post-induction temperature and IPTG concentration on total titre, extracellular titre and total SPR were performed. The results demonstrated that the microbioreactor fed-batch process is predictive of the 1L scale process (Section 4.10 and Table 4.2).

Chapter 5: Evaluation of the microbioreactor system as a scale-down model for pilot scale, fed-batch fermentation process development

5.1. Introduction and aim

In Chapter 4, a direct fed-batch feeding approach was established at microwell scale (Section 4.9) and it was demonstrated that the microbioreactor can be predictive of 1L-scale fed-batch fermentation process performance (Section 4.10). This justifies the use of the fed-batch microbioreactor platform as a tool for bioprocess optimisation experiments. The aim of this chapter is to demonstrate the scalability of the microbioreactor process, in terms of cell growth, product expression and product quality. To this end 1L laboratory scale and 50L pilot scale fermentations were performed under optimum conditions, and the harvest samples were analysed for aggregation and fragmentation. In addition, the microbioreactor was characterised in terms of the oxygen mass transfer coefficient (k_La) and the fluid mixing time (t_m), to give an insight into the differences in process conditions between scales. The microbioreactor data was compared to experimental k_La data for the 1L vessel, the predicted k_La of the 50L vessel using literature correlations, and the predicted mixing times of the 1L and 50L vessels using literature correlations.

5.2. Comparison of the k_La of the 1L and 50L vessels and the microbioreactor

5.2.1. Micro-24 k_La characterisation

The k_La values of the microbioreactor for each cassette geometry were determined using the static gassing out method under shaking conditions suitable for microbial cultivation (van't Riet, 1979; Betts *et al.*, 2014). Experiments were performed using two different solutions; deionised water and complex media containing antifoam (Section 2.3.2) A DoE approach was used as described in Section 2.8.1. A 3 factor-2 level face centred central composite design with 6 centre points was used (Islam *et al.*, 2007). The factors studied were agitation speed (500-800 rpm), air flow rate (0.1-20.0 mL min^{-1}) and fill volume (4-7mL) as described in Table 2.5. For the BFL cassette the fill volume range investigated was 4-5mL, due to splashing at higher fill volumes.

The k_La values in just water were greater in the REG and BFL cassettes compared to the PRC cassette, which is consistent with the presence of a dispersed gas phase; the maximum k_La values with deionised water for the REG, BFL and PRC cassettes were 101h^{-1}, 136h^{-1} and 64h^{-1}

respectively (Figure 5.1). The BFL cassette had the highest k_La with water due to enhanced mixing with the single baffle. However, despite this, the BFL cassette was not used for any fermentations, and was only evaluated in regard to oxygen mass transfer with water as a comparison. The BFL cassette was considered unsuitable for fed batch cultures due to the fill volume restrictions to prevent splashing, and the increased foaming compared to the REG cassette.

The measured k_La values were not corrected for the optical sensor spot probe response time (τ_p), the time taken for a stepwise increase in the DO from 0 to 63%, (van't Riet, 1979; Lamping *et al.*, 2003; Betts, Doig and Baganz, 2006), as the sensor spots are fixed *in situ* meaning it is not possible to transfer the optical sensors from a 100% DO environment to a 0% DO environment. The accuracy of k_La measurements is likely to be affected if τ_p is not significantly less than $1/k_La$ (Badino et al. 2000; Betts et al. 2006; Van 't Riet 1979). The response time of the optical sensor spots stated in the specification is <6 seconds (PreSens, 2018), and $1/k_La_{max}$ of the microbioreactor (REG cassette) was ~35 seconds, therefore the probe response time is unlikely to have affected the accuracy of the k_La measurements.

For measurements made using complex media containing antifoam, the maximum k_La of the REG cassette were approximately 45% lower at 56h^{-1} (Figures 5.1(a) and(b)), compared to deionised water. Similarly, the maximum k_La of the PRC cassettes was 28% lower with a k_La of 43h^{-1} (Figures 5.1c and d). This decrease in k_La is due to adsorption of antifoam at the gas-liquid interface providing an extra barrier to oxygen transfer, and hence a decrease in the k_La. The presence of a dispersed gas phase in the REG cassette results in a greater reduction in the k_La compared to the PRC cassette, due the greater gas-liquid interfacial area. The increased viscosity of the media containing glycerol is likely to cause a decrease in both the interfacial area (a), and the liquid film mass transfer coefficient k_L. Bubble coalescence is enhanced at higher viscosities leading to an increase in bubble rise velocity and therefore a reduction in bubble residence time (Kantarci, Borak and Ulgen, 2005). The oxygen solubility (L_{O2}) in media was determined to be 95% the solubility in water, which would also result a reduction in k_L in addition to the increase in viscosity (Hermann *et al.*, 2003).

The maximum k_La was achieved at a shaking frequency of 800rpm, total gas flow rate of 20 mL min^{-1} for all cassette geometries, a fill volume of 4mL with the REG and PRC cassettes, and a 5mL fill volume for the BFL cassette, using water (Figure 5.1(a), (c) and (e). With complex media containing antifoam the maximum k_La was achieved under the same conditions as with water for the REG and PRC cassettes (Figure 5.1b and d). The shaking frequency and total gas flow rate had a significant impact on the k_La values measured in all cassette geometries, whereas the fill volume did not affect the k_La response in all cases with the exception of the PRC cassette using complex media (Tables 5.1-5.4). In the case of the PRC cassette using complex media, the

k_La response decreased with increasing fill volume due to the decrease in the surface-area-to-volume-ratio, and the reduced oxygen transfer in complex media compared to water. There was a significant interaction between shaking frequency and total gas flow rate with all cassette geometries, using both water and complex media; the total gas flow rate had a greater effect on the k_La response at higher shaking frequencies (Tables 5.1-5.5). This is likely due to the improved fluid mixing at higher shaking frequencies. There was also an interaction between total gas flow rate and fill volume for the PRC cassette using both water and complex media; the total gas flow rate had a greater impact on the k_La response with lower fill volumes (Tables 5.3 and 5.4). This is consistent with the higher surface-area-to-volume-ratio at lower fill volumes. This interaction was not observed with the REG or BFL cassettes with water, or REG cassette with complex media, as oxygen transfer is not dependant on headspace aeration (Tables 5.1, 5.2 and 5.5). In general these data show that the microbioreactor k_La is mainly determined by shaking frequency and the presence of dispersed gas phase.

The k_La values for the microbioreactor (Micro-24) in this work are comparable to data reported by Betts *et al.* (2014) and Ramirez-Vargasa *et al.*, (2014) for the microbioreactor using cell culture media. Betts *et al.* 2014 reported k_La values for the microbioreactor at a 7mL fill volume, shaking frequencies 500-800rpm and gas flow rates of 0.1-10 mL min^{-1}, ranging from 4-22h^{-1} and 4-53h^{-1} for the PRC and REG cassette designs respectively. Ramirez-Vargassa *et al* (2014) have also reported k_La values for the PRC cassette and BFL geometries in a cassette similar range of 8-40h^{-1} and 15–90h^{-1} respectively using tap water under a range of experimental conditions, These values are lower than the experimental values reported in this work as different well closures were used that do not allow two-way gaseous exchange. The microbioreactor k_La values are also comparable to k_La values reported for other shaken MBRs (Table 1.2) and conventional microtitre plates. Doig *et al.* (2005) reported k_La values between 36 and 180h^{-1} for a 24-well plate, with a fill volume of 1182μL, shaking frequencies of 200 to 800rpm shaking diameters of 3-8mm, and also derived a correlation for predicting k_La in shaken microwell plates. Micheletti *et al.*, (2006) predicted k_La values for a 96-DSW plate of 64 to 260h^{-1} using the correlation described by Doig *et al.*, using a fill volume of 1000μL, shaking diameter of 3mm and shaking frequencies of 500-100rpm. Hermann *et al.* (2003) determined the k_La of both round and square 96-well plates at shaking diameters of 3-50mm, fill volume of 200μL and shaking frequencies of up to 800rpm using the sodium sulphite oxidation method; under these conditions the k_La values were in the range 25-1500h^{-1}.

In order to use microbioreactors as a scale-down model of larger scale stirred reactors, it is also necessary to compare k_La values in conventional STRs to the k_La values in microbioreactors. In general, the k_La values of microbioreactors are at the lower end of the reported range for STRs over the size range of 0.025 - 20L. Ali *et al.*, (2012) reported k_La values of 250h^{-1} and 210h^{-1} for a 25mL STR and 20L STR respectively at agitation speeds of 2000-7000rpm and 1VVM gas

flow rate. Yawalkar *et al.*, (2002) derived a k_La correlation for air-water systems based on a relative dispersion parameter, N/N_{cd}, where N_{cd} is rotational speed at which the complete dispersion of the gas phase occurs and the superficial gas velocity, v. The literature experimental k_La values used to derive the correlation were in the range 30-490h^{-1}, for a variety of STR configurations ($D_T = 0.39$-1.2m).

Table 5.1. Model parameter estimates for the k_La characterisation of the REG cassette with water

Term	Estimate	Std Error	t Ratio	Prob>|t|
Intercept	58.53	3.66	15.99	<.0001
Shaking frequency (rpm)(500,800)	13.25	3.37	3.94	0.003
Gas flow rate (mL min^{-1})(0.1,20)	33.83	3.37	10.05	<.0001
Fill volume (mL)(4,7)	-4.08	3.37	-1.21	0.253
Shaking frequency (rpm)*Gas flow rate (mL min^{-1})	10.63	3.76	2.83	0.018
Shaking frequency (rpm)*Fill volume (mL)	-0.16	3.76	-0.04	0.968
Gas flow rate (mL min^{-1})*Fill volume (mL)	-2.70	3.76	-0.72	0.489
Shaking frequency (rpm)*Shaking frequency (rpm)	2.65	6.42	0.41	0.689
Gas flow rate (mL min^{-1})*Gas flow rate (mL min^{-1})	-23.04	6.42	-3.59	0.005
Fill volume (mL)*Fill volume (mL)	2.90	6.42	0.45	0.662

Table 5.2. Model parameter estimates for the k_La characterisation of the REG cassette with complex media containing 500ppm of antifoam

Term	Estimate	Std Error	t Ratio	Prob>|t|
Intercept	29.39	1.47	19.96	<.0001
Shaking frequency (rpm)(500,800)	9.69	1.35	7.15	<.0001
Gas flow rate (mL min^{-1})(0.1,20)	16.39	1.35	12.1	<.0001
Fill volume (mL)(4,7)	-2.97	1.35	-2.19	0.053
Shaking frequency (rpm)*Gas flow rate (mL min^{-1})	8.21	1.51	5.42	0.000
Shaking frequency (rpm)*Fill volume (mL)	0.72	1.51	0.47	0.647
Gas flow rate (mL min^{-1})*Fill volume (mL)	-1.68	1.51	-1.11	0.293
Shaking frequency (rpm)*Shaking frequency (rpm)	-3.59	2.58	-1.39	0.195
Gas flow rate (mL min^{-1})*Gas flow rate (mL min^{-1})	-9.15	2.58	-3.54	0.005
Fill volume (mL)*Fill volume (mL)	3.67	2.58	1.42	0.186

Table 5.3. Model parameter estimates for the k_La characterisation of the PRC cassette with water

Term	Estimate	Std Error	t Ratio	Prob>|t|
Intercept	26.02	0.87	29.87	<.0001
Shaking frequency (rpm)(500,800)	11.39	0.80	14.21	<.0001
Gas flow rate (mL min^{-1})(0.1,20)	16.29	0.80	20.33	<.0001
Fill volume (mL)(4,7)	-0.81	0.80	-1.02	0.334
Shaking frequency (rpm)*Gas flow rate (mL min^{-1})	9.93	0.90	11.08	<.0001
Shaking frequency (rpm)*Fill volume (mL)	1.52	0.90	1.70	0.120
Gas flow rate (mL min^{-1})*Fill volume (mL)	-2.74	0.90	-3.06	0.012
Shaking frequency (rpm)*Shaking frequency (rpm)	5.92	1.53	3.87	0.003
Gas flow rate (mL min^{-1})*Gas flow rate (mL min^{-1})	-4.45	1.53	-2.91	0.015
Fill volume (mL)*Fill volume (mL)	-3.11	1.53	-2.03	0.070

Table 5.4. Model parameter estimates for the k_La characterisation of the PRC cassette with complex media containing 500ppm antifoam

Term	Estimate	Std Error	t Ratio	Prob>|t|
Intercept	19.03	0.76	25.06	<.0001
Shaking frequency (rpm)(500,800)	6.26	0.70	8.97	<.0001
Gas flow rate (mL min^{-1})(0.1,20)	9.34	0.70	13.37	<.0001
Fill volume (mL)(4,7)	-1.99	0.70	-2.85	0.017
Shaking frequency (rpm)*Gas flow rate (mL min^{-1})	4.89	0.78	6.26	<.0001
Shaking frequency (rpm)*Fill volume (mL)	-0.94	0.78	-1.21	0.255
Gas flow rate (mL min^{-1})*Fill volume (mL)	-3.12	0.78	-4.00	0.003
Shaking frequency (rpm)*Shaking frequency (rpm)	-2.26	1.33	-1.70	0.120
Gas flow rate (mL min^{-1})*Gas flow rate (mL min^{-1})	-5.04	1.33	-3.78	0.004
Fill volume (mL)*Fill volume (mL)	2.90	1.33	2.18	0.054

Table 5.5. Model parameter estimates for the k_La characterisation of the BFL cassette with water

Term	Estimate	Std Error	t Ratio	Prob>|t|
Intercept	87.24	4.21	20.74	<.0001
Shaking frequency (rpm)(500,800)	15.19	3.87	3.93	0.003
Gas flow rate (mL min⁻¹)(0.1,20)	48.07	3.87	12.42	<.0001
Fill volume (mL)(4,5)	-0.94	3.87	-0.24	0.813
Shaking frequency (rpm)*Gas flow rate (mL min⁻¹)	14.25	4.33	3.29	0.008
Shaking frequency (rpm)*Fill volume (mL)	1.95	4.33	0.45	0.662
Gas flow rate (mL min⁻¹)*Fill volume (mL)	0.93	4.33	0.21	0.834
Shaking frequency (rpm)*Shaking frequency (rpm)	-10.61	7.38	-1.44	0.181
Gas flow rate (mL min⁻¹)*Gas flow rate (mL min⁻¹)	-27.04	7.38	-3.66	0.004
Fill volume (mL)*Fill volume (mL)	4.64	7.38	0.63	0.544
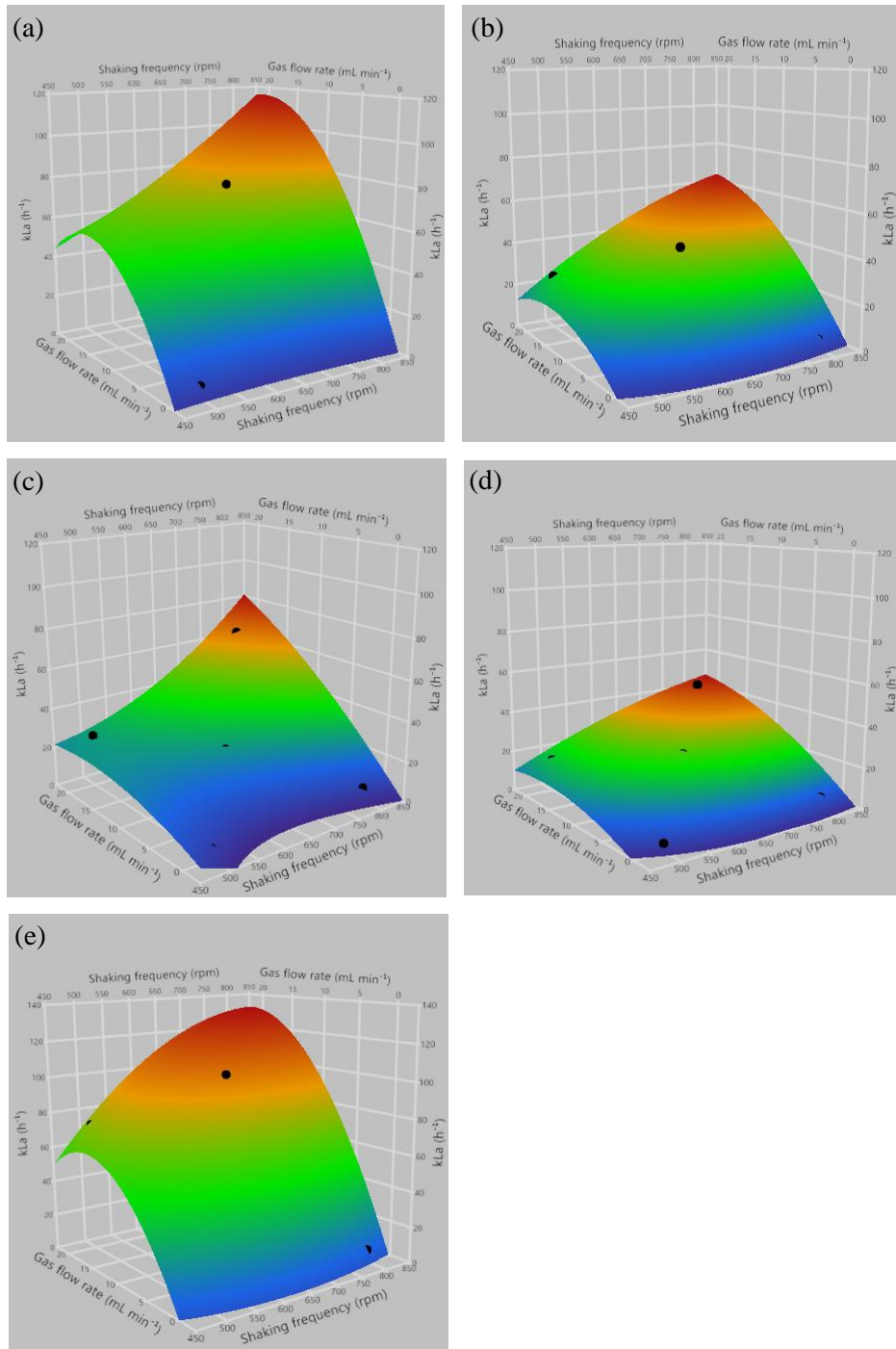
Figure 5.1. Surface response plots showing the effect of shaking frequency (rpm), and gas flow rate (mL min^{-1}) on the measured k_La of the Micro-24 for: (a) REG cassette design filled with 4mL water; (b) REG cassette design filled with 4mL complex media containing antifoam; (c) PRC cassette design filled with 4mL of water; (d) PRC cassette designs filled with 4mL of complex media containing antifoam; (e) BFL cassette design filled with 4mL water. All experiments were performed at 30°C as described in Section 2.8.1. A 3-factor-3-level, face-centered, central composite design (fcCCD) with six centre points was used, and all experiments were performed in duplicate. The DoE response models were generated using JMP® 13 software (SAS Institute, North Carolina, USA). The black dots represent the actual data points measured in the experimental design.

5.2.2. Predicted k_La values of the 50L and 1L vessels from literature correlations

The k_La of the 1L vessel (Section 2.3.1) was predicted using the correlations reported in the literature described in Table 5.7, and compared to historical data generated in-house at GSK. The gassed power (P_g) was predicted using the gassed-ungassed power ratio (P_g/P_{ug}) correlations reported in the literature described in Table 5.6, assuming a power number of 6 for a Rushton turbine impeller in the turbulent region (Nienow, 1998). The correlation described by Hughmark, (1980) was used for the k_La predictions (Figure 5.2(a)), since it was developed from literature data (391 data sets) and has an average absolute deviation of the experimental values from the calculated values of 0.117, meaning it is considered to be reliable. In addition, the data sets included in correlation development included a range of vessel configurations with diameters in the range 0.165m to 1m, and fluid viscosities up to 90 cP, meaning it should be suitable for P_g/P_{ug} predictions at both 1L laboratory and 50L pilot scales, with both water and complex media.

The correlations used to predict the 1L scale k_La are shown in Table 5.7. Figure 5.2(b) shows that the correlation described by Zhu, Bandopadhyay and Wu (2001) gives the best predictions of the experimental data both in terms of the magnitude of the k_La values and also how they vary as a function of N. Gas hold-up was not accounted for in these predictions, therefore the predicted k_La is likely to be an overestimation of the actual k_La (Möckel *et al.*, 1990). The k_La correlation described by Zhu, Bandopadhyay and Wu, (2001), and the P_g/P_{ug} correlation described by Hughmark, (1980) were also used to predict the k_La for the 50L vessel (Figure 5.3). Figure 5.3 shows that the predicted k_La of the 50L and 1L vessel, experimental data for the 1L vessel, and the microbioreactor data for the REG cassette generated by the model described in Section 5.2.1 and Equation 5.1. All predicted and experimental data was generated using the maximum gas flow rate used in a standard fermentation. Figure 5.3 shows that the microbioreactor k_La is significantly less than both the 50L and 1L vessels, even at the highest shaking frequency of 800rpm. At all three scales the oxygen transfer can be enhanced by oxygen enrichment; in the microbioreactor fermentations 100% oxygen is used for DO control, which enhances the oxygen concentration gradient (C_L^*-C_L) (Clarke, 2013).

Equation 5.1

$$
\begin{aligned}
k_L a \;=\; & 58.530681818 \\[4pt]
& + 13.2487 \cdot \left(\frac{\left(\text{Shaking frequency (rpm)} -650 \right)}{150} \right) \\[4pt]
& + 33.8339 \cdot \left(\frac{\left(\text{Gas flow rate (mL min}^{-1}\text{)} -10.05 \right)}{9.95} \right) \\[4pt]
& + \text{-4.0803} \cdot \left(\frac{\left(\text{Fill volume (mL)} -5.5 \right)}{1.5} \right) \\[4pt]
& + \left(\frac{\left(\text{Shaking frequency (rpm)} -650 \right)}{150} \right) \cdot \left(\left(\frac{\left(\text{Gas flow rate (mL min}^{-1}\text{)} -10.05 \right)}{9.95} \right) \cdot 10.633625 \right) \\[4pt]
& + \left(\frac{\left(\text{Shaking frequency (rpm)} -650 \right)}{150} \right) \cdot \left(\left(\frac{\left(\text{Fill volume (mL)} -5.5 \right)}{1.5} \right) \cdot \text{-0.156625} \right) \\[4pt]
& + \left(\frac{\left(\text{Gas flow rate (mL min}^{-1}\text{)} -10.05 \right)}{9.95} \right) \cdot \left(\left(\frac{\left(\text{Fill volume (mL)} -5.5 \right)}{1.5} \right) \cdot \text{-2.702375} \right) \\[4pt]
& + \left(\frac{\left(\text{Shaking frequency (rpm)} -650 \right)}{150} \right) \cdot \left(\left(\frac{\left(\text{Shaking frequency (rpm)} -650 \right)}{150} \right) \cdot 2.6495454545 \right) \\[4pt]
& + \left(\frac{\left(\text{Gas flow rate (mL min}^{-1}\text{)} -10.05 \right)}{9.95} \right) \cdot \left(\left(\frac{\left(\text{Gas flow rate (mL min}^{-1}\text{)} -10.05 \right)}{9.95} \right) \cdot \text{-23.03645455} \right) \\[4pt]
& + \left(\frac{\left(\text{Fill volume (mL)} -5.5 \right)}{1.5} \right) \cdot \left(\left(\frac{\left(\text{Fill volume (mL)} -5.5 \right)}{1.5} \right) \cdot 2.8965454545 \right)
\end{aligned}
$$

Table 5.6. Summary of literature P_g/P_{ug} correlations for stirred tanks. P_g = gassed power input (W), P_{ug} = ungassed power input (W), Q = volumetric gas flow rate ($m^3 s^{-1}$), N = stir speed (s^{-1}), d_i = impeller diameter (m).

Equation number.	Author(s)	Equation	Symbols	Notes
5.2	(Mockel *et al.*, (1990)	$$\frac{P_g}{P_{ug}} = \frac{1}{\sqrt{1 + Z\left(\frac{Q}{\sqrt{gd_i}}\right)}}$$	Z , constant based on number of impellers Z = 750 (1 impeller) Z = 490 (2 impellers) Z = 375 (3 impellers) g = acceleration of gravity = 9.2 m S^{-2}	
5.3	Cui, van der Lans and Luyben, (1996)	$$1 - \frac{P_g}{P_{ug}} = 0.52 + 0.62\left(\frac{QN^{0.25}}{d_i^2}\right)$$		Apply equation when: $\frac{QN^{0.25}}{d_i^2} > 0.055$
5.4	(Cui, van der Lans and Luyben, 1996)	$$1 - \frac{P_g}{P_{ug}} = 9.9\left(\frac{QN^{0.25}}{d_i^2}\right)$$		Apply equation when: $\frac{QN^{0.25}}{d_i^2} \leq 0.055$
5.5	Luong and Volesky, (1979)	$$\frac{P_g}{P_{ug}}$$ $$= 0.417\left(\frac{Q}{Nd_i^3}\right)^{-0.38}\left(\frac{N^3 d_i^3}{\sigma}\right)^{-0.18}$$	σ = air-liquid surface tension (N m^{-1})	
5.6	Calderbank, (1958)	$$\frac{P_g}{P_{ug}} = 0.62 - 18.5\left(\frac{Q}{ND_i}\right)$$		Apply equation when $Fl > 0.035$

Equation number.	Author(s)	Equation	Symbols	Notes
5.7	Calderbank, (1958)	$\dfrac{P_g}{P_{ug}} = 1 - 1.26\left(\dfrac{Q}{ND_i}\right)$		Apply equation when $Fl < 0.035$
5.8	Hughmark, (1980)	$\dfrac{P_g}{P_{ug}} = 0.10\left(\dfrac{Q}{NV}\right)^{-0.25}\left(\dfrac{N^2 D_i^{\,4}}{gW_i V^{0.67}}\right)^{-0.2}$	W_i = impeller blade width (m) V_L = liquid volume (m^3)	

Table 5.7. Summary of literature $k_L a$ correlations for Rushton turbines in stirred tanks. . P_g = gassed power input (W), v_s = superficial gas velocity (m s^{-1}), N = stir speed (s^{-1}), d_T = tank diameter (m).

Equation number	Author(s)	Equation	$k_L a$ measurement method	Type of fluid	Notes
5.9	van't Riet, (1979)	$k_L a = 0.026\left(\dfrac{P_g}{V}\right)^{0.4} v_s^{\,0.5}$	Static gassing out	Air- water	
5.10	Nishikawa *et al.*, (1981)	$k_L a$ $= 3.92 \times 10^{-6}\left(\dfrac{P_g}{V}\right)^{0.33}(v_s g)^{0.2}$	Static gassing out	Air - water	
5.11	Chandrasekharan and Calderbank, (1981)	$k_L a$ $= \left(\dfrac{0.0248}{d_T^{\,4}}\right)\left(\dfrac{P_g}{V}\right)^{0.551} v_s^{\,0.551 d_T^{-0.5}}$	Static gassing out	Air – water	
5.12	Gibilaro *et al.*, (1985)	$k_L a = 0.49\left(\dfrac{P_g}{V}\right)^{0.76} v_s^{\,0.45}$	Static gassing out	Air - water	
5.13	Linek *et al.*, (2004)	$k_L a = 0.0108\left(\dfrac{P_g}{V}\right)^{0.699} v_s^{\,0.581}$	Dynamic pressure	Air – water	

Equation number	Author(s)	Equation	k_La measurement method	Type of fluid	Notes
5.14	Gagnon *et al.*, (1998)	$k_La = 0.0092\left(\frac{P_g}{V}\right)^{0.60} v_s^{0.503}$	Static gassing out	Air – water	3 Rushton turbines
5.15	Arjunwadkar *et al.*, (1998)	$k_La = 0.002\left(\frac{P_g}{V}\right)^{0.68} v_s^{0.58}$	Static gassing out	Air – water with ions	2 Rushton turbines
5.16	Vasconcelos *et al.*, (2000)	$k_La = 0.0083\left(\frac{P_g}{V}\right)^{0.62} v_s^{0.49}$	Peroxide decomposition	Air – water with ions	2 Rushton Turbines, magnesium sulphate catalyst used
5.17	Puthli, Rathod and Pandit, (2005)	$k_La = 1.9 \times 10^{-4}\left(\frac{P_g}{V}\right)^{0.67} v_s^{0.53}$	Static gassing out	Air – water	3 Rushton turbines
5.18	Vilaca *et al.*, (2000)	$k_La = 0.00676\left(\frac{P_g}{V}\right)^{0.94} v_s^{0.65}$	Sodium sulphite	Air – water – sodium sulphite	2 Rushton Turbines, copper sulphate catalyst
5.19	Smith *et al.,* (1977)	$k_La = 0.01\left(\frac{P_g}{V}\right)^{0.475} v_s^{0.4}$	Static gassing out	Air - water	
5.20	Zhu *et al.,* (2001)	$k_La = 0.224\left(\frac{P_g}{V}\right)^{0.35} v_s^{0.52}$	Static gassing out	Air - water	
5.21	Gill *et al.* (2008b)	$k_La = 0.031\left(\frac{P_g}{V}\right)^{0.4} v_s^{0.5}$	Static gassing out	Air – water with ions	100mL miniature stirred bioreactor with a single turbine impeller

(a)

(b)
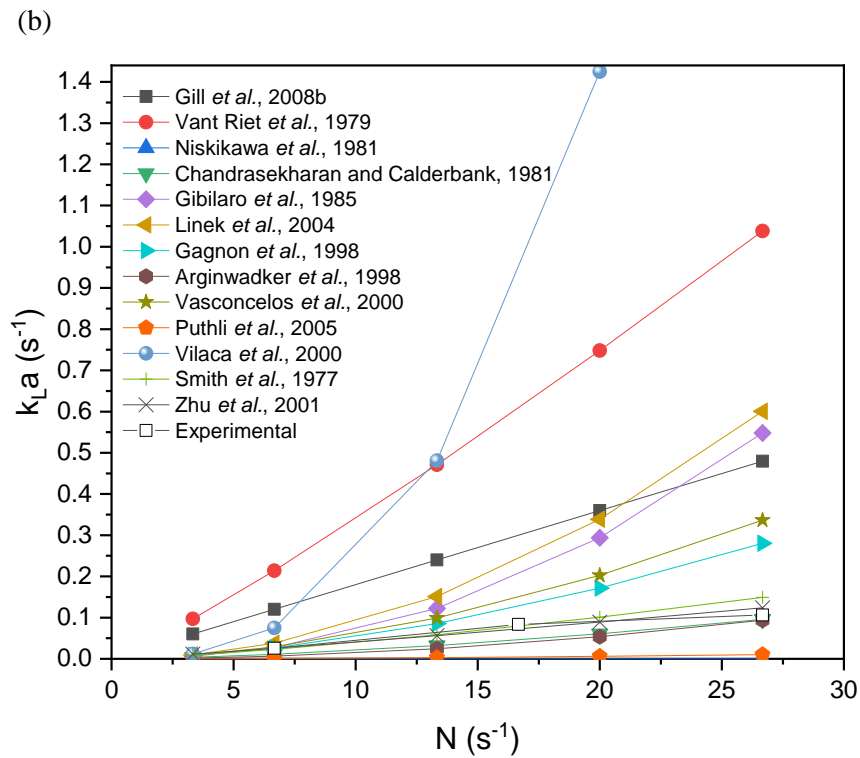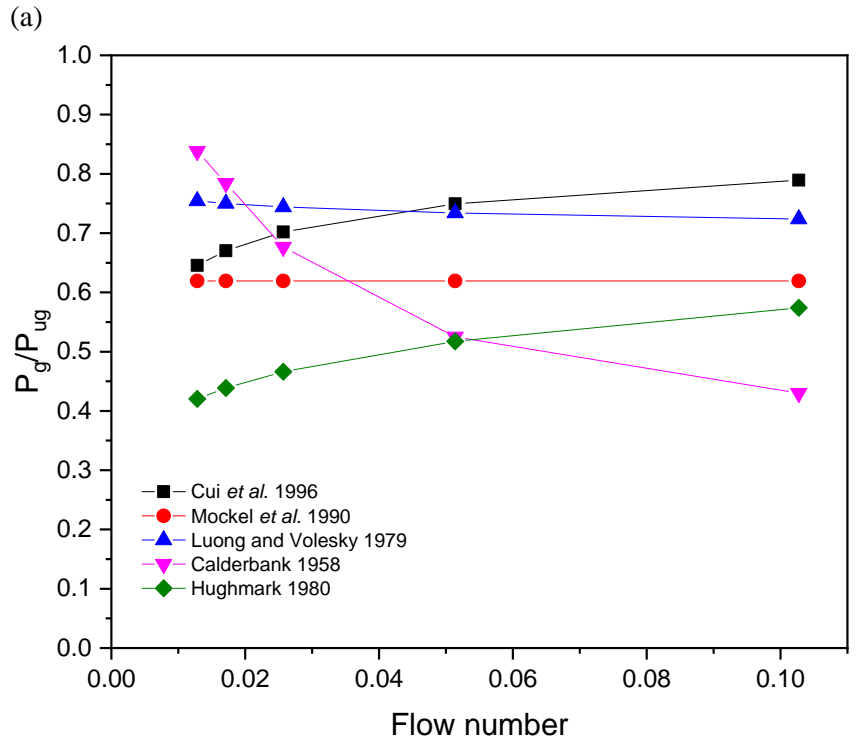
Figure 5.2. Gassed-ungassed power consumption ratios and k_La values for the 1L scale vessel calculated from literature correlations. (a) Gassed-ungassed power consumption ratios for the 1L vessel using the literature correlations described in Table 5.6. (b) Comparison of the 1L scale k_La experimental data with the literature correlations described in Table 5.7., using the gassed power correlation described by Hughmark. (1980). The 1L scale historical experimental data was generated with 1L water using the static gassing out method in-house at GSK., as described in
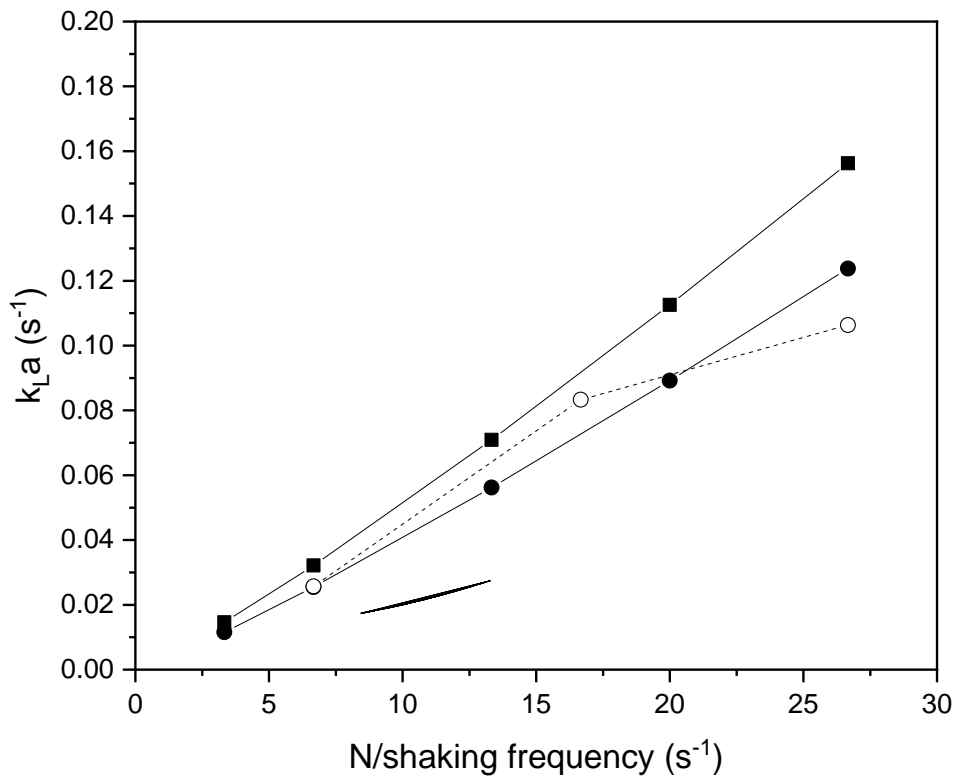
Figure 5.3. Comparison of the predicted k_La values ($\bullet$, solid line) and experimental k_La values ($\circ$, dashed line) of the 1L scale vessels, and the predicted k_La values of the 50L vessel ($\blacksquare$, solid line) with increasing stir speed, and predicted Micro-24 k_La values (solid line) with increasing shaking frequency.   The predicted 1L scale and 50L k_La was determined using the correlation described by Zhu *et al.,* 2001, and the gassed-ungassed power consumption ratio described by Hughmark (1980). The Micro-24 k_La data was generated using the DoE model (Equation 5.1). The 1L scale k_La was determined/ predicted using a volumetric gas flow rate of 2 vvm, the 50L k_La was predicted using a volumetric gas flow rate of 1.2 vvm, and the Micro-24 k_La was predicted using a volumetric gas flow rate of 3.75 vvm and a fill volume of 4mL. The 1L scale historical experimental data was generated with 1L deionised water using the static gassing out method in-house at GSK as described in Section 2.8.1 for the Micro-24 k_La characterisation experiments.

5.3. Microbioreactor fluid mixing time (t_m) determination

Efficient mixing of microbial cultivations is critical for rapid oxygen transfer, and for the blending of liquid additions in the case of fed-batch fermentations. Therefore, understanding mixing in small-scale shaken reactors is important for the development of effective scale-down models of small-scale STRs. The fluid mixing times (t_m) of the microbioreactor REG and PRC cassettes (Section 2.4.) were measured using the iodine decolourisation method (Carreau, Patterson and Yap, 1976; Takahashi *et al.*, 1985; Betts *et al.*, 2014). The colour change was determined using a DVR Fastcam as described in Section 2.8.2.

Figure 5.4. shows representative images from the DVR for both the REG and PRC cassettes. Buchs *et al.*, (2001) described a phenomenon unique to fluid flow in shaken bioreactors, and identified two flow regimes: 'in-phase' and 'out-of-phase'. The' in-phase' flow regime occurs when the majority of the liquid circulates around the vessel wall in sync with the motion of the shaking platform. Fluid flow is 'out-of-phase' when only a small fraction of liquid moves along the vessel wall and the majority of the liquid remaining stationary on the base of the flask reducing mixing efficiency. A non-dimensional number, the phase number (Ph) describes this phenomenon. The phase number can be calculated from Equation 1.9. Where d_o is the shaker diameter, d_f is the inner diameter of the shaken vessel, V is the liquid volume and N is the shaking frequency. According to Buchs *et al*, for operating conditions where $Ph<1.26$ fluid flow will be 'in-phase' and for $Ph<1.26$ fluid flow will be 'out-of phase. It was not possible to calculate the Ph for the fill volumes tested (3-7mL) as a negative value in the square root was obtained, however the fluid motion depicted in Figure 5.4 indicates the fluid flow is 'in-phase' with the orbital shaking platform in both the REG and PRC cassettes.

The measured microbioreactor mixing times were 0.5-3.0s for the REG cassette and 0.6-15s for the PRC cassette. For both cassette designs mixing time decreased with increasing shaking frequency and decreasing fill volume (Figure 5.5), although the shaking frequency has a much greater effect on mixing time than fill volume (Tables 5.8 and 5.9). There was a significant interaction between fill volume and agitation for the PRC cassette design; at low shaking frequencies the fill volume had a greater impact on the mixing time. This interaction was not observed with the REG cassette indicating it is an artefact of the central vent of the PRC cassette. Overall at lower fill volumes (4mL) the mixing times for both cassette geometries were comparable.

The microbioreactor (Micro-24) mixing times determined here are comparable to values previously reported for the microbioreactor by Betts *et al* (2014) who reported mixing times of 0.8-2s at shaking speeds of 650-800rpm and fill volumes of 5-7mL for the REG and PRC cassettes. The mixing times are also comparable to those reported by Barrett *et al.* (2010) for shaken microwell plates. Barrett *et al.*, (2010) reported mixing times for a 24-well SRW

cassette of 1.7 ± 0.06s for both 800μL and 1000μL fill volumes at $Re = 1830$; the Micro-24 mixing times were comparable at 0.5-3s at $Re = 2133$-3413, with the exception of the mixing times of the PRC cassette at low shaking speeds. The Micro-24 Re and the microtitre plate Re described by Barrett *et al.* were calculated using Re for shaking systems (Equation 1.8) as defined by Büchs *et al.*, (2000).

The mixing time values reported here are also of a similar magnitude to those reported for conventional STRs. Gogate, Beenackers and Pandit, (2000) reported mixing times for an STR multiple impeller geometries at agitation speeds up to 1200rpm of less than 40s and less than 10s for a single Rushton turbine. Saito *et al*. (1992) reported mixing times in a similar range of 5-20s for 6-blade RSGT and Rushton turbine impellers at agitation speeds of 100 to 450rpm and gas flow rates of 0.5-1 VVM.

Cooke, (1993) described a correlation for '90% mixing times' (t_{90}), which was defined as the time taken for the conductivity of a tracer to reach $\pm10\%$ of the equilibrium, for 20-60 litre STRs with aspect ratios of 1-3 and three Rushton Turbines. The mixing time correlation is shown in Equation 1.7, where H_L is the liquid height and P_0 is the power number. Equation 1.7 was used to predict the mixing time of the 1L and 50L scale vessels (Figure 5.6.) under non-aerated conditions. Figure 5.6 shows that the predicted mixing times of the 1L scale under the agitation speeds typically used in fed-batch fermentations, are comparable to the microbioreactor mixing times under microbial operating conditions, whereas the mixing time of the 50L vessel is predicted to be significantly higher. Table 5.10 summarises the engineering parameters of the 50L-scale, 1L-scale and microbioreactor processes under standard fed-batch fermentation conditions.

Bulk mixing is less efficient at larger volumes at equivalent agitation speeds due to the decrease in P_g/V (Cooke, 1993; Nienow, 1998). Rushton turbines are radial-flow impellers and it has been shown that 60% of the energy input is dissipated in the immediate impeller and jet flow regions, which can lead to longitudinal gradients (Wu and Patterson, 1989; You *et al.*, 2014). This can lead to dissolved oxygen, temperature and nutrient concentration gradients, and compromised process control (Oosterhuis and Kossen, 1984; Larsson *et al.*, 1996; Lara *et al.*, 2006); this could explain the lower biomass concentration and product expression achieved with the 50L scale process compared to the 1L scale process (see later in Section 5.4.) .

Additional microbioreactor mixing time experiments were performed at a fill volume of 3mL, to establish if the removal of 1mL of culture broth prior to feeding (Sections 2.6.3.1. and 4.5), to allow sufficient volume for feed additions, was likely to affect fluid mixing. Figure 5.7 shows that for both the REG and PRC cassettes the mixing time increases with increasing fill volume in the range 3-7mL; at all fill volumes the mixing time of both cassette types was less that 2s indicating that mixing is efficient. The images obtain from the DVR Fastcam also indicated that

the fluid motion was 'in phase' and therefore the fluid was well mixed at all fill volumes. Therefore the mixing of the cultures should not have been negatively impacted by the change in volume due to feed additions

The microbioreactor mixing time experiments were performed using aqueous media, whereas under fermentation conditions the viscosity is greater due to the glycerol in the media and feed, and the presence of cells and cell debris such a DNA (Balasundaram *et al.*, 2009; Newton *et al.*, 2016). Therefore the mixing times determined may be an underestimation of the mixing times under fed-batch fermentation conditions (Tan, Eberhard and Büchs, 2011; Rodriguez, Micheletti and Ducci, 2018), however the system should still be well-mixed. Betts *et al.* (2014) showed that aeration decreases the mixing time of the shaken microbioreactor, which is consistent with the occurrence of enhanced gas-induced mixing. In theory, in STRs the mixing time will increase with aeration, as it is inversely proportional to P_o (Cooke, 1993). However, the reduction in mechanical mixing efficiency with aeration, is usually compensated for by the gas-induced liquid flow, meaning mixing of aerated and unaerated systems is comparable (VraH bel *et al.*, 2000). The absence of mechanical agitation in the microbioreactor means that the gas-induced flow has a greater effect on mixing than in conventional STRs.

Table 5.8. Model parameter estimates for mixing time determination of the REG cassette

Term	Estimate	Std Error	t Ratio	Prob>|t|
Intercept	3.720	0.525	7.09	0.0001*
Shaking frequency (rpm)	-0.004	0.001	-7.01	0.0001*
Fill volume (mL)	0.171	0.061	2.80	0.0233*
(Shaking frequency (rpm)-650)*(Fill volume (mL)-5.5)	0.000	0.000	-0.07	0.9484

Table 5.9. Model parameter estimates for mixing time determination of the PRC cassette

Term	Estimate	Std Error	t Ratio	Prob>|t|
Intercept	10.181	5.515	1.85	0.0980
Shaking frequency (rpm)	-0.023	0.006	-3.65	0.0053*
Fill volume (mL)	1.416	0.643	2.20	0.0552
(Shaking frequency (rpm)-650)*(Fill volume (mL)-5.5)	-0.013	0.005	-2.52	0.0327*
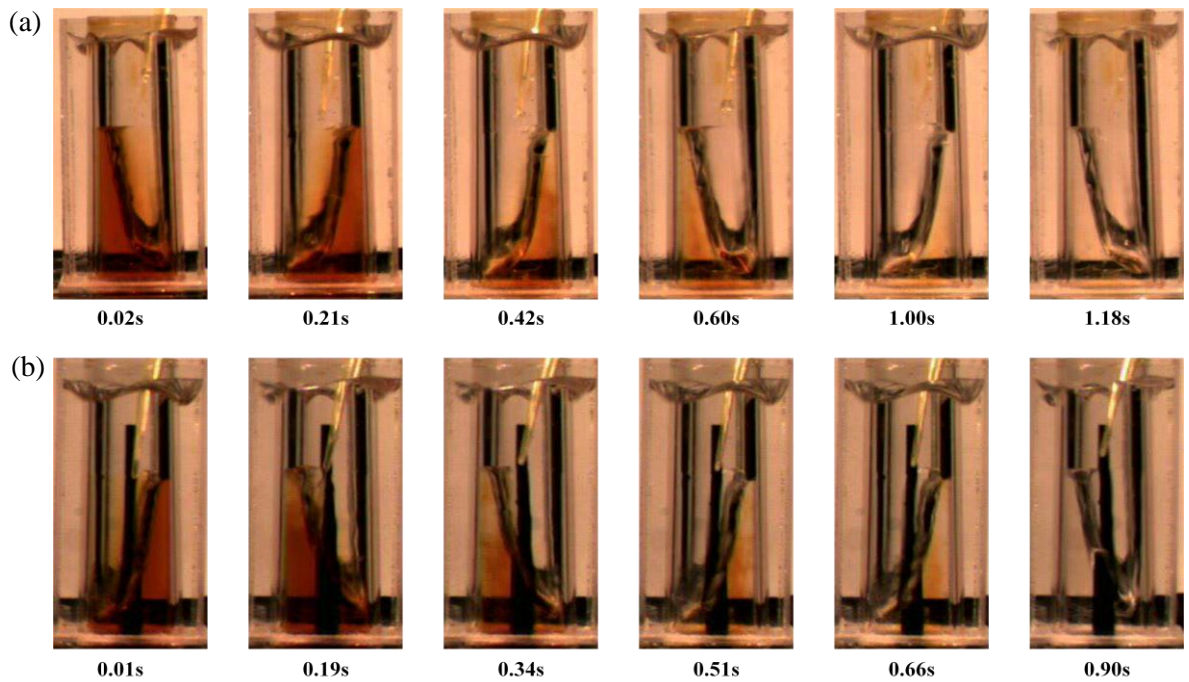
Figure 5.4. Representative high speed video images during Micro-24 mixing time experiments using the iodine discoloration method for: (a) REG cassette design and (b) PRC cassette design. Conditions for all experiments: dynamic start; 4mL fill volume; 800rpm shaking frequency; d_o 5mm; 30°C. The experiments were performed as described in Section 2.8.2 and images were acquired using a DVR Fastcam (Photron, California, USA).

Equation 5.22

$$t_m = 3.72$$
$$+ -0.004288889 \cdot \text{Shaking frequency (rpm)}$$
$$+ 0.1711111111 \cdot \text{Fill volume (mL)}$$
$$+ \left(\text{Shaking frequency (rpm)} - 650 \right) \cdot \left(\left(\text{Fill volume (mL)} - 5.5 \right) \cdot -0.000033333 \right)$$
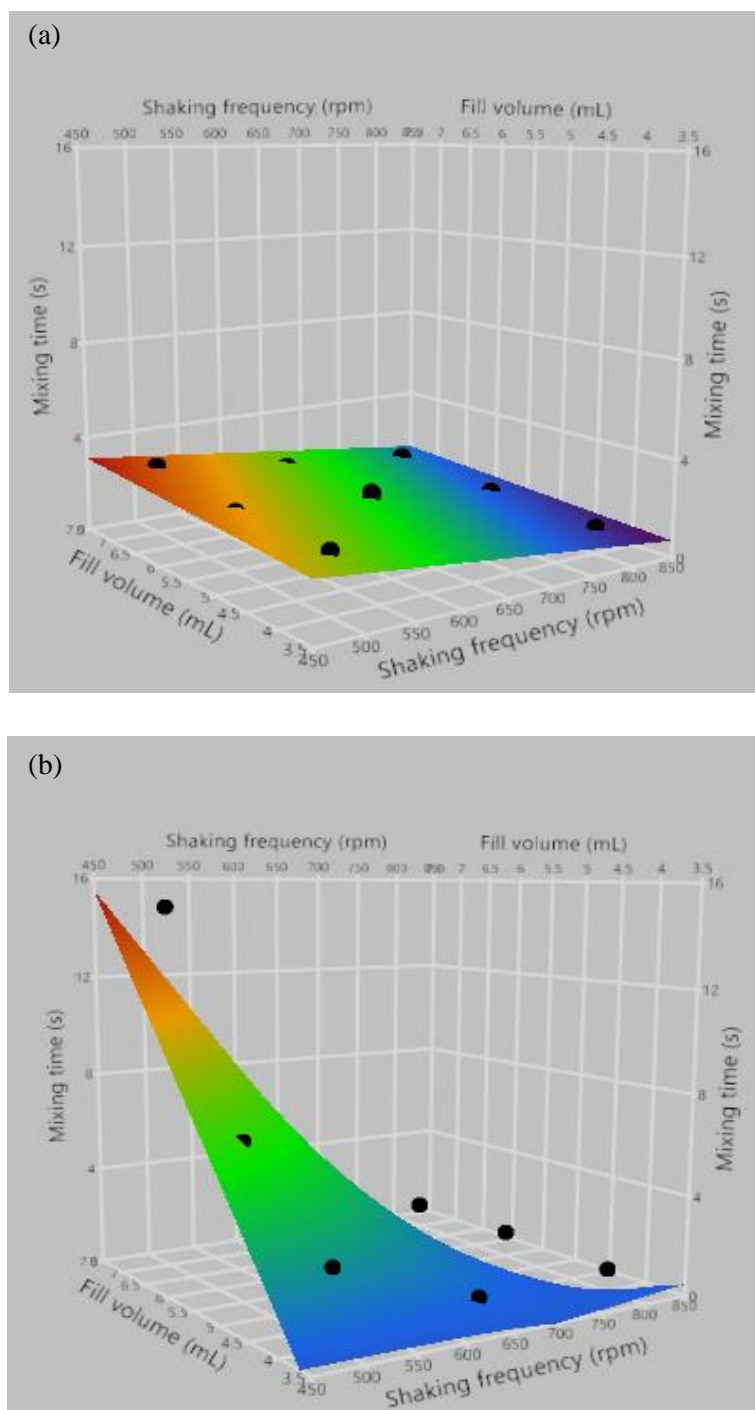
Figure 5.5. Surface response plots showing the effect of a shaking frequency (rpm), and fill volume (mL) on the mixing time of the Micro-24 **(a)** REG cassette and **(b)** PRC cassette designs. All experiments were performed under non-aerated conditions at 30°C. A 2-factor-3-level, face-centered, central composite design (fcCCD) with six centre points was used, and the DoE design was run in duplicate. The DoE response models were generated using JMP® 13 software (SAS Institute, North Carolina, USA). These experiments were performed using a DVR Fastcam (Photron, California, USA) as described in Section 2.8.2. The black dots represent the actual data points measured in the experimental design.
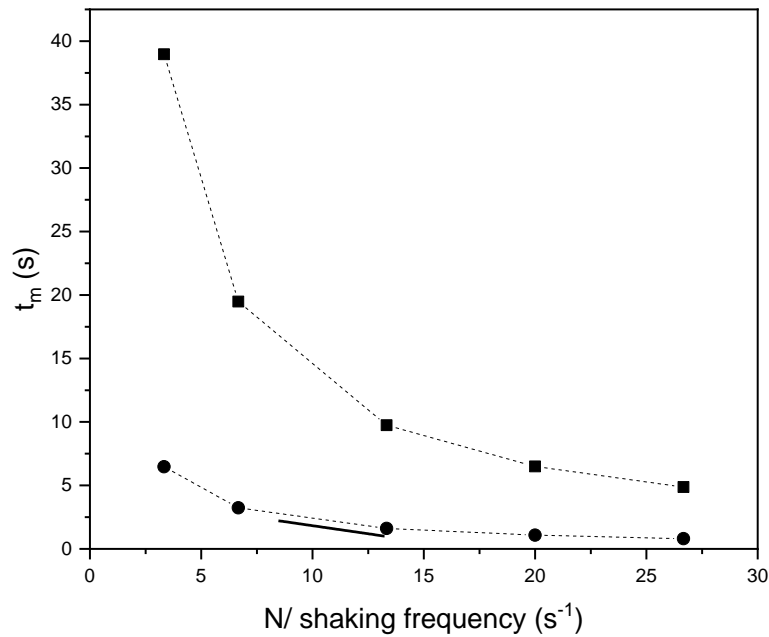
Figure 5.6. Comparison of the predicted 50L (■, dashed line) and 1L scale (●, dashed line) mixing times with increasing stir speed under non-aerated conditions, and Micro-24 mixing time data (solid line) with increasing shaking frequency under non-aerated conditions. The predicted 1L scale and 50L mixing time was determined using the correlation described by Cooke, 1993, and the Micro-24 mixing time data was generated using the DoE model (Equation 5.22) using a fill volume of 4mL. The Micro-24 mixing time was measured using a DVR Fastcam (Photron, California, USA) as described in Section 2.8.2
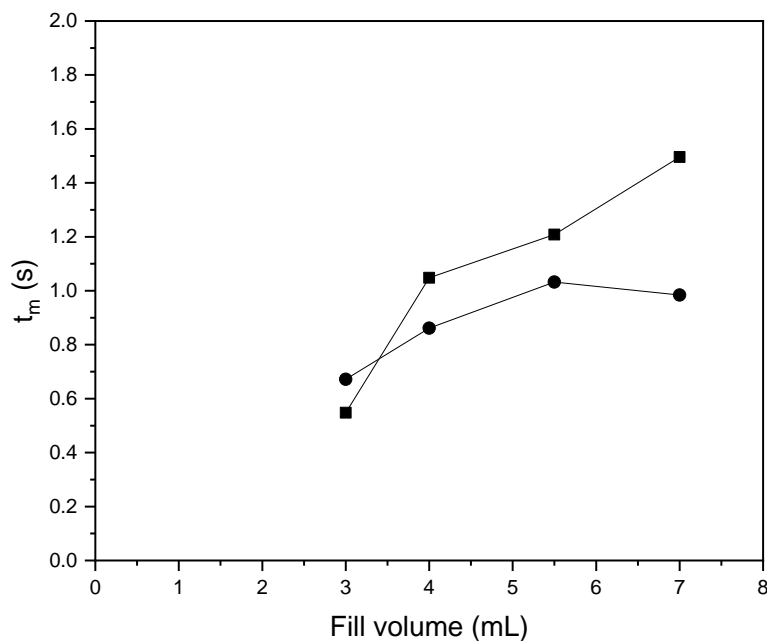
Figure 5.7. Effect of fill volume on the mixing time of the REG (■) and PRC (●) cassettes under non-aerated conditions. The Micro-24 mixing time data was generated using a shaking frequency of 800rpm at 30°C, and was measured using a DVR Fastcam (Photron, California, USA) as described in Section 2.8.2.

5.4. Comparison of cell growth, product expression and product quality of the microbioreactor fed-batch process to the 1L scale and 50L processes

50L pilot scale, 1L laboratory scale and Micro-24 fermentations were performed under optimum conditions i.e. platform conditions for the 50L and 1L scale fermentations, and the refined microbioreactor fed-batch fermentation process described in Section 4.9 (Figure 4.11). Table 5.10 summarises the oxygen transfer and fluid mixing characteristics under fermentation conditions. The three processes were compared in terms of cell growth and product expression (Figure 5.8), and dAb product quality (Figure 5.9). Table 5.11 summarises the 50L scale, 1L scale and microbioreactor processes in terms of cell growth, product expression and product quality.

Figure 5.8a shows that the highest pre-induction biomass concentration was achieved at 1L scale; an OD_{600} value of ~60 was acheived compared to ~50 and ~42 at 50L and microbioreactor scale respectively. As previously described in Section 5.2 the lower biomass in the microbioreactor may be attributed to the lower oxygen mass transfer capacity of the microbioreactor. The lower pre-induction biomass at 50L scale may be due could be a result of less efficient mixing compared to the 1L scale vessel. The pre-feeding acetate concentration decreased with increasing scale, which could be result of differences the in oxygen mass transfer and the growth rate of the cells. The pre-feeding acetate concentration at 50L scale was minimal at 0.05 g L^{-1}, which is 4-fold and 8-fold lower that the 1L scale and microbioreactor processes respectively. The sample port was situated at the bottom of the vessel, so the sample is likely to have been taken from a well-mixed region, therefore the metabolite concentrations may be an underestimation of the average concentration of the bulk fluid (Wu and Patterson, 1989; You *et al.*, 2014).

Figure 5.8(c) shows the titres achieved at 50L, 1L and microbioreactor scale. The total titres at 1L and 50L scale were 1.39 g L^{-1} and 0.86 g L^{-1} respectively. The microbioreactor total titre was 0.48 g L^{-1} indicating that it may be a better model of the 50L scale process than the 1L-scale process. The specific productivity data also suggests that the microbioreactor processes better predicts the 50L scale process than the 1L scale process (Figure 5.8(d) and Table 5.11). The 50L and microbioreactor processes, were also comparable in terms of product distribution, with 74.2% and 70.9% extracellular product respectively; the proportion of extracellular product was lower for the 1L-scale process at 50.5% (Table 5.11). This suggests that the metabolic state of cells is comparable in the microbioreactor and 50L scale processes.

The product quality of the 50L scale, 1L scale and microbioreactor processes was compared; aggregation and fragmentation were assessed by size exclusion chromatography (SEC) HPLC as described in Section 2.10.6. Figure 5.9 shows the chromatograms for the 50L scale harvest samples with and without the addition of PEI at harvest, the 1L scale harvest samples, and the

microbioreactor harvest samples. The shape of the chromatograms were comparable for all samples, however there were some differences in the peak heights (Figure 5.9). This indicates that not all the samples were at a concentration of 1 mg mL^{-1} possibly due to the presence of unpurified material, as a result of liquid handling errors on the Tecan. The presence of unpurified protein would interfere with the NanoDrop™ absorbance measurements, resulting in an overestimation in the dilution factor required to achieve a final concentration of 1 mg mL^{-1}.

The product quality characteristics of the 50L-scale and microbioreactor processes were similar in terms of aggregation , at 92-93% monomer and 7-8% aggregates , whereas there aggregation at 1L scale was higher at 10%, and the percentage monomer was lower at ~89% (Table 5.11). This shows that the modifications made to the microbioreactor process i.e. implementation of a pre-feeding hold period and refinement of the feeding strategy, did not have adverse affects on aggregation. Also, the less efficient process control in the microbioreactor compared to the 1L and 50L processes does not appear to have an effect on product quality. It appears that in terms of product quality, the microbioreactor is a better match to the 50L pilot-scale processes, than the 1L laboratory-scale process. To confirm this observation, further investigations would be required to determine if the higher aggregation levels at 1L-scale is an artefact of the fermentation process, or the sample preparation or purification procedures. Due to the limited sample volumes from the microbioreactor, HPLC-SEC was the only product quality assay performed; to confirm that the product quality is comparable to the 50L-scale process, other product quality and process-related impurity assays should be performed e.g. HCP and DNA enzyme-linked immunosorbent assays (ELISAs), mass spectrometry and capillary gel electrophoresis assays (Kumaraswamy, 2012; Welsh *et al.*, 2016; Oshinbolu *et al.*, 2018).

Table 5.10. Engineering parameters of the 50L vessel, 1L vessel, and microbioreactor under operating conditions used for a standard fed-batch fermentation.

Parameter	50L	1L	Microbioreactor (4mL)
Air flow rate (vvm)	0.72 - 1.20	2.00	0 - 3.75[1]
Stir speed/ shaking frequency (rpm)	300 - 900	400 - 1200	800
k_La (h^{-1})	83 – 292[2]	64 - 383[3]	5 - 101
P/V (KW m^{-3})	0.4 – 10.2[4]	0.9 – 13.0[4]	ND
Mixing time (s)	8.7 – 26.0[5]	1.1 – 3.2[5]	1.1[6]

[1] Intermittent sparging of 100% oxygen

[2] Predicted using the P_g/Pug correlation proposed by Hughmark (1980) using the density of water, and k_La correlation proposed by Zhu *et al.,* 2001.

[3] Measured using deionised water

[4] Predicted using the P_g/Pug correlation proposed by Hughmark (1980) using the density of water

[5] Predicted using the mixing time correlation proposed by Cooke (1993) under non-aerated conditions

[6] Measured under non-aerated conditions

Table 5.11. Comparison of cell growth dAb formation and product quality in the 50L scale, 1L scale and Micro-24 processes.

	Fed-batch Fermentation Scale		
	50L	**1L**	**Microbioreactor (4 mL)**
End of batch DCW (g L^{-1})	18.3	26.3	19.3
Harvest DCW (g L^{-1})	28.9	36.7	22.5
End of batch $Y_{x/s}$ (g g^{-1})	0.73	0.90	0.72
Pre-induction $Y_{x/s}$ (g g^{-1})	0.56	0.66	ND*
Pre-feeding [acetate] (g L^{-1})	0.05	0.17	0.40
Harvest total titre (g L^{-1})	0.86	1.39	0.48
% Extracellular	74.2	50.5	70.9
Harvest total SPR (g g^{-1})	29.8	37.9	21.0
% Monomer	92.7	89.2	91.9
% Aggregate	7.1	10.0	8.11
% Fragment	0.3	0.90	0.01<

*Insufficient volume of pre-induction sample for cell weight determination.
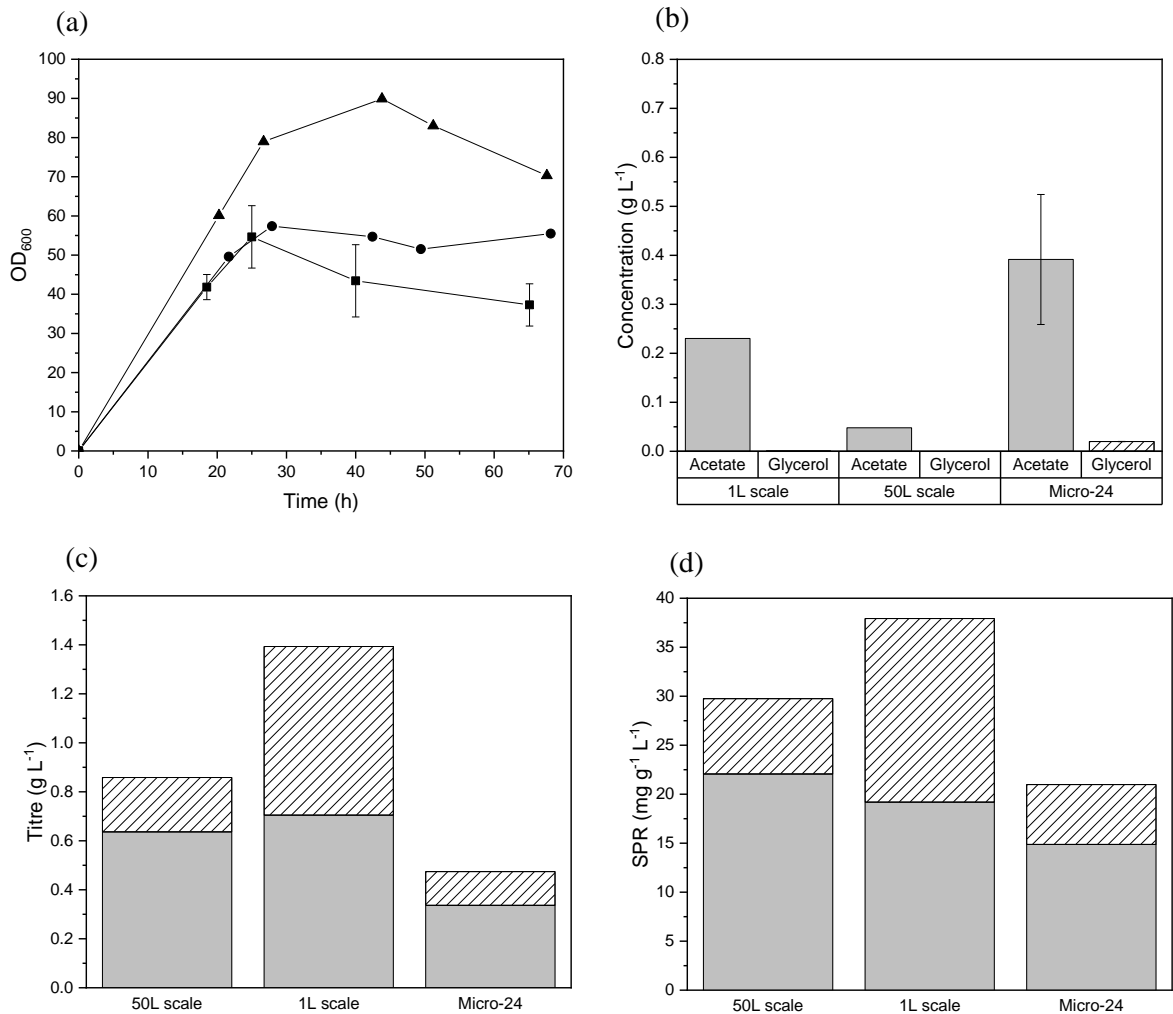
Figure 5.8. Cell growth and antibody production in 50L scale, 1L scale and Micro-24 fed-batch cultures of w3110 *E. coli* producing a dAb protein. (a) Cell growth kinetics: 50L OD_{600} profile (●), 1L OD_{600} profile (▲), and Micro-24 OD_{600} profile (■). The error bars represent one standard deviation from the mean (n=8). (b) Pre-feeding glycerol (shaded bars) and acetate (filled grey bars) concentration (c) Harvest dAb titres for the 50L scale, 1L scale and Micro-24 processes. The grey filled bars represent extracellular titre and the shaded bars represent intracellular titre (d) Harvest SPRs for the 50L scale, 1L scale and Micro-24 processes. The grey filled bars represent extracellular SPR and the shaded bars represent intracellular SPR. The Micro-24, 1L scale and 50L scale fermentations were performed as described in Sections 2.3.2., 2.6.3.4. and 2.9. respectively. The analytical assays were carried out as described in Section 2.10. The DO, pH and temperature set points were 40% (50L and 1L scale) and 60% (Micro-24), pH7 and 30°C respectively.
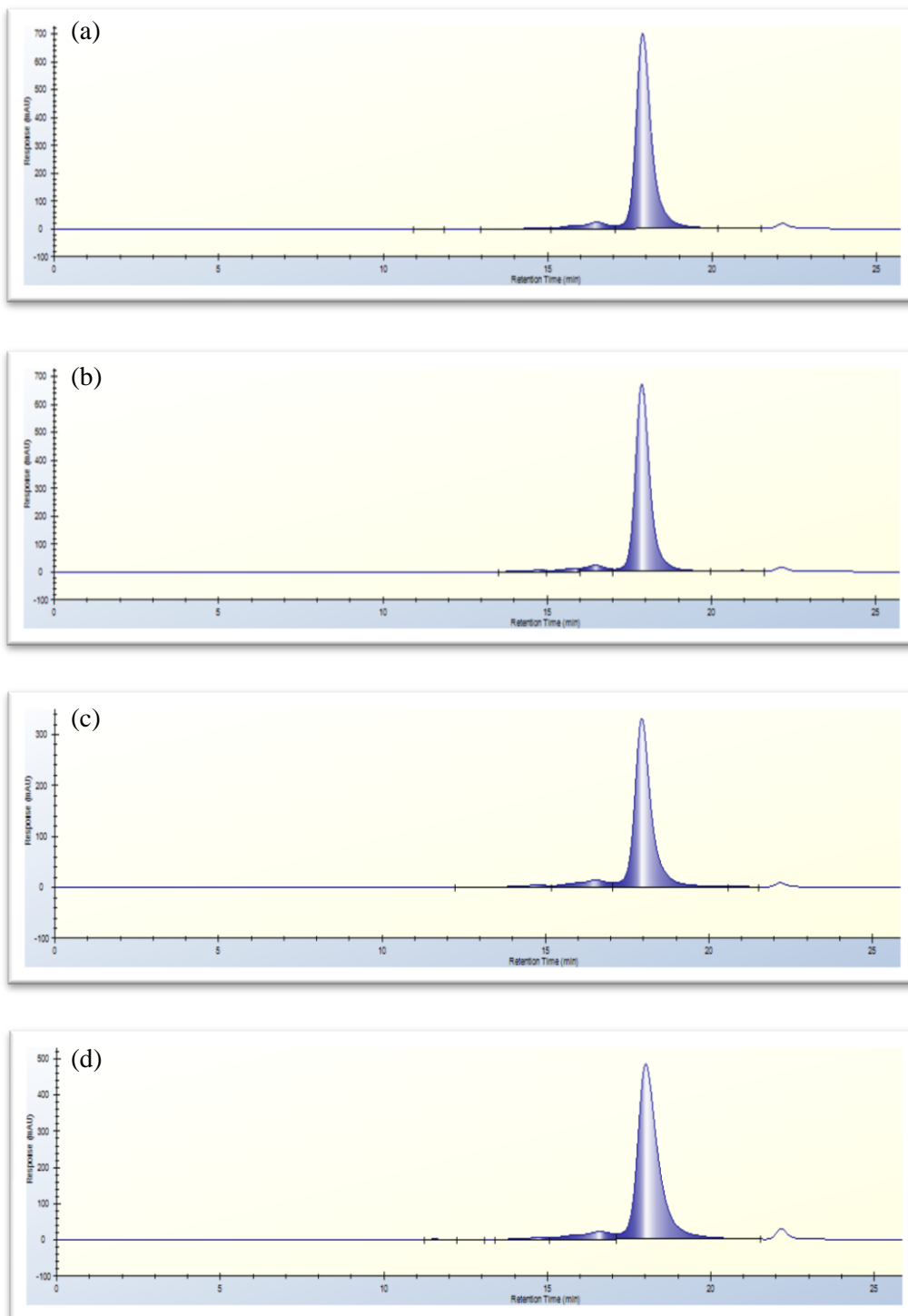
Figure 5.9. 50L scale, 1L scale and Micro-24 harvest sample SEC-HPLC chromatograms. (a) 50L scale without PEI addition at harvest (b) 50L scale with PEI addition at harvest (c) 1L scale, and (d) Micro-24. The Micro-24, 1L scale and 50L scale fermentations were performed as described in Sections 2.3.2., 2.6.3.4. and 2.9. respectively. The HPLC-SEC assay and sample preparation were performed as described in Section 2.10.6.

5.5. Summary

The aim of this chapter was to demonstrate the scalability of the microbioreactor process, in terms of cell growth, product expression and product quality. To this end, the microbioreactor was characterised in terms of oxygen mass transfer and fluid mixing, and a direct comparison to 1L-scale and 50L-scale processes under optimum conditions was performed.

The k_La of the microbioreactor under standard fermentation operating conditions was inferior to the k_La of the 1L scale vessel and the predicted k_La of the 50L vessel; however in a microbioreactor fermentation oxygen transfer is enhanced by using 100% oxygen instead of air for DO control for the duration of the cultivation (Table 5.10). The mixing time of the REG cassette and PRC cassette at high shaking frequencies were comparable to literature data for both shaken microtitre plates and conventional STRs. Images from the high speed camera indicate that the fluid in the microbioreactor moves 'in phase' with orbital shaking platform and therefore the system should be well mixed under fermentation conditions.

The data presented in this chapter indicates that the microbioreactor fed-batch process better predicts the 50L pilot scale process than the 1L scale process, based on cell growth, product expression and product quality (Table 5.11). This is likely due to mixing and oxygen mass transfer phenomena. At 1L scale, both oxygen mass transfer and fluid mixing are highly efficient, resulting in the highest cell growth and productivity of the three processes (Tables 5.10 and 5.11). The limitations in oxygen mass transfer in the microbioreactor, and fluid mixing in the 50L scale vessel appear to result in a comparable cellular environment, and therefore cell growth, productivity and product quality (Tables 5.10 a d 5.11).

Chapter 6: Conclusions and Future Work

6.1. Conclusions

The original aim of this thesis was to develop a scale-down fermentation platform suitable for the study and optimisation of high cell density cultures (Section 1.9). As shown in Figure 4.13 an existing 24-well microbioreactor platform was modified to facilitate fed-batch culture operation. It was demonstrated that this could be used for screening of microbial fermentation conditions (Figure 4.15) and to predict pilot scale fermentation process performance (Figure 5.8). The overall aim of the work has therefore been achieved.

The first objective was to establish a feeding system to enable fed-batch *E. coli* cultures to be performed in an existing 24-well microbioreactor platform, the Pall Micro-24 microbioreactor. This was chosen as it enabled control of culture conditions in individual wells (Section 2.4). In Chapter 3 two feeding strategies were investigated; *in situ* feeding by the enzymatic release of glucose (Section 3.3.1), and direct feeding using a preliminary version of a bespoke feed delivery system (Section 3.3.2). It was demonstrated that specific productivity was enhanced with *in situ* feeding in comparison to the batch cultures at 1L scale (Table 3.1). However, the rate of glucose release was insufficient to sustain the high cell densities comparable to the 1L laboratory scale process. The second feeding strategy investigated was direct, continuous feeding. A bespoke feed delivery system was developed to allow for twelve wells to be fed directly in parallel (Figure 4.12). The final feeding system design consisted of a 3D-printed device to connect the feed lines to the microbioreactor cassette, a lid to maintain the environment temperature and accommodate the feed lines, and a sampling stand (Figures 3.14, 3.15 and 4.12).

The second objective was to establish an industrially relevant feeding strategy in the microbioreactor. Therefore, the culture conditions used with the direct feeding strategy were refined and optimised in terms of cell growth and product expression. This was achieved by modifying the feed rate and concentration (Sections 4.5 and 4.7), increasing the DO set point (Figure 4.7), implementing a pre-feeding hold period to reduce the concentration of inhibitory by-products (Section 4.7), and improvement of the sampling procedure to reduce sampling time (Section 3.3.2.1). The initial cell densities and SPRs attained using the microbioreactor direct feeding system were approximately 70% and 60% of the benchmark 1L scale process respectively (Table 3.1). There was significant well-to-well variation in the microbioreactor, which was shown to be due to excessive acetate production in the batch phase (Figure 4.6). It was demonstrated that cell growth and product expression were inhibited at high pre-feeding acetate concentrations (>1 g L^{-1}). The variation in the pre-feeding acetate concentration was consistent between experiments; wells with a high pre-feeding acetate concentration were

consistently high in repeat runs. Therefore, the variability appears to be related to the microbioreactor itself, rather than the fermentation process.

The third objective was to demonstrate the applicability of the bespoke feeding system as a tool for high throughput fermentation process optimisation experiments. Process optimisation experiments investigating the effect of IPTG concentration and post-induction temperature on product expression, were performed using the microbioreactor feeding system and the 1L scale laboratory process (Section 4.10). The data obtained were consistent between scales; in both cases product expression was enhanced at a higher post-induction temperature, and IPTG concentration did not affect product expression over the concentration range tested (Section 4.10). This demonstrates that the modified microbioreactor platform can be used to explore the response of the strain to changes in culture conditions (Section 4.10).

The fourth objective was to characterise the microbioreactor in terms of oxygen transfer capability and fluid mixing, to compare to the laboratory scale and pilot scale bioreactors. The microbioreactor was characterised in terms of oxygen transfer capacity (Section 5.2) and mixing time (Section 5.3)The maximum k_La values with water for the REG and PRC cassettes were 101h^{-1} and 64h^{-1} respectively (Figure 5.1), which in both cases is inferior to the k_La of the 1L scale vessel and the predicted k_La of the 50L scale vessel (Section 5.2.2). The measured microbioreactor mixing times were 0.5-3s for the REG cassette and 0.6-15s for the PRC cassette; at high shaking frequencies the mixing times were comparable to literature data for conventional STRs and the predicted mixing times of the 1L vessel (Section 5.3). The lower k_La of the microbioreactor compared to the 1L scale process could explain the greater acetate production and therefore lower biomass concentration and specific productivity in the microbioreactor.

The final objective was to show scalability of the microbioreactor by directly comparing it to laboratory and pilot scale processes in terms of cell growth, product expression, and product quality. 50L pilot-scale, 1L laboratory scale and 4mL microbioreactor fed-batch fermentations were performed under optimum conditions (Section 5.4). The 4mL microbioreactor process was shown to better predict the 50L pilot-scale process than the 1L laboratory-scale process based on cell growth, product expression and product quality (Table 5.11). This is likely due to mixing and oxygen mass transfer phenomena. At 1L scale, both oxygen mass transfer and fluid mixing are most efficient, meaning cell growth and productivity was the highest of the three processes. It appears that the limitations in oxygen mass transfer in the microbioreactor and fluid mixing in the 50L scale vessel (Table 5.10), results in a comparable cellular environment, and therefore cell growth, productivity and product quality (Table 5.11).

Overall, in this work the ability to conduct high cell density, fed-batch microbial cultures in parallel shaken miniature bioreactors has been demonstrated. A bespoke, 3D-printed feeding

system for a shaken miniature bioreactor was developed, that enabled twelve 4mL fed-batch cultures to be performed in parallel. The microbioreactor fed-batch process was shown to be predictive of an industrially relevant 50L pilot-scale process in terms of cell growth, product expression and product quality (Table 5.11). In addition, it was demonstrated that the microbioreactor can be used as a tool for small scale process optimisation experiments under industrially relevant, fed-batch conditions (Figure 4.16).

6.2. Future work

This work was specifically addressed replicating the GSK platform process in the microbioreactor. This process utilised a semi-complex media. Complex media is nutrient-rich and is undefined meaning cell growth is less controlled than using a defined media; this may have contributed to the high pre-feeding acetate concentration. Therefore to further investigate strategies to improve the reproducibility of the microbioreactor, a process using defined media could be established at 1L scale and then replicated using the microbioreactor feeding system.

Due to intellectual property reasons only one *E. coli* strain was investigated, so future work could be to further demonstrate the applicability of the microbioreactor fed-batch process as a scale-down platform. Possible experiments would be to run a low acetate producing strain in the microbioreactor as a comparison to the high acetate producing strain used in this work. Running multiple strains in parallel would also allow investigation of the application of the microbioreactor for strain screening experiments. To fully demonstrate the versatility of the system other host organisms e.g. *Saccharomyces cerevisiae* should be run in the microbioreactor. It would be particularly interesting to evaluate the microbioreactor with host organism with a lower growth rate than *E. coli* to see if the reproducibility of the system is improved.

Further engineering characterisation studies could also be performed. To better understand how mixing may vary during the course of fed-batch fermentation, additional mixing time experiments at a range of gas flow rates and viscosities should be performed. An engineering characterisation approach that could provide additional information about the fluid flow in the microbioreactor would be computational fluid dynamics (CFD). This would allow for prediction of parameters that are difficult to determine experimentally such as energy dissipation rates and gas hold up. Also this could provide an insight into the reasons for the retardation in mixing times in the PRC cassette at low shaking speeds, and the differences in bubble coalescence between water, and the complex media containing antifoam used in the fermentations (Kelly, 2008; Sharma, Malhotra and Rathore, 2011)

The scalability of the microbioreactor feeding system should ideally be further investigated. Additional product quality assays such as capillary gel electrophoresis and mass spectrometry should be performed. Also, in this work the 50L scale, 1L scale and microbioreactor processes were compared under optimum operating conditions. To try and improve comparability between scales, various scale-up criteria such as equivalent k_La, *OTR* or *P/V* should be investigated.

The feeding system could also potentially be adapted for continuous cultivation. This would be an interesting application of the system as the growth rates (or dilution rates) are more controlled than in batch or fed-batch cultivation, therefore the reproducibility may be improved (Monod, 1950; Novick and Szilard, 1950; Herbert, Elsworth and Telling, 1956). However, this would require the accommodation of a second line into each well.

To make the bespoke feed delivery system commercially viable, further development in terms of both user-friendliness and fermentation performance, would be required. The feed line assembly would need to be refined as the current system requires each syringe to be filled manually which is time consuming and risks the introduction of air bubbles into the tubing. Also, hypodermic needles are used to insert the feed lines into the well closures, which could be a safety concern in some research laboratories. The feed line assembly could made more user-friendly by fabricating bespoke well closures with integrated feed line ports and bespoke connectors to connect to the feed lines. In addition, the use of an automated syringe filling system would simply and improve the accuracy of the syringe filling process.

Modifications to the feed delivery system and microbioreactor well geometry would be desirable to further improve fermentation performance. Integrating a feed line dip tube into a bespoke well closure would be beneficial as it would enable a more uniform feed addition profile, and therefore reduce the oscillations in the DO control (Section 4.5). To enhance the k_La of the microbioreactor so that it is more comparable to conventional STRs under microbial operating conditions, the REG cassette wells could be modified by fabricating a sparger to sit on top of the gas injection membrane. This would reduce gas bubble size and therefore enhance the interfacial area *a*. To minimise the risk of contamination during assembly of the feed delivery system, the components should be 3D-printed using an autoclavable resin; this would be particularly important if the system were to be used for cell culture applications.

Chapter 7: References

A study of the effect of specific growth-rate and acetate on recombinant protein-production of Echerichia coli JM107Turner, C., Gregory, M. E. and Turner, M. K. (1994) 'A study of the effect of specific growth-rate and acetate on recombinant protein-production of Echerichia coli JM107', *Biotechnology Letters*, 16(9), pp. 891–896. doi: 10.1007/bf00128620.

Ali, S., Perez-Pardo, M. A., Aucamp, J. P., Craig, A., Bracewell, D. G. and Baganz, F. (2012) 'Characterization and feasibility of a miniaturized stirred tank bioreactor to perform E. coli high cell density fed-batch fermentations', *Biotechnology Progress*, 28(1), pp. 66–75. doi: 10.1002/btpr.708.

Anane, E., Lopez, C. D. C., Neubauer, P. and Bournazou, M. N. C. (2017) 'Modelling overflow metabolism in Escherichia coli by acetate cycling', *Biochemical Engineering Journal*, 125, pp. 23–30. doi: 10.1016/j.bej.2017.05.013.

Applikon (2018) 'micro-Matrix: 24 bioreactors in a convenient microtiter format'. Available at: https://www.applikon-biotechnology.com/files/applikon-micromatrix.pdf.

Applikon (2020) 'Generating scalable results in micro-bioreactors'. Available at: <https://www.applikon-biotechnology.com/files/applikon-white-paper-generating-scalable-results-in-micro-bioreactors.pdf>.

Arjunwadkar, S. J., Sarvanan, K., Kulkarni, P. R. and Pandit, A. B. (1998) 'Gas-liquid mass transfer in dual impeller bioreactor', *Biochemical Engineering Journal*, 1(2), pp. 99–106. doi: 10.1016/s1385-8947(97)00083-1.

Badino, A. C., Facciotti, M. C. R. and Schmidell, W. (2000) 'Improving kLa determination in fungal fermentation, taking into account electrode response time', *Journal of Chemical Technology & Biotechnology*. Wiley-Blackwell, 75(6), pp. 469–474. doi: 10.1002/1097-4660(200006)75:6<469::AID-JCTB236>3.0.CO;2-4.

Balasundaram, B., Nesbeth, D., Ward, J. M., Keshavarz-Moore, E. and Bracewell, D. G. (2009) 'Step change in the efficiency of centrifugation through cell engineering: co-expression of *Staphylococcal nuclease* to reduce the viscosity of the bioprocess feedstock', *Biotechnology and Bioengineering*. Wiley-Blackwell, 104(1), pp. 134–142. doi: 10.1002/bit.22369.

Bang, H. B., Lee, K., Lee, Y. J. and Jeong, K. J. (2018) 'High-level production of trans - cinnamic acid by fed-batch cultivation of Escherichia coli', *Process Biochemistry*, 68, pp. 30–36. doi: 10.1016/j.procbio.2018.01.026.

Bao, X., Xu, L., Lu, X. and Jia, L. (2016) 'Optimization of dilution refolding conditions for a camelid single domain antibody against human beta-2-microglobulin', *Protein Expression and*

Purification journal, 117, pp. 59–66. doi: 10.1016/j.pep.2015.09.019.

Bareither, R., Bargh, N., Oakeshott, R., Watts, K. and Pollard, D. (2013) 'Automated disposable small scale reactor for high throughput bioprocess development: A proof of concept study', *Biotechnology and Bioengineering*. Wiley-Blackwell, 110(12), pp. 3126–3138. doi: 10.1002/bit.24978.

Bareither, R. and Pollard, D. (2011) 'A review of advanced small-scale parallel bioreactor technology for accelerated process development: current state and future need', *Biotechnol Prog*, 27(1), pp. 2–14. doi: 10.1002/btpr.522.

Barrett, T. A., Wu, A., Zhang, H., Levy, M. S. and Lye, G. J. (2010) 'Microwell Engineering Characterization for Mammalian Cell Culture Process Development', *Biotechnology and Bioengineering*, 105(2), pp. 260–275. doi: 10.1002/bit.22531.

Bates, R. L., Fondy, P. L. and Corpstein, R. R. (1963) 'Examination of Some Geometric Parameters of Impeller Power', *Industrial & Engineering Chemistry Process Design and Development*. American Chemical Society, 2(4), pp. 310–314. doi: 10.1021/i260008a011.

Becker, P., Fierfort, N., Fernandes, C. and Bernal, C. (2017) 'High cell density fed-batch fermentation in micro-scale bioreactors – feed rate optimisation and strain selection for the production of HMO in E. coli', in *RAFT^{TM} 2017*. Bonita Springs.

Berlec, A. and Strukelj, B. (2013) 'Current state and recent advances in biopharmaceutical production in Escherichia coli, yeasts and mammalian cells', *Journal of Industrial Microbiology & Biotechnology*, 40(3–4), pp. 257–274. doi: 10.1007/s10295-013-1235-0.

Betts, J. I. and Baganz, F. (2006) 'Miniature bioreactors: current practices and future opportunities', *Microbial Cell Factories*, 5. doi: 10.1186/1475-2859-5-21.

Betts, J. I. I., Doig, S. D. D. and Baganz, F. (2006) 'Characterization and application of a miniature 10 mL stirred-tank bioreactor, showing scale-down equivalence with a conventional 7 L reactor', *Biotechnology Progress*. American Chemical Society (ACS), 22(3), pp. 681–688. doi: 10.1021/bp050369y.

Betts, J. P. J., Warr, S. R. C., Finka, G. B., Uden, M., Town, M., Janda, J. M., Baganz, F. and Lye, G. J. (2014) 'Impact of aeration strategies on fed-batch cell culture kinetics in a single-use 24-well miniature bioreactor', *Biochemical Engineering Journal*. Elsevier B.V., 82, pp. 105–116. doi: 10.1016/j.bej.2013.11.010.

Boder, E. T. and Jiang, W. (2011) 'Engineering Antibodies for Cancer Therapy', in Prausnitz, J. M. (ed.) *Annual Review of Chemical and Biomolecular Engineering, Vol 2*. Palo Alto: Annual Reviews, pp. 53–75. doi: 10.1146/annurev-chembioeng-061010-114142.

Bothmann, H. and Pluckthun, A. (2000) 'The periplasmic Escherichia coli peptidylprolyl cis,trans-isomerase FkpA. I. Increased functional expression of antibody fragments with and without cis-prolines.', *The Journal of biological chemistry*. American Society for Biochemistry and Molecular Biology, 275(22), pp. 17100–5. doi: 10.1074/jbc.M910233199.

Bournazou, M. N. C., Barz, T., Nickel, D. B., Cardenas, D. C. L., Glauche, F., Knepper, A. and Neubauer, P. (2017) 'Online optimal experimental re-design in robotic parallel fed-batch cultivation facilities', *Biotechnology and Bioengineering*, 114(3), pp. 610–619. doi: 10.1002/bit.26192.

Buchenauer, A., Hofmann, M. C., Funke, M., Buchs, J., Mokwa, W. and Schnakenberg, U. (2009) 'Micro-bioreactors for fed-batch fermentations with integrated online monitoring and microfluidic devices', *Biosensors and Bioelectronics*, 24(5), pp. 1411–1416. doi: 10.1016/j.bios.2008.08.043.

Buchs, J., Lotter, S., Milbradt, C., Büchs, J., Lotter, S. and Milbradt, C. (2001) 'Out-of-phase operating conditions, a hitherto unknown phenomenon in shaking bioreactors', *Biochemical Engineering Journal*. Elsevier, 7(2), pp. 135–141. doi: 10.1016/s1369-703x(00)00113-3.

Büchs, J., Maier, U., Milbradt, C. and Zoels, B. (2000) 'Power consumption in shaking flasks on rotary shaking machines: I. Power consumption measurement in unbaffled flasks at low liquid viscosity', *Biotechnology and Bioengineering*. Wiley-Blackwell, 68(6), pp. 589–593. doi: 10.1002/(SICI)1097-0290(20000620)68:6<589::AID-BIT1>3.0.CO;2-J.

Buss, N., Henderson, S. J., McFarlane, M., Shenton, J. M. and de Haan, L. (2012) 'Monoclonal antibody therapeutics: history and future', *Current Opinion in Pharmacology*, 12(5), pp. 615–622. doi: 10.1016/j.coph.2012.08.001.

Butler, M. (2005) 'Animal cell cultures: recent achievements and perspectives in the production of biopharmaceuticals', *Appl Microbiol Biotechnol*, 68, pp. 283–291. doi: 10.1007/s00253-005-1980-8.

Cabilly, S. (1989) 'Growth at suboptimal temperatures allows the production of functional, antigen-binding fab fragments in Escherichia coli', *Gene*, 85(2), pp. 553–557. doi: 10.1016/0378-1119(89)90451-4.

Calderbank, P. H. (1958) 'Physical Rate Processes in Industrial Fermentations Part Ⅰ: The Interfacial Area in Gas-Liquid Contacting with Mechanical Agitation', *Trans. Inst. Chem. Engrs*, 36, pp. 443–463. Available at: http://ci.nii.ac.jp/naid/10013410643/en/ (Accessed: 26 August 2019).

Çalik, P., Yilgör, P. and Demir, A. S. (2006) 'Influence of controlled-pH and uncontrolled-pH

operations on recombinant benzaldehyde lyase production by Escherichia coli', *Enzyme and Microbial Technology*, 38, pp. 617–627. doi: 10.1016/j.enzmictec.2005.07.029.

Carreau, P. J., Patterson, I. and Yap, C. Y. (1976) 'Mixing of viscoelastic fluids with helical-ribbon agitators. I - Mixing time and flow patterns', *The Canadian Journal of Chemical Engineering*. Wiley-Blackwell, 54(3), pp. 135–142. doi: 10.1002/cjce.5450540303.

Chalmers, J. J., Kim, E., Telford, J. N., Wong, E. Y., Tacon, W. C., Shuler, M. L. and Wilson, D. B. (1990) 'Effects of temperature on Escherichia coli overproducing beta-lactamase or human epidermal growth-factor', *Applied and Environmental Microbiology*, 56(1), pp. 104–111.

Chandrasekharan, K. and Calderbank, P. H. (1981) 'Further observations on the scale-up of aerated mixing vessels', *Chemical Engineering Science*, 36(5), pp. 819–823. Available at: https://pdf.sciencedirectassets.com/271348/1-s2.0-S0009250900X03879/1-s2.0-0009250981850336/main.pdf?X-Amz-Security-Token=AgoJb3JpZ2luX2VjEMH%2F%2F%2F%2F%2F%2F%2F%2F%2F%2FwEaCXVzLWVhc3QtMSJGMEQCIAgF3RQCsYD%2BE9FcIqPt5aUYfEaR%2B0I4A91VdD3hKpsaAiBvbOioVWnHZ (Accessed: 6 August 2019).

Chen, A., Chitta, R., Chang, D. and Anianullah, A. (2009) 'Twenty-Four Well Plate Miniature Bioreactor System as a Scale-Down Model for Cell Culture Process Development', *Biotechnology and Bioengineering*, 102(1), pp. 148–160. doi: 10.1002/bit.22031.

Chung, J. (2017) 'Special issue on therapeutic antibodies and biopharmaceuticals', *Experimental & Molecular Medicine*, 49. doi: 10.1038/emm.2017.46.

Clarke, K. (2013) *Bioprocess Engineering - An Introductory Engineering and Life Science Approach - Knovel*. Philadelphia: Woodland Publishing. Available at: https://app-knovel-com.libproxy.ucl.ac.uk/web/toc.v/cid:kpBEAIELS6/viewerType:toc/root_slug:viewerType%3Atoc/url_slug:root_slug%3Abioprocess-engineering?kpromoter=federation (Accessed: 31 May 2018).

Contiero, J., Beatty, C., Kumari, S., DeSanti, C. L., Strohl, W. R. and Wolfe, A. (2000) 'Effects of mutations in acetate metabolism on high-cell-density growth of Escherichia coli', *Journal of Industrial Microbiology & Biotechnology*, 24(6), pp. 421–430. doi: 10.1038/sj.jim.7000014.

Cooke, M. (1993) 'Application of model suspensions in the design of fermenters', in Shamlou, P. A. (ed.) *Solid-liquid suspensions*. Oxford: Butterworth-Heinemann, pp. 192–221.

Cui, Y. Q., vanderLans, R. and Luyben, K. (1996) 'Local power uptake in gas-liquid systems with single and multiple Rushton turbines', *Chemical Engineering Science*, 51(11), pp. 2631–

2636. doi: 10.1016/0009-2509(96)00128-5.

Deantonio, C., Sedini, V., Cesaro, P., Quasso, F., Cotella, D., Persichetti, F., Santoro, C. and Sblattero, D. (2014) 'An Air-well sparging minifermenter system for high-throughput protein production', *Microbial Cell Factories*, 13(1), pp. 1–9. doi: 10.1186/s12934-014-0132-1.

Death, A. and Ferenci, T. (1994) *Between Feast and Famine: Endogenous Inducer Synthesis in the Adaptation of Escherichia coli to Growth with Limiting Carbohydrates*, *Journal of Bacteriology*. Available at: http://jb.asm.org/ (Accessed: 16 June 2019).

Diaz, A. and Acevedo, F. (1999) 'Scale-up strategy for bioreactors with Newtonian and non-Newtonian broths', *Bioprocess Engineering*, 21(1), pp. 21–23. doi: 10.1007/s004490050634.

Doherty, A. J., Connolly, B. A. and Worrall, A. F. (1993) 'Overproduction of the toxic protein, bovine pancreatic DNAseI, in Escherichia coli using a tightly controlled T7-promoter-based vector', *Gene*, 136(1–2), pp. 337–340. doi: 10.1016/0378-1119(93)90491-k.

Doig, S. D., Baganz, F. and Lye, G. J. (2006) 'High-throughput screening and process optimisation', in *Basic Biotechnology*. doi: 10.1017/CBO9780511802409.014.

Doig, S. D., Pickering, S. C. R., Lye, G. J. and Baganz, F. (2005) 'Modelling surface aeration rates in shaken microtitre plates using dimensionless groups', *Chemical Engineering Science*, 60(10), pp. 2741–2750. doi: 10.1016/j.ces.2004.12.025.

Dong, H. J., Nilsson, L. and Kurland, C. G. (1995) 'Gratuitous overexpression of genes in Escherichia coli leads to growth-inhibition and ribosome destruction', *Journal of Bacteriology*, 177(6), pp. 1497–1504. doi: 10.1128/jb.177.6.1497-1504.1995.

Donovan, R. S., Robinson, C. W. and Glick, B. R. (1996) 'Review: Optimizing inducer and culture conditions for expression of foreign proteins under the control of the lac promoter', *Journal of Industrial Microbiology*, 16(3), pp. 145–154. doi: 10.1007/bf01569997.

Doran, P. M. (2013) *Bioprocess engineering principles*. Elsevier/Academic Press.

Duetz, W. A. (2007) 'Microtiter plates as mini-bioreactors: miniaturization of fermentation methods', *Trends in Microbiology*, 15(10), pp. 469–475. doi: 10.1016/j.tim.2007.09.004.

Dumon-Seignovert, L., Cariot, G. and Vuillard, L. (2004) 'The toxicity of recombinant proteins in Escherichia coli: A comparison of overexpression in BL21(DE3), C41(DE3), and C43(DE3)', *Protein Expression and Purification*, 37(1), pp. 203–206. doi: 10.1016/j.pep.2004.04.025.

Eiteman, M. A. and Altman, E. (2006) 'Overcoming acetate in Escherichia coli recombinant protein fermentations', *Trends in Biotechnology*, 24(11), pp. 530–536. doi:

10.1016/j.tibtech.2006.09.001.

El-Dessouky, H. T., Ettouney, H. M., Alatiqi, I. M. and Al-Shamari, M. A. (2002) 'Evaporation rates from fresh and saline water in moving air', *Industrial & Engineering Chemistry Research*, 41(3), p. 642–+. doi: 10.1021/ie010327o.

Enjalbert, B., Cocaign-Bousquet, M., Portais, J. C. and Letisse, F. (2015) 'Acetate Exposure Determines the Diauxic Behavior of Escherichia coli during the Glucose-Acetate Transition', *Journal of Bacteriology*, 197(19), pp. 3173–3181. doi: 10.1128/jb.00128-15.

Esfandiar, S., Hashemi-Najafabadi, S., Shojaosadati, S. A., Sarrafzadeh, S. A. and Pourpak, Z. (2010) 'Purification and refolding of Escherichia coli-expressed recombinant human interleukin-2', *Biotechnology and Applied Biochemistry*, 55, pp. 209–214. doi: 10.1042/ba20090256.

Farewell, A. and Neidhardt, F. C. (1998) 'Effect of temperature on in vivo protein synthetic capacity in Escherichia coli', *Journal of Bacteriology*, 180(17), pp. 4704–4710.

FDA (2011) *Guidance for Industry Process Validation : General Principles and Practices Guidance for Industry Process Validation : General Principles and Practices*. Available at: https://www.fda.gov/downloads/drugs/guidances/ucm070336.pdf.

Ferenci, T. (1999) '"Growth of bacterial cultures" 50 years on: towards an uncertainty principle instead of constants in bacterial growth kinetics', *Research in Microbiology*, 150(7), pp. 431–438. Available at: https://pdf.sciencedirectassets.com/272130/1-s2.0-S0923250800X00344/1-s2.0-S092325089900114X/main.pdf?x-amz-security-token=AgoJb3JpZ2luX2VjED0aCXVzLWVhc3QtMSJHMEUCIQDaTfuKoCXX7rkh1bSHP8%2Fm%2FGveMO%2FMWhO2PE1%2FiJs31QIgO7Vo%2F5WZZkbj%2F0sHF3DlIeb9bolxKexy.

Fischer, S., Handrick, R. and Otte, K. (2015) 'The art of CHO cell engineering: A comprehensive retrospect and future perspectives'. doi: 10.1016/j.biotechadv.2015.10.015.

Frenzel, A., Hust, M. and Schirrmann, T. (2013) 'Expression of Recombinant Antibodies', *Frontiers in Immunology*. Frontiers, 4, p. 217. doi: 10.3389/fimmu.2013.00217.

Funke, M., Buchenauer, A., Schnakenberg, U., Mokwa, W., Diederichs, S., Mertens, A., Muller, C., Kensy, F. and Buchs, J. (2010) 'Microfluidic BioLector-Microfluidic Bioprocess Control in Microtiter Plates', *Biotechnology and Bioengineering*, 107(3), pp. 497–505. doi: 10.1002/bit.22825.

Gagnon, H., Lounès, M., Thibault, J., Lounes, M. and Thibault, J. (1998) 'Power consumption and mass transfer in agitated gas-liquid columns: a comparative study', *Canadian Journal of*

Chemical Engineering, 76(3), pp. 379–389. doi: 10.1002/cjce.5450760306.

Garcia-Ochoa, F. and Gomez, E. (2009) 'Bioreactor scale-up and oxygen transfer rate in microbial processes: An overview', *Biotechnology Advances*. Elsevier, 27(2), pp. 153–176. doi: 10.1016/J.BIOTECHADV.2008.10.006.

Gibilaro, L. G., Davies, S. N., Cooke, M., Lynch, P. M. and Middleton, J. C. (1985) 'Initial response analysis of mass-transfer in a gas sparged stirred vessel', *Chemical Engineering Sconce*, 40(181). Available at: https://ac-els-cdn-com.libproxy.ucl.ac.uk/0009250985801159/1-s2.0-0009250985801159-main.pdf?_tid=201ea85d-bf0c-4a33-bff5-c6fef77e59a0&acdnat=1527683722_1a83b08f8170b4e230d315c06ed9d3fa.

Gill, N. K., Appleton, M., Baganz, F. and Lye, G. J. (2008a) 'Design and characterisation of a miniature stirred bioreactor system for parallel microbial fermentations', *Biochemical Engineering Journal*, 39(1), pp. 164–176. doi: 10.1016/j.bej.2007.09.001.

Gill, N. K., Appleton, M., Baganz, F. and Lye, G. J. (2008b) 'Quantification of power consumption and oxygen transfer characteristics of a stirred miniature bioreactor for predictive fermentation scale-up', *Biotechnology and Bioengineering*. Wiley-Blackwell, 100(6), pp. 1144–1155. doi: 10.1002/bit.21852.

Glazyrina, J., Krause, M., Junne, S., Glauche, F., Strom, D. and Neubauer, P. (2012) 'Glucose-limited high cell density cultivations from small to pilot plant scale using an enzyme-controlled glucose delivery system', *New Biotechnology*, 29(2), pp. 235–242. doi: 10.1016/j.nbt.2011.11.004.

Glazyrina, J., Materne, E. M., Dreher, T., Storm, D., Junne, S., Adams, T., Greller, G. and Neubauer, P. (2010) 'High cell density cultivation and recombinant protein production with Escherichia coli in a rocking- motion- type bioreactor', *Microbial Cell Factories*, 9. doi: 10.1186/1475-2859-9-42.

Gogate, P. R., Beenackers, A. A. C. . C. M. and Pandit, A. B. (2000) 'Multiple-impeller systems with a special emphasis on bioreactors: a critical review', *Biochemical Engineering Journal*. Elsevier, 6(2), pp. 109–144. doi: 10.1016/S1369-703X(00)00081-4.

Gu, M. B., Dhurjati, P. S., Van Dyk, T. K. and LaRossa, R. A. (1996) 'A Miniature Bioreactor for Sensing Toxicity Using Recombinant Bioluminescent Escherichia coli Cells', *Biotechnology Progress*. American Chemical Society (ACS), 12(3), pp. 393–397. doi: 10.1021/bp9600142.

Harms, P., Kostov, Y., French, J. A., Soliman, M., Anjanappa, M., Ram, A. and Rao, G. (2006) 'Design and performance of a 24-station high throughput microbioreactor', *Biotechnology and Bioengineering*, 93(1), pp. 6–13. doi: 10.1002/bit.20742.

Hegarty, T. W. (1973) 'Temperature coefficient (q10), seed-germination and other biological processes', *Nature*, 243(5405), pp. 305–306. doi: 10.1038/243305a0.

Herbert, D., Elsworth, R. and Telling, R. C. (1956) 'The Continuous Culture of Bacteria; a Theoretical and Experimental Study', *Journal of Applied Microbiology*, 14, p. 601622. Available at: https://www.microbiologyresearch.org/docserver/fulltext/micro/14/3/mic-14-3-601.pdf?expires=1566849955&id=id&accname=guest&checksum=29A79261C3B9D11AB17B 31B7451D884C.

Herendeen, S. L., Vanbogelen, R. A. and Neidhardt, F. C. (1979) 'Levels of major proteins of Escherichia coli during growth at different temperatures', *Journal of Bacteriology*, 139(1), pp. 185–194.

Hermann, R., Lehmann, M., Buchs, J., Büchs, J. and Buchs, J. (2003) 'Characterization of gas-liquid mass transfer phenomena in microtiter plates', *Biotechnology and Bioengineering*, 81(2), pp. 178–186. doi: 10.1002/bit.10456.

Heyland, J., Blank, L. M. and Schmid, A. (2011) 'Quantification of metabolic limitations during recombinant protein production in Escherichia coli', *Journal of Biotechnology*, 155(2), pp. 178–184. doi: 10.1016/j.jbiotec.2011.06.016.

Holt, L. J., Herring, C., Jespers, L. S., Woolven, B. P. and Tomlinson, I. M. (2003) 'Domain antibodies: proteins for therapy', *Trends in Biotechnology*, 21(11), pp. 484–490. doi: 10.1016/j.tibtech.2003.08.007.

Hortsch, R., Stratmann, A. and Weuster-Botz, D. (2010) 'New Milliliter-Scale Stirred Tank Bioreactors for the Cultivation of Mycelium Forming Microorganisms', *Biotechnology and Bioengineering*, 106(3), pp. 443–451. doi: 10.1002/bit.22706.

Huang, C. J., Lin, H. and Yang, X. M. (2012) 'Industrial production of recombinant therapeutics in Escherichia coli and its recent advancements', *Journal of Industrial Microbiology & Biotechnology*, 39(3), pp. 383–399. doi: 10.1007/s10295-011-1082-9.

Huber, R., Ritter, D., Hering, T., Hillmer, A. K., Kensy, F., Muller, C., Wang, L. and Buchs, J. (2009) 'Robo-Lector - a novel platform for automated high-throughput cultivations in microtiter plates with high information content', *Microbial Cell Factories*, 8. doi: 10.1186/1475-2859-8-42.

Huber, R., Scheidle, M., Dittrich, B., Klee, D. and Büchs, J. (2009) 'Equalizing growth in high-throughput small scale cultivations via precultures operated in fed-batch mode', *Biotechnology and Bioengineering*, 103(6), pp. 1095–1102. doi: 10.1002/bit.22349.

Hughmark, G. A. (1980) 'Power requirements and interfacial area in gas-liquid turbine agitated

systems', *Industrial & Engineering Chemistry Process Design and Development*, 19(4), pp. 638–641. doi: 10.1021/i260076a023.

Isett, K., George, H., Herber, W. and Amanullah, A. (2007) 'Twenty-four-well plate miniature Bioreactor high-throughput system: Assessment for microbial cultivations', *Biotechnology and Bioengineering*, 98(5), pp. 1017–1028. doi: 10.1002/bit.21484.

Islam, R. S., Tisi, D., Levy, M. S. and Lye, G. J. (2007) 'Framework for the rapid optimization of soluble protein expression in Escherichia coli combining microscale experiments and statistical experimental design', *Biotechnology Progress*, 23(4), pp. 785–793. doi: 10.1021/bp070059a.

Jensen, E. B. and Carlsen, S. (1990) 'Production of recombinant human growth-hormone in Escherichia coli: expression of different precursors and physiological effects of glucose, acetate and salts', *Biotechnology and Bioengineering*, 36(1), pp. 1–11. doi: 10.1002/bit.260360102.

Jeude, M., Dittrich, B., Niederschulte, H., Anderlei, T., Knocke, C., Klee, D. and Buchs, J. (2006) 'Fed-batch mode in shake flasks by slow-release technique', *Biotechnology and Bioengineering*, 95(3), pp. 433–445. doi: 10.1002/bit.21012.

Junker, B. H. (2004) 'Scale-up methodologies for Escherichia coli and yeast fermentation processes', *Journal of Bioscience and Bioengineering*. Elsevier, 97(6), pp. 347–364. doi: 10.1016/S1389-1723(04)70218-2.

Kantarci, N., Borak, F. and Ulgen, K. O. (2005) 'Bubble column reactors', *Process Biochemistry*, 40(7), pp. 2263–2283. doi: 10.1016/j.procbio.2004.10.004.

Kaprelyants, A. S., Mukamolova, G. V and Kell, D. B. (1994) 'Estimation of dormant Micrococcus luteus cells by penicillin lysis and by resuscitation in cell-free spent culture-medium at high dilution', *Fems Microbiology Letters*, 115(2–3), pp. 347–352. doi: 10.1111/j.1574-6968.1994.tb06662.x.

Kar, T., Destain, J., Thonart, P. and Delvigne, F. (2010) 'Impact of scaled-down on dissolved oxygen fluctuations at different levels of the lipase synthesis pathway of Yarrowia lipolytica', *Biotechnology, Agronomy and Society and Environment*, 14(spec. issue 2), pp. 523–529.

Kato, I. and Tanaka, H. (1998) 'Development of a novel box-shaped shake flask with efficient gas exchange capacity', *Journal of Fermentation and Bioengineering*, 85(4), pp. 404–409. doi: 10.1016/s0922-338x(98)80084-6.

Kelly, W. J. (2008) 'Using computational fluid dynamics to characterize and improve bioreactor performance', *Biotechnology and Applied Biochemistry*. Wiley-Blackwell, 49(4), p. 225. doi: 10.1042/BA20070177.

Kensy, F., Zang, E., Faulhammer, C., Tan, R. K. and Buchs, J. (2009) 'Validation of a high-throughput fermentation system based on online monitoring of biomass and fluorescence in continuously shaken microtiter plates', *Microbial Cell Factories*, 8. doi: 10.1186/1475-2859-8-31.

Kesik-Brodacka, M. (2018) 'Progress in biopharmaceutical development', *Biotechnology and Applied Biochemistry*. Wiley-Blackwell, 65(3), pp. 306–322. doi: 10.1002/bab.1617.

Klein, T., Schneider, K. and Heinzle, E. (2013) 'A system of miniaturized stirred bioreactors for parallel continuous cultivation of yeast with online measurement of dissolved oxygen and off-gas', *Biotechnology and Bioengineering*, 110(2), pp. 535–542. doi: 10.1002/bit.24633.

Kocincova, A. S., Nagl, S., Arain, S., Krause, C., Borisov, S. M., Arnold, M. and Wolfbeis, O. S. (2008) 'Multiplex bacterial growth monitoring in 24-well microplates using a dual optical sensor for dissolved oxygen and pH', *Biotechnology and Bioengineering*, 100(3), pp. 430–438. doi: 10.1002/bit.21793.

Kosinski, M. J., Rinas, U. and Bailey, J. E. (1992) 'Proteolytic response to the expression of an abnormal beta-galactosidase in Escherichia coli', *Applied Microbiology and Biotechnology*, 37(3), pp. 335–341. doi: 10.1007/bf00210989.

Kostov, Y., Harms, P., Randers-Eichhorn, L. and Rao, G. (2001) 'Low-cost microbioreactor for high-throughput bioprocessing', *Biotechnology and Bioengineering*, 72(3), pp. 346–352. doi: 10.1002/1097-0290(20010205)72:3<346::aid-bit12>3.0.co;2-x.

Kumaraswamy, S. (2012) 'Biosensors in the Processing and Analysis of Biopharmaceuticals', in Subramanian, G. (ed.) *Biopharmaceutical Production Technology*. Weinheim: Wiley- VCH Verlag GmbH & Co. KGaA, pp. 445–471. doi: 10.1002/9783527653096.

Laffend, L. and Shuler, M. L. (1994) 'Structured model of genetic-control via the lac promoter in Escherichia coli', *Biotechnology and Bioengineering*, 43(5), pp. 399–410. doi: 10.1002/bit.260430508.

Lamping, S. R., Zhang, H., Allen, B. and Shamlou, P. A. (2003) 'Design of a prototype miniature bioreactor for high throughput automated bioprocessing', *Chemical Engineering Science*, 58, pp. 747–758. doi: 10.1016/S0009-2509(02)00604-8.

Landwall, P. and Holme, T. (1977) 'Removal of inhibitors of bacterial-growth by dialysis culture', *Journal of General Microbiology*, 103(DEC), pp. 345–352. doi: 10.1099/00221287-103-2-345.

Lara, A. R., Galindo, E., Ramírez, O. T. and Palomares, L. A. (2006) 'Living With Heterogeneities in Bioreactors Understanding the Effects of Environmental Gradients on Cells',

Molecular Biotechnology, 34(3), pp. 355–381. Available at: https://search-proquest-com.libproxy.ucl.ac.uk/docview/236776615?accountid=14511.

Larsson, G., T6rnkvist, M., Noorman, H., Enfors, S.-O., Wernersson, E. S. and Tr~ig~rdh, C. (1996) 'Substrate gradients in bioreactors: origin and consequences', *Bioprocess Engineering*. Springer-Verlag, 14(289). Available at: https://link-springer-com.libproxy.ucl.ac.uk/content/pdf/10.1007%2FBF00369471.pdf.

Lasko, D. R., Zamboni, N. and Sauer, U. (2000) 'Bacterial response to acetate challenge: a comparison of tolerance among species', *Applied Microbiology and Biotechnology*, 54(2), pp. 243–247. doi: 10.1007/s002530000339.

Lecina, M., Sarro, E., Casablancas, A., Godia, F. and Cairo, J. J. (2013) 'IPTG limitation avoids metabolic burden and acetic acid accumulation in induced fed-batch cultures of Escherichia coli M15 under glucose limiting conditions', *Biochemical Engineering Journal*, 70, pp. 78–83. doi: 10.1016/j.bej.2012.10.006.

Lee, S. Y. (1996) 'High cell-density culture of Escherichia coli', *Trends in Biotechnology*, 14(3), pp. 98–105. doi: 10.1016/0167-7799(96)80930-9.

Lee, Y. J. and Jeong, K. J. (2015) 'Challenges to production of antibodies in bacteria and yeast', *Journal of Bioscience and Bioengineering*, 120, pp. 483–490. doi: 10.1016/j.jbiosc.2015.03.009.

van Leeuwen, M., Buijs, N. A. A., Canelas, A. B., Oudshoorn, A., Heijnen, J. J. and van Gulik, W. M. (2009) 'The Hagen–Poiseuille pump for parallel fed-batch cultivations in microbioreactors', *Chemical Engineering Science*, 64(8), pp. 1877–1884. doi: http://dx.doi.org/10.1016/j.ces.2009.01.015.

Liew, M. W. O., Rajendran, A. and Middelberg, A. P. J. (2010) 'Microbial production of virus-like particle vaccine protein at gram-per-litre levels', *Journal of Biotechnology*, 150(2), pp. 224–231. doi: 10.1016/j.jbiotec.2010.08.010.

Linek, V., Kordač, M., Fujasová, M. and Moucha, T. (2004) 'Gas-liquid mass transfer coefficient in stirred tanks interpreted through models of idealized eddy structure of turbulence in the bubble vicinity', *Chemical Engineering and Processing*, 43, pp. 1511–1517. doi: 10.1016/j.cep.2004.02.009.

Luli, G. W. and Strohl, W. R. (1990) 'Comparison of growth, acetate production, and acetate inhibition of Escherichia coli strains in batch and fed-batch fermentations', *Applied and Environmental Microbiology*, 56(4), pp. 1004–1011.

Luong, H. T. and Volesky, B. (1979) 'Mechanical power requirements of gas-liquid agitated systems', *AIChE Journal*. Wiley-Blackwell, 25(5), pp. 893–895. doi: 10.1002/aic.690250520.

Lye, G. J., Ayazi-Shamlou, P., Baganz, F., Dalby, P. A. and Woodley, J. M. (2003) 'Accelerated design of bioconversion processes using automated microscale processing techniques', *Trends in Biotechnology*, 21(1), pp. 29–37. Available at: http://www.hamiltoncomp.com (Accessed: 4 November 2019).

Macdonald, H. L. and Neway, J. O. (1990) 'Effects of medium quality on the expression of human interleukin-2 at high cell-density in fermenter cultures of Escherichia coli K-12', *Applied and Environmental Microbiology*, 56(3), pp. 640–645.

Maggi, M. and Scotti, C. (2017) 'Enhanced expression and purification of camelid single domain VHH antibodies from classical inclusion bodies'. doi: 10.1016/j.pep.2017.02.007.

Maharbiz, M. M., Holtz, W. J., Howe, R. T. and Keasling, J. D. (2004) 'Microbioreactor arrays with parametric control for high-throughput experimentation', *Biotechnology and Bioengineering*, 85(4), pp. 376–381. doi: 10.1002/bit.10835.

Mayer, S., Junne, S., Ukkonen, K., Glazyrina, J., Glauche, F., Neubauer, P. and Vasala, A. (2014) 'Lactose autoinduction with enzymatic glucose release: Characterization of the cultivation system in bioreactor', *Protein Expression and Purification*, 94, pp. 67–72. doi: 10.1016/j.pep.2013.10.024.

Mccleary, W. R. and Stock, J. B. (1994) 'Acetyl Phosphate and the Activation of Two-component Response Regulators*', *The Journal of Biological Chemistry*, 269(50), p. 3156731572. Available at: http://www.jbc.org.libproxy.ucl.ac.uk/content/269/50/31567.full.pdf (Accessed: 7 October 2018).

McDougald, D., Rice, S. A., Weichart, D. and Kjelleberg, S. (1998) 'Nonculturability: adaptation or debilitation?', *Fems Microbiology Ecology*, 25(1), pp. 1–9.

Meyer, H. P., Leist, C. and Fiechter, A. (1984) 'Acetate formation in continuous culture of Escherichia coli K12-D1 on defined and complex media', *Journal of Biotechnology*, 1(5–6), pp. 355–358. doi: 10.1016/0168-1656(84)90027-0.

Micheletti, M., Barrett, T., Doig, S. D., Baganz, F., Levy, M. S., Woodley, J. M. and Lye, G. J. (2006) 'Fluid mixing in shaken bioreactors: Implications for scale-up predictions from microlitre-scale microbial and mammalian cell cultures', *Chemical Engineering Science*, 61(9), pp. 2939–2949. doi: 10.1016/j.ces.2005.11.028.

Micheletti, M. and Lye, G. J. (2006) 'Microscalle bioprocess optimisation', *Current Opinion in Biotechnology*, 17(6), pp. 611–618. doi: 10.1016/j.copbio.2006.10.006.

Miroux, B. and Walker, J. E. (1996) 'Over-production of proteins in Escherichia coli: Mutant hosts that allow synthesis of some membrane proteins and globular proteins at high levels',

Journal of Molecular Biology, 260(3), pp. 289–298. doi: 10.1006/jmbi.1996.0399.

Möckel, H.-O., Wolleschensky, E., Drewas, S., Drewas, S. and Rahner, H.-J. (1990) 'Modelling of the calculation of the power input for aerated single- and multistage impellers with special respect to scale-up', *Acta Biotechnologica*. Wiley-Blackwell, 10(3), pp. 215–224. doi: 10.1002/abio.370100302.

Mockel, H. O., Wolleschensky, E., Drewas, S. and Rahner, H. J. (1990) 'Modeling of the calculation of the power input for aerated single-stage and multistage impellers with special respect to scale-up', *Acta Biotechnologica*, 10(3), pp. 215–224. doi: 10.1002/abio.370100302.

Monod, J. (1950) 'La Technique de Culture Continue Theorie et Applications', *Annales de L'Institut Pasteur*. Paris: Masson Editeur, 79(4), pp. 390–410.

Moorkens, E., Meuwissen, N., Huys, I., Declerck, P., Vulto, A. G. and Simoens, S. (2017) 'The Market of Biopharmaceutical Medicines: A Snapshot of a Diverse Industrial Landscape', *Frontiers in Pharmacology*. Frontiers, 8, p. 314. doi: 10.3389/fphar.2017.00314.

Mori, H., Yano, T., Kobayashi, T. and Shimizu, S. (1979) 'High density cultivation of biomass in fed-batch system with DO-stat', *Journal of Chemical Engineering of Japan*, 12(4), pp. 313–319. Available at: https://www-jstage-jst-go-jp.libproxy.ucl.ac.uk/article/jcej1968/12/4/12_4_313/_pdf.

Mukhopadhyay, T. K., Allison, N., Charlton, S., Hudson, M. J., Hallis, B., King, A., Baker, R., Noonan, S., Mcglashan, J., West, K., Levy, M. S., Ward, J. M. and Lye, G. J. (2010) 'Evaluation of anthrax vaccine production by Bacillus anthracis Sterne 34F 2 in stirred suspension culture using a miniature bioreactor: A useful scale-down tool for studies on fermentations at high containment', *Biochemical Engineering Journal*. Elsevier, 50(3), pp. 139–144. doi: 10.1016/j.bej.2010.03.011.

Najafpour, G. D. (2007) 'Bioprocess Scale-up', in *Biochemical Engineering and Biotechnology*, pp. 287–331. Available at: https://app-knovel-com.libproxy.ucl.ac.uk/web/toc.v/cid:kpBEB00001/viewerType:toc//root_slug:viewerType%3Atoc/url_slug:root_slug%3Abiochemical-engineering?kpromoter=federation

Nakano, K., Rischke, M., Sato, S., Markl, H. and Märkl, H. (1997) 'Influence of acetic acid on the growth of Escherichia coli K12 during high-cell-density cultivation in a dialysis reactor', *Applied Microbiology and Biotechnology*, 48(5), pp. 597–601. doi: 10.1007/s002530051101.

Nandakumar, M. P., Cheung, A. and Marten, M. R. (2006) 'Proteomic analysis of extracellular proteins from Escherichia coli W3110', *Journal of Proteome Research*, 5(5), pp. 1155–1161. doi: 10.1021/pr050401j.

Navascues, G. (1979) 'Liquid surfaces - theory of surface tension', *Reports on Progress in Physics*, 42(7), p. 1131-. doi: 10.1088/0034-4885/42/7/002.

Newton, J. M., Schofield, D., Vlahopoulou, J. and Zhou, Y. (2016) 'Detecting cell lysis using viscosity monitoring in *E. coli* fermentation to prevent product loss', *Biotechnology Progress*. American Chemical Society (ACS), 32(4), pp. 1069–1076. doi: 10.1002/btpr.2292.

Ni, Y. and Chen, R. (2009) 'Extracellular recombinant protein production from Escherichia coli', *Biotechnology Letters*, 31(11), pp. 1661–1670. doi: 10.1007/s10529-009-0077-3.

Nienow, A. W. (1997) 'On impeller circulation and mixing effectiveness in the turbulent flow regime', *Chemical Engineering Science*, 52(15), pp. 2557–2565. doi: 10.1016/S0009-2509(97)00072-9.

Nienow, A. W. (1998) 'Hydrodynamics of Stirred Bioreactors', *Applied Mechanics Reviews*, 51(1), p. 3. doi: 10.1115/1.3098990.

Nishikawa, M., Nakamura, M., Yagi, H. and Hashimoto, K. (1981) 'GAS-ABSORPTION IN AERATED MIXING VESSELS', *Journal of Chemical Engineering of Japan*, 14(3), pp. 219–226. doi: 10.1252/jcej.14.219.

Novick, A. and Szilard, L. (1950) 'Description of the Chemostat', *Science*. Washington: Amer Assoc Advancement Science, 112(2920), pp. 715–716. doi: 10.1126/science.112.2920.715.

Oosterhuis, N. M. G. and Kossen, N. W. F. (1981) 'Power input measurements in a production scale bioreactor', *Biotechnology Letters*. Kluwer Academic Publishers, 3(11), pp. 645–650. doi: 10.1007/BF00158694.

Oosterhuis, N. M. G. and Kossen, N. W. F. (1984) 'Dissolved oxygen concentration profiles in a production-scale bioreactor', *Biotechnology and Bioengineering*. Wiley-Blackwell, 26(5), pp. 546–550. doi: 10.1002/bit.260260522.

Orphanou, C. and Gervais, D. (2018) 'Mini-review Higher-order structure and conformational change in biopharmaceuticals'. doi: 10.1002/jctb.5682.

Oshinbolu, S., Wilson, L. J., Lewis, W., Shah, R. and Bracewell, D. G. (2018) 'Measurement of impurities to support process development and manufacture of biopharmaceuticals', *TrAC Trends in Analytical Chemistry*. Elsevier, 101, pp. 120–128. doi: 10.1016/J.TRAC.2017.10.026.

Pall (no date) Pall ForteBio : Octet Systems. Available at: https://www.fortebio.com/octet-platform.html

Pall Corporation (2012) 'Micro-24 MicroReactor System'. Available at: www.pall.com.

Pan, J. G., Rhee, J. S. and Lebeault, J. M. (1987) 'Physiological constraints in increasing biomass concentration of Escherichia coli B in fed-batch culture', *Biotechnology Letters*, 9(2), pp. 89–94. doi: 10.1007/bf01032744.

Panula-Perala, J., Siurkus, J., Vasala, A., Wilmanowski, R., Casteleijn, M. G. and Neubauer, P. (2008) 'Enzyme controlled glucose auto-delivery for high cell density cultivations in microplates and shake flasks', *Microbial Cell Factories*, 7. doi: 10.1186/1475-2859-7-31.

Pinto, D., Almeida, V., Santos, M. A. and Chambel, L. (2011) 'Resuscitation of Escherichia coli VBNC cells depends on a variety of environmental or chemical stimuli', *Journal of Applied Microbiology*, 110(6), pp. 1601–1611. doi: 10.1111/j.1365-2672.2011.05016.x.

Pinto, D., Santos, M. A. and Chambel, L. (2015) 'Thirty years of viable but nonculturable state research: Unsolved molecular mechanisms', *Critical Reviews in Microbiology*, 41(1), pp. 61–76. doi: 10.3109/1040841x.2013.794127.

PreSens (2018) *Optical Oxygen Sensors & Meters Variety of sensors for industrial and scientific applications μL up to m 3 range Pre-calibrated Insertion in plant and animal tissue For microbial and cell culture www.PreSens.de/o2 CONTENT*. Available at: https://www.presens.de/fileadmin/user_upload/brochures/180517_char_Presens_O2_Broschuere_01-18_dv2_web_2.pdf.

Puskeiler, R., Kaufmann, K. and Weuster-Botz, D. (2005) 'Development, parallelization, and automation of a gas-inducing milliliter-scale bioreactor for high-throughput bioprocess design (HTBD)', *Biotechnology and Bioengineering*, 89(5), pp. 512–523. doi: 10.1002/bit.20352.

Puskeiler, R., Kusterer, A., John, G. T. and Weuster-Botz, D. (2005) 'Miniature bioreactors for automated high-throughput bioprocess design (HTBD): reproducibility of parallel fed-batch cultivations with Escherichia coli', *Biotechnology and Applied Biochemistry*, 42, pp. 227–235. doi: 10.1042/ba20040197.

Puskeiler, R. and Weuster-Botz, D. (2005) 'Combined sulfite method for the measurement of the oxygen transfer coefficient k(L)a in bioreactors', *Journal of Biotechnology*, 120(4), pp. 430–438. doi: 10.1016/j.jbiotec.2005.06.016.

Puthli, M. S., Rathod, V. K. and Pandit, A. B. (2005) 'Gas-liquid mass transfer studies with triple impeller system on a laboratory scale bioreactor', *Biochemical Engineering Journal*, 23(1), pp. 25–30. doi: 10.1016/j.bej.2004.10.006.

Rai, M. and Padh, H. (2001) 'Expression systems for production of heterologous proteins', *Current Science*, 80(9), pp. 1121–1128.

Ramirez-Vargasa, R., Vital-Jacome, M., Camacho-Perez, E., Hubbard, L. and Thalasso, F.

(2014) 'Characterization of oxygen transfer in a 24-well microbioreactor system and potential respirometric applications', *Journal of Biotechnology*, 186, pp. 58–65. doi: 10.1016/j.jbiotec.2014.06.031.

Rathore, A. S. and Winkle, H. (2009) 'Quality by design for biopharmaceuticals', *Nature Biotechnology*, 27(1), pp. 26–34. doi: 10.1038/nbt0109-26.

Riesenberg, D., Schulz, V., Knorre, W. A., Pohl, H.-D., Korz, D., Sanders, E. A., Roß, A. and Deckwer, W.-D. (1991) 'High cell density cultivation of Escherichia coli at controlled specific growth rate', *Journal of Biotechnology*, 20(1), pp. 17–27. doi: 10.1016/0168-1656(91)90032-Q.

Rodriguez, G., Micheletti, M. and Ducci, A. (2018) 'Macro- and micro-scale mixing in a shaken bioreactor for fluids of high viscosity', *Chemical Engineering Research and Design*. Elsevier, 132, pp. 890–901. doi: 10.1016/J.CHERD.2018.01.018.

Rosano, G. L. and Ceccarelli, E. A. (2014) 'Recombinant protein expression in Escherichia coli: advances and challenges', *Frontiers in Microbiology*, 5, p. 17. doi: 10.3389/fmicb.2014.00172.

Saito, F., Nienow, A. W., Chatwin, S. and Moore, I. P. T. (1992) 'Power, gas dispersion and homogenisation characteristics of Scaba SRGT and rushton turbine impellers.', *JOURNAL OF CHEMICAL ENGINEERING OF JAPAN*. The Society of Chemical Engineers, Japan, 25(3), pp. 281–287. doi: 10.1252/jcej.25.281.

Salehmin, M. N. I., Annuar, M. S. M. and Chisti, Y. (2013) 'High cell density fed-batch fermentations for lipase production: feeding strategies and oxygen transfer', *Bioprocess and Biosystems Engineering*, 36(11), pp. 1527–1543. doi: 10.1007/s00449-013-0943-1.

Sanil, R., Maralingannavar, V. and Gadgil, M. (2014) 'In situ pH management for microbial culture in shake flasks and its application to increase plasmid yield', *Journal of Industrial Microbiology and Biotechnology*, 41(4), pp. 647–655. doi: 10.1007/s10295-014-1405-8.

Sartorius Stedim (no date) *ambr 15 fermentation - System Overview*. Available at: https://www.tapbiosystems.com/tap/cell_culture/ambr_15_fermentation.htm (Accessed: 13 September 2018).

Schapper, D., Alam, M., Szita, N., Lantz, A. E. and Gernaey, K. V (2009) 'Application of microbioreactors in fermentation process development: a review', *Analytical and Bioanalytical Chemistry*, 395(3), pp. 679–695. doi: 10.1007/s00216-009-2955-x.

Schmidt, F. R. (2005) 'Optimization and scale up of industrial fermentation processes', *Applied Microbiology and Biotechnology*, 68(4), pp. 425–435. doi: 10.1007/s00253-005-0003-0.

Schofield, D. M., Templar, A., Newton, J. and Nesbeth, D. N. (2016) 'Promoter engineering to

optimize recombinant periplasmic Fab fragment production in Escherichia coli', *Biotechnology Progress*, 32(4), pp. 840–847. doi: 10.1002/btpr.2273.

Sharma, C., Malhotra, D. and Rathore, A. S. (2011) 'Review of Computational fluid dynamics applications in biotechnology processes', *Biotechnology Progress*. American Chemical Society (ACS), 27(6), pp. 1497–1510. doi: 10.1002/btpr.689.

Sharma, S. K. (1986) 'Recovery of soluble human renin from inclusion-bodies produced in recombinant Escherichia coli', *Journal of Biotechnology*, 4(2), pp. 119–124. doi: 10.1016/0168-1656(86)90023-4.

Shepherd, C. B., Hadlock, C. and Brewer, R. C. (1938) 'Drying materials in trays - Evaporation of surface moisture', *Industrial and Engineering Chemistry*, 30, pp. 388–397. doi: 10.1021/ie50340a006.

Shiloach, J. and Fass, R. (2005) 'Growing E-coli to high cell density - A historical perspective on method development', *Biotechnology Advances*, 23(5), pp. 345–357. doi: 10.1016/j.biotechadv.2005.04.004.

Shimizu, N., Fukuzono, S., Fujimori, K., Nishimura, N. and Odawara, Y. (1988) 'Fed-batch cultures of recombinant Escherichia coli with inhibitory substance concentration monitoring', *Journal of Fermentation Technology*, 66(2), pp. 187–191. doi: 10.1016/0385-6380(88)90046-5.

Shimoni, Y., Goudar, C., Jenne, M., Scrinivasan, V. and Srinivasan, V. (2014) 'Qualification of Scale-Down Bioreactors Validation of Process Changes in Commercial Production of Animal-Cell–Derived Products, Part 1 — Concept', *Bioprocess Engineering*, 12(5), pp. 38–45.

Silk, N. J., Denby, S., Lewis, G., Kuiper, M., Hatton, D., Field, R., Baganz, F. and Lye, G. J. (2010) 'Fed-batch operation of an industrial cell culture process in shaken microwells', *Biotechnology Letters*, 32(1), pp. 73–78. doi: 10.1007/s10529-009-0124-0.

Skerra, A. and Pluckthun, A. (1991) 'Secretion and invivo folding of the fab fragment of the antibody McPC603 in Escherichia coli - influence of disulfides and cis-prolines', *Protein Engineering*, 4(8), pp. 971–979. doi: 10.1093/protein/4.8.971.

Smith, G. W., Tavlarides, L. L. and Placek, J. (1990) 'Turbulent flow in stirred tanks: scale-up computations for vessel hydrodynamics', *Chemical Engineering Communications*. Taylor & Francis Group, 93(1), pp. 49–73. doi: 10.1080/00986449008911436.

Soini, J., Ukkonen, K. and Neubauer, P. (2008) 'High cell density media for Escherichia coli are generally designed for aerobic cultivations – consequences for large-scale bioprocesses and shake flask cultures', *Microbial Cell Factories*. BioMed Central, 7(1), p. 26. doi: 10.1186/1475-2859-7-26.

Sonoda, H., Kumada, Y., Katsuda, T. and Yamaji, H. (2011) 'Effects of cytoplasmic and periplasmic chaperones on secretory production of single-chain Fv antibody in Escherichia coli', *Journal of Bioscience and Bioengineering*, 111(4), pp. 465–470. doi: 10.1016/j.jbiosc.2010.12.015.

Spadiut, O., Capone, S., Krainer, F., Glieder, A. and Herwig, C. (2014) 'Microbials for the production of monoclonal antibodies and antibody fragments', *Trends in Biotechnology*, 32(1), pp. 54–60. doi: 10.1016/j.tibtech.2013.10.002.

Steinmeyer, D. E. and McCormick, E. L. (2008) 'The art of antibody process development', *Drug Discovery Today*, 13(13–14), pp. 613–618. doi: 10.1016/j.drudis.2008.04.005.

Sun, W. J., Lee, C., George, H. A., Powell, A. L., Dahlgren, M. E., Greasham, R. and Park, C. H. (1993) 'Acetate inhibition on growth of recombinant escherichia-coli and expression of fusion protein TGF-alpha-PE40', *Biotechnology Letters*, 15(8), pp. 809–814.

Szita, N., Boccazzi, P., Zhang, Z., Boyle, P., Sinskey, A. J. and Jensen, K. F. (2005) 'Development of a multiplexed microbioreactor system for high-throughput bioprocessing'. doi: 10.1039/b504243g.

T Vasconcelos, J. M., P Orvalho, S. C., A F Rodrigues, A. M., Alves, S. S., Vasconcelos, J. M. T., Orvalho, S. C. P., Rodrigues, A. and Alves, S. S. (2000) 'Effect of blade shape on the performance of six-bladed disk turbine impellers', *Industrial & Engineering Chemistry Research*, 39(1), pp. 203–213. doi: 10.1021/ie9904145.

Takagi, H., Morinaga, Y., Tsuchiya, M., Ikemura, H. and Inouye, M. (1988) 'Control of folding of proteins secreted by a high expression secretion vector, pIN-III-ompA: 16-fold increase in production of active Subtilisin E in Escherichia coli', *Bio-Technology*, 6(8), pp. 948–950. doi: 10.1038/nbt0888-948.

Takahashi, K., Takahata, Y., Yokota, T. and Konno, H. (1985) 'Mixing of two miscible highly viscous Newtonian liquids in a helical ribbon agitator.', *Journal of Chemical Engineering of Japan*. The Society of Chemical Engineers, Japan, 18(2), pp. 159–162. doi: 10.1252/jcej.18.159.

Tan, J. S., Abbasiliasi, S., Kadkhodaei, S., Tam, Y. J., Tang, T.-K., Lee, Y.-Y. and Ariff, A. B. (2018) 'Microtiter miniature shaken bioreactor system as a scale-down model for process development of production of therapeutic alpha-interferon2b by recombinant Escherichia coli', *BMC Microbiology*. BioMed Central, 18(1), p. 3. doi: 10.1186/s12866-017-1145-9.

Tan, R.-K., Eberhard, W. and Büchs, J. (2011) 'Measurement and characterization of mixing time in shake flasks', *Chemical Engineering Science*. Pergamon, 66(3), pp. 440–447. doi: 10.1016/J.CES.2010.11.001.

Tang, Y. J. J., Laidlaw, D., Gani, K. and Keasling, J. D. (2006) 'Evaluation of the effects of various culture conditions on Cr(VI) reduction by Shewanella oneidensis MR-1 in a novel high-throughput mini-bioreactor', *Biotechnology and Bioengineering*, 95(1), pp. 176–184. doi: 10.1002/bit.21002.

Toeroek, C., Cserjan-Puschmann, M., Bayer, K. and Striedner, G. (2015) 'Fed-batch like cultivation in a micro-bioreactor: screening conditions relevant for Escherichia coli based production processes', *Springerplus*. Springer International Publishing, 4(1), p. 490. doi: 10.1186/s40064-015-1313-z.

Tolman, R. C. (1949) 'The effect of droplet size on surface tension', *Journal of Chemical Physics*, 17(3), pp. 333–337. doi: 10.1063/1.1747247.

van't Riet, K. (1979) 'Review of Measuring Methods and Results in Nonviscous Gas-Liquid Mass Transfer in Stirred Vessels', *Ind. Eng. Chem. Process Des. Dev*, 18(3). Available at: https://pubs-acs-org.libproxy.ucl.ac.uk/doi/pdf/10.1021/i260071a001 (Accessed: 30 May 2018).

van't Riet, K. and van der Lans, R. G. J. M. (2011) 'Mixing in Bioreactor Vessels', in *Comprehensive Biotechnology*. Elsevier, pp. 63–80. doi: 10.1016/B978-0-08-088504-9.00083-0.

Velez-Suberbie, M. L., Betts, J. P. J., Walker, K. L., Robinson, C., Zoro, B. and Keshavarz-Moore, E. (2018) 'High throughput automated microbial bioreactor system used for clone selection and rapid scale-down process optimization', *Biotechnology Progress*. American Chemical Society (ACS), 34(1), pp. 58–68. doi: 10.1002/btpr.2534.

Vilaca, P. R., Badino, A. C., Facciotti, M. C. R. and Schmidell, W. (2000) 'Determination of power consumption and volumetric oxygen transfer coefficient in bioreactors', *Bioprocess Engineering*, 22(3), pp. 261–265. doi: 10.1007/s004490050730.

VraH bel, P., J M van der Lans, R. G., Ch M Luyben, K. A., Boon, L. and Nienow, A. W. (2000) 'Mixing in large-scale vessels stirred with multiple radial or radial and axial up-pumping impellers: modelling and measurements', *Chemical Engineering Science*, 55, pp. 5881–5896. Available at: https://ac-els-cdn-com.libproxy.ucl.ac.uk/S0009250900001755/1-s2.0-S0009250900001755-main.pdf?_tid=920bfc55-50e9-4df4-8490-469e97af8c96&acdnat=1527025509_7f1182a1c73289a00b099beafc9f6b9c.

Wang, R., Xiang, S., Feng, Y., Srinivas, S., Zhang, Y., Lin, M. and Wang, S. (2013) 'Engineering production of functional scFv antibody in E. coli by co-expressing the molecule chaperone Skp', *Frontiers in Cellular and Infection Microbiology*. Frontiers, 3, p. 72. doi: 10.3389/fcimb.2013.00072.

Weichart, D. H. and Kell, D. B. (2001) 'Characterization of an autostimulatory substance produced by Escherichia coli', *Microbiology-Sgm*, 147, pp. 1875–1885. doi: 10.1099/00221287-147-7-1875.

Weir, M. P. and Sparks, J. (1987) 'Purification and renaturation of recombinant human interleukin-2', *Biochemical Journal*, 245(1), pp. 85–91. doi: 10.1042/bj2450085.

Welsh, J. P., Rauscher, M. A., Bao, H., Meissner, S., Han, I., Linden, T. O. and Pollard, J. M. (2016) 'Domain antibody downstream process optimization: High-throughput strategy and analytical methods', *Engineering in Life Sciences*. Wiley-Blackwell, 16(2), pp. 133–142. doi: 10.1002/elsc.201400255.

Weuster-Botz, D., Altenbach-Rehm, J. and Arnold, M. (2001) 'Parallel substrate feeding and pH-control in shaking-flasks', *Biochemical Engineering Journal*, 7(2), pp. 163–170. doi: 10.1016/s1369-703x(00)00117-0.

Wiegmann, V., Martinez, C. B. and Baganz, F. (2018) 'A simple method to determine evaporation and compensate for liquid losses in small-scale cell culture systems', *Biotechnology Letters*, 40, pp. 1029–1036. doi: 10.1007/s10529-018-2556-x.

Wittmann, C., Kim, H. M., John, G. and Heinzle, E. (2003) 'Characterization and application of an optical sensor for quantification of dissolved O-2 in shake-flasks', *Biotechnology Letters*, 25(5), pp. 377–380. doi: 10.1023/a:1022402212537.

Wu, H. and Patterson, G. K. (1989) 'Laser-doppler measurements of turbulent-flow parameters in a stirred mixer', *Chemical Engineering Science*. Pergaman Press pk, 44(8). Available at: https://ac-els-cdn-com.libproxy.ucl.ac.uk/0009250989851553/1-s2.0-0009250989851553-main.pdf?_tid=25435ec6-7444-49d6-bc29-e447a5a89b43&acdnat=1527262808_b56a9b517cd89fc3ad5a2f514fef4fa5.

Wypych, G. (2016) *Handbook of Polymers (2nd Edition)*. ChemTec Publishing. Available at: app.knovel.com/hotlink/toc/id:kpHPE00012/handbook-polymers-2nd/handbook-polymers-2nd.

Xu, B., Jahic, M. and Enfors, S. O. (1999) 'Modeling of overflow metabolism in batch and fed-batch cultures of Escherichia coli', *Biotechnology Progress*, 15(1), pp. 81–90. doi: 10.1021/bp9801087.

Xu, X., Nagarajan, H., Lewis, N. E., Pan, S., Cai, Z., Liu, X., Chen, W., Xie, M., Wang, W., Hammond, S., Andersen, M. R., Neff, N., Passarelli, B., Koh, W., Fan, C., Wang, J., Gui, Y., Lee, K. H., Betenbaugh, M. J., Quake, S. R., Famili, I., Palsson, B. O. and Wang, J. (2011) 'The genomic sequence of the Chinese hamster ovary (CHO)-K1 cell line', *Nature Biotechnology*, 29. doi: 10.1038/nbt.1932.

Yang, X. M. (1992) 'Optimization of a cultivation process for recombinant protein-production by Escherichia coli', *Journal of Biotechnology*, 23(3), pp. 271–289. doi: 10.1016/0168-1656(92)90075-k.

Yawalkar, A. A., Heesink, A. B. M., Versteeg, G. F. and Pangarkar, V. G. (2002) 'Gas-liquid mass transfer coefficient in stirred tank reactors', *Canadian Journal of Chemical Engineering*, 80(5), pp. 840–848.

Yee, L. and Blanch, H. W. (1992) 'Recombinant Protein Expression in High Cell Density Fed-Batch Cultures of Escherichia Coli', *Nature Biotechnology*. Nature Publishing Group, 10(12), pp. 1550–1556. doi: 10.1038/nbt1292-1550.

You, S. T., Aziz, A., Raman, A., Shazrin, R., Raja, S., Shah, E., Iskandr, M. and Nor, M. (2014) 'Multiple-impeller stirred vessel studies', *Rev Chem Eng*, 30(3), pp. 323–336. doi: 10.1515/revce-2013-0028.

Zarschler, K., Witecy, S., Kapplusch, F., Foerster, C. and Stephan, H. (2013) 'High-yield production of functional soluble single-domain antibodies in the cytoplasm of Escherichia coli', *Microbial Cell Factories*. Microbial Cell Factories, 12(1), p. 1. doi: 10.1186/1475-2859-12-97.

Zhang, Z., Szita, N., Boccazzi, P., Sinskey, A. J. and Jensen, K. F. (2006) 'A well-mixed, polymer-based microbioreactor with integrated optical measurements', *Biotechnology and Bioengineering*. Wiley-Blackwell, 93(2), pp. 286–296. doi: 10.1002/bit.20678.

Zhong, J. J. (2010) 'Recent advances in bioreactor engineering', *Korean Journal of Chemical Engineering*, 27(4), pp. 1035–1041. doi: 10.1007/s11814-010-0277-5.

Zhu, J. (2012) 'Mammalian cell protein expression for biopharmaceutical production'. doi: 10.1016/j.biotechadv.2011.08.022.

Zhu, Y. G., Bandopadhyay, P. C. and Wu, J. (2001) 'Measurement of gas-liquid mass transfer in an agitated vessel - A comparison between different impellers'', *Journal of Chemical Engineering of Japan*, 34(5), pp. 579–584. doi: 10.1252/jcej.34.579.

Appendix A: DoE T-test tables

A.1. Micro-24 Evaporation rate experiments

Table A.1. Micro-24 evaporation rate model parameter estimates

Term	Estimate	Std Error	t Ratio	Prob>|t|
Intercept	443.48464	21.91427	20.24	<.0001*
Temperature (ºC)(28,32)	103.535	20.1582	5.14	0.0004*
Fill volume (mL)(3,5)	1.762	20.1582	0.09	0.9321
Gas flow rate (mL min⁻¹)(0,15)	284.455	20.1582	14.11	<.0001*
Temperature (ºC)*Fill volume (mL)	46.73125	22.53755	2.07	0.0649
Temperature (ºC)*Gas flow rate (mL min⁻¹)	132.09625	22.53755	5.86	0.0002*
Fill volume (mL)*Gas flow rate (mL min⁻¹)	-18.21125	22.53755	-0.81	0.4379
Temperature (ºC)*Temperature (ºC)	-6.329091	38.44017	-0.16	0.8725
Fill volume (mL)*Fill volume (mL)	-37.65409	38.44017	-0.98	0.3504
Gas flow rate (mL min⁻¹)*Gas flow rate (mL min⁻¹)	-40.35909	38.44017	-1.05	0.3185

A.2. Micro-24 and 1L scale process optimisation DoE experiments

Table A.2. Micro-24 process optimisation model parameter estimates for total titre

Term	Estimate	Std Error	t Ratio	Prob>|t|
Intercept	0.3238042	0.024094	13.44	<.0001*
Temperature (ºC)(25,30)	0.0885292	0.024094	3.67	0.0032*
IPTG concentration (µM)(100,250)	-0.030429	0.024094	-1.26	0.2306
Temperature (ºC)*IPTG concentration (µM)	-0.011904	0.024094	-0.49	0.6302

Table A.3. Micro-24 process optimisation model parameter estimates for extracellular titre

Term	Estimate	Std Error	t Ratio	Prob>|t|
Intercept	0.2098667	0.011789	17.80	<.0001*
Temperature (ºC)(25,30)	0.0657167	0.011789	5.57	0.0001*
IPTG concentration (µM)(100,250)	-0.015117	0.011789	-1.28	0.2240
Temperature (ºC)*IPTG concentration (µM)	-0.007467	0.011789	-0.63	0.5384

Table A.4. Micro-24 process optimisation model parameter estimates for total SPR

Term	Estimate	Std Error	t Ratio	Prob>|t|
Intercept	15.053342	1.262836	11.92	<.0001*
Temperature (ºC)(25,30)	3.0822417	1.262836	2.44	0.0311*
IPTG concentration (µM)(100,250)	-1.283342	1.262836	-1.02	0.3296
Temperature (ºC)*IPTG concentration (µM)	-0.552242	1.262836	-0.44	0.6697

Table A.5. 1L scale process optimisation model parameter estimates for total titre

Term	Estimate	Std Error	t Ratio	Prob>|t|
Intercept	0.942375	0.032411	29.08	<.0001*
Temperature (ºC)(25,30)	0.344875	0.032411	10.64	0.0004*
IPTG concentration (µM)(100,250)	-0.036625	0.032411	-1.13	0.3216
Temperature (ºC)*IPTG concentration (µM)	-0.069125	0.032411	-2.13	0.0999

Table A.6. 1L scale process optimisation model parameter estimates for extracellular titre

Term	Estimate	Std Error	t Ratio	Prob>|t|
Intercept	0.426375	0.022049	19.34	<.0001*
Temperature (ºC)(25,30)	0.231625	0.022049	10.51	0.0005*
IPTG concentration (µM)(100,250)	-0.029625	0.022049	-1.34	0.2502
Temperature (ºC)*IPTG concentration (µM)	-0.017375	0.022049	-0.79	0.4748

Table A.7. 1L scale process optimisation model parameter estimates for total SPR

Term	Estimate	Std Error	t Ratio	Prob>|t|
Intercept	26.10875	0.865981	30.15	<.0001*
Temperature (ºC)(25,30)	9.24125	0.865981	10.67	0.0004*
IPTG concentration (µM)(100,250)	-0.95375	0.865981	-1.10	0.3326
Temperature (ºC)*IPTG concentration (µM)	-1.63125	0.865981	-1.88	0.1327

A.2. EngD chapter k_La characterisation DoE

Table A.8. Model parameter estimates for the k_La characterisation of the prototype miniature bioreactor described in the EngD chapter (Appendix E)

Term	Estimate	Std Error	t Ratio	Prob>|t|
Intercept	180.16071	9.92398	18.15	<.0001*
Agitation (rpm)(1000,3000)	75.91	7.977262	9.52	<.0001*
Gas flow rate (mL min⁻¹)(7,30)	22.74	7.977262	2.85	0.0215*
Fill volume (mL)(7,15)	25.21	7.977262	3.16	0.0134*
Agitation (rpm)*Gas flow rate (mL min⁻¹)	13.05	8.91885	1.46	0.1816
Agitation (rpm)*Fill volume (mL)	25.7	8.91885	2.88	0.0205*
Gas flow rate (mL min⁻¹)*Fill volume (mL)	24.5	8.91885	2.75	0.0252*
Agitation (rpm)*Agitation (rpm)	-14.39643	15.32481	-0.94	0.3750
Gas flow rate (mL min⁻¹)*Gas flow rate (mL min⁻¹)	-3.546429	15.32481	-0.23	0.8228
Fill volume (mL)*Fill volume (mL)	-61.09643	15.32481	-3.99	0.0040*

Appendix B: Micro-24 Feeding System CAD Drawings

Figure B.1. Feeding device Version 4 full assembly
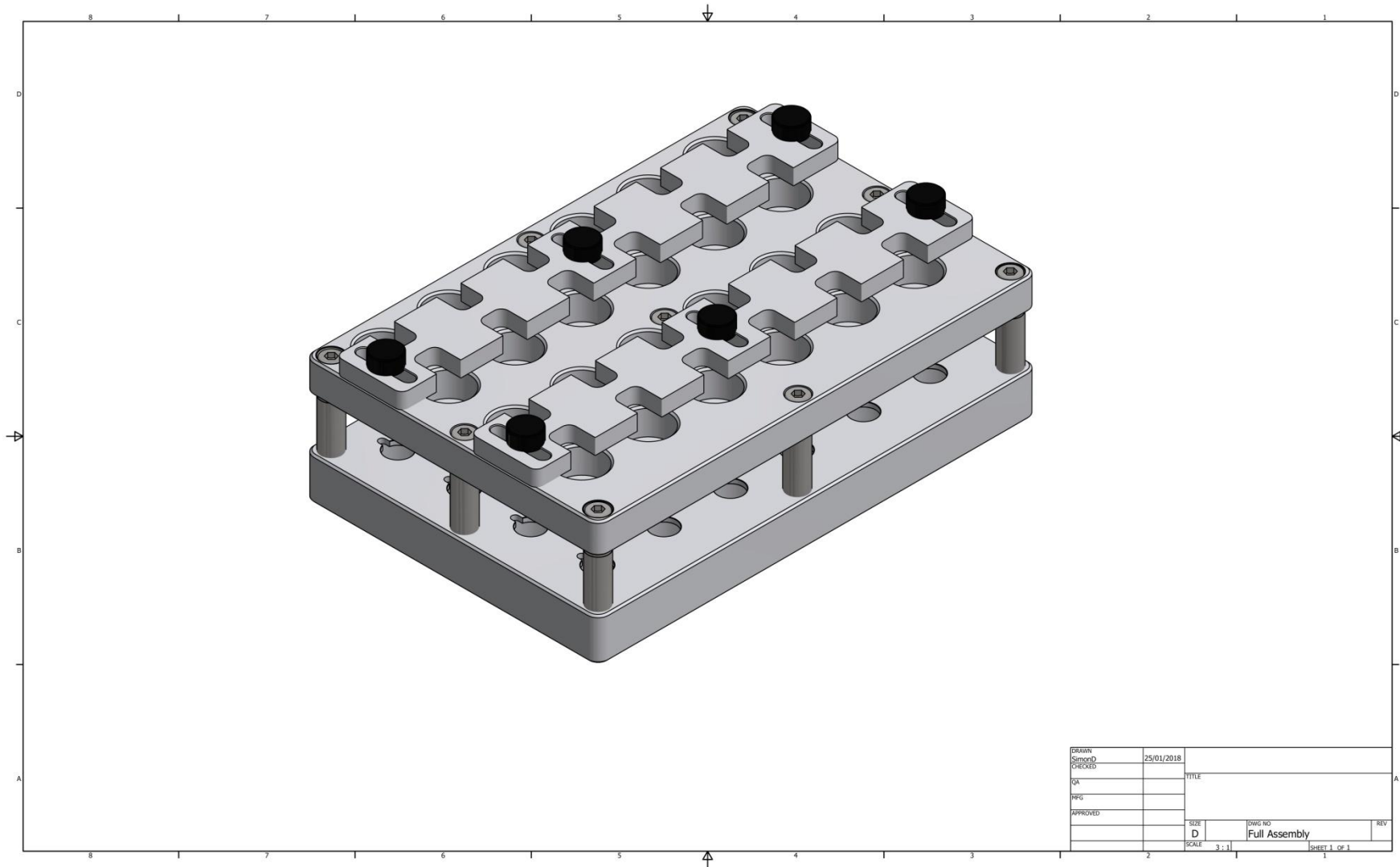
**Figure B.2.** Feeding device Version 4 bottom plate
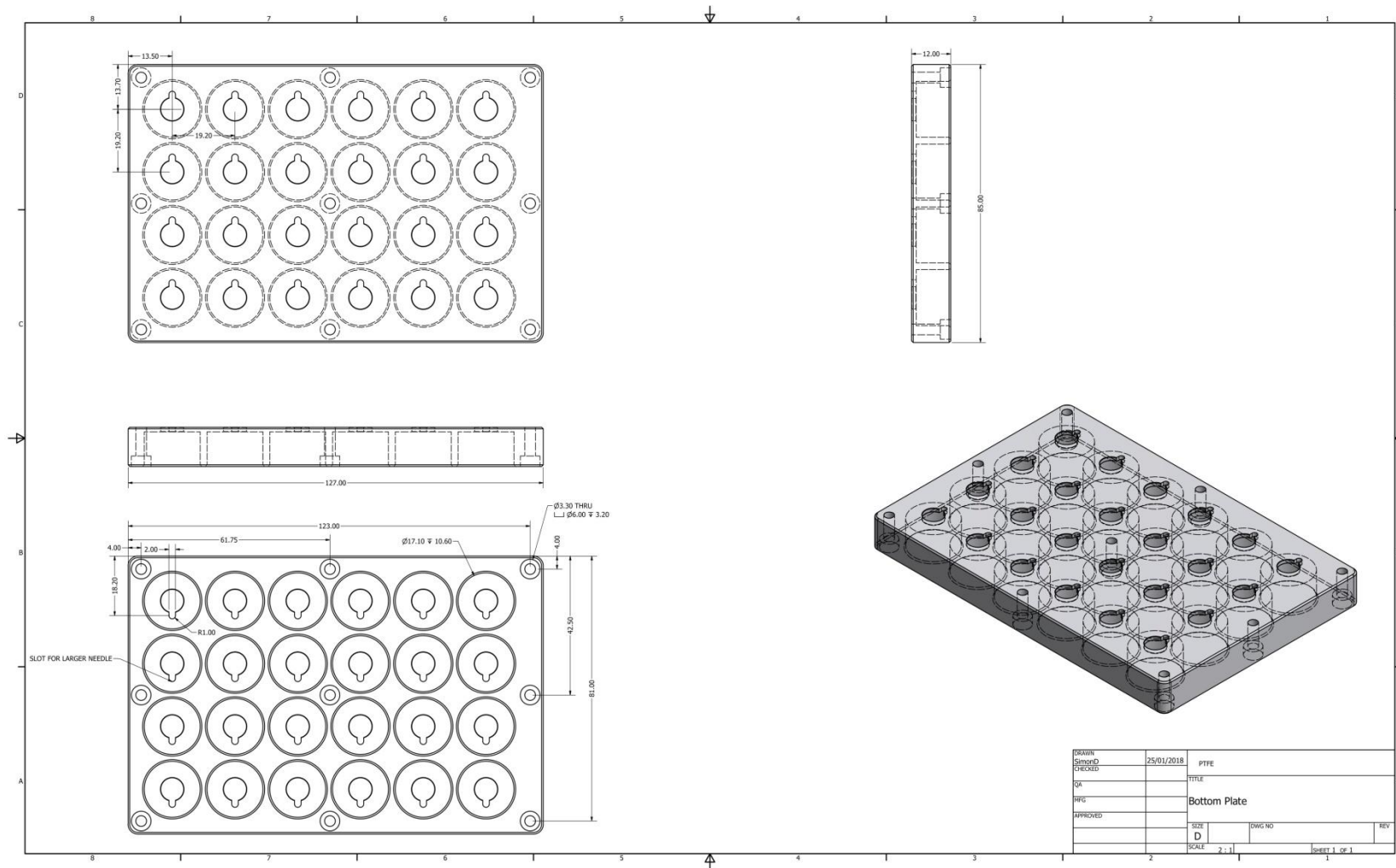
Figure B.3. Micro-24 feeding device Version 4 middle plate
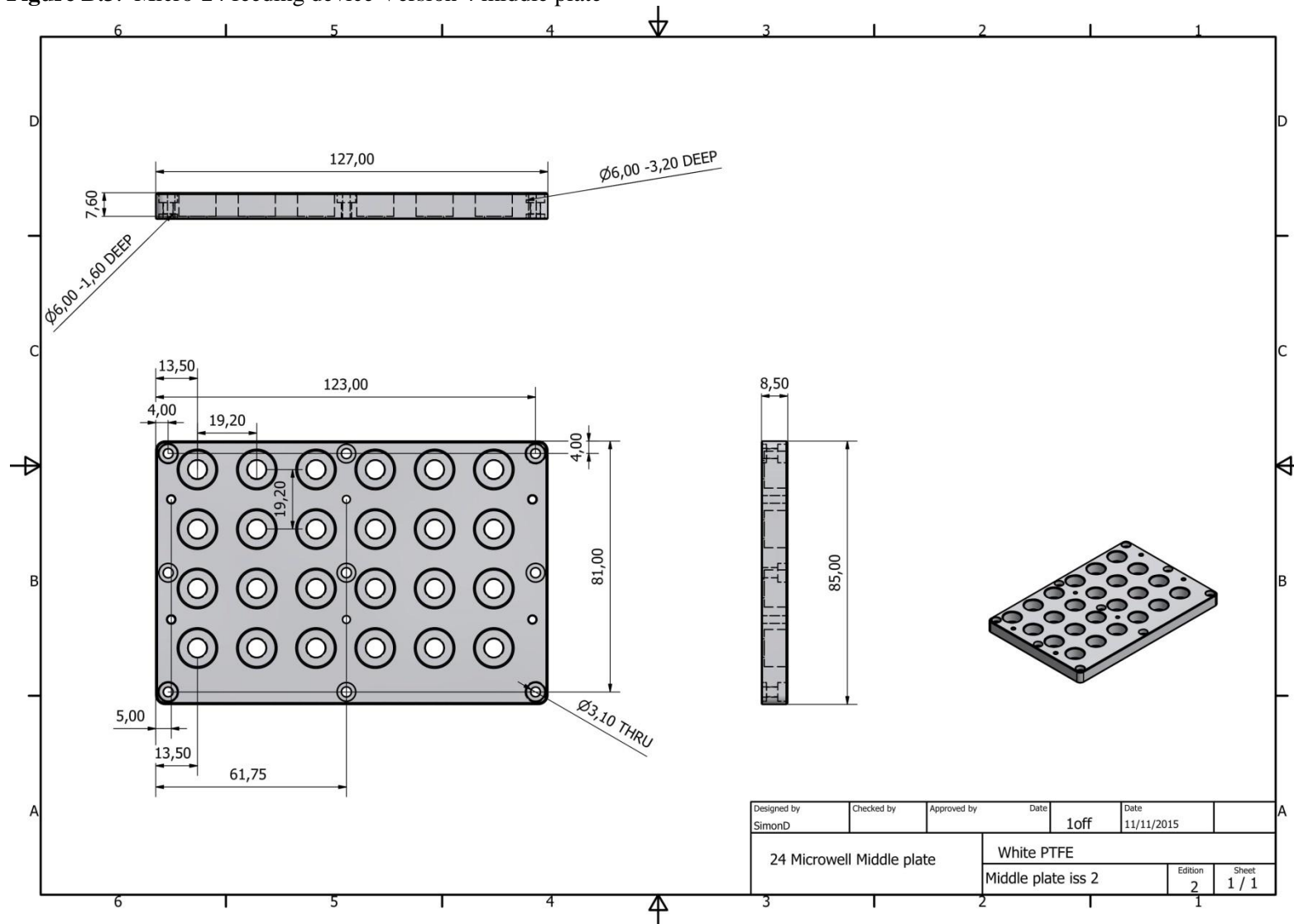
Figure B.4. Micro-24 feeding device Version 4 adjustable plate (clamps)
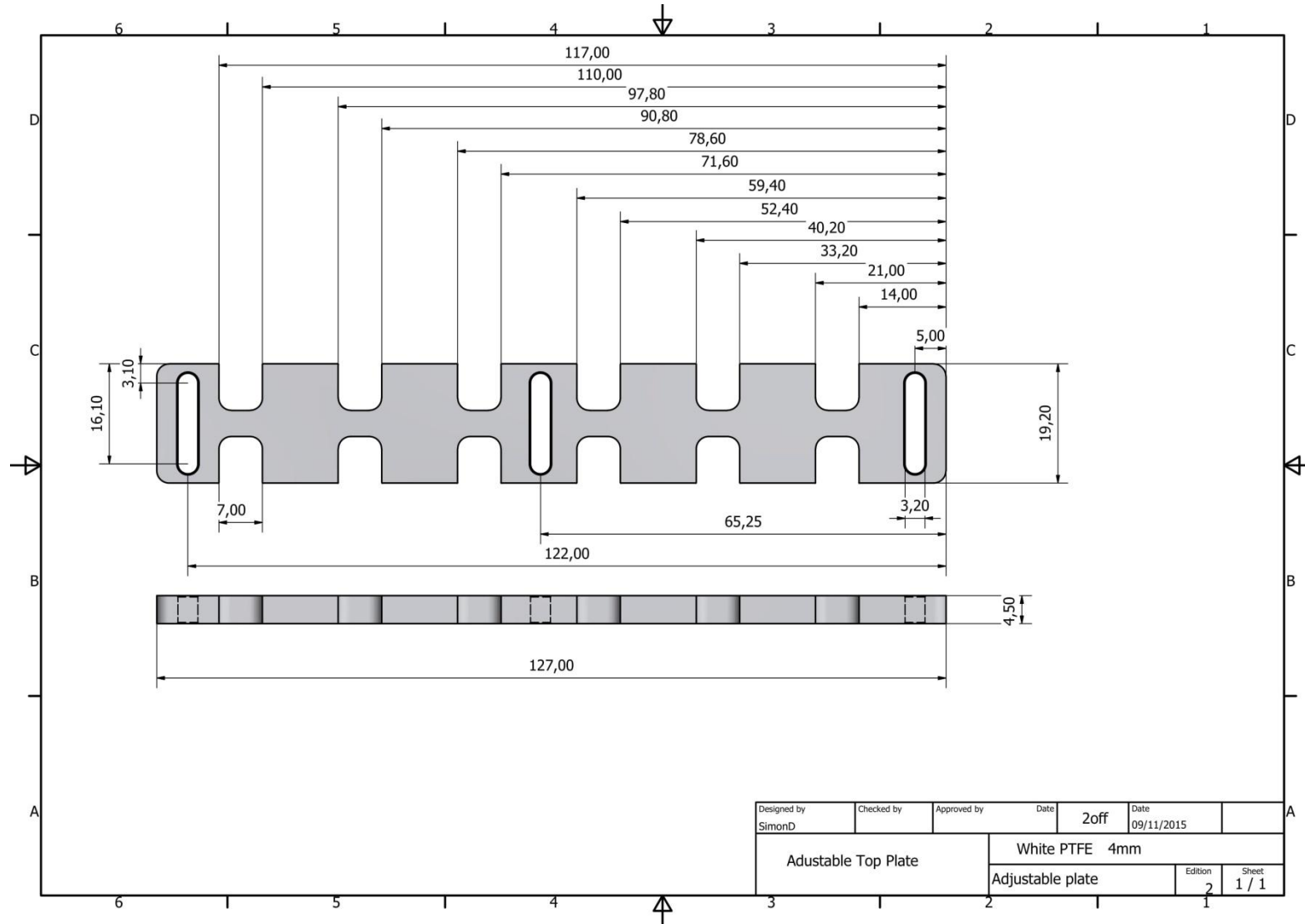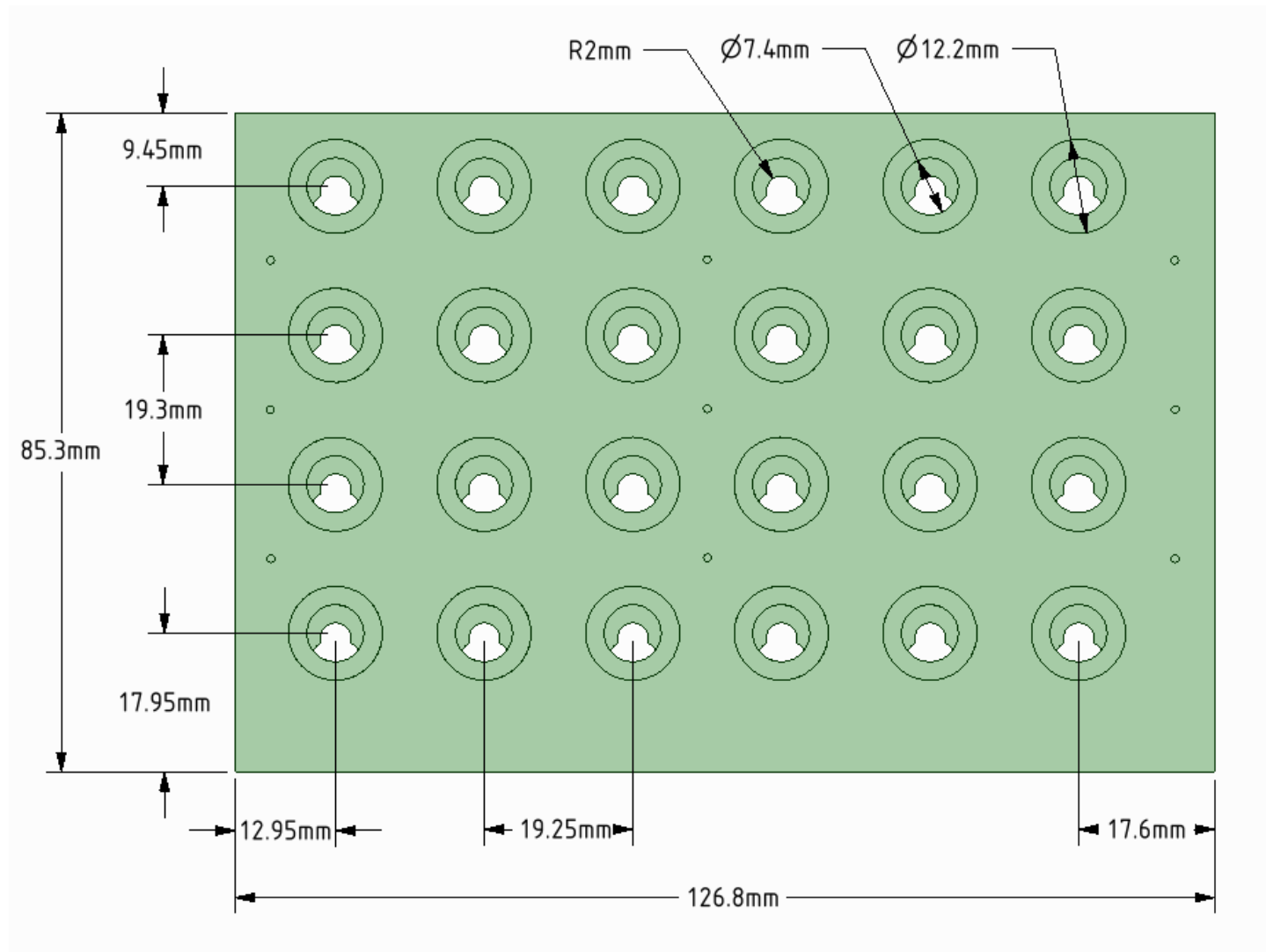
Figure B.5. Micro-24 feeding device Version 5 (top)
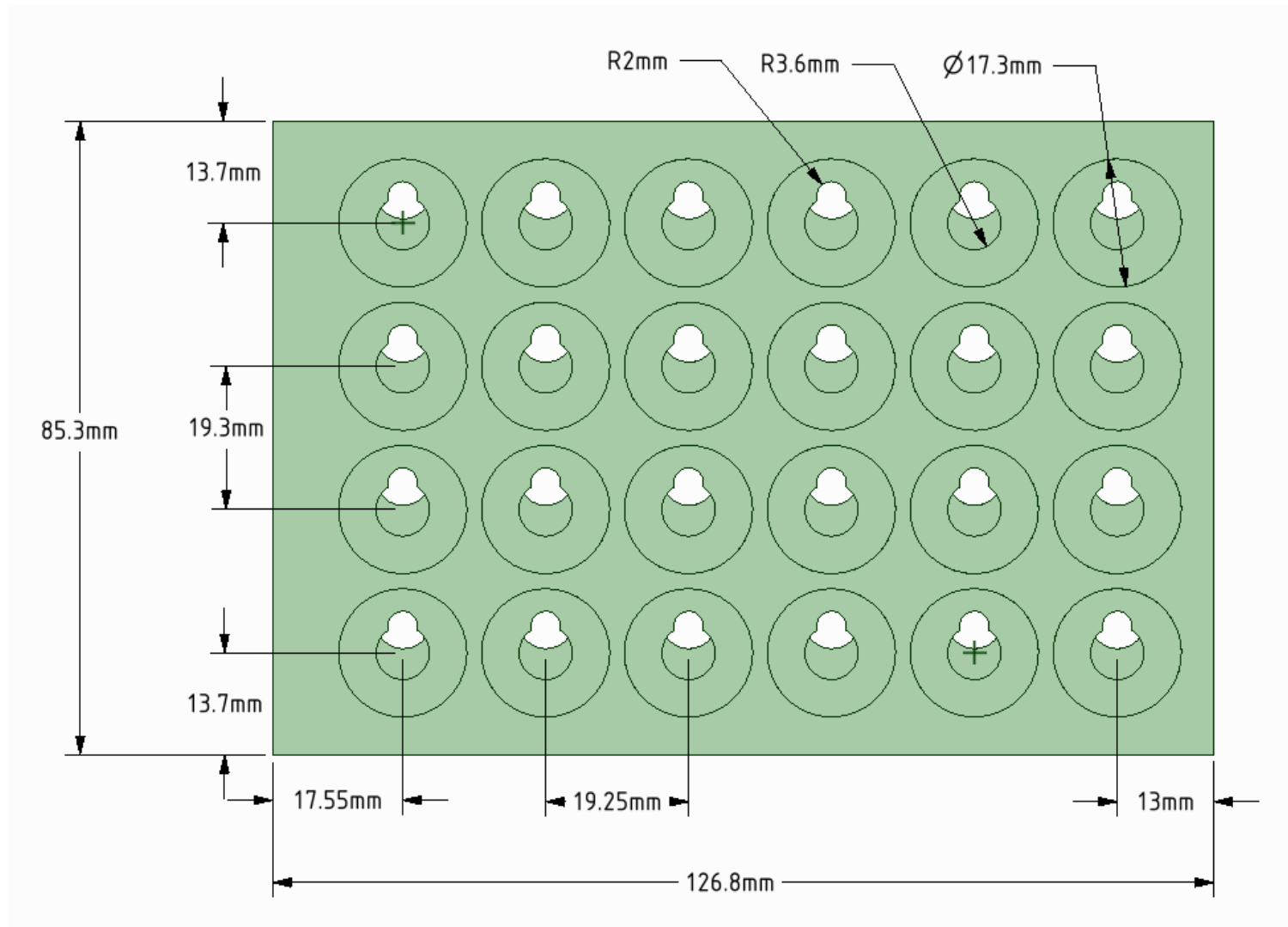
Figure B.6. Feeding device Version 5 (underside)
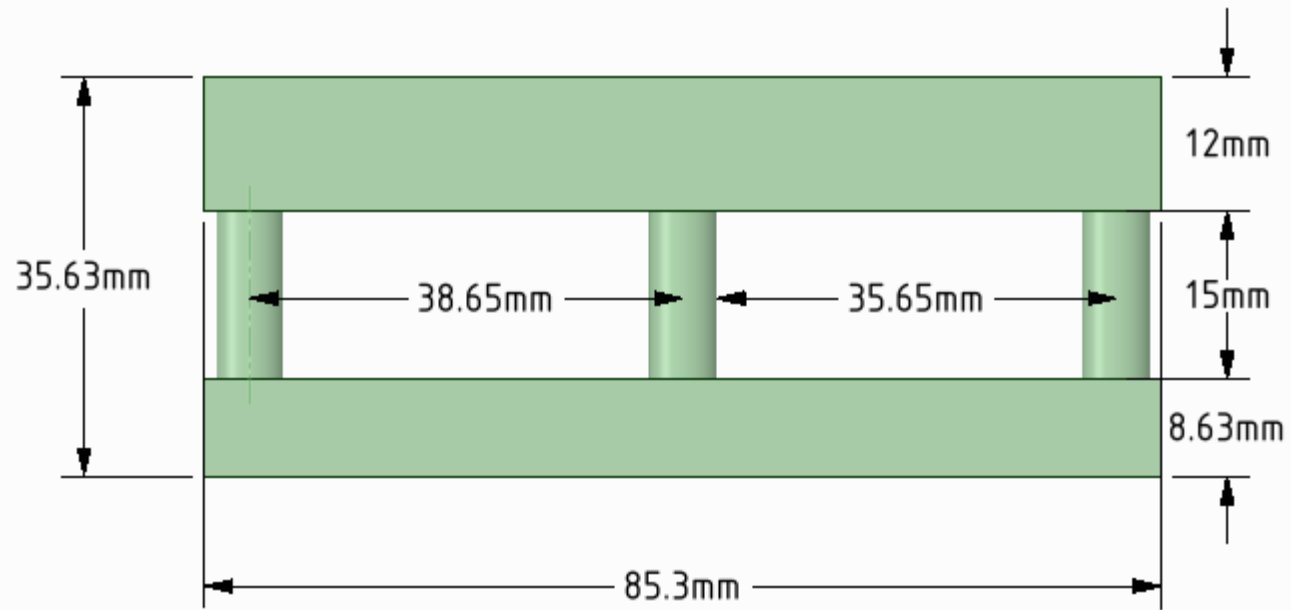
Figure B.7. Micro-24 feeding device Version 5 (front)
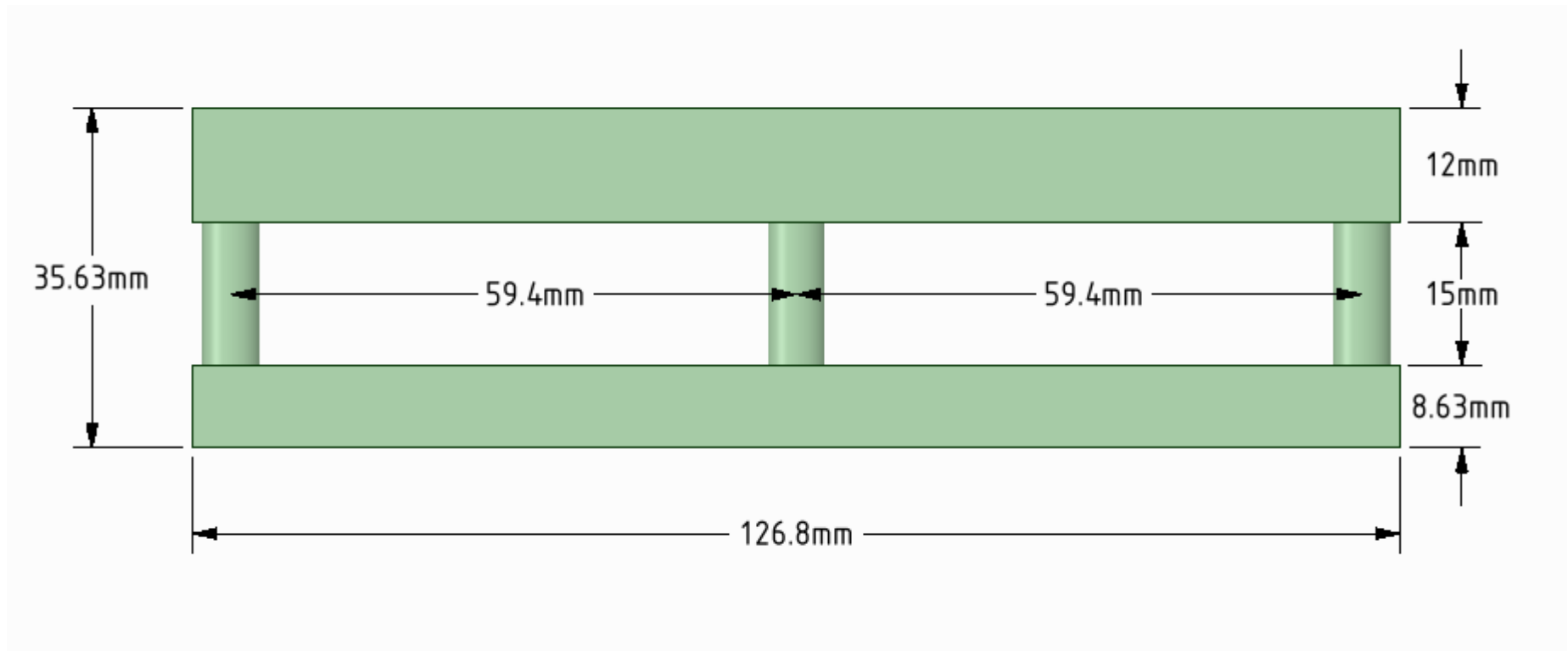
Figure B.8. Micro-24 feeding device Version 5 (side)
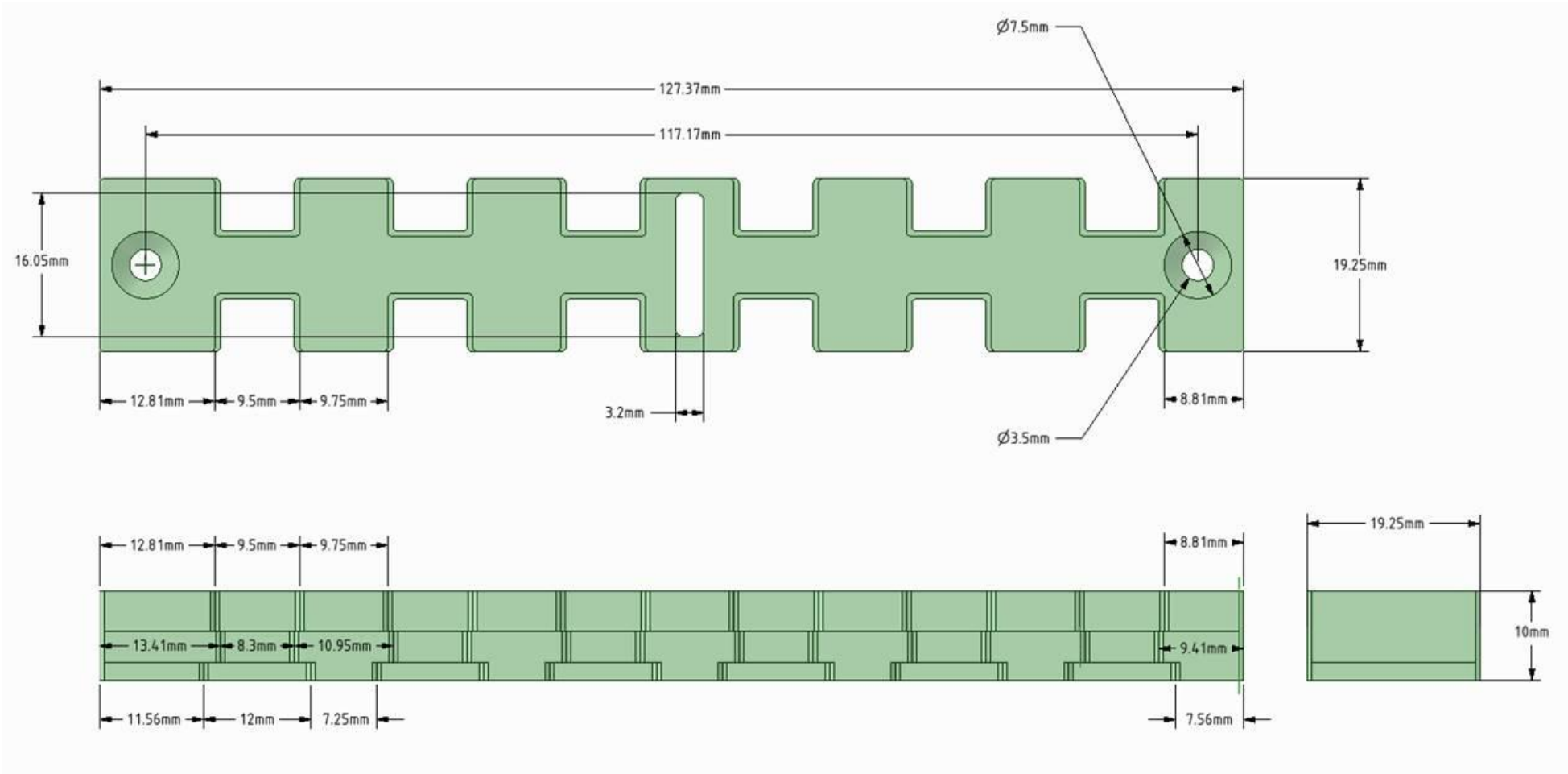
**Figure B.9**. Micro-24 feeding device Version 5 clamps
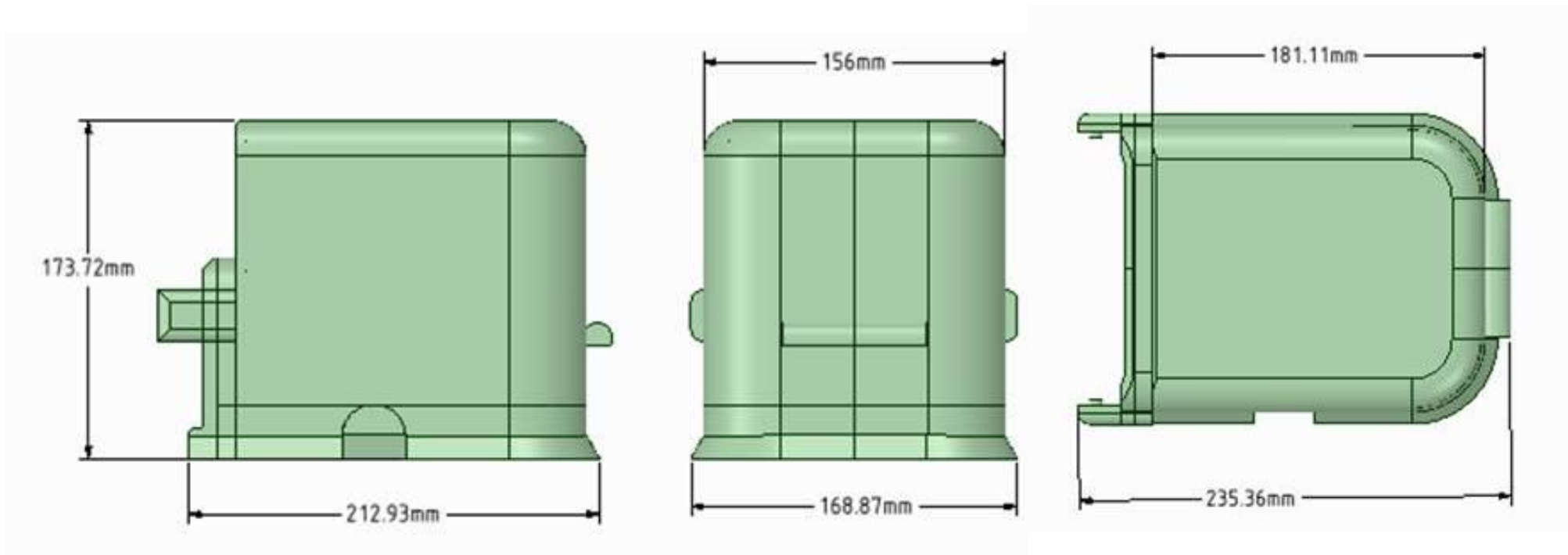
Figure B.10. Micro-24 feeding system temperature control lid.
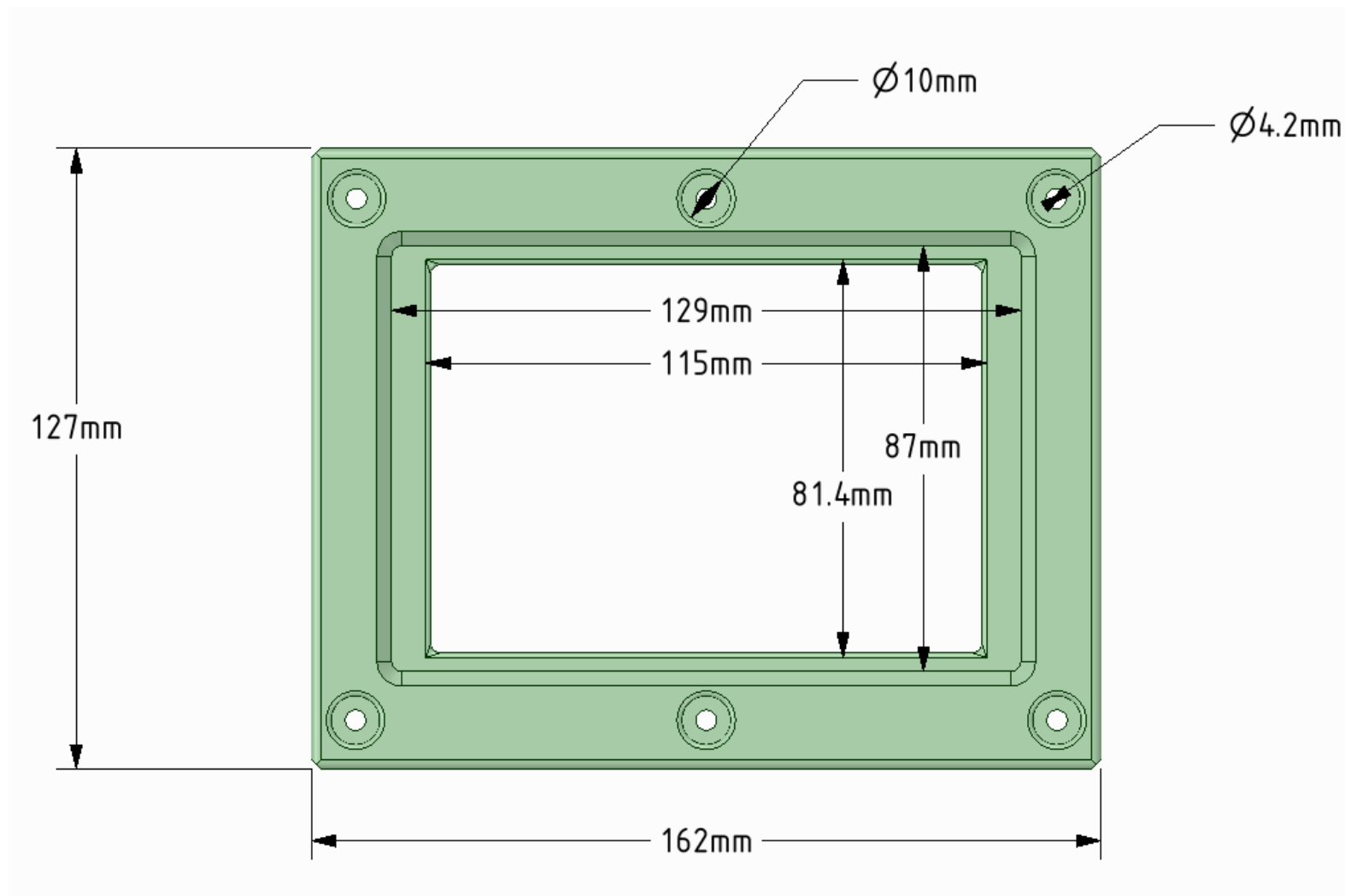
**Figure B.11.** Micro-24 feeding system sampling stand (top)
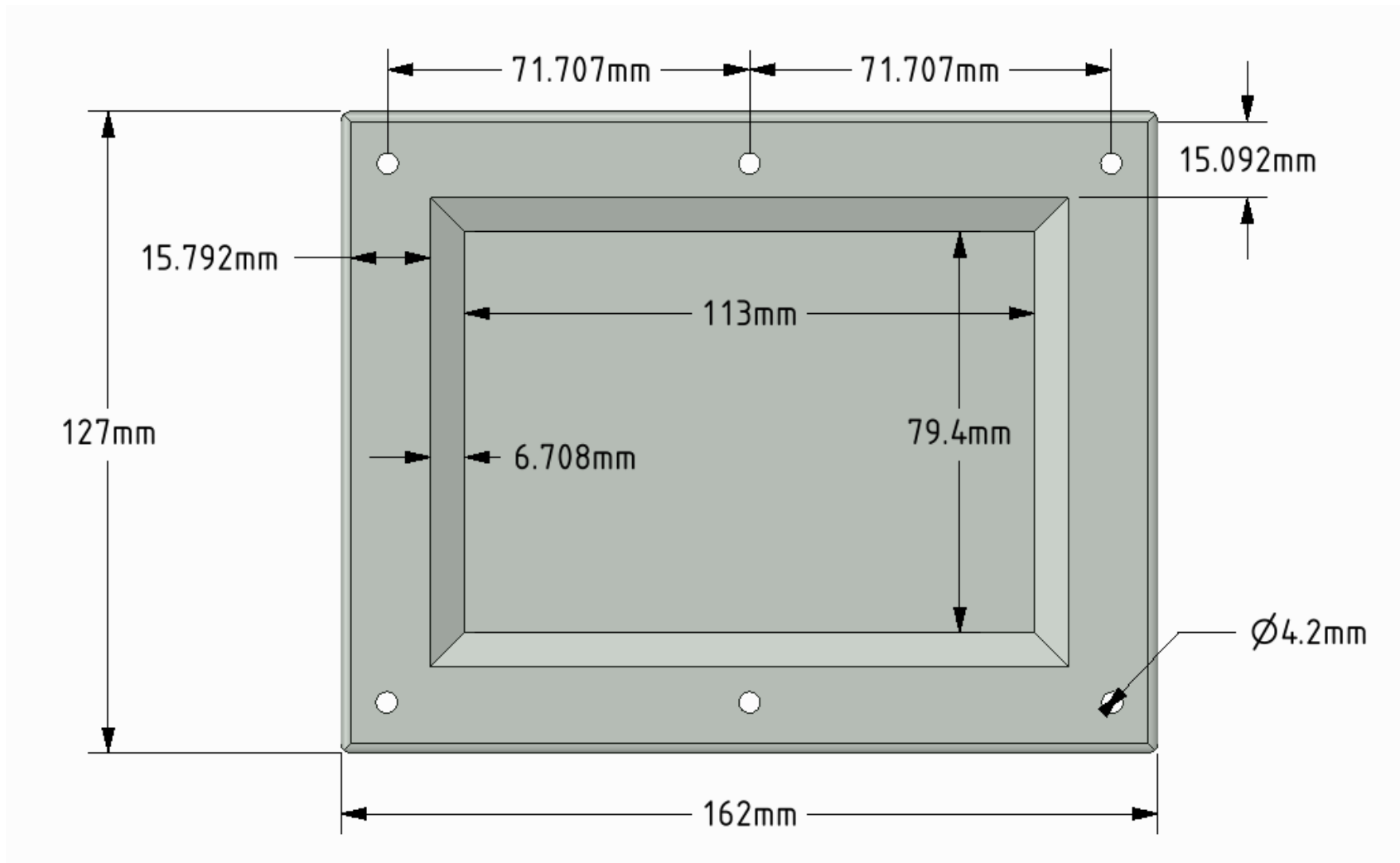
**Figure B.12.** Micro-24 feeding system sampling stand base (top)
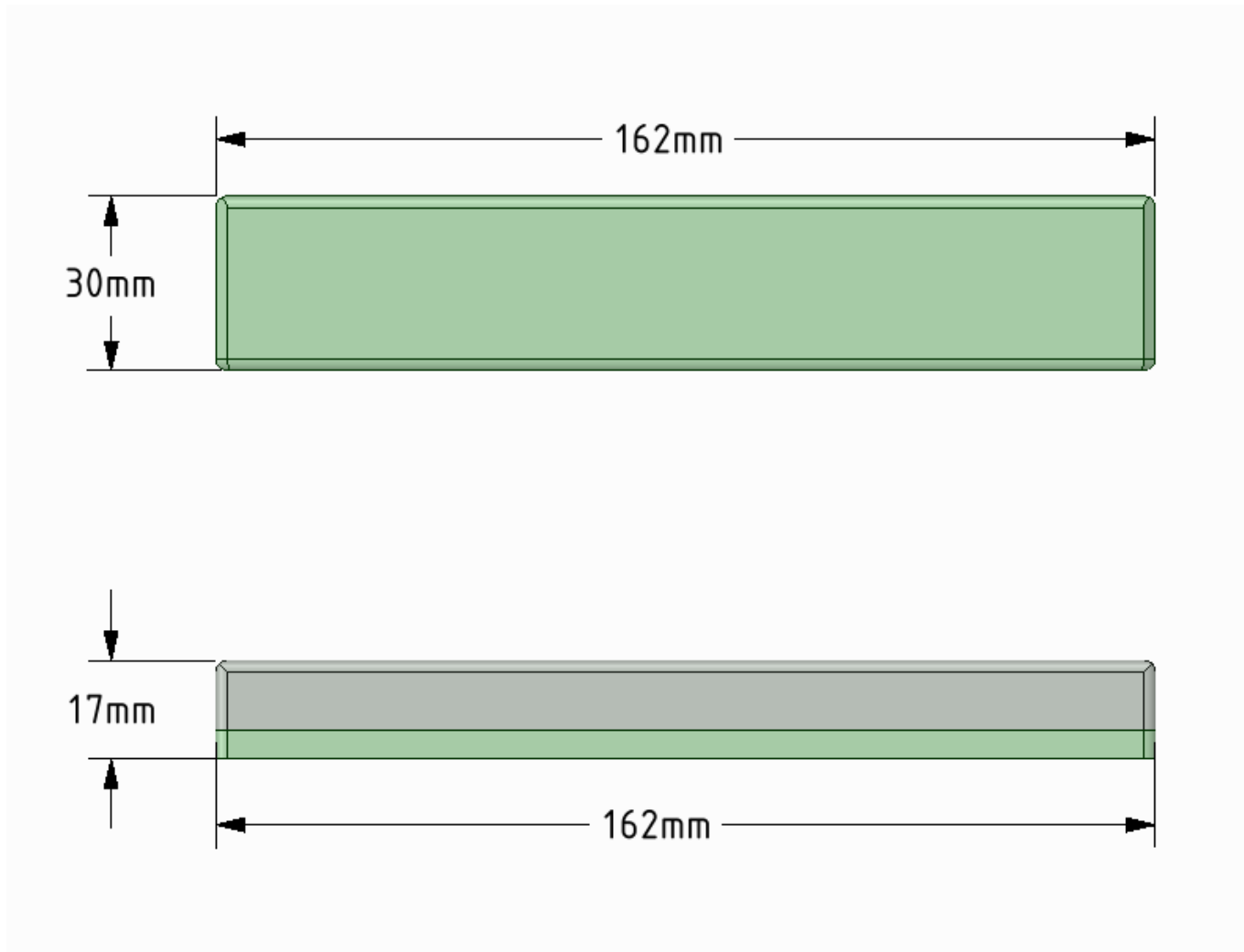
Figure B.13. Micro-24 feeding system sampling stand without the metal spacers (side)

# Appendix C: HPLC-SEC Data and Chromatograms

Table C.1. HPLC-SEC Data for the 50L scale, 1L scale and Micro-24 fed-batch processes

| Sample	%Aggregate	%Monomer	%Fragment	%total	Monomer peak area (units)	Total peak area (units)	Retention time of monomer (minutes)	Aggregate peak count	Monomer peak count	Fragment peak count
50L Sample 1 (without PEI)	6.87	92.63	0.50	100	23665.67	25547.81	17.89	3	1	1
50L Sample 2 (without PEI)	7.30	92.70	0.00	100	24434.52	26358.04	17.93	3	1	0
1L scale Bioreactor 1 Sample 1	10.70	88.53	0.78	100	11089.78	12526.81	17.93	2	1	1
1L scale Bioreactor 1 Sample 2	9.55	90.03	0.42	100	12059.72	13395.58	17.95	2	1	1
1L scale Bioreactor 2 Sample 1	9.66	88.88	1.47	100	8033.56	9038.74	17.96	3	1	1
Micro-24 Sample 1	7.88	92.12	0.00	100	21569.27	23413.54	17.99	4	1	0
Micro-24 Sample 2	8.33	91.67	0.00	100.001	21715.38	23689.19	18.02	4	1	0
50L Sample 1 (with PEI)	7.24	91.95	0.81	100	21345.13	23214.45	17.88	3	1	1
50L Sample 2 (with PEI)	5.60	93.22	1.18	100	21071.49	22604.23	17.9	3	1	1
50L Sample 3 (with PEI)	6.92	92.42	0.67	99.999	21774.48	23560.79	17.91	1	1	1
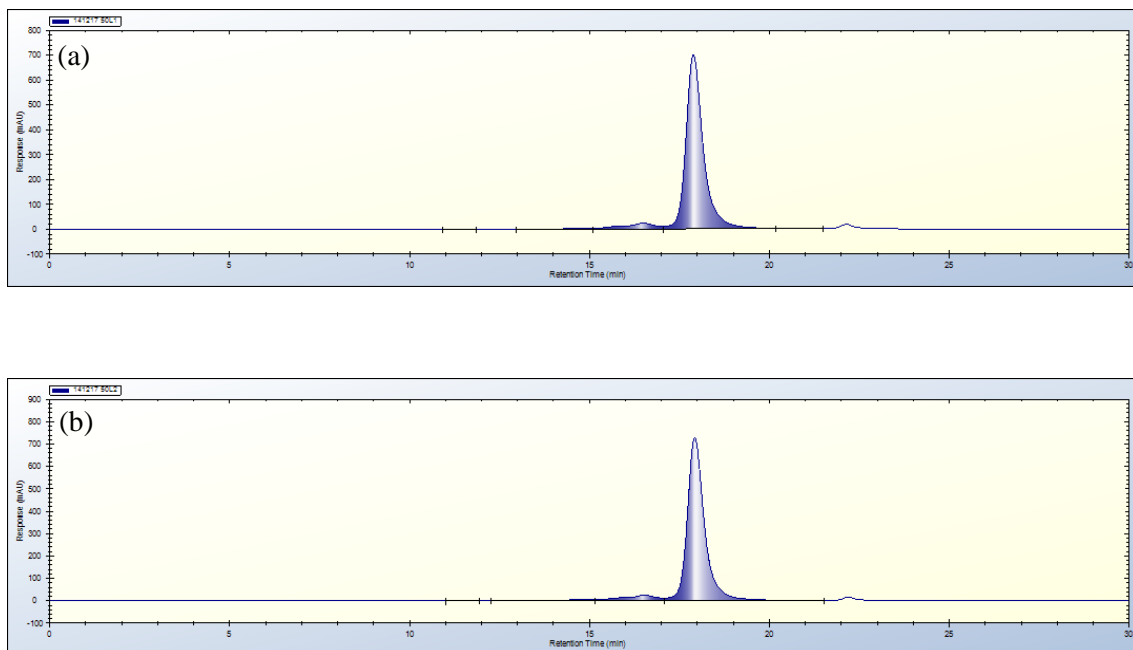
Figure C.1 HPLC-SEC chromatograms for the 50L samples without the addition of PEI at harvest. (a) Sample 1 (b) Sample 2. The fermentations were performed as described in Section 2.9. The HPLC-SEC assay and sample preparation were performed as described in Section 2.10.6.
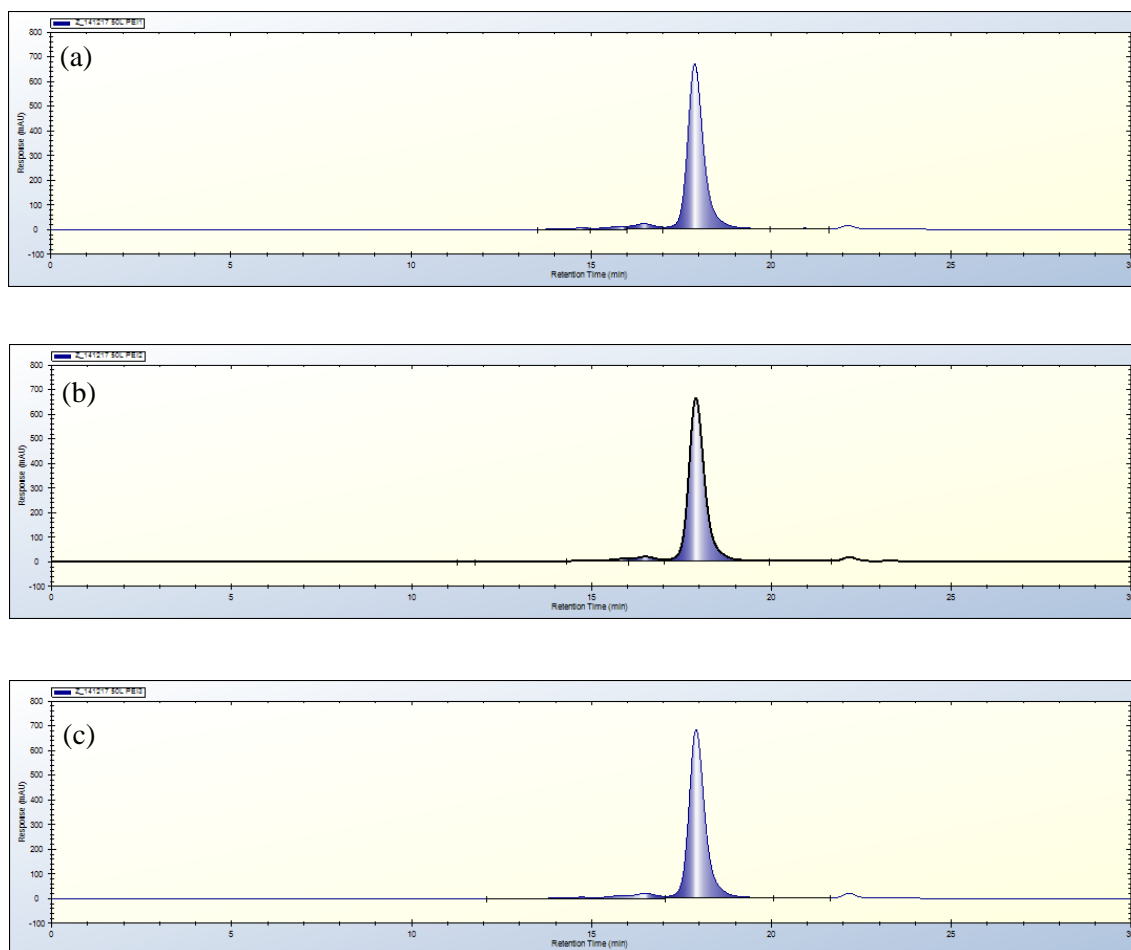
Figure C.2 HPLC-SEC chromatograms for the 50L samples with the addition of PEI at harvest. (a) Sample 1 (b) Sample 2 (c) Sample 3. The fermentations were performed as described in Sections 2.9. The HPLC-SEC assay and sample preparation were performed as described in Section 2.10.6.
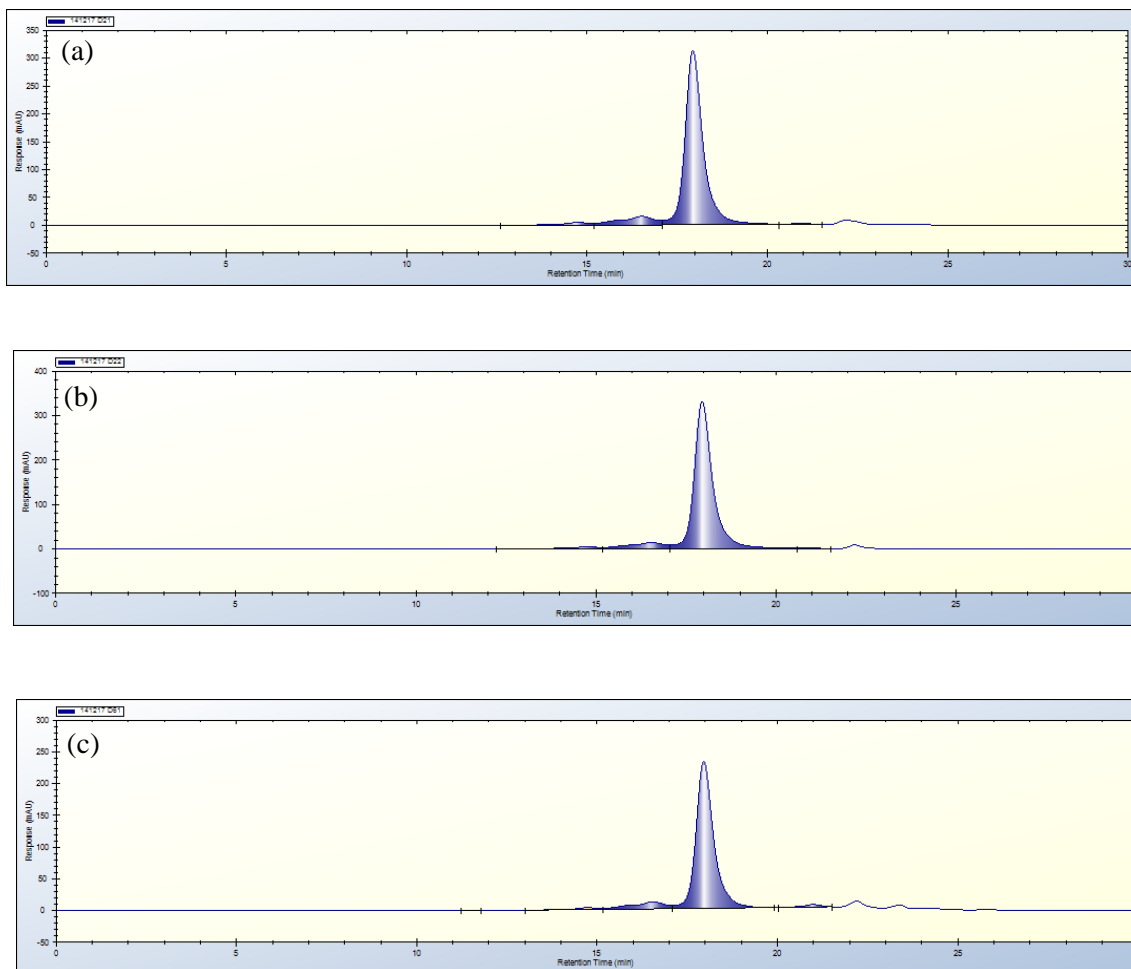
Figure C.3 HPLC-SEC chromatograms for the 1L samples. (a) Bioreactor 1 Sample 1 (b) Bioreactor 2 Sample 2 (c) Bioreactor 2 Sample 1. The fermentations were performed as described in Sections 2.3.2. The HPLC-SEC assay and sample preparation were performed as described in Section 2.10.6.
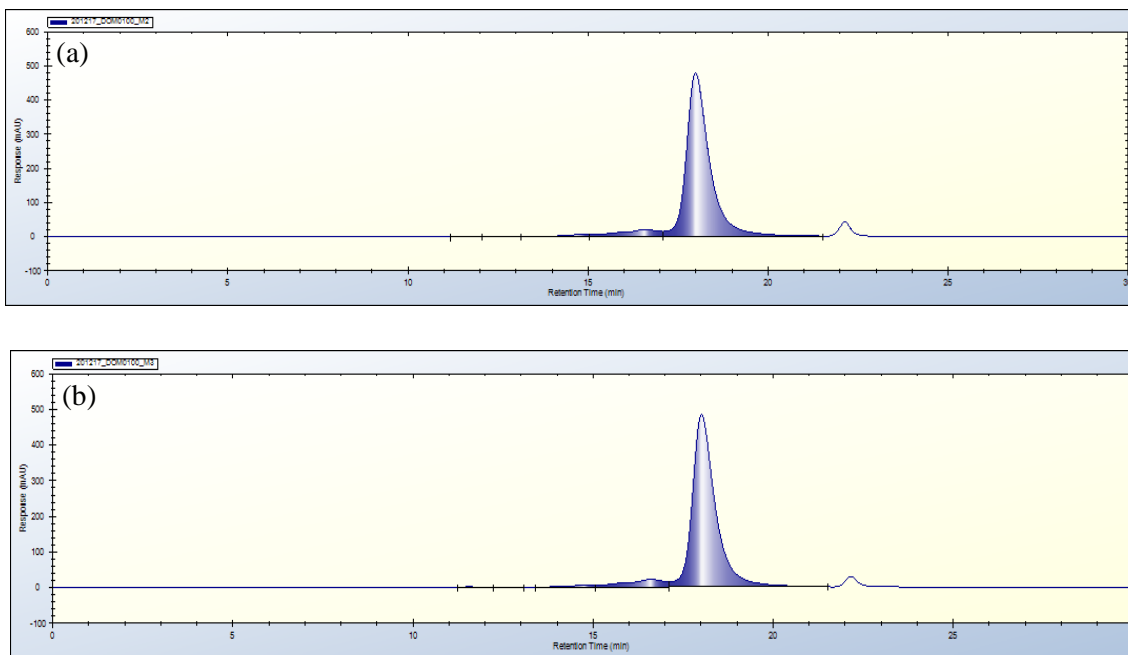
Figure C.4 HPLC-SEC chromatograms for the Micro-24 samples. (a) Sample 1 (b) Sample 2. The fermentations were performed as described in Sections 2.6.3.4. The HPLC-SEC assay and sample preparation were performed as described in Section 2.10.6.

Appendix D. Octet® RED Standard Curve Examples

(a)

(b)
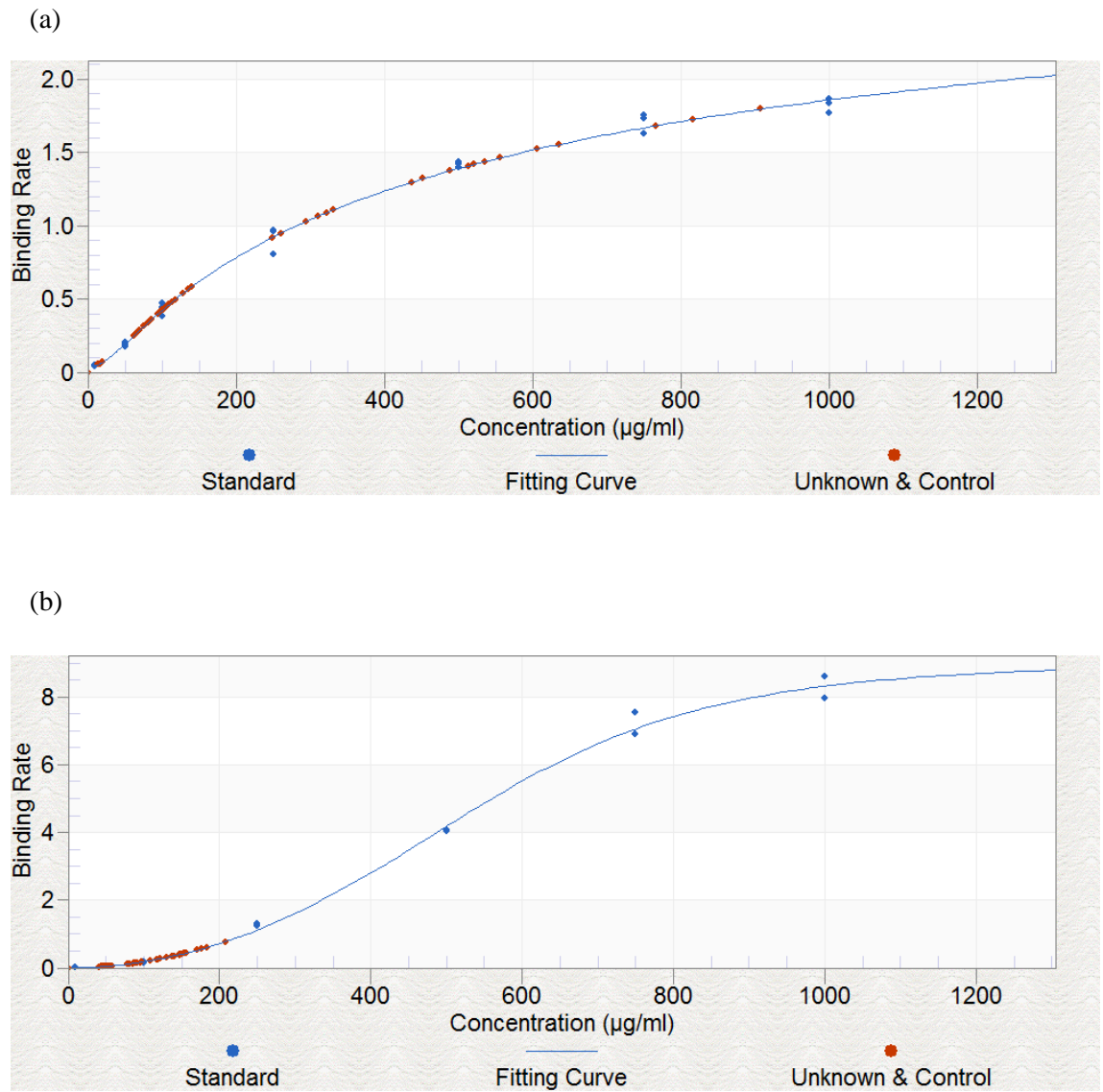
Figure D.1. Octet® RED standard curve examples. (a) supernatant samples and (b) lysed cell samples. The blue dots represent the dAb standard, and the red dots represent the dAb samples. The Octet® RED titre assay was performed as described in Section 2.10.4.

Appendix E: Qualification of a Prototype Stirred miniature bioreactor for use as a validation tool in biopharmaceutical development[1]

E.1. Background

The application of miniature bioreactors in biopharmaceutical development enables new medicines to become available to patients more quickly and at a lower cost. The rate limiting step of biopharmaceutical process development is strain evaluation and process optimisation; improving the efficiency of this step is key to minimising development time and cost (Bareither and Pollard, 2011). Scale-down models can be used for screening experiments and to predict the large scale process performance (FDA, 2011); this allows large amount of process data to be generated. Quality by Design (QbD) principles can be applied to establish a process design space, which allows for the translation of more efficient and robust processes to manufacturing scale. This improvement in efficiency of biopharmaceutical development and lower cost of goods allows for a greater number of products to enter clinical trials in a shorter time frame.

A scale-down model used as a tool in process validation needs to be shown to be adequate for this purpose (Shimoni et al, 2014). A scale-down bioreactor qualification package should consist of three key components: bioreactor design, bioreactor performance and product quality (Shimoni *et al.*, 2014). The bioreactor design refers to the specification and geometry of the system. Ideally the scale down bioreactor should be geometrically similar to the production scale bioreactor; however this can be difficult at microscale due to availability of equipment. The aeration and mixing strategies often differ significantly between scales due to the geometric differences, and also because there are a number of key physical phenomena that cannot be directly scaled down such as bubble size and size distribution and the surface area to volume ratio (Duetz, 2007; Betts *et al.*, 2014; Shimoni *et al.*, 2014). Although the mechanisms of heat and mass transfer and control may differ, provided that the conditions experienced by the cells are the same between scales, the scale-down model should be suitable for validation purposes.

---

[1] This chapter is included as part of the requirements for award of a UCL EngD in Bioprocess Engineering.

E.2. Objectives

A number of different parallel miniature bioreactor platforms are currently commercially available or are in development by vendor companies. Although the focus of this thesis was on miniature shaken bioreactors, the opportunity emerged during the course of this EngD to undertake a short, end user evaluation of a miniature stirred bioreactor technology. The aim was to characterise and briefly evaluate a beta-test design against an industrial fermentation processes and end user specifications.

The studies described below summarise the results of this evaluation and are included as part of the EngD requirements. Limited details of the stirred bioreactor are provided as this represents an active product development programme of a commercial partner.

E.3. Engineering Characterisation

To demonstrate that the conditions experienced by the cells in scale-down system are representative of the conditions of lab and pilot scale bioreactors, a small scale bioreactor should be characterised in terms of oxygen transfer and fluid mixing. Engineering parameters used to characterise bioreactors are described in Section 1.4. Figure E.1 shows k_La data for a prototype miniature STR system, which allows for up to 48 fed-batch fermentations to be run simultaneously. The DO control cascade of the prototype miniature bioreactor differs from a conventional STR as the increase in agitation speed is the final response rather than first response. This is due to the system level control of agitation meaning that increasing the agitation in one vessel would result in an increase in agitation of multiple vessels. The measured k_La values for the prototype miniature bioreactor were in the range 17-292h^{-1}, which are within the range for conventional STRs (Yawalkar *et al.*, 2002). Table E.1 shows the maximum k_La for the prototype miniature bioreactor and a 1L scale STR, and the operating conditions at which the maximum k_La was achieved. The maximum agitation speed was defined by the operating ranges of the bioreactor systems. Engineering characterisation data generated under and range of process conditions can be used to establish optimum operating conditions and appropriate scale-up criteria e.g. matched k_La, *OTR* or *P/V*, and the required operating conditions at both scales to achieve these criteria (Figure E.1).

Table E.1. Comparison of the k_La_{max} of the prototype miniature STR and the 1L scale STR

| Vessel	Working volume (L)	Impeller type	Number of impellers	Agitation (rpm)	Gas flow rate (vvm)	k_La_{max} (h^{-1})
Prototype miniature STR	0.008	Rushton-type	1	3000	2	292
1L STR	1	Rushton turbine	3	1600	2	393
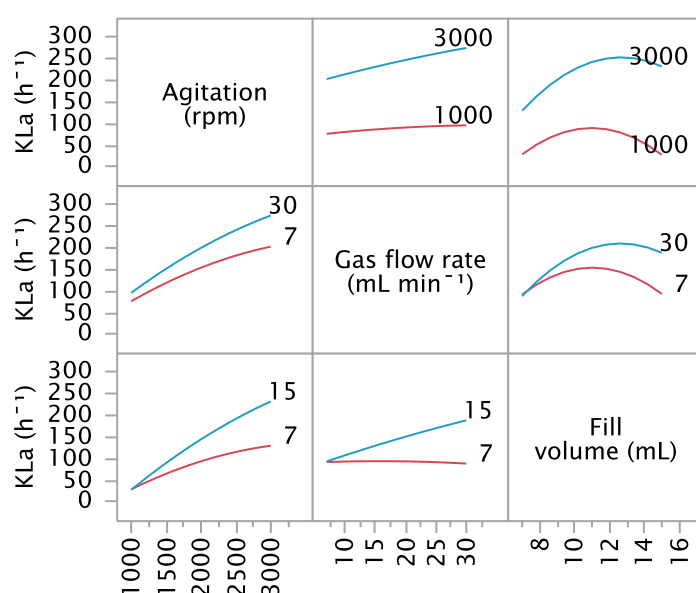
Figure E.1. Effect of agitation speed, total gas flow rate and fill volume on the k_La of the prototype miniature STR

## E.4. Parallel fermentation performance

The performance of the scale-down bioreactor refers to the reproducibility and scalability system. The performance qualification (PQ) package should demonstrate that the scale-down model is reproducible; batch variability should be less or equal to the large scale bioreactor. Figure E.2 shows the OD$_{600}$ profiles and harvest titres for twelve vessels of the prototype miniature bioreactor system. The prototype miniature bioreactor system was reproducible in terms of cell growth, with CVs of 8-15% and harvest titre, with a CV of ~15% (Figure E.2). For the prototype miniature STR to be used as a validation tool it would need to be demonstrated that these CVs are equivalent or better than the laboratory and pilot scale vessels. In order to

establish reproducible cultures, refinements of the control loop parameters, sampling procedures, operating conditions e.g. fill volume and feed rate, and vessel geometry were performed. The DO control loop required tuning as initially the control cascade was not functioning properly due to issues with the control software; aeration was achieved via fixed gassing and fixed agitation (Figure E.3(a)). Rectifying the software issues and refining the calibration settings dramatically improved the DO control (Figure E.3(b)), however there was still oscillations in the DO caused by the fluctuations in the oxygen demand of the cells with feed additions. Modification of the feed line dip tube resulted in a more uniform feed delivery profile, and therefore a reduction in the oscillations in the DO control (Figure E.3(c)).

A scale-down bioreactor should be representative of the large scale bioreactor, and operating conditions that will attain equivalent performance to the production scale process should be established. In general volume-independent set points should be maintained between scales and scale-dependant parameters should be adjusted in proportion to the volume e.g. feed rates. Linear scaling is often not accurate, particularly if geometric similarity cannot be achieved and there are differences in mixing and oxygen transfer between scales. Operational settings should maintain equivalent operating conditions between scales. Criteria frequently used to establish equivalent operating conditions are DO set point, $k_L a$, OTR, U_{tip}, Re number and P/V (Shimoni *et al.*, 2014) .
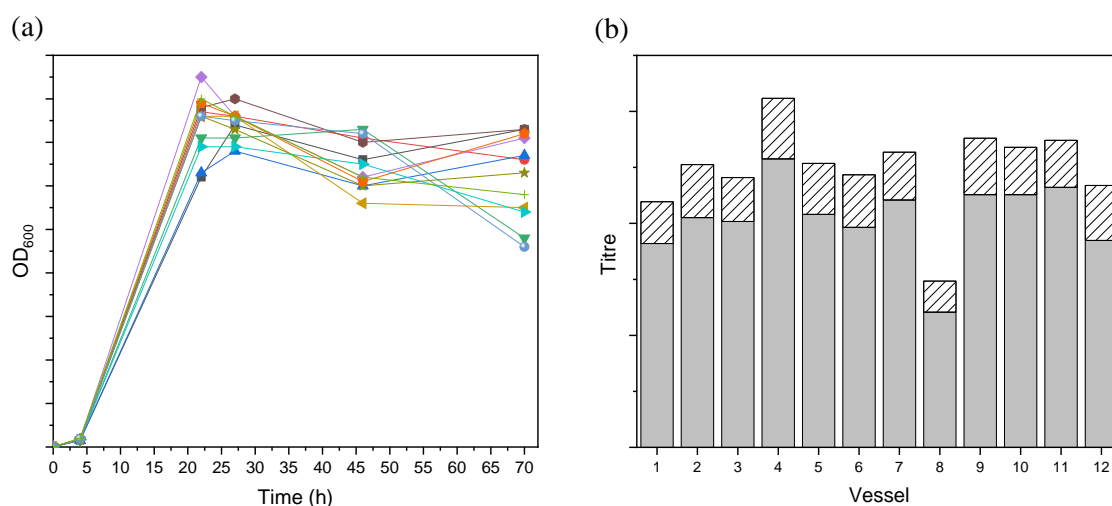
Figure E.2. Cell growth and product expression of 12 parallel fed-batch cultures of *E. coli* expressing a dAb protein using the prototype miniature bioreactor. (a) OD_{600} profiles of the 12 vessels, (b) Harvest product titres of the 12 vessels. The grey bars represent the extracellular titre, and the shaded bars represent the intracellular titre.

(a)

(b)

(c)
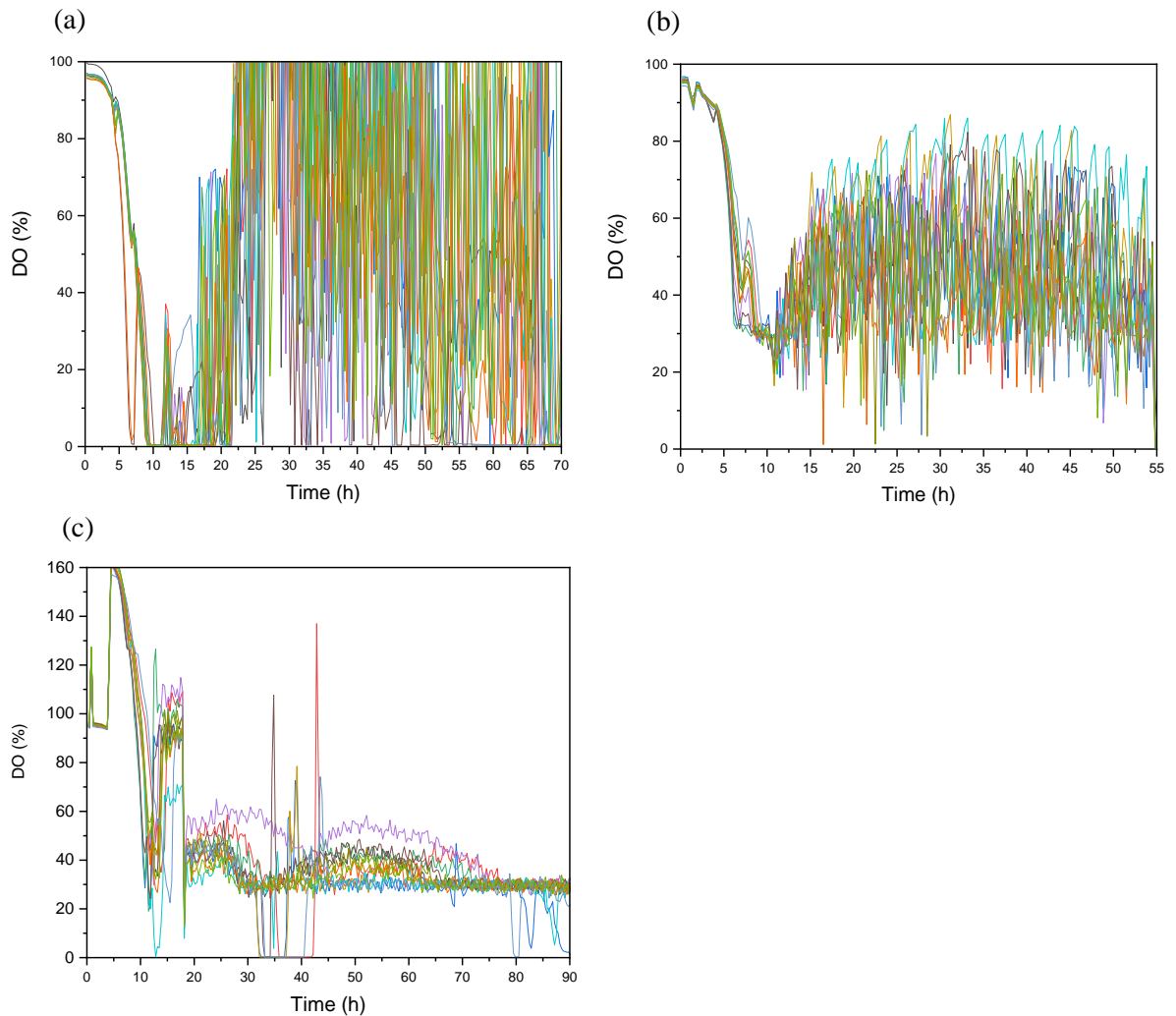
Figure E.3. DO profiles of 12 parallel fed-batch *E. coli* cultures using the prototype miniature bioreactor. (a) DO controlled via fixed gassing and fixed agitation, (b) DO controlled via a control cascade, (c) DO controlled via a control cascade and the use of a modified feed line dip tube.

The scope of the qualification package should be determined by evaluating the feasible processes, this should include a range of products, host organisms and process conditions (Shimoni *et al.*, 2014). Four different *E .coli* strains were run in both the prototype miniature STR and a 1L scale STR at equivalent DO set points, under optimum operating conditions. Table E.2 summarises the differences between the strains. Figure E.4. shows a comparison of cell growth and product expression of the four strains in the prototype STR and the 1L scale STR. The SPRs (per gram of WCW) of strains A and C were comparable between scales, however the SPRs of clones B and D were significantly greater at 1L scale than with the prototype miniature STR. This indicates that the strains that contain leader sequence 2 are more scalable than the strains using leader sequence 1. This suggests that the miniature bioreactor is

predictive of the 1L scale process under certain conditions, but refinements of the scale-up criteria would be required to improve the robustness of the system.

Table E.2. Summary of the strains run in the prototype miniature STR and 1L scale STR

E .coli strain	Product variant	Leader sequence
A	1	1
B	1	2
C	2	1
D	2	2

(a)   (b)
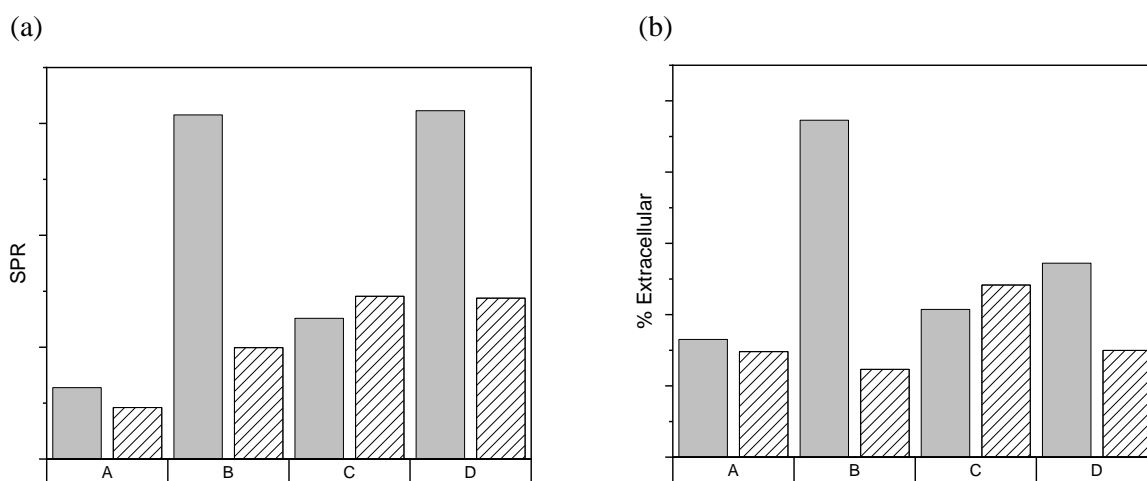
Figure E.4. Comparison of product expression of four *E. coli* clones (A, B, C and D) using the prototype miniature bioreactor and a 1L scale STR (a) SPR per gram of WCW and (b) % extracellular product. The grey bars represent the 1L scale process and the shaded bars represent the prototype miniature bioreactor process.

Product quality is the most important factor in the qualification of a scale-down bioreactor and should be consistent between scales (Shimoni *et al.*, 2014). Sensitivity of a scale down-model system to changes that could affect product quality should be equivalent or better than the large scale system. The bioreactor qualification programme should provide evidence of equivalent in-process and release specifications; therefore ideally equivalent sampling regimes, analytical assays and acceptance criteria should be used at both scales, (Shimoni *et al.*, 2014). This may require reduction of assay sample volume and/or modification of the purification procedure to

enable sample analysis to be performed on the small volumes of material generated from miniature bioreactor cultures. Product quality prioritisation should be the same at both scales; critical quality attributes (CQAs) e.g. purity and potency, and critical process parameters (CPPs) e.g. cell growth and titre of the large scale process should also be defined as the CQAs and CPPs of the scales-down process (Shimoni *et al.*, 2014). Product quality comparability studies are yet to be performed using the prototype miniature bioreactor. This would be the final stage of the qualification of the prototype miniature bioreactor, if it were to be used as a tool for validation of process modifications.

E.5. Summary

The implementation of scale-down models in fermentation process development enables new medicines to become available to patients more quickly and at a lower cost, due to increased experimental throughput and lower cost of goods. In this chapter the qualification of a prototype miniature stirred bioreactor was described. The prototype miniature bioreactor was characterised in terms of the oxygen mass transfer coefficient, k_La; the k_La values were shown to be in a similar range to a 1L-scale laboratory vessel, meaning the cells should experience similar process conditions at both scales if suitable scale-up criteria are used e.g. matched *P/V*. Parallel fermentations showed good reproducibility in terms of cell growth and product expression, demonstrating the robustness of the miniature bioreactor as a scale-down model. Clone screening experiments showed that the miniature bioreactor is predictive of an industrially relevant 1L-scale fermentation process; however the leader sequence used appeared to impact the scalability of the fermentation process. To complete the qualification of the miniature bioreactor, a product quality evaluation should be completed. The sensitivity of the miniature bioreactor to process changes that could impact product quality should be demonstrated to be equivalent or better than the 1L-scale process.

E.6. Bibliography

Betts, J. P. J., Warr, S. R. C., Finka, G. B., Uden, M., Town, M., Janda, J. M., Baganz, F. and Lye, G. J. (2014) 'Impact of aeration strategies on fed-batch cell culture kinetics in a single-use 24-well miniature bioreactor', *Biochemical Engineering Journal*. Elsevier B.V., 82, pp. 105–116. doi: 10.1016/j.bej.2013.11.010.

Duetz, W. A. (2007) 'Microtiter plates as mini-bioreactors: miniaturization of fermentation methods', *Trends in Microbiology*, 15(10), pp. 469–475. doi: 10.1016/j.tim.2007.09.004.

FDA (2011) *Guidance for Industry Process Validation : General Principles and Practices Guidance for Industry Process Validation : General Principles and Practices*. Available at: https://www.fda.gov/downloads/drugs/guidances/ucm070336.pdf.

Shimoni, Y., Goudar, C., Jenne, M., Scrinivasan, V. and Srinivasan, V. (2014) 'Qualification of Scale-Down Bioreactors Validation of Process Changes in Commercial Production of Animal-Cell–Derived Products, Part 1 — Concept', *Bioprocess Engineering*, 12(5), pp. 38–45.

Yawalkar, A. A., Heesink, A. B. M., Versteeg, G. F. and Pangarkar, V. G. (2002) 'Gas-liquid mass transfer coefficient in stirred tank reactors', *Canadian Journal of Chemical Engineering*, 80(5), pp. 840–848.